The role of redox balance in pulmonary innate immunity

Thesis submitted in accordance with the requirements of

the University of Liverpool for the degree of Doctor in Philosophy

by

Jamie Rylance

January 2013

Declaration

This thesis is the result of my own work and effort. In some instances, work was done in conjunction with other colleagues and institutions. Table details in full the attribution of work and responsibility related to the project.

This research was carried out at Liverpool School of Tropical Medicine and the Malawi-Liverpool-Wellcome Clinical Research Programme.

The material contained in the thesis has not been presented, nor is currently being presented, either wholly or in part, for any other degree or other qualification.

Table I ***Declaration of work and responsibilities within the project***

Activity	**Responsibility**
Image analysis software development	Dr S Barrett (Department of Physics, University of Liverpool) Duncan Fullerton (University of Liverpool)
Bronchoscopy	J Rylance shared responsibility with A Kankwatira (MLW) A Collins (Liverpool School of Tropical Medicine)
Spirometry measurements	J Rylance shared responsibility with A Kankwatira (MLW) R Malamba (MLW)
Sample processing	J Rylance shared responsibility with C Chimpini (MLW)
Image analysis and acquisition	J Rylance shared responsibility with C Chimpini (MLW)
Multiplex bead array	J Rylance solely responsible
Inductively coupled plasma mass spectrometry for trace elements	Biochemistry Department, Royal Liverpool University Hospital, Liverpool, UK
Glutathione peroxidase activity	Randox Laboratories Ltd, UK solely responsible
Western blotting	J Rylance, with supportive supervision from O Olayanju (Translational Medicine, University of Liverpool)
Preparation of reporter beads for intraphagosomal assays	J Rylance shared responsibility with Prof DG Russell, Cornell University, US
Intraphagosomal reporter bead assays	J Rylance solely responsible
Flow cytometry analysis	J Rylance solely responsible
Statistical data analysis and presentation	J Rylance solely responsible
Thesis Preparation	J Rylance solely responsible
Mathematical modelling	P Diggle (Lancaster University)

Abstract

Introduction: Household air pollution (HAP) affects one half of the world population, comprises 90% of global particulate exposure, and is associated with mortality from respiratory infections. Particulates are known to alter cellular redox balance, including that of the alveolar macrophage (AM). We investigate redox balance as a mechanism to explain the link between particulate exposure and failure of innate immune function.

Methods: Bronchoalveolar lavage was performed on healthy human volunteers in the UK (low HAP) and Malawi (high HAP). Antioxidant capacity was determined (concentrations of oxidised and reduced glutathione, and antioxidant capacities of glutathione peroxidase and superoxide dismutase). AM function was assessed by capacity to phagocytose, and to produce oxidative burst and proteolysis activity within the phagosome using reporter-fluorophore coated silica beads. AM cytokine responses to lipopolysaccharide and to respirable size wood smoke particles were measured before and after *ex vivo* treatment to reduce glutathione content. Personal exposure to particulates was estimated by the cytoplasmic content of black carbon within AM.

Results: AM glutathione was similar in UK and Malawi non-smokers (of which 4.3% was in oxidised form). One quarter of Malawians exhibited a high oxidised glutathione phenotype (8.6% of total). Malawians exhibited higher levels of extracellular glutathione, and intracellular malondialdehyde and particulate content than UK volunteers. Nrf2 levels in Malawian AM were proportional to levels of particulate matter. We demonstrated no association between particulate matter content and AM cytokine responses to lipopolysaccharide or wood. Glutathione depletion did not consistently alter AM cytokine production.

In vivo particulate exposure correlates with reduced AM phagosomal oxidative capacity, and increased cellular Nrf-2 concentration, but phagocytosis and phagosomal proteolysis are unaffected.

Conclusion: Malawians have high levels of AM particulate exposure, as expected from HAP surveys. This is associated with evidence of oxidative stress (lipid peroxidation), antioxidant upregulation (raised extracellular glutathione, intracellular Nrf2) and a specific defect in AM function (reduced oxidative burst).

Antibacterial function of the AM is key to preventing pulmonary infection: in a population subjected to high levels of household air pollution, particulate related defects in AM function could explain the high prevalence of infective respiratory illness.

Abbreviations

Abbreviations are explained at their first use. The following list may also be useful.

BAL	bronchoalveolar lavage
CFU	colony forming units
CumOOH	cumene hydroperoxide
CV	coefficient of variation
DMSO	dimethyl sulfoxide
DTNB	5,5'-Dithio-bis(2-nitrobenzoic acid), Ellman's reagent
EDTA	ethylenediaminetetraacetic acid
ELF	epithelial lining fluid
H_2DCFDA-SE	2',7'-dichlorodihydrofluorescein diacetate, succinimidyl ester
FCS	fetal calf serum
FITC	fluorescein isothiocyanate
fMLP	formyl-methionyl-leucyl-phenylalanine
FSC	forward scatter (flow cytometry)
γ GCS	γ-glutamylcysteine synthase
GPx	glutathione peroxidase
GR	glutathione reductase
Grx	glutaredoxin
GSH	reduced glutathione
GSSG	oxidised glutathione
GST	glutathione-S-transferases
HAM	human alveolar macrophage
Hb	haemoglobin
IFNγ	interferon γ
LPS	lipopolysaccharide
LTA	lipoteichoic acid
MDA	malondialdehyde
MDM	monocyte derived macrophage
NADPH	nicotinamide adenine dinucleotide phosphate
NF-κB	nuclear factor κB
Nrf2	nuclear factor (erythroid-derived 2)-like 2
PBS	phosphate buffered saline
PBMC	peripheral blood mononuclear cell
PE	phycoerythrin
SOD	superoxide dismutase
5-SSA	5-sulfasalicylic acid
SSC	side scatter (flow cytometry)
TEA	triethanolamine
TBARS	thiobarbituric acid reacting substance
TNB	5-thio-2-nitrobenzoic acid
TNFα	tumour necrosis factor α
Trx	thioredoxin
TrxR	thioredoxin reductase
ufCB	ultrafine carbon black (Printex 90, Degussa, GmBH)

Contents

Tables

Figures

Acknowledgments

This work has been funded by the Wellcome Trust. While this work is submitted as my own, it has also been variously supported, questioned, guided, critiqued and facilitated by a large number of people. My wife, Sarah, has been hugely loving, helpful and supportive throughout, demonstrating both sharp insight and wilful blindness as required. My children, Arthur and Arwen, while not directly helpful to the writing process have provided a reality check when I've been tempted to ask "what's the point?" While perhaps not strictly heritable traits, I have acquired from my dad the disposition to ask "why?", and from my mum the sense to stop. To both Maggie and George I owe a great (unpayable) debt: I am hugely grateful for their lifetime of love and support.

Supervisory support has been necessarily excellent. Stephen Gordon has been unswervingly optimistic, and relentlessly energetic. His personal kindness and professional encouragement have been fantastic. I wish I had collated the Gordonisms in a small volume to accompany this one. Rob Heyderman has carefully listened and incisively commented on this project from its inception. His thorough and helpful analysis has been inspirational. Thanks also to Malcolm Jackson and Frank McArdle for their time and scientific insight. I have been extremely fortunate in having friendly colleagues and laboratory scientists who have tolerated the ignorant clinician in their midst with great humour and understanding. These include: Sarah Glennie; Daniela Ferreira; Kondwani Jambo; Mathieu Bangert; Adam Wright; Helen Tolmie. Also thanks to: Rose Malamba, Anstead Kankwatira, Marie Kunkeyani; Chikondi Chimpini, Sade Ajibade (Laboratory technicians); Angie Wright, Lorna Roche (Specialist nurses); Kate Jones, Carolyn O'Leary (WTTC); David Russell (Cornell University); Ian Copple, Dammy Olayanju (Clinical Pharmacology); Alieu Amara, Lea Zibrik (IACD). Lastly, my thanks to the volunteers involved in both UK and Malawi without whom this project would have been impossible.

"If you thought hard enough, he'd always considered, you could work out everything. The wind, for example. It had always puzzled him until the day he'd realised that it was caused by all the trees waving about."

Terry Pratchett

1 Introduction

This project investigates the relationship between innate immune function, particularly in alveolar macrophages and redox balance in the lung. These topics are introduced separately below for orientation. Subsequently, their overlap and 'crosstalk' is discussed.

1.1 Innate immunity in the lung

1.1.1 Importance of intact innate immunity in the lung

Pneumonia is the consequence of a failed immune response in the lung following entry of a pathogen into the alveolar space. This disease causes death worldwide particularly in the young, elderly and immunocompromised[1, 2]. In US cohorts the strongest risk factor is cigarette smoking[3]. In developing countries, where the burden of disease is highest, the most important risk factors among children for acute respiratory infection are: malnutrition and micronutrient deficiency[4]; indoor air pollution[5, 6]; lack of breastfeeding and measles immunisation; overcrowding[7]. Despite lower rates of pneumococcal infection, there is also a significant burden of disease in otherwise healthy adults. In the absence of systemic immunocompromise such as HIV, biological mechanisms of susceptibility are not well understood.

The link between inhaled particulate exposure and respiratory disease was historically demonstrated by respiratory deaths during the 1952 London smog. Subsequent emphasis on, and funding to reduce environmental particulates within Western countries has been associated with significant increases in life expectancy[8].

In developing countries however, indoor air pollution in particular is widespread, affecting half of the world's population[9]. Intense particulate exposures due to burning of organic material for cooking, heating and lighting are common, and

associated with pneumonia in adults as well as children[10] Recent meta-analysis showed a relative risk for pneumonia of 1.8 from unprocessed solid fuel burning in the home[6]. Interventions to improve indoor air quality using improved stoves for cooking can reduce pneumonia[11].

It is evident from these epidemiological studies that, apart from the infective agent, other challenges to the lung are important in predisposing individuals to disease. Enhancing our understanding of the effect of particulates on innate immunity, for example, might help to more efficiently direct or target interventions to improve lung health.

1.1.2 Overview of the innate immune system in the lung

The innate immune system comprises a group of defences against potentially infectious agents which are similarly implemented in wide range of organisms, suggesting an ancient and common origin[12]. These defence systems incorporate a number of mechanisms by which the host avoids injury. They include: avoidance, compromise or removal of infectious agents by a physical or chemical means; targeting or effecting extracellular killing responses; initiating containment and killing responses within specialised cells; recruiting of further innate components; priming the adaptive immune system to identify and react to the infective agent. A key feature of innate immune responses is that they are rapid, but non-specific in their response[13, 14]. Innate immune mechanisms are central to pulmonary defence against infection; Table 1-1 shows a summary of these strategies and effectors within the lung. Tolerance to a pathogen's presence is an increasingly recognised defence mechanism[15] which is important in limiting harm to the host caused by its own immune system.

Table 1-1 Overview of the innate immune system strategies and effectors within the lung

Strategy	**Component**
Avoid, compromise or remove infectious agents	Unbroken respiratory epithelium, mucociliary escalator and cough reflex remove particles including infectious agents[16]
Chemical means	Lysozyme, lactoferrin, defensins, surfactant, proteases, complement and others (predominantly secreted from epithelial cells) [17] Cause reduced attachment of agent to epithelium and directly impairs the function or fitness of the agent
Target & initiate extracellular killing responses	Complement causes cytolysis, opsonises and targets inflammatory responses[18]. Immunoglobulin A (IgA) binding triggers localised inflammatory responses
Initiate containment and killing responses within cells	Phagocytic cells *i.e.* macrophages, monocytes, neutrophils. The action of the phagolysosome on ingested particles inactivates and destroys infectious agents by processes such as oxidative burst and proteolysis[19] Natural killer [NK] cells cause destruction of compromised host cells
Recruit further innate cells	Inflammatory cytokines and chemokine secretion (macrophage, epithelial cells) increases local anti-infective capacity
Prime the adaptive immune system to identify and react more specifically	Recognition of pathogen associated molecular patterns [PAMPs] by macrophages and dendritic cells causes inflammatory responses Antigen presentation (dendritic cells, macrophages)[20]
Regulate subsequent responses	Removal of apoptosis inflammatory cells (efferocytosis) and anti-inflammatory cytokine secretion prevent over-activation of immune response and subsequent tissue damage[21]

1.1.3 Lower airway cellular defences

It is noted that a large proportion of aerosolised particles is deposited proximal to the terminal airways, and that likelihood of deposition changes with particle diameter and content[22, 23]; larger particles tend to be filtered in the nasopharynx and larger airways, whereas particles of around 1μm and less may more commonly be encountered in the terminal bronchioles and alveoli.

At this level, the respiratory interface is populated mostly by epithelial cells. Alveolar macrophages (AM) occur at the approximate frequency of 1 per alveolus[24]. It is possible to obtain these cells in humans via a well-tolerated bronchoscopic procedure (bronchoalveolar lavage): isotonic fluid (normal saline) is instilled into a sub-segmental bronchus of the lung, and removed by suction. In healthy volunteers, the resulting suspension usually contains around 90% AM and, at an order of magnitude less frequent, lymphocytes[25]. Proportions of lymphocytes change with age: Figure 1-1illustrates normal values for differential counts of bronchoalveolar lavage in volunteers aged 19-36 years.

Figure 1-1 Proportional area diagram showing the cells present in bronchoalveolar lavage fluid

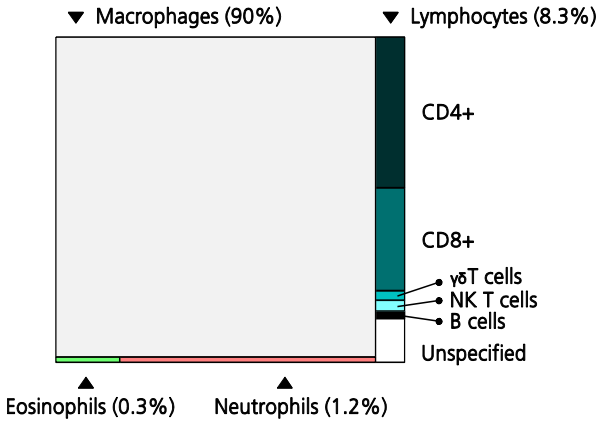

Data in Meyer et al[26]

The alveolar epithelium also incorporates type 2 cells which secrete surfactant proteins[17]. Submucosal dendritic cells and other macrophages lie amongst the framework of blood vessels and extracellular matrix[27]. During inflammatory or ectopic processes, neutrophils and eosinophils may also be present in increased number and proportion[28].

1.1.4 Alveolar macrophage

Even with intact upper airway defences, microbial pathogens due to their size may be deposited directly in the terminal airways[29]. This may occur following aerosol inhalation derived from another host (as for *Mycobacterium tuberculosis*), or from autologous colonisation in the upper airways (as for *Streptococcus pneumoniae)*.

The alveolar macrophage (AM), as part of the pulmonary innate immune system, is importantly placed to defend against organic and non-organic insults. As the primary resident macrophages in the lungs, they are key sentinel cells which have roles in cytokine response, neutrophil recruitment, antigen presentation and efferocytosis (the removal of apoptosed cells)[24, 30]. The following section describes the interaction between AM and pathogen, focussing on *Streptococcus pneumoniae*.

1.1.4.1 Alveolar macrophage-pathogen interactions

S. pneumoniae is the commonest cause of mortality from pneumonia, accounting for 1.2 million deaths per year in infants, and may well exceed this in adults[31]. Streptococcal pneumonia is necessarily preceded by nasopharyngeal colonisation. During childhood, rates of both disease and colonisation fall with age following repeated exposure to the pathogen[32]. It is presumed that the lungs are frequently challenged with colonising bacteria, but that frank pneumonia results from failure of the innate immune system[24].

S. pneumoniae (the pneumococcus) is a gram positive alpha haemolytic bacterium. Encapsulated forms are the most capable of colonisation and of causing invasive disease. The polysaccharide capsule inhibits phagocytosis, complement and immunoglobulin binding. More than 90 serotypes have been isolated. Each serotype has a unique variation in the composition of the polysaccharide coating which is recognised by antisera[33]. Various other virulence factors also subvert the innate

immune response: preferential binding to epithelial surfaces (PspA); reduction of complement activity (cbpA); increased resistance to oxidative burst (PspA); cleavage of mucosal immunoglobulin (IgA protease). *S. pneumoniae* also secretes pneumolysin which damages ciliary transport and oxidative burst through cytotoxic effects, causes inflammation through activation of complement, and activates innate immune responses through the TLR4 pathway[34]. Pro-inflammatory signalling is also propagated through TLR2 receptors by lipoteichoic acid[35] and internalised peptidoglycan by Nod –like receptor 2 (Nod2)[36].

The alveolar macrophage co-ordinates the host response in the lung, balancing the need for robust reaction against the potential for damage caused by excessive inflammation[37]. In early infection, AM are killed due to cytotoxicity of this response[38], which involves: phagocytosis; internalised killing responses; antigen presentation; inflammatory response and recruitment. At a critical stage in the infection, the AM response becomes less inflammatory. This resolution phase is typified by alveolar macrophage apoptosis, efferocytosis (the clearance of apoptotic bodies) and anti-inflammatory signalling. These functions of the AM throughout the course of infection are summarised below.

Phagocytosis

Phagocytosis requires co-ordinated change to the cell membrane and actin structure to allow internalisation of the particle and time critical maturation of the phagolysosome. A large number of cell surface receptors exist to facilitate uptake of microbes and other material. Depending on which receptor system is engaged, such ingested material is differently dealt with. Bacteria which have been opsonised are targeted for phagocytosis through specific cell surface receptors on the AM (such as Fcγ receptor recognises IgG, and CR3 and CR4 recognise complement protein C3b)[39]. The Fcγ receptor directs internalisation to maturing phagosome marked by

lysosomal associated membrane protein LAMP-1. Complement deposition enhances, but is not necessary for this activity in alveolar macrophages[40].

Without bound IgG, alternative pathways exist which may converge on these killing and antigen presentation end points. This is mediated by pattern associated molecular pattern (PAMP) recognition receptors on the AM[41]. PAMPs are broadly phylogenetically conserved bacterial structures which afford the host an opportunity for bacterial recognition without relying on the cognate response *i.e.* without prior exposure. PAMP receptors are genetically encoded in the host, and unlike T and B cell receptors do not require somatic recombination. Alveolar macrophages exhibit a number of PAMP receptors including CD14, toll-like receptors (TLRs),"scavenger receptors" such as SR-A, MARCO, mannose receptor (CD163) [42, 43] which recognise bacterial and other foreign structures, and promote pathogen phagocytosis. There is overlap within these recognition pathways, for example *Streptococcus pneumoniae* is recognised by type A scavenger receptors, mannose receptor and others such as DC-SIGN[44].

Action of the phagosome *i.e.* killing responses

Bacterial killing is enacted by progressive and carefully choreographed endosomal fusion[45] Oxidative burst occurs relatively early in this pathway[46] and is succeeded by other reactions such as further acidification, proteolysis and other destructive processes[39]. There are significant differences between these processes in macrophages and the more often studied neutrophil.

NADPH oxidase produces the oxidative burst by catalytic formation of superoxide ions from molecular oxygen (see Equation 1). This enzyme is assembled from inactive cytosolic components as the macrophage becomes activated (see Figure 1-2). Subunits include the membrane spanning $gp91^{phox}$ and $p22^{phox}$ proteins

collectively termed flavocytochrome b_{558}. Three other cytosolic proteins ($p47^{phox}$, $p67^{phox}$ and Rac2) complete the active complex in macrophages[47]. Another protein, p40, is not necessary for oxidative burst but increases the affinity of p47 for the flavocytochrome b_{558} unit[48]. Other antibacterial functions of the phagolysosome, including mechanisms for trafficking the phagosome are reviewed elsewhere, and not discussed further here[20, 49].

Figure 1-2 Diagramatic structure of NADPH oxidase

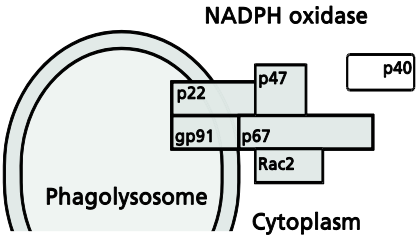

Equation 1 NADPH oxidase

$$NADPH + 2O_2 \xrightarrow{NADPH\ oxidase} NADP^+ + H^+ + 2O_2^{-\bullet}$$

Antigen presentation

The AM may present bacterial peptides in association with MHC class II causing specific T cell responses. Viral peptides may also be presented, on MHC class I. Although AM are less effective antigen presenters than monocytes[50], they are more adapted to this function than other tissue phagocytes[51]. The extent to which AM act as antigen presenting cells in pulmonary infection is not known, although lung macrophages can pass antigen to dendritic cells which may then migrate to regional lymph nodes[52].

Inflammatory response and recruitment

In response to infectious agents, alveolar macrophages produce inflammatory cytokines such as TNFα, IL-1β, IL-8 and IFNγ. TNFα and IL-1β stimulate further inflammatory mediators from macrophages and epithelial cells. IL-8, a chemokine,

operates as a chemo-attractant causing an influx of monocytes and neutrophils which may then themselves release pro-inflammatory mediators. IFNγ is important in priming immune cells for further activation[53].

Recognition of the bacteria by the AM, and subsequent signal transduction is fully described in a recent review[54]. Multiple pathways exist, but the best described are the Toll-like receptors (TLRs). These PAMP receptors, such as TLR2 and TLR4 propagate intracellular inflammatory signals by multiple pathways including MAPK[55], but are commonly dependent on the MyD88adapter molecule[56] and converge on NF-κB upregulation.

TLR4 recognises pneumolysin[57] and, in combination with CD14, lipopolysaccharide (LPS). TLR2 is important in gram positive bacterial recognition due to its affinity to lipoteichoic acid and bacterial lipopeptides. Mice lacking TLR2 have impaired cytokine responses to *Streptococcus pneumoniae*, although lung infection resolves normally provided pneumolysin is present to activate TLR4 pathways[58].

Oxidative and inflammatory pathways in the macrophage are closely related (see Figure 1-3). NADPH oxidase can limit pro-inflammatory NF-κB related cytokine release through suppression of NF-κB relating to Nrf2 activation[59]. Pro-inflammatory NF-κB also positively regulates the activity of NADPH oxidase through the gp91 subunit[60], and through the TNFα mediated phosphorylation of the $p47^{phox}$ subunit[61].

Figure 1-3 Interrelationships between oxidative burst and inflammatory pathways in the alveolar macrophage

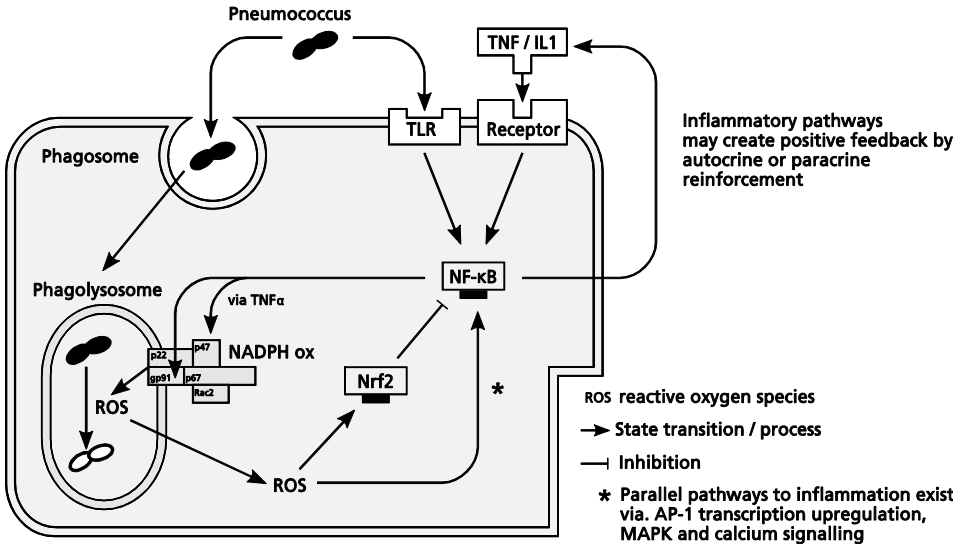

Central to regulation of the inflammatory response is the balance between NF-κB and inflammatory signalling responses, and those of Nrf2 by which the host protects itself against oxidative stress by upregulation of antioxidants
This diagram is necessarily simplified. Multiple inflammatory cytokines exist, and signals are transduced through multiple parallel pathways. See text for details.

Surprisingly, in p47^{phox} deficient mice, a lack of NADPH oxidase activity leads to improved microbial killing in low dose pneumococcal infection in mice[62]. In this model, increased neutrophil recruitment compensates for the loss of AM function. However, the exaggerated response to pro-inflammatory stimuli causes host lung damage[63].

Phenotypic shift of AM in response to bacterial stimulus

Macrophages, in response to Th1 type cytokines in their environment (*e.g.* TNFα, INFγ), undergo a reversible phenotypic shift towards an "activated" phenotype (designated M1: see section 2.9.1 for more detail). Transcriptomic analysis of activated macrophages demonstrates this common host response to a broad range of bacteria, and involves upregulation of MHCII, increased cytokine release and oxidative burst activity, and down-regulation of scavenger type receptors whose usual function is in internalisation of inert particles[64, 65].

By these mechanisms, the pneumococcus might be both recognised, phagocytosed and initiate an inflammatory signalling cascade. Once controlled, the AM becomes key to resolving these inflammatory changes.

Resolution of inflammatory changes

AM then adopt an anti-inflammatory phenotype (M2) and undergo apoptosis. While programmed cell death in early infection results in poor bacterial handling, delayed apoptosis limits inflammation and enhances antigen presentation[66-68]. Phagocytosis of these apoptosis cells (efferocytosis) limits further release of IL-1β, IL-8 and TNF-α[69]. This reduces the potential for tissue destruction, conferring a survival benefit to the host[70]. Prolonged responses to persistent bacterial products are limited by down-regulating the inflammatory response by an unknown mechanism. Macrophages appear to preserve the ability to recruit neutrophils even after this tolerance develops[71].

1.1.4.2 Alveolar macrophage – particulate interactions

Airborne products of combustion, cigarette smoke and less commonly, inorganic dusts are all encountered by the AM in the alveoli. Inhaled particles are conventionally designated by diameter as coarse (2.5-10μm), fine (0.1 to 2.5μm) and ultrafine (less than 0.1μm). Real world exposures are necessarily more complex, with considerable variation in size, surface charge and aggregation. Nevertheless, upper airways and the nasopharynx filter most coarse particles (see Figure 1-4). Alveolar macrophages typically encounter fine and ultrafine particles. Most commonly, these are internalised by AM phagocytosis, although direct penetration into the submucosal and wider circulation may occur particularly with ultrafine particles[72].

Figure 1-4 Particulate size classification, and deposition in the respiratory tract

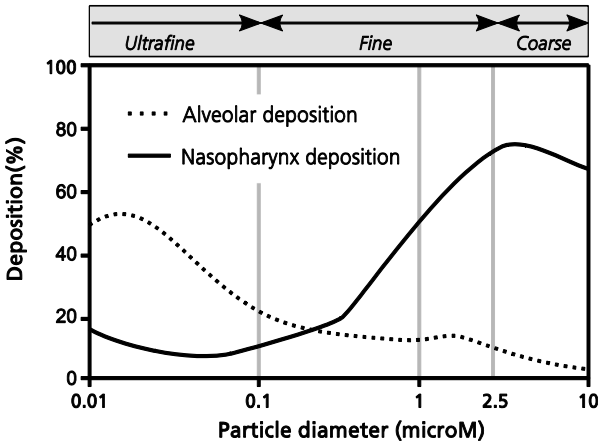

Modelling data for nasal breathing subjects shows the deposition fraction for nasopharynx and alveolar regions. This is based on 'ideal' particles in non-agregated form in a human breathing nasally at normal tidal volumes. Adapted from Oberdorster et al[73]

The toxicity of particles to the alveolar macrophage is in part caused by the inflammatory response which is turn is dependent on particle type[74]. Toxicity is inversely related to particle size[75, 76], and is compounded by the adsorbed transition metals, aromatic hydrocarbons and other volatile organic compounds[77]. Activation

of inflammatory signalling pathways and phagosomal activity is potentiated by hydrocarbons through the action of reactive oxygen species in either an autocrine or paracrine manner[75, 78, 79]. This is discussed further in 1.2.1.2.

In this project, we focus on the particulates which are most commonly used as "biomass fuels" by around 2.4 billion people worldwide[80]. These are energy sources derived from living organisms. Typically, wood, charcoal, dung and crop residue are used for heating, lighting and cooking provide more than half of domestic energy in developing countries[81].

Wood smoke has many constituents including carbon monoxide, benzene, nitrogen oxides and polyaromatics hydrocarbons[9] which may cause direct toxicity, generate reactive oxygen species and enhance inflammatory pathways. Endotoxins, of which lipopolysaccharide (LPS) is the archetypal example, also potentiate inflammation[82], and are present in relatively high quantities in homes burning biomass fuels[83].

Table 1-2 summarises key features of the innate response to particulates, and supporting evidence from the literature. Considerable knowledge exists for concentrated ambient particles (CAP) and diesel exhaust particulates (DEP), which have some commonality with biomass fuels in terms of the end products of combustion, and their potential for toxicity. DEP and CAP are therefore included for comparison: this table is not exhaustive; where possible human studies are reported in preference to animal experiments. It should be noted that most of these studies model acute exposure, and not chronic or repeated particulate challenge.

A number of generalisations may be made regarding particulate exposure, supported by evidence from Table 1-2:

- Particulates have a pro-inflammatory effect on alveolar macrophages and the lung in general. This is partially mediated by endotoxin and transition metal content. NF-κB is central to the inflammatory response, and may be antagonised by Nrf2 activity. This is strongly dose and particle dependent, and for "clean" particles there is a threshold effect for surface area below which inflammation is not induced[75].
- Chronic particulate exposure may reduce baseline or maximal inflammatory response, although evidence is patchy.
- Anti-inflammatory cytokine production has not been as widely assessed, and the effects are unknown.
- Neutrophil influx is a common observation in acute and chronic studies
- Phagocytosis is reduced by particulate exposure in the acute setting. This is unknown for chronic exposures
- Maximal respiratory burst is reduced by particulate exposure in the acute setting, and in chronic wood smoke exposure
- Microbial killing is reduced by acute exposure, but where prior exposure to particulates has caused an inflammatory stimulus, killing may be increased
- Apoptosis in the alveolar macrophage is induced by particulates

Detailed review of toxicological aspects may be found in recent peer reviewed articles[84-86] and are not further described here. Specific constituents of wood smoke which have harmful effects on health are given in Naeher et al[87].

1.1.5 Need for human studies in particulate exposure research

Study of particulate exposure has often been limited by *in vitro* experiments based on submerged monoculture. Problems with these include:

- difficulty establishing a model of physiological relevance, particularly for doses
- particle behaviour in collection and re-suspension *i.e.* the effect of solvents on particles, agglutination
- interaction with the cells in a non-confluent cell layer
- *in vitro* study: the lack of surrounding extracellular milieu and interaction with other cell types

Air-liquid interface experiments are possible, and might provide a more physiological laboratory apparatus for exposure and probing of cell cultures[88, 89] but are not widely used. Co-culture models have also been developed which allow some assessment of the interplay between macrophage and epithelium[90]. Human *in vivo* exposure studies have some advantages compared with *in vitro* testing in terms of relevance of exposure and physiology, but use lower doses and shorter exposures to particulates than those from "natural" human exposures. Exposure chamber experiments have used 200–300μg/m^3 $PM_{2.5}$ for 4 hours[91]).

A database of studies for indoor particulate levels[92] shows 24 hour time weighted averages of PM2.5 to be in a wide range: of the 10 studies available, concentrations were 56.8 - 1102μg/m^3 (geometric mean 391μg/m^3). Meal time and 1 hour exposures were available in 8 cases, with time weighted average concentrations of 130 to 27000μg/m^3 $PM_{2.5}$ (geometric mean 2531μg/m^3).

For these reasons, and because chronic and acute exposures have potential to differ widely in effect, human studies examining real-world exposures will be of key importance in defining our understanding of indoor air pollution.

Table 1-2 ***Effect of particulate exposure on the alveolar macrophage***

Inflammatory mediators	**Baseline levels increase** ↑ TNFα, IL-1β, IL-6, MIP-2 in HAM[93-95] ↑ IL-6 in humans after controlled exposure[96] ↑ MIP1β, GMCSF, IL-6, TNFα, IL-1beta, IL8, MCP-1 in rabbit AM[97] ↑ mRNA for MIPs, IL-1β, CCR1 in INFγ primed lungs of mice with *S. pneumoniae*[98] **Endotoxin is significant contributor** Blocking endotoxin reduces effect on IL-6 and IL-8[94, 99, 100] Priming with endotoxin amplifies effect[101] **Iron is significant contributor** Removing Fe^{2+} reduces effect of particulate source[100, 102]	**Baseline levels increase** ↑ TNFα, IL-8 in MDM[103] ↑ BAL IL-13, but not IL-10 and IL-18 in humans[104] ↑ Th2 response in HAM[105] **But maximal production decreases** ↓ TNFα, IL-8, PGE2 in LPS stimulated HAM[106] ↓ TNFα in LTA stimulated HAM[106] ↓ TNFα, IL-1β, IL-2 in *Listeria monocytogenes* infection in rats[107] **Surface area is a contributor** IL- 1β in mice lungs is dependent on particle surface area[75]	**Baseline levels increase** ↑ IL-6, TNFα but → MCSF, MIP1beta, IL1beta, MCP-1in rabbit AM[97] ↑ TNFα, IL-6 Histological inflammation in rats[108] **Surface area is a contributor** IL- 1β in mice lungs is dependent on particle surface area[75] Inflammation is surface area dependent at low doses, but mass dependent at higher doses[109]	**Baseline levels increase in some studies** ↑ TNFα in RAW264.7[110] → TNFα, IL- 1β, MCP-1 in mice[111] → TNFα, MIP-2 in rats[112] ↑ TNFα, IL-6, IL-8 but → IL-1β in co-cultured monocyte/ pneumocytes model[90] **Baseline levels decrease in chronic exposure** ↓ INFγ, IL-1β in rat BAL (chronic)[113]

Pathways	↑ NF-κB[114] Nrf2 protects against inflammation[115]	↑ NF-κB in RAW 264.7 cells[116] Nrf2 protects against inflammation[115]	NK	↑ NF-κB in RAW264.7[110]
Neutrophil recruitment	**BAL neutrophilia in acute and chronic exposures** ↑ recruitment in INFγ primed lungs of mice with *S. pneumoniae*[98], but ↓ in rats when infection preceded exposure[117] ↑ in mice in Paris subway[118] (chronic exposure)	**BAL neutrophilia in acute exposure** ↑ BAL neutrophils in mice[119] ↑ BAL neutrophils in humans[120]	**BAL neutrophilia in acute exposure** ↑ monocyte recruitment with rabbit AM[97]	**BAL neutrophilia in acute and chronic exposure** ↑ in rabbits[121] ↑ in humans[122] ↑ in rats (chronic)[123]
Chemotaxis	↓ in *ex vivo* rat AM[124] ↑ monocyte recruitment with rabbit AM[97]	→ in ex-vivo HAM[125], chemotactic agents in MDM[103]	↓ in rat AM after chronic *in vivo* exposure[74]	↓ in HAM[126]
Microbial binding	↑ in mouse AM with *S. pneumoniae*[127]	NK	→ in HAM with *S. pneumoniae*[127]	↓ with *Pseudomonas* sp by rabbit AM[121]
Phagocytosis or microbe internalisation	↓ in murine macrophages with *S. pneumoniae* (related to Fe^{2+})[127] ↓ in INFγ primed lungs of mice with *S. pneumoniae*[98] ↓ with silica particles in rat AM[124]	↓ in rats[107, 128]	→ in HAM with *S. pneumoniae*[127]. ↓ silica uptake in rat AM & HAM primed with INFγ[129, 130] ↓ in HAM challenged with silica beads[130]	↓ in rabbit AM[121] ↓ in human MDMs with *S. pneumoniae*[131]

Respiratory burst	↓ in rabbit AMs[132] ↓ basal rate in rats AM, but ↑ zymosan induced rate[117]	↓ in HAM[133]	↓ in canine AM exposed to UFCB, mediated by PGE_2[134]	↓ in rat AM[135] ↓ in rat lung (chronic)[87]
Microbial killing	**Killing reduced** → rate but ↓ absolute number killed[127] in murine macrophages with *S. pneumoniae* ↓ in rats with *Listeria* sp[136] ↓ in rats lungs with *S. pneumoniae*[117]	**Killing reduced** ↓ in rat AM with *S. pneumoniae*[137] and *Listeria sp*[107]	**Killing reduced** ↓ in rat AM with *S. pneumoniae*[137] ↓ with *S. aureus.* in rats[138] ↓ with *Listeria* in rat AM[107, 138] **Killing increased by priming inflammatory response** ↑ in mice with *S. pneumoniae* primed with UFCB[139]	**Killing reduced** ↓ in rabbit AM with *Pseudomonas*[121] ↓ in rats with *S. aureus*[135] **Killing increased by priming inflammatory response** ↑ in mice with *Listeria* primed with wood smoke[111]
Apoptosis	**Apoptosis increased** ↑ in HAM, mediated by transition metal content[93]	**Apoptosis increased** ↑ in HAM[93]	**Apoptosis increased** ↑ in RAW 264.7 macrophages, mediated by TNFα[79]	**Apoptosis increased in monoculture** ↑ in guinea pigs with chronic exposure[140] → in co-cultured monocyte/pneumocyte, but ↓ viable cells[90]

Oxidative stress	**Oxidative stress increased** ↑ in HAM and monocytes[95] ↑ in INFγ primed lungs of mice with *S. pneumoniae*[98]	**Oxidative stress increased** ↑ in HAM and monocytes[95] ↑ 8-isoprostane, mediated by arachidonic acid in canine AM[76] ↑ lipid peroxidation of surfactant in rat AM with *S. pneumoniae*[137] ↓ glutathione and urate in humans[120]	**Oxidative stress increased** ↑ 8-isoprostane, mediated by arachidonic acid in canine AM[76] ↑ 8-isoprostane in rats[108] ↑ lipid peroxidation of surfactant in rat AM with *S. pneumoniae*[137] **Oxidative stress is surface area dependent** 8-isoprostane correlates well with surface area of particles[76]	**Oxidative stress increased** ↑ Clara cell protein in blood and urine in human exposure[91] ↑ free radicals produced in mouse peritoneal macrophages[110] → 8-oxodG in rat lungs[141] ↑ DNA strand breaks and lipid peroxidation in RAW 264.7[110]

Studies are models of acute exposure unless explicitly stated.
Symbols: ↑Increased or upregulated; ↓Decreased or downregulated; →Unchanged
Abbreviations: AA = arachidonic acid; AM = alveolar macrophage (HAM = human alveolar macrophage); BAL = bronchoalveolar lavage; IFN = interferon IL = interleukin; LPS = lipopolysaccharide; LTA = lipoteichoic acid; MDM = monocyte derived macrophage; MTB = Mycobacterium tuberculosis; PBMC = peripheral blood derived mononuclear cells; TNF = tumour necrosis factor; UFCB = ultrafine carbon black, NK = not known

1.2 Redox balance in the lung

Redox balance is the equilibrium between production and metabolism of oxidising substances within a biological system[142]. Such oxidants include reactive oxygen species (ROS) and reactive nitrogen species (RNS). Adequate antioxidant capacity is required to prevent their deleterious effects, and to repair damage once done. Inadequate physiological defences may result in downstream effects involving the altered function of lipids, proteins and DNA[143]. Cellular behaviour may be profoundly affected during this so called 'oxidative stress', but is also attenuated by less destructive, lower amplitude fluctuations in redox balance: so called redox signalling[144].

Lung tissue is uniquely vulnerable to alteration in redox balance. Exogenous factors such as high tissue concentrations of oxygen and inhaled particulate matter[145] may compound endogenous production of oxidants[146]. Concurrently, low level bacterial challenge should be dealt with by the innate immune system in order to prevent pneumonia and invasive infection (see section 1.1.3). Where pulmonary redox balance is altered, so is the response to infection: oxidative stress has the potential to impair innate immune defences. Tight control of immune responses, inflammatory mediators and extracellular antioxidant buffering avoids excessive cellular recruitment and tissue oedema which would compromise normal lung function[147].

1.2.1 Definitions of terms

A number of terms are used to describe redox balance, and are explained in Table 1-3. Examples have been chosen to be relevant to the text which follows.

Table 1-3 Definition and explanation of terms relating to redox balance

Term	Definition / explanation	Examples
Redox reactions	[***Red***uction-***Ox***idation reactions] Any reaction in which components undergo changes to their oxidation state	$GSSG + NADPH + H^+ \rightarrow 2GSH + NADP^+$
Oxidation	Loss of electrons (within an atom, molecule or ion). Synonymous with increasing oxidation state	$2GSH \rightarrow GSSG + 2H^+ + 2e^-$ Here, the reduced form of glutathione (GSH) is oxidised
Reduction	Gain of electrons (within an atom, molecule or ion). Synonymous with decreasing oxidation state	$GSSG + 2H^+ + 2e^- \rightarrow 2GSH$ Here, the oxidised form of glutathione (GSSG) is reduced. The other half of the equation might be: $NADPH \rightarrow NADP^+ + H + e^-$ Combining both of these half equations gives the full equation at the top of this table
Redox couple[148]	The oxidised and the reduced forms of a molecule, atom or ion in a given redox reaction	Oxidised glutathione (GSSG) and reduced glutathione (GSH)
Redox potential[148]	The electric potential given by redox couples given by the Nernst equation (see section 7.2)	At 25°C, the redox potential of glutathione (GSSG/GSH) is -59.1mV
Redox state[148]	Not well defined, but refers to the redox environment of a cell as represented by multiple redox pairs	See Figure 1-5
Free radical	Molecules, atoms or ions with unpaired electrons in the outer orbit	Superoxide ($\bullet O_2^-$), Hydroxyl ($\bullet OH$) Nitric oxide ($NO\bullet$)
Reactive oxygen species[149]	Partially reduced metabolites of O_2 with high oxidizing capacity Not all ROS are free radicals (*e.g.* H_2O_2)	Superoxide ($\bullet O_2^-$), Hydroxyl ($\bullet OH$) Hydrogen peroxide (H_2O_2)
Reactive nitrogen species	Partially reduced metabolites of N_2 with high oxidizing capacity Not all RNS are free radicals (*e.g.* $ONOO^-$)	Nitric oxide ($NO\bullet$) Peroxynitrite ($ONOO^-$)
Oxidative stress	Excess ROS/RNS production compared with cellular antioxidant capacity	

1.2.1.1 Describing the redox balance

As noted in Table 1-3, the cellular redox balance is not tightly defined, but describes the predominant redox state of the most common redox pairs. It may be derived mathematically if the concentrations of contributing molecules are known[148], but methodologically this is not feasible.

Experimental studies often therefore equate redox balance with that of the most abundant intracellular redox buffer: glutathione. This tripeptide (*γ-GluCysGly)* exists at concentrations of 1-10mmol/l in the cytoplasm depending on cell type[150]. This allows proxy measurement of redox state by analysis of only one component. This approach has been criticised by Martinovich[151] who notes that it is possible for oxidants to preferentially oxidise specific redox pairs without affecting glutathione. Evidence for this has been seen in *ex-vivo* exposure of human epithelial lining fluid to nitrogen dioxide[152]. This is practically very uncommon, and the state of the glutathione redox pair both correlates well with the degree of oxidative stress, and has relevance to cellular behaviour[148].

Figure 1-5 shows examples of a number of intracellular redox pairs; these do not exist in isolation, and electrons may pass between sets of redox pairs (as seen with glutathione and NADPH in Table 1-3).

Many processes contribute to redox balance. Both endogenous generators of redox active substances and exogenous sources are introduced below.

Figure 1-5 Examples of redox pairs, and their relationship to intracellular redox balance

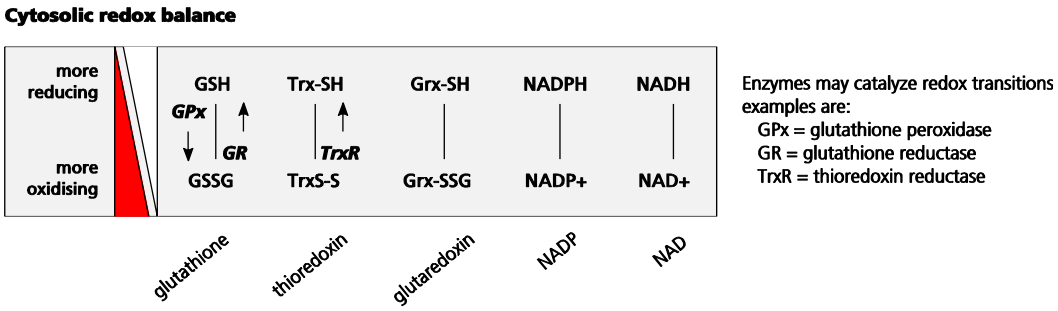

1.2.1.2 Endogenous sources of redox reactive substances

1.2.1.3 Mitochondria

Reactive oxygen species are produced endogenously in a number of ways in the alveolar macrophage (see Table 1-4). Usually, aerobic respiration uses oxygen as the final electron acceptor, resulting in carbon dioxide and water formation. However, during the process of electron transfer in the mitochondrial membrane, electrons may "leak" and react prematurely with oxygen. This occurs particularly from the ubiquinone component of the electron transport chain, and resulting in superoxide radical formation, for accounting for 1-3% of oxygen consumption[153].

1.2.1.4 Cytochrome P450

Secondly, nicotinamide adenine dinucleotide phosphate (NADPH) is used to drive important cellular processes. Cytochrome P450 enzymes use NADPH to drive redox reactions to metabolise wide varieties of substances, and different forms exhibit tissue specificity. Alveolar macrophages express multiple forms including CYP2E1, which is known to produce the most ROS of all cytochrome P450 forms as a result of loss of electrons from the metabolic pathway[154], predominantly as superoxide.

1.2.1.5 NADPH oxidase

Superoxide is also formed by the action of NADPH oxidase in generating the oxidative burst of phagocytes (see Equation 1 and section 1.2.1.5).

Superoxide is extremely short lived, causing oxidation immediate to its site of production. It dismutes spontaneously, a reaction which is diffusion limited when catalysed by superoxide dismutase (see Equation 2). Steady state concentrations from physiological processes are around 10^{-11}mol/l[150].

Equation 2 superoxide dismutation

$$2O_2^{-\bullet} + 2H^+ \xrightarrow{superoxide\ dismutase} H_2O_2 + O^2$$

The resulting hydrogen peroxide, although a weaker oxidant, more easily diffuses across phagosomal membranes[155]. It is found in the cytoplasm at concentrations of 10^{-8}mol/l[156], and up to 15μM in activated polymorphonuclear cells.

1.2.1.6 Inducible nitric oxide synthase (iNOS)

Alveolar macrophages may be induced to express by inducible nitric oxide synthase (iNOS) by inflammatory signals from epithelial cells[157].

1.2.1.7 Peroxisomes

Peroxisomes also generate ROS during their oxidation of long chain fatty acids and amino acids. Multiple enzymes are involved, predominantly producing H_2O_2, although xanthine oxidase and inducible nitric oxide synthase (iNOS) generate superoxide and nitric oxide respectively[158]. Peroxisomes are well equipped with antioxidant systems including catalase and Cu-Zn-superoxide dismutase, peroxiredoxin[158]. Their relative role in macrophage redox balance is not well defined.

Table 1-4 Endogenous sources of free radicals in the lung

Process	**Activity**	**Produces**
Oxidative burst within macrophage phagosome	NADPH oxidase[159]	$\bullet O_2^-$
Electron transport chain within mitochondria	Ubiquinone pathway[153]	$\bullet O_2^-$
Metabolism of long chain fatty acids and amino acids within peroxisomes	Multiple enzymes, including: xanthine oxidase; iNOS[158]	H_2O_2 $\bullet O_2^-$ NO•
Signalling pathways	iNOS (inducible nitric oxide synthase)	NO• Indirectly, $ONOO^-$
Metabolism of sterols and xenobiotics e.g. polyaromatics hydrocarbons in inhaled matter	Cytochrome P450 *e.g.* CYP2E1[154]	$\bullet O_2^-$ •OH H_2O_2

In addition to the primary products of these reactions, combinations of ROS can generate other, more reactive products. One example is the Fenton reaction. In the presence of ferrous iron (Fe^{2+}) or other transition metal, H_2O_2 can react to form the highly destructive hydroxyl radical (see Equation 3). This radical is short lived (half-life 10^{-9}s)[160]

Equation 3 hydroxyl formation

$$Fe^{2+} + H_2O_2 \xrightarrow{vie\ intermediate\ complexes} Fe^{3+} + HO^{\bullet} + HO^-$$

Another such reaction is for formation of peroxynitrite ($ONOO^-$) from superoxide and nitric oxide (see Equation 4). Peroxynitrite anions, and their downstream derivatives have cellular effects similar to ROS[161], and a half-life of 0.05-1s[160].

Equation 4 peroxynitrite formation

$$\cdot O_2^- + \cdot NO \rightarrow ONOO^-$$

ROS and RNS are created in the cell as a result of these fundamentally important processes: energy use; metabolism; cellular signalling; defence against pathogens

and xenobiotics. Antioxidant pathways are of central importance in maintaining redox equilibrium and limiting the potential for adverse effects on the host. These are summarised below.

1.2.2 Glutathione – central to antioxidant defence in the lung

Glutathione is the most abundant redox buffer, and is found in particularly high concentrations in alveolar macrophages compared to other cell types within the lung[162]. Estimates suggest total concentrations in AM are 6.64μmol/10^6 cells (4.8mM in the cytoplasm)[163]. This concentration is nine times higher than lung epithelial cells.

The vast majority of glutathione is held in the reduced form (GSH) which is regenerated from its oxidised form (GSSG) by the enzyme glutathione reductase, using energy from NADPH oxidation. Due to its high intracellular and extracellular concentrations, it acts as a buffer against ROS and RNS. Glutathione acts as an electron donor in preference to other molecules whose oxidation might have adverse functional effects. It is then recycled to its reduced form by the specific GR enzyme system.

As noted in section 1.2.1.1, the oxidation state of glutathione generally equates with cellular redox state. The proportion of GSH of total glutathione is estimated at 89% in *ex vivo* rabbit AM[163], and over 99% in macrophage cell lines[164]. This is considerably procedure dependent, as *ex-vivo* data from humans suggests figures of around 50% by induced sputum[165], whereas data from this project estimate around 96% by bronchoalveolar lavage (see section 4.3.3.3). Glutathione is more oxidized in lung than other tissue[166], perhaps due to high tissue oxygen concentrations. Certainly, supra-physiological O_2 levels cause oxidative stress in AM in human neonates[167] and upregulation of antioxidant enzymes in adults[168].

1.2.2.1 *Intracellular and extracellular glutathione are related, but separate*

Glutathione is also excreted by AM, lymphocytes and fibroblasts to form a redox buffer in the epithelial lining fluid at 400μM (around 140 fold higher than in plasma) of which 96% is in reduced form[169, 170]. Extracellular glutathione can metabolised by γ-glutamyl transferase (GGT) which is present at low levels in epithelial lining fluid to increase availability of cysteine to the cells[171]. Alveolar macrophages rely on GGT secreted from type 2 epithelial cells in order to maintain a normal redox balance[172, 173]. Using this mechanism, AMs constitute intracellular glutathione from extracellular amino acids either via the rate limiting γ-GCS conjugation of cysteine, or bypassing this step by utilising γ-glutamylcysteine directly[174] (see Figure 1-6, and review by Deneke[169]).

Figure 1-6 Glutathione transport and synthesis pathways

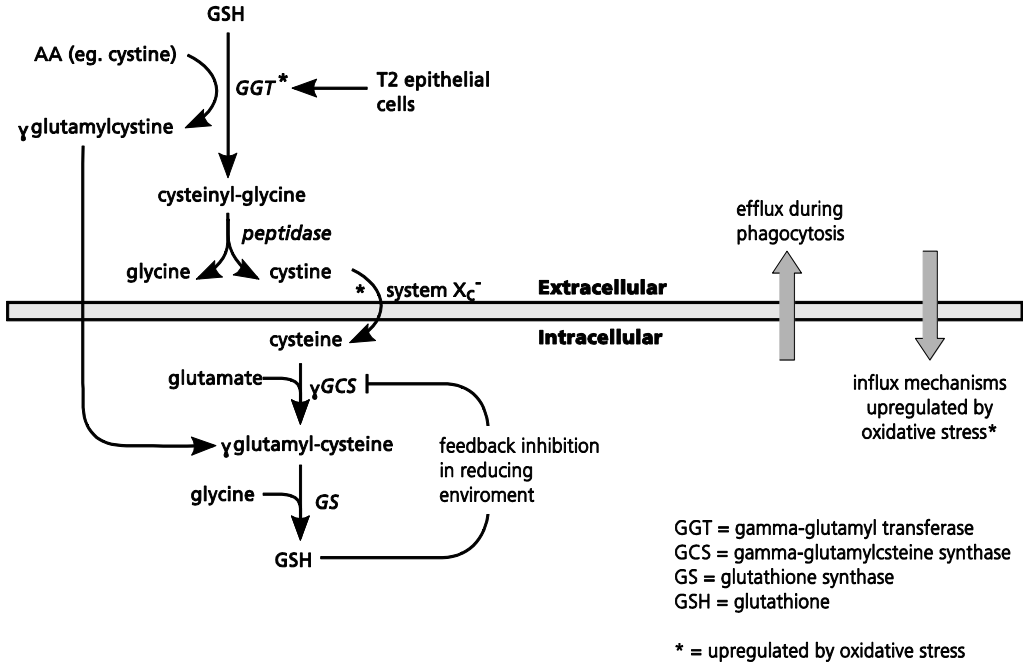

Pathways derived from description by Deneke[169]. During times of oxidative stress, glutathione may be transported into the cell from extracellular fluid

During phagocytosis, there is efflux of glutathione from macrophages, although the reason for this is unclear[175]. In reducing environments, feedback inhibition of γ-GCS

limits GSH production and helps maintain homeostasis[176]. Conversely, oxidative stress in airway epithelial cells induces γ-GCS associated with AP-1 transcription response elements. This allows rapid resolution of intracellular GSH after initial falls[177, 178]. Consistent with this, during oxidative stress, both GGT production and cysteine uptake are induced, thereby providing extra glutathione for the AM[170, 179]. Experimental data in mouse knockout models confirms the physiological importance of these pathways: reduced availability of extracellular GGT causes intracellular GSH depletion and oxidative stress[172, 173] due to decreased cysteine availability[180].

By these mechanisms, some degree of redox homeostasis is achieved.

1.2.2.2 Other extracellular antioxidants

Multiple other non-enzymatic buffers are present in the epithelial lining fluid including surfactant protein[181] and urea[152]. Transferrin prevents hydroxyl ion formation as a result of Fenton reactions by sequestration of iron as intracellular lactoferrin/ferritin[182, 183]. Caeruloplasmin is produced throughout the airway, but inducible mostly in the larger airways[184]; its relevance at physiological concentrations is debatable[185]. Ascorbate is present, and at lower concentrations in cigarette smokers[186], but the degree to which it acts as an antioxidant is variable[187]. As for glutathione, there is potential for transport of ascorbate into the cell during times of oxidative stress[188]. Bilirubin has potential physiological relevance at tissue concentrations of 2% oxygen, but is less effective at the higher levels found at the lung/air interface[189]. Albumin and alpha-1-antitrypsin are also present, but at low levels compared to that required for antioxidant effect[185]. Experiments using synthetic lung epithelial lining fluid suggest that glutathione and ascorbate contribute most to antioxidant effect[190].

1.2.3 Enzymatic antioxidants

1.2.3.1 Superoxide dismutases (SOD)

Superoxide dismutase enzymes are phylogenetically nearly ubiquitous, although these are co-factored by different metal ions depending on cellular location and species. Copper and zinc SOD (CuZnSOD) are cytosolic proteins common to eukaryotes. The manganese co-factored form (MnSOD) is employed by some prokaryotes and nearly all mitochondria[191]. It catalyses the dismutation of superoxide (see Equation 2). Alveolar macrophages predominantly express MnSOD and the extracellular form (EC-SOD). MnSOD is found at concentrations 5 times higher than neutrophils, and 3 times higher than monocytes[192]. Both forms are up-regulated by oxidative stress[193], although the predominant source of EC-SOD is the airway epithelium[194].

1.2.3.2 Glutathione peroxidase and catalase

Two enzyme systems are produced by cells specifically to catalyse the reduction of hydrogen peroxide: glutathione peroxidase (GPx, see Equation 6) and catalase (see Equation 5.

GPx activity is optimal at lower concentrations of substrate than catalase (at 5mM concentrations of glutathione, Michaelis constant* [K_m] =25-60μmol/l for GPx and K_m=1.1mol/l for catalase[195, 196]). This suggests different roles for these two enzymes. Catalase is found in high concentrations in neutrophils which have high endogenous production of H_2O_2[197] in order to provide substrate for

---

* The Michaelis constant is the concentration of substrate at which the rate of enzyme-catalyzed-reaction is half of the maximum rate.
This relates to the model: $E + S \xrightarrow{k_{forward}} ES \xrightarrow{k_{cat}} E + P$
Where: E = enzyme; S = substrate; P = product; $k_{forward}$ and k_{cat} = rate constants for the reactions
The following assumptions are made: 1) ES is at steady state ie. $k_{forward}$ is fast and k_{cat} is rate limiting; 2) the reverse reaction ES →E+S is negligible; 3) substrate is in excess compared with enzyme

myeloperoxidase. Alveolar macrophages, by contrast, have much lower levels of catalase expression, and higher GPx[198]. AM have higher intracellular GPx activity than other lung cell types, predominantly in mitochondria and to a lesser degree the cytoplasm[199]. The lower K_m makes GPx efficient at reducing hydroperoxides even when they occur at low concentrations.

GPx is present in multiple forms resulting from different genes: each has different distribution, structure and avidity, but the main four depend on selenium as a central co-factor[200]. Selenium availability limits GPx function in the AM[201]. Key features of the main four GPx types are given in Table 1-5. Of note, in addition to its effect on H_2O_2, GPx is also an important reducer of peroxynitrite[202] and the only enzyme which is able to reduce harmful lipid peroxides in AMs[203].

GPx-3 is present in the epithelial lining fluid and is excreted by AM and epithelial cells in response to oxidative stress[177]. GPx-3 accounts for over half the alveolar GPx activity[204]. Unlike in the upper airways where lactoperoxidase is the most active peroxidase in ELF[205], GPx is the most important terminal airway defence against H_2O_2[206].

Table 1-5 Glutathione peroxidases – key features

		Location	Electron donor	Substrate and notes
GPX-1 (cGPx)	Tetramer	Cytosol	GSH only	Substrates: H_2O_2, Organic and fatty acid hydroperoxides, but **Not** phospholipid hydroperoxides
GPX-2	Tetramer	Cytosol	GSH only	Substrates: as for GPX-1 Found in GI tract and liver only
GPX-3 (eGPx)	Tetramer	Extracellular Plasma ELF	GSH TrxR, Grx	Substrates: as for GPX-1 Requires GSH>0.5mM, and may require TrxR or Grx for function physiologically[207]
GPX-4	Monomer	Membrane associated	Multiple inc. GSH	Substrates: H_2O_2, Phospholipid hydroperoxides More conserved when Se availability is low[208] Not GSH restricted. May use other thiols[209]

For a full review see Arthur[200, 206, 209]. Other GPx forms exist, but are not relevant to this topic. ELF = epithelial lining fluid in the lung; TrxR = thioredoxin reductase; Grx = glutaredoxin reductase; Se = selenium; GI = gastrointestinal

The high level of GPx in AM has important implications for cell signalling[210], and will be described later.

Equation 5 Catalase action

$$2H_2O_2 \xrightarrow{catalase} H_2O + O_2$$

Equation 6 GPx action

$$H_2O_2 + 2GSH \xrightarrow{glutathione\ peroxidase} 2H_2O + GSSG$$

1.2.3.3 Thioredoxins

In a parallel system to GPx, thioredoxins are also potent reducing enzymes. They are also selenium dependent. Various isoforms are found depending on cellular location; mitochondrial, cytoplasmic and excreted forms exist in mammals. Thioredoxin, once oxidised, is itself reduced by thioredoxin reductase (peroxiredoxin)[211]. These proteins have a significant antioxidant effect and roles in redox signalling as discussed in section 1.2.4.1.

1.2.3.4 Heme oxygenase-1

Heme oxygenase-1 (HO-1) is another enzymatic antioxidant expressed in alveolar macrophages which may be induced by oxidative stress[212]. It is up-regulated by the antioxidant response element (ARE) in response to particulates and other oxidants, leading to catalysis of heme breakdown to elemental iron and bilirubin. Free iron is rapidly stored[213] as ferritin to prevent Fenton reactions, while bilirubin may act as an antioxidant, and HO-1 also alters iron efflux from cells[214].

1.2.3.5 Exogenous effects on redox balance in the lung

Exogenous oxidants are commonly encountered by the alveolar macrophage, and have been extensively investigated *ex-vivo* and in the context of cell line studies. Particulates including $PM_{2.5}$, wood smoke and concentrated ambient particles (CAP) are consistently shown to cause oxidative stress in alveolar macrophages *in vitro* and ex-vivo (see Table 1-2). Response to this oxidative stress, is different in granulocytes, monocytes and alveolar macrophages. The degree of inflammation and generation of ROS in the macrophage depends on particle type[74], is inversely related to particle size[75, 76], and is compounded by the adsorbed transition metals[77]. Finer particles are more potent in generating ROS, and inducing protective responses (particularly HO-1) in macrophages and epithelial cells[215]. However, as noted previously, coarse particles may induce ROS through inflammatory pathways where they are associated with adsorbed endotoxin. This is particularly true for concentrated ambient particles[94, 100, 216]. AMs are relatively less sensitive to cytotoxic effects of oxidative stress than epithelium, perhaps in part due to differences in the metabolism of glutathione precursors, or to the relative concentration of antioxidant enzymes[164]. However, AM are susceptible to upregulation of NADPH oxidase subunit $p47^{phox}$ by aryl hydrocarbons which increases oxidative stress[78].

Increasing antioxidant availability may reduce oxidative stress resultant from particulate exposure. N-acetylcysteine and catalase supplementation reduces ambient particle induced inflammatory signalling in the alveolar macrophage[84]. Increasing extracellular superoxide dismutase has a similar effect: levels of glutathione oxidation are lower in cells exposed to products of oil combustion when they over-express the enzyme[217].

Redox balance also mediates the response to bacterial peptides. Endotoxins (such as LPS), which are associated with respiratory infection[218] also potentiate inflammation[82]. Superoxide dismutase supplementation offsets this NF-κB mediated inflammatory response[219] .

To investigate more physiological exposures, *in vivo* studies of humans and animals have been performed, and effects on glutathione measured. These are summarised in Table 1-6. This table excludes occupational particulate and cigarette smoke exposure which have been extensively reviewed. Table 1-6 shows for a broad range of inhalable particulates oxidants that glutathione is depleted in the acute exposure (hours afterwards), before synthetic enzyme function is up-regulated. After this (usually 24 hours), glutathione concentrations in the lung, ELF or AM tend to be higher than baseline levels.

Other studies have examined these stressors for the effects of that oxidative stress *i.e.* changes to antioxidant concentration or activity (see Table 1-7 for a summary). There are no direct studies of *in vivo* exposure to wood smoke. In general, any particulate causes an immediate fall in antioxidant enzyme function, and this is noted to last after 2 weeks for CAP, DEP and NO_2 exposures. Acutely, mRNA for antioxidant enzymes is reduced, but no data are available for more chronic exposures.

Table 1-6 Glutathione and acute toxicity

Reference	Model*	Condition	Measured	Effect	Notes
Concentrated ambient particles (CAP)					
Li[220]	Rat (BAL)	PM_{10} (*in vivo*, intratracheal, 50-125µg)	Total glutathione GSSG:GSH	↓ ↑	At 6h Associated TNFα
Pradhan[221]	Rat (BAL)	$PM_{2.5}$ urban CAP (*in vivo*, 15d, intratracheal 2.5-10mg)	Total glutathione	→	Lipid peroxides ↑
Schins[216]	Rat (BAL)	$PM_{2.5}$ and PM_{10} CAP (*in vivo*, intratracheal)	Total glutathione	↓	At 18h
Residual oil fly ash (ROFA)					
Ghio[217]	Mouse (BAL)	ROFA (*in vivo*, intratracheal 50µg)	Total glutathione GSSG:GSH	↑ ↓	At 24 hours Glutathione, TNFα, MIP-2 increases were ↓ in extracellular SOD overexpressing mice
Norwood[222]	Guinea pig (BAL)	ROFA (*in vivo*, 19-25mg/m^3 for 2h)	Total glutathione	↑	At 24 hours. GSH depletion caused ↑ LDH and ↑ inflammatory influx
Kerosene and diesel combustion particulates (DEP)					
Al-Humadi[223]	Rat (BAL)	DEP (*in vivo*, intratracheal, 5mg/kg)	Total glutathione	↑	Peak at 24h. Augmented with increased cysteine availability. *cf*: Lymphocytes which showed ↓ GSH. DEP does absorb some GSH.
Arif[224]	Rat (BAL)	Kerosene soot (*in vivo*, intratracheal, 5mg)	Total glutathione	↓	Progressively from day 1-16 Associated ↑MDA.

Reference	Model*	Condition	Measured	Effect	Notes
Behndi[120]	Human (BAL)	DEP (*in vivo*, 100µg/m^3 for 2h)	Total glutathione	↑	At 18 hours
			Urate	↑	Inflammatory mediators ↑ (IL-8 and neutrophil influx)
Ultrafine carbon					
Li[109]	Rat (BAL + lung)	Ultrafine carbon (intratracheal, 125µg)	Total glutathione in BAL + lung	↓	At 6 hours
				↑	At 24 hours. Associated with ↑ LDH and TNFα
Wilson[225]	Rat (BAL)	Ultrafine carbon (*in vivo*, intratracheal, 125µg))	Total glutathione	↓	Mirrored ↑ ROS, but unlike ROS did not depend on transition metals at low concentrations
Zhong[226]	Rat (BAL)	Ultrafine iron and soot (*in vivo*, 100µg/m^3 iron + 100µg/m^3 soot for 6h/day for 3days)	GSSG: GSH	↑	Inflammatory mediators ↑ (IL-1β)
Zhou[227]	Rat (BAL)	Ultrafine soot + iron particles (57-90µg/m^3 for 6h/day for 3 days)	Total glutathione	→	BAL and lung tissue showed same results
			GSSG	↑	Changes mirrored in pro-inflammatory cytokines (TNF, IL-1β)
Wood smoke					
Seagrave[112]	Rat (AM)	Hard wood smoke (*in vivo*, (1mg/m^3, 6h/day, 6mo)	Total glutathione	↑	Lower dose show large ↑ total GSH
			GSSG	↓	Higher doses show minimal increase
Sehlstedt[228]	Human (BAL)	Wood smoke (*in vivo*, $PM_{2.5}$, mean 224µg/m^3)	Total glutathione	↑	At 24 hours, but no inflammatory change

** Model details the subject with target compartment in parentheses*
Search terms in PubMed: (particulate OR smoke OR wood[Title]) AND bronchoalveolar lavage AND glutathione

Table 1-7 *Enzymatic antioxidants and acute toxicity*

Paper	Model	Condition	Measured	Effect	Notes
Concentrated ambient particles (CAP)					
Pradhan[221]	Rat (BAL)	$PM_{2.5}$ urban CAP (*in vivo*, 15d, intratracheal 2.5-10mg)	SOD activity CAT activity	↓ ↓	At 15 days ↑ in RNS formed
Rhoden[229]	Rat (Lung)	CAP (*in vivo*, intratracheal SRM1649, 10mg/kg)	Lung chemi-luminescence	↑	At 4 hours Pre-administration of SOD analogue (MnTBAP) normalised this
Rouse[230]	Mouse (BAL)	Butadiene soot (*in vivo*, 5mg/m^3 4h/day, 4days)	Microarray data	See notes	At 4 days ↑ oxidative stress related genes: GCLC; GPX2; HMOX1; NFE2L2; TXNRD1 ↑ inflammatory and aryl hydrocarbon receptor responsive genes including CYP1A1
Van Winkle[231]	Rat (dissected lower airways))	Flame soot mean particle size 192nm (170µg/m^3 for 6 hours)	GCL protein GSTµ mRNA CAT mRNA GPx-1 mRNA	↑ → ↓ ↓	At 24 hours Reduction in RT-PCR microarray based measurement of many antioxidant genes including: peroxiredoxin, GPx (multiple forms), catalase. mRNA and immunohistochemistry showed discrepancy – upregulation of GPx and Cat proteins was apparent
Residual oil fly ash (ROFA) / soot					
Wallenborn[232]	Rat (Lung)	ROFA (*in vivo*, intratracheal, 8.3mg/mL/kg)	SOD activity Ferritin protein	↓ →	At 24 hours
Kerosene and diesel combustion particulates (DEP)					

Paper	Model	Condition	Measured	Effect	Notes
Arif[224]	Rat (BAL)	Kerosene soot (*in vivo*, intratracheal, 5mg)	GPx activity GR activity	↓ ↓	Most abnormality noted on day 1, with subsequent recovery towards normal (for GPx) and supranormal (for GR) by day 16
Sagai[233]	Mouse (Lung)	DEP (*in vivo*, intratracheal, 0.4mg)	GPx + SOD activity GST activity GR activity	↓ ↓ →	At 24 hours
Sunil[234]	Mouse (BAL)	DEP (*in vivo*, 1mg/m^3 for 3h/day for 3 days)	MnSOD protein	↓	At 24 hours Immunohistochemical assessment: reduction in MnSOD following exposure in young mice. No change in older mice (who had undetectable baseline)
Rengasamy[235]	Rat (Lung)	DEP (*in vivo*, intratracheal, 35mg/kg)	CYP1A1 activity CAT activity	↑ ↓	At 24 hours, normalised by 7 days At 24 hours and 7 days
Nitrogen dioxide					
Olker[236]	Rat (AM)	NO_2 (*in vivo*, 10ppm for 20 days)	GPx1 mRNA GPx3 mRNA CuZnSOD mRNA GPx + SOD activity	→ ↑ ↑ ↑	Chemoluminescence following zymosan stimulation decreased in time dependent manner 1, 3 and 20 days GPX and SOD activity increased at 20 days, but not before
Van Bree[237]	Rat (AM)	NO_2 (*in vivo*, 10.6ppm for 4 days)	GPx activity GR activity	↑ ↑	At 4 days

** Model names the animal or cell line, and details the compartment measured in parentheses Search terms in PubMed: (particulate OR smoke OR wood[Title]) AND bronchoalveolar lavage AND (superoxide dismutase OR glutathione peroxidase OR catalase). Abbreviations: CAT = catalase; GCL = glutamate cysteine ligase; GPx = glutathione peroxidase; GR = glutathione reductase; GSTμ = glutathione-S-transferase mu isoform; SOD = superoxide dismutase*

1.2.3.6 Particulate related oxidative stress – feedback mechanisms in AMs

Acute particulate exposure cause macrophages to generate ROS and inflammatory mediators including TNFα and IL-6, IL-8, MCP-1[238] which have potential to cause tissue oedema and architectural changes in the lung. Acute toxicity to the alveolar macrophage leads to apoptosis and can diminish the population of these cells leading to impaired immunity (see Table 1-2). Oxidative stress caused by these particulates also causes DNA adduct formation[110] with potential for cellular harm.

In the AM of healthy people, such adverse effects of exogenous oxidative stress are prevented by a number of mechanisms:

1) **Inherent hypo-responsiveness**. Multiple stimuli are required for ROS to cause an inflammatory response. For example. in the alveolar macrophage, activation of NADPH oxidase and ROS generated by ROFA particles are not sufficient to induce NF-κB or inflammatory cytokines[100, 239]. However, mechanistic studies show that higher level source of ROS (H_2O_2) can stimulate NF-κB signalling[240] and TNFα production[241]. Downstream of this, alveolar macrophages have weaker TNFα responses than monocytes which relates to lower p38 MAP kinase activation by oxidants[210]
2) **Decoupling of NADPH oxidase activity and ROS signalling**. For example, hydrogen peroxide produced from the respiratory burst does not cause ERK protein kinase signalling even though H_2O_2 at the same concentration when produced from alternative (zymosan) activation can propagate inflammatory signalling[242].
3) **Specificity of response to phagocytosed particles**. Unopsonised particle ingestion in AM is mediated by scavenger receptors and is associated with reduced oxidative burst by comparison to Fc dependent phagocytosis of opsonised particles, presumably to limit the generation of ROS caused by inert material[243, 244].
4) **Sequestration of iron during inflammatory response**. Iron loading of lysosomes due to environmental exposure can exacerbate oxidative stress. In

these circumstances, TNFα enhances lysosomal iron storage by upregulation of heavy chain ferritin, and reduces free cellular iron[245].

5) **Antioxidant upregulation**. Compensatory increases in antioxidants occur *in vivo* as a result of chronic cigarette smoke exposure[246]. Presumably this also occurs in other particulate exposure[247] although data are few. Human responses to *in vivo* wood smoke include upregulation of glutathione in the epithelial lining fluid[228]. Nrf2 has a central role in up-regulating antioxidant responses to DEP[115] and cigarette smoke[248].
   Nrf2 can also dampen chronic inflammation in macrophages by its negative effect on NF-κB[249]. The transcription factor AP-1 is also implicated, particularly for GPx upregulation[206]

   HO-1 (an enzyme regulated by Nrf2) is up-regulated in smokers, and provides protection against inhaled oxidants[212]. GPx prevents AM death by inhibiting apoptosis through the caspase 3 pathway and by maintaining Bcl-2 levels[250]. Additionally, GPx reduces NF-κB activity by reducing phosphorylation of its inhibitor (IκB)[250, 251]. It is likely that this explains the beneficial dampening effect of pulmonary inflammation in response to cigarette smoke[252]. *Ex vivo*, antioxidant treatment with glutathione donors attenuates the inflammatory cytokine response of AM to wood dust[253]. Similarly, AM from mice overexpressing EC-SOD or from knockout NADPH oxidase strains have dampened inflammatory response to inhaled smoke[254]. Where particulates have induced inflammation by another pathway (such as arachidonic acid metabolic pathways[76], calcium signalling[255, 256], transition metal or endotoxin[257]), antioxidants reduce the magnitude of response[258]. Lastly, circumstantial data suggest that antioxidant GPx and SOD have an inhibitory effect on NADPH oxidase activity: in animal neonate models, levels of GPx and SOD are high and associated with reduced AM respiratory burst capacity[259]. The corollary is that while antioxidant upregulation is necessary to protect the host, it may indirectly have negative effects *e.g.* on bactericidal activity or inflammatory response in early infection.

1.2.4 Redox signalling in the alveolar macrophage

From previous sections, maintaining redox balance in the alveolar macrophage by antioxidant regulation might be understood to be a necessary defence against endogenous and exogenous oxidative stressors. While this is no doubt true, recent observations have suggested a finer role for ROS: signalling of cellular behaviour. This section reviews mechanisms by which the redox state of the cell might alter its function, and mediate inflammatory and other signals.

1.2.4.1 Signalling aspects of glutathione

Glutathione may be seen to be a passive buffer against alterations in the cellular redox state, but it also plays a role in adapting cell behaviour to cope with future oxidative stress. Its oxidation state can determine cellular behaviour: cellular proliferation is favoured by GSH while GSSG promotes cellular differentiation and apoptosis[148, 260]. This is redox signalling, and the same processes may mediate inflammatory response. A key mechanism for this is the conjugation of glutathione with intracellular proteins[261].

Glutathionylation protects proteins and alters signalling pathways

With increasing concentration or production of ROS/RNS a number of changes to intracellular proteins can occur[149], notably reversible conjugation with glutathione (S-glutathiolation) – see Figure 1-7. This has two potential functions; firstly, protecting proteins against irreversible structural changes in times of increased ROS production: S-glutathiolation occurs early in the respiratory burst (up to 20 minutes) [262]. Secondly, post-translational conjugation with glutathione effects a temporary change in protein function, including those involved in signalling. These are not fully elucidated, but known to include: reduced activation of caspase-3; reduced polymerization of actin; reduced binding of transcription factors NF-κB and AP-1 (by altering binding of the p50[263] and cJun[264] subunits respectively). However, some

protein functions are increased: increased chaperone activity of heat shock protein hsp70[265]; increased sarcoplasmic or endoplasmic-reticulum Ca^{2+}-ATPase (SARCA) activity[266]. Recently, it has been reported that epithelial antibacterial peptide beta-defensin 1 is only active in its reduced state, and that redox balance therefore has a direct effect on the capacity of innate immune responses[267].

The redox balance in the lung certainly determines the cytokine response of alveolar macrophages. An increase in total intracellular glutathione reduces NF-κB activation[268], and hydrogen peroxide activates IKK[269] (an upstream regulator NF-κB). However, oxidative glutathionylation of the IKKβ subunit results in reduction of NF-κB activity[38] presumably to prevent irreversible inhibition. After such insults, glutaredoxin is critical in restoring an adequate inflammatory response in alveolar macrophages[270, 271]. These processes have been recently reviewed[272 273]. Similar pathways are modulated downstream by redox dependant NF-κB binding to DNA[274, 275]. AP-1 transcription factor complex activity[276] and the mitogen-activated protein kinase (MAPK) and ERK1 cascades may also be affected. However, alveolar macrophages are deficient in AP-1 binding activity compared with monocytes[277].

Thioredoxins also reduce oxidised proteins, though in a less specific manner. They also decrease DNA binding of NF-κB, but increase that of AP-1[278]. Specifically both cJun-terminal kinases and the $p38^{MAPK}$ have a common upstream mediator, apoptosis-signal regulating kinase-1, which is released from its thioredoxin inhibitor by the action of ROS, thereby causing activation of the pathway[150, 279]. In AMs, via this pathway, respiratory burst may cause activation of inflammatory JNK-1/c-Jun pathway[280]. The relationship between thioredoxins and the glutathione system have been recently reviewed[281].

Figure 1-7 Interactions of proteins and the glutathione / glutaredoxin / thioredoxin systems

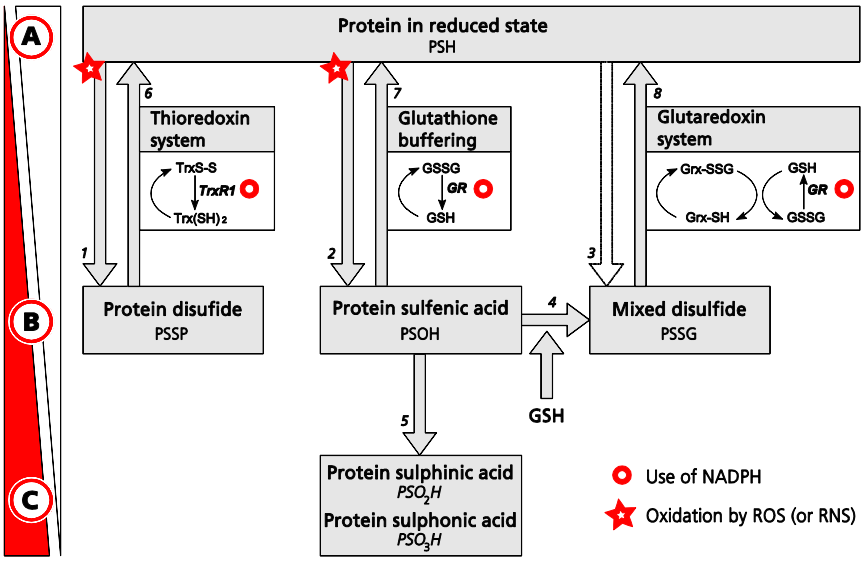

	Notes
A	Normal redox state: Proteins have SH groups intact
B	Oxidative stress adequately buffered by cellular antioxidants: Reversible changes to proteins leads to temporarily altered protein function. This may result in cellular redox signalling, and protects proteins from further oxidation.
C	Oxidative capacity exceeds cellular antioxidant supply: Irreversible changes to proteins leads to loss of function
1	Formation of disulfide bonds within or between proteins alters them structurally with resulting change in biologic activity[282].
2	Oxidation of the thiol group (-SH) to an unstable intermediate state (-SOH), which can in turn lead to: Further oxidation results in permanent detrimental alteration to the protein (reaction 5); Reversal of the oxidation by GSH with restoration of normal function (reaction 7); Conjugation with GSH to form a 'mixed disulfide' (reaction 4)
3	In theory, the formation of a mixed disulfide is possible by reaction with GSSG directly. However, for most conjugations this would require an unphysiologic derangement of the GSH:GSSG ratio (c-Jun being an exception[264]). In practice, mixed disulfides are likely to be formed via reactions 2 & 4.
6	The thioredoxin system has broad specificity to reduce disulfide bonds within proteins.
7	Glutathione, due to high concentrations, buffers proteins against oxidation.
8	Glutaredoxin assists the reversal of S-glutathiolation and is very substrate specific compared to the thioredoxin system[283]. It is highly expressed in AM[284].

Nrf2 and redox signalling

Nrf2 is another important regulator. It is a basic leucine zipper protein which recognises the antioxidant response element (ARE). Its binding to DNA up-regulates transcription of ARE associated genes, especially cytoprotective proteins and antioxidant enzymes. It is implicated in many disease processes including COPD. Nrf2 has a cytoplasmic half-life or around 20 minutes; it is usually bound to the Keap1 dimer which allows ubiquitination by ubiquitin E3 ligase and rapid proteasomal degradation[285]. Keap1 contains cysteine residues which when oxidised reduce the E3 ligase activity, and hence increase Nrf2 levels and nuclear translocation[286]. Phosphorylation of Nrf2 by the protein kinase C signalling pathway, and possibly others, also lends it stability[287].

Nrf2 binds to promoter elements of target genes leading to their transcription. Such targets include: Nrf2 itself[288]; glutathione; enzymes for GSH production (GCLM, GCLC)[289]; GSH recycling enzymes (GR)[260]; the regulator of GSH influx (cysteine/glutamate exchange transporter)[290]; enzymes using GSH as cofactor for reducing other oxidants and electrophiles (GPx[288, 291], GST[288]); other enzymatic antioxidants (SOD, catalase, HO-1); components of the parallel thioredoxin system (peroxiredoxin, thioredoxin, thioredoxin reductase).[292, 293]

Knockout studies have demonstrated the absence of Nrf-2 results in pneumotoxicity of hyperbaric oxygen[294], emphysema[295] and increased oxidation of glutathione in response to LPS[296]. Where oxidative stress leads to moderate glutathione depletion, Nrf2 effects allows macrophages to avoid apoptosis[260, 297]. Nrf2 upregulation improves bacterial phagocytosis, in association with increased expression of scavenger receptors[298].

Within cells, crosstalk between Nrf2 and NF-κB pathways exists to moderate inflammation; in the absence of Nrf2, NF-κB activation is enhanced during lipopolysaccharide challenge, and is associated with increased mortality in septic shock[296]. It seems likely that Nrf2 plays a role in limiting NF-κB activation in response to such inflammatory stimuli. Conversely, some of the effects of Nrf2 may be mediated by the AP-1 / NF-κB pathways, including transcription of glutathione related GCL[299], and initial stimulation of Nrf2 by oxidants in the lung is followed by a restorative response involving MAP and JNK kinases[300]. Such Nrf2 responses may therefore by short lived. Paracrine effects are also important in modulating the cytokine response to oxidative stress[301].

Pro-inflammatory signalling is dampened by antioxidants. Pre-treatment of mice with glutathione or its components (such as N-acetylcysteine) reduces *in vivo* TNFα production to lipopolysaccharide[302, 303]. Similarly, ex-vivo human AMs have an enhanced inflammatory cytokine profile when glutathione availability is reduced, which is normalised with NAC supplementation[304]. Moreover, oxidants may also antagonise the suppression of pro-inflammatory cytokines pathways by TGF-β by inducing $p38^{MAPK}$ activation[305].

Membrane lipids also contribute to redox signalling

Lipids are most potently affected by peroxidation which may, usually after initiation by hydroxyl ions, a reaction which can be propagated down a chain of adjacent lipid molecules. Oxidation of phospholipids within lipid rafts is common[306], and seen systemically in humans in chronic exposure to smoke from domestic fuel or cigarettes[307]. Lipid peroxidation in AM reduces sensing of the external environment through TLR-2, TLR-4[308]. Once inflammation is established, however, oxidation of phosphatidylserine in other cells' membranes facilitates their efferocytosis by macrophages[309].

ROS/RNS effects on DNA

Changes to DNA are well documented after alveolar macrophage exposure to extrinsic particles[310], potentially resulting in altered signalling, cell death and mutagenesis. These are widely thought to be pathological phenomena, and multiple mechanisms for repair of such damage exist, although these themselves may also be impaired by PM[311].

1.3 Effect of redox signalling on bacterial infection

The following section examines the overlap between redox signalling, and innate immunity in the context of bacterial infection. Finally, therapeutic implications and limitations are discussed.

1.3.1 Early or controlled infection

In early pneumococcal infection, NF-κB signalling is important in generating sufficient cytokine response[312]. Alveolar macrophages subjected to oxidative stress (those from smokers, with high levels of glutathione) have less nuclear NF-κB binding[313], and may be less sensitive to bacterial signals. Where acute upregulation of antioxidants is expected, due to environmental tobacco smoke, some pathogens (e.g. *Mycoplasma pneumoniae*) interfere with this mechanism which may partly explain their association with chest infections in smokers[314]. Chronic derangement of the redox balance of rat AM may reduce antibacterial capacity, which can be normalised by supplementation of glutathione pre-cursors[315]. In chronic oxidative stress, such as human COPD, AM responses to pneumonia are less inflammatory than non-COPD controls[316], and associated with reduced phagocytosis. The situation is complicated, however: using AM from COPD patients, increasing *antioxidant* signalling through the Nrf2 pathway pharmacologically (using sulphorafane) leads to improved bacterial clearance by macrophages[317], perhaps by upregulation of

pattern recognition receptors. It seems that both inflammatory and anti-inflammatory pathways can be blunted by oxidative stress.

Epithelial responses are also altered. For example, bacterial binding to respiratory epithelium is increased by particulate matter generated oxidative stress[318], and this may increase the chances of invasive disease.

1.3.2 Established pneumonia

Macrophage responses to overwhelming infection are characterised by ROS generation for bacterial killing and neutrophil recruitment which further exacerbate oxidative stress. Myeloperoxidase (a potent producer of ROS) from neutrophils exacerbates inflammatory recruitment. Cytokine release is also increased, perhaps due to a bystander effect on other cell types[319]. Changes in local environmental oxygen tension (hypoxia) can exacerbate inflammatory responses[320].

As a result, acute pneumonia in children is associated with whole body depletion of antioxidants measured in the serum (retinol, ascorbate, α-tocopherol, GSH), and decreasing levels of enzymatic antioxidants (GPx, SOD), and markers of molecular oxidative damage (MDA)[321-323]. Similar patterns of GSH and antioxidant depletion are noted in TB[324, 325]. Ventilator associated pneumonia is associated with lower GPx activity in BAL and increased lipid peroxidation, which is mirrored in the circulation[326].

Usually, antioxidant (Nrf2) pathways limit ROS production in phagocytes in response to bacterial peptides such as LPS[327] (see Figure 1-3); defective antioxidant upregulation is associated with lower survival from sepsis[296]. Indeed, ROS may be less important than previously thought in bacterial killing: $gp91^{phox}$ knockout mice improve killing responses, maintain higher pulmonary neutrophil numbers with lower apoptosis rates and stronger pro-inflammatory signalling[62].

Despite considerable evidence of antioxidant depletion in uncomplicated pneumonia, supplementation trials in humans are lacking. In mouse influenza pneumonia, inhaled catalase improves mortality and histopathological appearance[328]. Efferocytosis seems to require some oxidation of the target cell phosphatidylserine[329] by endogenous NADPH[330]. Exogenous oxidants, however, cause a defect in efferocytosis[331] and antioxidant treatment with NAC improves such cell clearance[332]. Quality evidence of antioxidant therapy in pneumonia is lacking, either at during the acute inflammatory stage or during resolution. Further clinical trials would therefore have a sound theoretical basis.

1.3.3 Antioxidants as prevention of pneumonia

Evidence of efficacy of clinical interventions through antioxidant supplementation is not strong. Although the use of zinc in children does prevent pneumonia[333], there is minimal robust evidence of effect of other supplements (for example Vitamin A outside of its use in measles)[334, 335]. Vitamin D supplementation does not work where deficiency is common[336]. In adults, less is known, but Vitamin E does not prevent community acquired pneumonia[337], and may have unintended risks, particularly of tuberculosis[338].

1.3.4 Redox balance in wider and systemic inflammatory syndromes

Where local control mechanisms fail, oxidative stress and inflammatory responses in the lung may lead to excessive tissue injury, as in Acute Respiratory Distress Syndrome (ARDS). Uncontrolled NF-κB activation leads to overproduction of cytokines. AM release mediators due to pulmonary stimuli (hypoxia and particulate exposure) which have systemic inflammatory effects, including MCP-1[339, 340] Oxidised phospholipids activating the TLR-4 pathway increase these inflammatory cytokines. This is associated with increased pulmonary oxidative stress in humans

with ARDS[341], and increased mortality in models of influenza infection and other acute lung infection[342].

Treating such patients with acute lung injury with antioxidants is an attractive option in order to reduce inflammatory response. However, trials with N-acetylcysteine have tended no show no mortality reduction, except in specific GST genotypes[343], but may shorten the duration of disease. Prevention of pneumonia with antioxidants in patients at high risk, has been trialled with varying results. Additional ascorbate and α-tocopherol did not reduce pneumonia incidence in critically unwell trauma patients, but did reduce that of subsequent ARDS[344]. Amongst burns patients, supplementation of high dose trace metals (Cu, Se, Zn) does reduce nosocomial pneumonia[345]. A lack of effect in many supplementation trials might represent late treatment in the evolution of disease. However, the lack of prevention effect suggests that straightforward antioxidant supplementation might not be an effective strategy.

1.4 Summary

Redox state in the lung, and more specifically in the alveolar macrophage is of major importance to proper homeostasis. Due to the high levels of endogenous oxidative processes in the macrophage, and exogenous oxidants in inhaled air, considerable resources are expended in maintaining antioxidant defences. These are responsive to changes in the redox state, and can be up-regulated as required.

Changes in the redox state, either acutely due to oxidative stress, or chronically as a result of up-regulated antioxidants, might have important effects on redox signalling. This collection of processes uses, at its core, glutathione and other redox sensitive thiols to sense changes in the environment, and to effect a response by alterations to cellular signals. By these pathways, which include NF-κB, AP-1 and Nrf2 transcription factors, and protein kinase cascades, inflammation and redox balance are tightly knitted.

Redox balance has the capacity to alter host immune responses, and is integral to the effective containment and disposal of infective and non-infective substances in the lung. Where high levels of particulates are encountered chronically, up-regulated antioxidant systems are likely to change the finely controlled balance between inflammatory and restorative responses. It is possible that the host response to oxidative stress, whilst immediately helpful to the host, is ultimately damaging to the innate immune responses.

This project focusses on redox balance and AM dysfunction in the context of the most widespread and overlooked form of particulate exposure in humans: household air pollution from the combustion of biomass fuels. Epidemiological evidence strongly associates such use with morbidity from chronic respiratory disease, and mortality from pneumonia. Work presented here aims to clarify the

extent to which redox balance impacts on innate immunity in the Malawian population: people to whom high particulate exposure in their own homes is a normal part of life.

Overall hypotheses

We have addressed three overarching hypotheses within this project.

1. Particulate exposure is associated with altered redox balance in the lung in both intracellular and extracellular compartments
2. Redox balance in the alveolar macrophage alters innate immune function
3. Particulate exposure is detrimental to alveolar macrophage function

2 Methods

This chapter includes all methodologies used in the project which generated the finalised data reported in subsequent results chapters. A number of methods were initially tested for fitness, and were unworkable in the context of this project. These are included in section 3, together with details of optimisation experiments for those methods which have been used.

2.1 Ethics

Ethical approval for the studies were granted as follows:

Table 2-1 Ethics committee approval for the project in the UK and in Malawi

Study	**Ethics body**	**Approval number**	**Date granted**
Antioxidant defence in the lung (UK)	Cheshire Research Ethics Committee (NHS)	09/H1017/82	14/07/2009
The role of redox balance in pulmonary innate immune responses (Malawi)	Liverpool School of Tropical Medicine, UK	09.69	14/01/2010 amended 19/05/2011
The role of redox balance in pulmonary innate immune responses (Malawi)	Malawi College of Medicine Research Ethics Committee (COMREC)	P.03/10/916	17/06/2010
The role of redox balance in pulmonary innate immune responses – phase 2 (Malawi)	Malawi College of Medicine Research Ethics Committee (COMREC)	P.03/11/1063	06/05/2011

2.2 Study participants

2.2.1 Liverpool, UK

Adult volunteers for bronchoalveolar lavage were recruited according to the ethics protocols listed above. This included advertising in the local university and hospital. Consent was performed in two stages: firstly, a preliminary meeting with a member of the study team in order to disseminate information both written and oral, and to provide opportunity for early exclusion of those individuals not meeting inclusion criteria; secondly, written informed consent in the presence of a different member of the study team with full medical examination in order to determine fitness for the study procedures.

All volunteers were healthy adults aged 18 to 50, who had no significant pre-existing chronic health problems. Exclusion criteria were pregnancy, recent (within six months) pulmonary infection, previous tuberculosis. Two cohorts were recruited: non-smokers who had not smoked any tobacco or marijuana in the last six months; smokers who admitted a regular smoking habits of 10 cigarettes per day or more.

2.2.2 Blantyre, Malawi

Volunteers were recruited by word-of-mouth, and relied on a formal community structures whereby village leaders (Chairmen) were asked to disseminate invitations to volunteer for the study. Thereafter all information and consent was taken in the hospital setting (Queen Elizabeth Central Hospital Blantyre). Consent procedures were identical to those used in the UK except that the local language (Chichewa) was used for both dissemination of information and consent.

2.2.3 Exclusion criteria and justification

Exclusion criteria were designed to minimise variability within the volunteers due to pathological processes and aging, and for reasons of safety relating to bronchoscopy. Exclusion criteria were:

- Pregnancy or lactation
- HIV infection (due to the potentially overwhelming confounding effect on results)
- Based on clinical history and examination findings, the presence of an underlying health problem which would potentially increase the risk associated with bronchoscopy, specifically:
    - Chronic lung disease, including COPD, recurrent chest infections,
    - Chronic heart disease, including heart failure and valvular heart disease
    - Previous maxillofacial surgery
    - Previous reactions to medications used during the procedure (benzodiazepines)
- Chest radiograph showing evidence of chronic or active lung or heart disease
- Use of prescribed medications excluding oral contraceptives (due to the potential for difficulty in interpreting results
- Use of antibiotics in the preceding 4 weeks
- FEV1 <75% predicted (on screening breathing tests)
- Potential for communication difficulties during bronchoscopy (due to language, hearing or understanding)
- Inability to give informed consent

2.3 Blood collection

Blood was drawn from the antecubital fossa using a Vacutainer system (BD Medical, UK). Skin was prepared with 75% isopropyl alcohol, and clean technique and universal precautions were used. Specific tubes were collected according to the sample required: serum into clot activator (SST tubes, BD); selenium, copper and zinc into trace elements tubes (BD); plasma and anti-coagulated blood into potassium (K2) EDTA tubes (BD). Samples for lipid peroxide measurement were stored on ice until used to prevent degradation. For preparation of peripherally derived mononuclear cells, blood was taken into a 50mL syringe, and immediately mixed with potassium EDTA to a final concentration of 1.8mg/mL of blood before being stored on ice for transport to the laboratory.

2.4 Urine collection

Urine was collected from volunteers on the day of bronchoscopy into a universal container, and kept on ice until laboratory preparation. Cellular debris was removed by centrifugation at 500g for 5minutes before storage in aliquots at -80°C. Urinary concentrations were subject to standardisation according to the formula given by Heavner[346]. This assumes that for a spot-test, the ratio of urinary analyte to total solute concentration remains constant even where urinary flow fluctuates. This formula is validated where paired serum and urinary creatinine values are not available, and where more specific details of the urinary excretion kinetics are unknown (*Equation 7*)

Equation 7:
$$[Analyte]_{corrected} = [Analyte] \,.\left(\frac{1.020 - 1}{specific\ gravity - 1}\right)$$

Urinary specific gravity was measured using a manual refractometer with automatic temperature compensation (Zhangzhou Sino Science & Technology Co., Ltd, China. Cat#RHC-200ATC) calibrated to a blank of distilled water.

2.5 Bronchoalveolar lavage

Primary human alveolar macrophages behave differently than other human cellular models (see section 4.3.1), and discrepancies with animal studies are common. This project aimed to study innate immunity in context of "natural" exposure in human populations, and this justifies the use of human alveolar macrophages. Previous research studies have found bronchoalveolar lavage (BAL) to be well tolerated and safe; the protocol detailed below is a development of those used by these projects[347-350]

Standard operating procedures for bronchoscopy were the same in both UK and Malawi sites, and consistent with guidelines issued from the British Thoracic Society[351]. Preparatory measurements of blood pressure, heart rate, pulse oximetry and respiratory rate were taken. The mucosal surface of the nasopharynx was anaesthetised with topical lignocaine gel (CliniMed Limited, UK), and with lignocaine spray to the oropharynx (Xylocain 10%, AstraZeneca, UK). Sedation of the volunteer was rarely performed, and only used in the UK. In these cases, intravenous midazolam was administered according to response with the aim of reaching a relaxed but coherent state in the volunteer. Further topical anaesthesia at the level of vocal cords was achieved with 4% lignocaine, and 2% lignocaine was used in the larger airways. The maximum dose used was 8.2 mg per kilogram. Bronchoalveolar lavage was performed by advancing the bronchoscope to a sub-segmental bronchus of the right middle lobe in order to achieve a seal. Warmed sterile normal saline was instilled in four aliquots to a total volume of 200mL. Lavage fluid was withdrawn by gentle suction after each aliquot, and stored on melting ice until laboratory preparation.

Supplemental oxygen was not routinely used, but was given in cases where pulse oximetry indicated saturations of less than 92% during the procedure. All volunteers were reviewed before discharge for immediate complications, and returned within 72 hours for further review and clinical examination.

2.6 Total and oxidised glutathione

2.6.1 Principle

Total glutathione was measured using the assay developed by Anderson[352] and Tietze[353] which is based on the reaction of glutathione with 5,5'-dithiobis-(2-nitrobenzoic acid) (DTNB). Reduced glutathione (GSH) is oxidised by DTNB to give oxidised glutathione (GSSG) with formation of 5-thio-2-nitrobenzoic acid:

Equation 8: $$2\ GSH + DTNB \rightarrow GSSG + TNB$$

GSSH is reduced to GSH by the specific enzyme GSSG reductase, which is dependent on nicotinamide adenine dinucleotide phosphate (NADPH):

Equation 9: $$GSSG + NADPH + H^+ \xrightarrow[GSSG\ reductase]{} 2\ GSH + NADP^+$$

From *Equation 8*, the rate of TNB formation is proportional to the sum of GSH and GSSG present, given constant temperature. It can be followed by measuring absorbance at 412nm, and used to determine total glutathione. In order to measure oxidised glutathione, 2-vinylpyridine is used to sequester GSH, and the assay repeated to measure GSSG only, and calculated as *Equation 10*.

Equation 10: $$[GSH] = [total\ glutathione] - [GSSG]$$

It should be noted that each molecule of GSSG is equivalent to two of GSH. Throughout this work, glutathione concentrations are reported in GSH equivalents.

2.6.2 Materials and reagents

- 5% (w/v) 5-sulphosalicylic acid (5-SSA. Sigma, UK. Cat#247006) in deionised water
- Glutathione reductase from yeast (600U/mL: Roche Diagnostics Ltd, UK. Cat#10105678001)
- Glutathione - oxidised form (GSSG) (Mw = 612.6, Sigma, UK)
- Glutathione - reduced form (GSH) (Mw = 307.3, Sigma, UK. Cat#G6529)
- Stock buffer: 143mM Disodium hydrogen phosphate Na_2HPO_4 (Mw = 141.96), 6.3mM tetrasodium EDTA dihydrate (Mw = 416.20), pH 7.5
- Reaction buffer: 0.3mM NADPH (Mw = 744.4, Sigma-Aldrich, UK. Cat#N1630) in stock buffer, made daily and stored on ice
- DTNB solution: 6mM 5,5′-dithiobis-(2-nitrobenzoic acid. Mw = 396.35. Sigma, UK. Cat#D8130) in stock buffer
- Triethanolamine 50% w/v (TEA. Sigma, UK. Cat#90278)
- 2-vinylpyridine (2VP. Sigma, UK. Cat#132292)

2.6.3 Preparation of bronchoalveolar lavage and cultured macrophages

When using cells from bronchoalveolar lavage, 30mL of whole BAL fluid was spun at 4°C at 500g for 5 minutes. The supernatant was saved, and the pellet (approximately 10^6 cells) was dissolved in 500µL cold 5% 5-SSA. For assays of plated macrophages, $2x10^6$ cells in 6 well plates were scraped into 250µL cold 5% 5-SSA using a cell scraper. These steps were performed as cold and as quickly as possible to prevent oxidation of GSH prior to the addition of 5-SSA. The resulting suspension of lysed cells was pelleted by centrifugation (10000rpm for 5 minutes, 4°C). The supernatant was assayed for glutathione, and the precipitate was frozen at -30°C pending total protein analysis by the Lowry method. Standards were made

fresh by serial dilution of a 50:50 mixture of oxidised and reduced glutathione in 5% 5-SSA to give a range of 10.4μM to 0.325μM. Blanks contained 5% 5-SSA only.

For total glutathione, sample supernatants were diluted 10x in 5% 5-SSA. Samples for oxidised glutathione were derivitivized in triplicate, each by the addition of 2μL 2-VP to 100μL sample, with vigorous vortexing. The pH of each derivitivized sample was brought to between 6 and 7 by addition of 50% triethanolamine in water, and samples were left at room temperature for 1 hour to allow full degradation of the 2-VP before analysis. Standards for the oxidised glutathione assay were obtained using the same process, giving a range of 5.2μM to 0.325μM.

Standards and samples (20μL each) were pipetted into 96 well plates in triplicate. Immediately before starting the kinetic assay, the reaction mixture (8.4mL daily buffer, 1.2mL DTNB, 1.2mL H_2O) was mixed with 120μL glutathione reductase. Immediately, 200μL of this solution was added to each well using a multichannel pipette, and the absorbance of each well at 412nm was recorded using a plate reader (Fluostar Omega, BMG Labtech, UK), reading every 20 seconds. The reaction undergoes linear kinetics until the DTNB oxidation is saturated or NADPH availability becomes limiting. Standard curves were derived from the linear portion (usually until 8 minutes), and used to calculate sample concentrations (see section 3.2).

2.7 Cytospin of bronchoalveolar lavage

2.7.1 Principle

Cytospin produce a relatively uniform scattered monolayer of cells from a suspension. Centripetal force acts to evenly disperse cells from a fine aperture plastic funnel outwards onto a microscope slide. These preparations were used to obtain a cellular differential count and in order to quantify cytoplasmic carbon area by image analysis (using Fields B stain, Sigma, UK). For differential counts, following fixation in methanol, slides were sequentially subjected to: May-Grunwald-Giemsa stain for 10 minutes; rinse buffer pH 6.8 briefly; Giemsa stain for 15 minutes; acetone briefly to dehydrate the sample.

2.7.2 Protocol

A volume of 70μL was used in each funnel, at cell concentrations of $3.3x10^5$/mL and $6.7x10^5$/mL. These were spun at 450rpm for 5 minutes in a Shandon Cytospin (Thermo Scientific, UK). Slides were air-dried. Fixation in methanol was used for staining purposes.

2.8 Trace metal analysis

2.8.1 Principle

Concentrations of selenium and other trace metals can be accurately quantified by Inductively Coupled Plasma Mass Spectrometry (ICP-MS), as previously published[354]. Within a plasma of argon formed in a radio frequency magnetic field, samples or interest are partially ionised, thus allowing detection of components of the sample, particularly metal ions. These are detected by mass spectroscopy

Samples used for calibration are blanks, 1.9μmol/L and 3.8μmol/L. Quality assurance was done using a stable lyophilised human based serum (Seronorm, Biostat, Norway). Indium is added to the sample as an internal standard[355].

For selenium, six isotopes stably exist (74, 76, 77, 78, 80, 82)[355]. Two of these are measured: ^{77}Se and ^{82}Se. Due to limitations of the ICP-MS the most abundant isotopes are not easily quantified (^{76}S and ^{80}S due to the presence of argon dimers formed from ^{40}Ar, and ^{38}Ar). However, these are considerably reduced in this assay by the use of butan-1-ol as diluent. Results assume that the ratio of isotopes is relatively constant; although abundance in soils varies considerably, the absolute proportion of each isotope varies by less than 3%[356].

2.8.2 Materials and reagents

- Diluent: 1% nitric acid, 0.2% butan-1-ol, 0.2% propan-2-ol, 10 ppb indium (VWR)
- Seronorm (Bio-Stat Diagnostics, Norway)
- Selenium atomic absorption standard solution 1000μg/mL (Sigma-Aldrich)

2.8.3 Protocol

All samples were prepared, analysed and reported by the Biochemistry department of the Royal Liverpool University Hospital as part of the routine analysis for NHS patients. After dilution 1:9 of the sample in diluent, 100μL was injected into the plasma and assayed using indium as an internal standard.

2.9 Alveolar macrophage characterisation

2.9.1 Background

Descriptions of macrophage phenotype have undergone considerable change in recent years. At least in mouse models, a spectrum of activation is accepted with variations in the degree of expression of certain receptors, and the phenotype of the macrophage[357, 358]. These have been divided into M1 and M2 designations to denote inflammatory and anti-inflammatory type macrophages respectively. Further subdivision of M2 types has been suggested (see Table 2-2) although plasticity of phenotype is well recognised, and *in vitro* macrophages may be switched between these phenotypes depending on external stimuli[359]. Transcriptional profiling has defined these macrophage populations more specifically. Genes may be defined by type: "M1" type if they are up-regulated in response to INFγ or LPS; M2 if up-regulated by Th2 cytokines IL-4 or IL-13 (designated alternately activated), IL-10 (deactivated), or another anti-inflammatory stimulus such as TGF-β or glucocorticoids[360].

Table 2-2 ***Surface markers of human macrophage activation***

	M1 "Classical"	**M2a "Alternative"**	**M2b "Type II"**	**M2c "Deactivated"**
Induced by	TNFα, INFγ, TLR2/4 agonists	IL-4, IL-13	LPS, IL-1R Immune complexes	IL-10 glucocorticoids
Function	Microbicidal Inflammatory Antigen presenting	Th2 type responses Immuno-modulatory Killing of parasites	Immunoregulatory	Immuno-modulatory Matrix deposition Remodelling
Cytokine	TNFα, IL-6 IL-12, IL-1β IL-23	IL-10	TNFα, IL-1, IL-6 IL-10 high IL12 lo	IL-10 TGF-β
Cytokine receptor	IL-7R, IL-15ra		IL-1ra	
Chemokine	CCL5 CXCL8, CCR7 CCL2/MCP-1	CCL2/MCP-1		CCL2/MCP-1
Others	NOS-2 CD80, CD86			
Surface markers				
CD14	+	++	++	++
CCR7	+	O	O	O
CD86	+	O	+	O
CD206 (MR)	-	+	O	+
CD163 (SR)	-	+	O	+
MHC II (HLR-DR)	+	+	+	O
CD11b	+	+	O	O
CD11c	+	-	O	O
CD16	-	O	O	O

Phenotypic classification is not complete: in some cases surface markers have not been specifically reported or are of variable expression; these are designated "O" above

In order to characterise human alveolar macrophages, we used a panel of surface markers, with mouse antibodies as detailed in Table 2-3.

2.9.2 Materials and reagents

Table 2-3 Antibody cocktail use for alveolar macrophage phenotyping

Target	Conjugated fluorophore	Laser excitation (nm)	Peak emission (nm)	Volume / 100µL cells	Manufacturer code
HLA-DR	Alexa Fluor 700 (AF700)	633	719	2.5µL	BD #560743
CD206	Allophycocyanin (APC)	633	660	10µL	BD #55089
CD11b	Pacific Blue (PB)	405	455	2.5µL	BD #558121
CD86	Fluorescein isothiocyanate (FITC)	488	525	3µL	BD #555657
CD163	Phycoerythrin (PE)	488	575	2.5µL	BD #347557
CCR7	PE-Cy7	488	767	3.5µL	BD#557648

2.9.3 Protocol

Ex vivo macrophages were washed twice in PBS with braked centrifugation at 500g for 5 minutes. Antibodies were added as above in a total volume of 100µL made up with PBS. After 20 minutes incubation at RT, three further washes were performed to remove unbound antibodies. Flow cytometry was performed using appropriate excitation and filter combinations. Colour compensation was also acquired using single-labelled samples. Analysis was performed in FlowJo software v7.64 (Tree Star, Inc. USA).

2.10 Quantification of cytoplasmic particulate loading

Particulate exposure in the lower airways may be quantified by light microscopy of alveolar macrophages[347]. Digital image analysis of cytospin preparations are stored and analysed using freely available ImageSXM software v1.92 (Dr Steve Barrett, University of Liverpool, UK. Available from: http://www.liv.ac.uk/~sdb/ImageSXM/

Slides fixed in methanol were stained with Fields B (Sigma, UK) in order to identify cytoplasm. An overview of the digital image processing and analysis is shown in Figure 2-2. Nuclear stain is not applied, as previous evaluation showed that this tends to make image analysis less accurate[361]. Accurate results rely on careful standardisation of both the staining and analysis protocols. Staining is standardised to 10 seconds exposure to stain with rapid draining; images were taken with the condenser focus fully raised, and the diaphragm fully open in order to reduce the dark appearances of cell outlines; at least 50 images were taken for each individual. Within the slide, images were taken according to a predetermined path in order to minimise operator bias (see Figure 2-1).

Figure 2-1 Path taken when recording digital images for analysis.

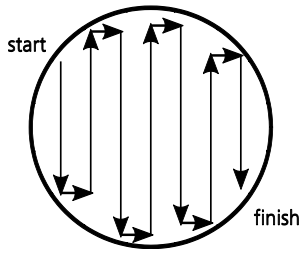

The circle in this diagram represents the outer border of the cell "spot" generated from cytospins.

Each image was visually assessed for accuracy by comparing the original slide to the computer generated map of cytoplasmic carbon. Images were excluded from the analysis only if slide artefact has introduced over-identification of particulate.

Figure 2-2 Overview of the digital image analysis performed by ImageSXM

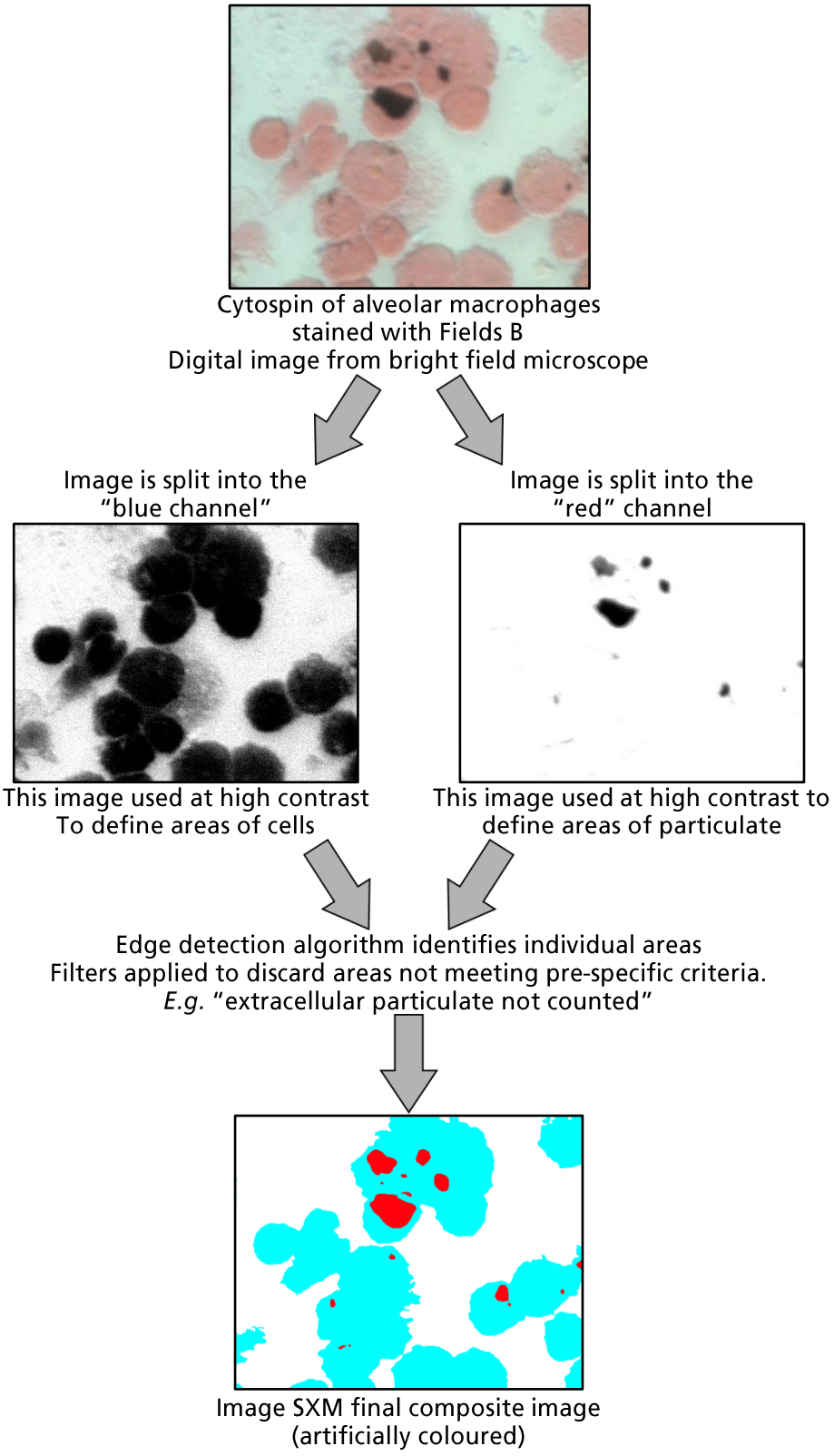

2.11 Preparation of smoke particulate suspension for *in vitro* challenge experiments

Two forms of particulate were used in challenge experiments. Ultrafine carbon black (Printex 90, Degussa, Germany) was used where relatively inert particles were required. These have relatively little adsorbed metal ions, and a consistent diameter of 90 nm. *In vitro* challenge experiments used a fine suspension of this powder created by sonication in culture medium to the required density.

In vivo smoke exposure was modelled using particulates obtained from a controlled combustion of wood commonly used in Malawi for cooking. Mopani wood from Blantyre was burnt at University of Aberdeen (Dr S Semple) and the method used resulted in collection of respirable size particles. The resulting smoke was drawn over a polycarbonate isopore filter with 2μm pore size (Millipore, MA USA), using an Apex pump (Casella CEL, Bedford, UK) attached to a Higgins-Dewell cyclone (respirable dust) at a flow rate of 2.2L/min. The filters were kept dry and cold (4^{o}C) until particulate extraction into methanol. Briefly, filters were weighed before submerging in HPLC grade methanol (Sigma, cat #34898). The particulate suspension was produced by serially sonicating in a water bath (Thermo Scientific, UK), each time for 2 minutes repeated five times. The filter was removed, air dried, and re-weighed in order to determine the mass particulates removed. Appropriate aliquots of the methanol suspension approximating 250μg of particulate were then made in glass vials and dried over nitrogen gas. In order to distribute the nitrogen to multiple vials and minimise exposure time, it was dispensed through a plate washer (Immuno Wash 12, Nunc, UK) as shown in Figure 2-3).

Figure 2-3 Preparation of smoke extract

Left: Plate washer used to dispense dry nitrogen gas for drying methanol suspensions.
Right: Resulting dehydrated particulate sample ready for resuspension in culture medium.

Dried particulate samples were stored at -80°C until required. Resuspension was performed by adding culture medium to the vial to the correct concentration, and sonicating in a water bath until a fine suspension was seen.

2.12 Preparation of pneumococcal culture supernatants

2.12.1 Background

Streptococcus pneumoniae was used as the bacterial model of infection due to epidemiological evidence that it is the most common cause of pneumonia in sub-Saharan Africa[362]. Clinical isolates of type 2 D39 serotype have been previously isolated (WT). Additionally, we used a mutated form from which amino acids 55 to 437 of the pneumolysin product have been removed by an in-frame deletion[363]. This type is referred to as ΔPly in the original work, and here.

Supernatants of the bacterial culture were used in stimulation experiments to test the potential effect of bacterial proteins on the alveolar macrophage during pneumococcal infection. The relative impact of pneumolysin could also be assessed by comparison of the D39 wild-type with ΔPly strain.

2.12.2 Protocol

Clinical isolates of D39 type *Streptococcus pneumoniae* were grown on blood agar overnight. The correlation of bacterial density to optical density was previously determined by removing small aliquots every hour, plating out according to Miles-Misra protocol (see 2.13, carried out by Dr E Sepako, MLW, Malawi) and quantifying colony forming units. Three colonies were transferred to Todd Hewitt broth, and grown to an estimated density of $1x10^8$/mL (OD=0.4 at 620nm).

Growth was terminated by centrifugation (3000g, 30 minutes), after which the supernatant was passed sequentially through 0.45µm and 0.2µm filters under suction (Nalgene 20mm filter unit, 250mL capacity, UK). Filtered supernatant was concentrated approximately 10x by centrifugal ultrafiltration across a polyethersulfone membrane (Vivaspin 20, Vivaproducts, UK). Protein concentration of the concentrate was determined by the Bradford method (see 2.15) in order that known concentration could be added to *in vitro* challenge experiments.

Using this method, bacterial suspensions were grown to mid-log phase before freezing aliquots at -80^{o}C with 10% glycerol for future use.

2.13 Miles and Misra technique for counting Colony Forming Units (CFUs)

Quantification of the bacterial concentration is used here for two purposes:

1. To enable correlation of optical density of media containing viable bacteria with concentration of those bacteria
2. To check post-hoc that bacteria numbers in some assays are consistent over time

The Miles and Misra technique[364] counts colony forming units (CFU) by surface counting on blood agar plates. In order to estimate counts over a wide range of

concentrations, sequential dilutions of the suspension to be assayed are made in phosphate buffered saline. Typically six log10 dilutions are made. Each resulting suspension is dropped onto a different demarcated area of a blood agar plate. A total of 30μL in 3 separate spots are used and left to air dry before overnight incubation at 37°C in an environment of 5% CO_2. Concentrations of bacteria are determined from the area with the most individually identifiable colonies. The CFU is given by Equation 11.

Equation 11: $$CFU\ (colonies/ml) = count \times \frac{30}{1000} \times dilution\ factor$$

2.14 Protein concentration determination – Lowry method

2.14.1 Background

A number of methods were used for determining protein concentration. This was due to the relative limitations of each method according to sample type, and convenience of measurement.

The Lowry method[365] was used specifically for analysis of highly alkaline sample required analysis: glutathione levels reported throughout this project are corrected to Lowry determined protein concentrations. Under alkaline conditions, an excess of divalent copper chelates peptide bonds, forming univalent copper ions in proportion to the concentration of peptide bonds (the Biuret reaction). This subsequently is used to reduce Folin-Ciocalteu reagent (a mixture of phosphomolybdate and phosphotungstate) which itself undergoes a colour change in the reduced state, thereby increasing the sensitivity of detection by ten times. Concentrations of reduced Folin-Ciocalteu reagent were measured by absorption at 750nm in a microplate. Bovine serum albumin (BSA) was used as a standard. Where samples fell outside the standard range, dilutions were performed, with appropriate corrections.

2.14.2 Materials and reagents

- Bovine serum albumin standard 1mg/mL (Sigma, UK. Cat #P0914)
- 2% sodium carbonate (Na2CO3, Mw = 106) in deionised water
- 2% sodium-potassium tartrate (KNaC4H4O6·4H2O, Mw = 282.1) in deionised water
- 40mM copper sulphate solution (CuSO4.5H2O, Mw = 249.68). Stored in the dark
- Folin-Ciocalteu reagent (Sigma-Aldrich, UK. Cat #47641)

2.14.3 Protocol

Samples were digested in 1M sodium hydroxide for 3 hours at 37°C. Standards were prepared fresh in the same diluent. In a microplate 20µL of standards and samples were pipetted in triplicate. 200µL of freshly prepared Biuret solution (1:1:100 mixture of copper sulphate, sodium tartrate, sodium carbonate) was added to each well using a multichannel pipette. The microplate was agitated and incubated in the dark. Exactly ten minutes after the introduction of Biuret solution, 20µL of 50% Folin-Ciocalteu reagent in water was added. After further two hour incubation in the dark[366], absorption was read from each well at 750 nm.

2.15 Protein concentration determination – Bradford method

The reaction of Coomassie brilliant blue G250 with proteins in solution causes a protein-dye complex to form. This results in a change of absorption in the solution from a peak of around 465 nm to 595 nm. Briefly, commercially obtained Bradford solution was used (Sigma, UK. Cat # B6916) according to the manufacturer's instructions against standards of BSA from 50µM to 1mg/mL (Sigma, UK. Cat #P0914). Samples and standards were run in triplicate, and absorption at 595 nm read by a plate reader (BMG Omega, BMG Labtech, UK).

2.16 Multiplex bead cytokine analysis

2.16.1 Background

Quantification of cytokines and chemokines in the experimental supernatants of *in vitro* challenge measurements was performed by multiplex bead cytokine array analysis using the Luminex platform. Custom kits were provided by R&D systems, UK.

In principle this is a sandwich ELISA technique couples with flow cytometric detection through which quantitative measurements of multiple target proteins can be made (see Figure 2-4). Sets of microbeads are variously identifiable by their size and degree of labelling with a fluorophore. Each set is also covalently bound to an antibody against a specific protein of interest (here, a cytokine). The "sandwich" formed by the bead, the target protein, and the reporter antibody conjugate (biotin-streptavidin-PE) can be detected by flow cytometry. As each bead set is unique, the concentration of each target protein can be measured indirectly by the intensity of PE wavelength fluorescence after comparison to a set of standards of known concentration.

Figure 2-4 Detection of protein by multiplex bead array

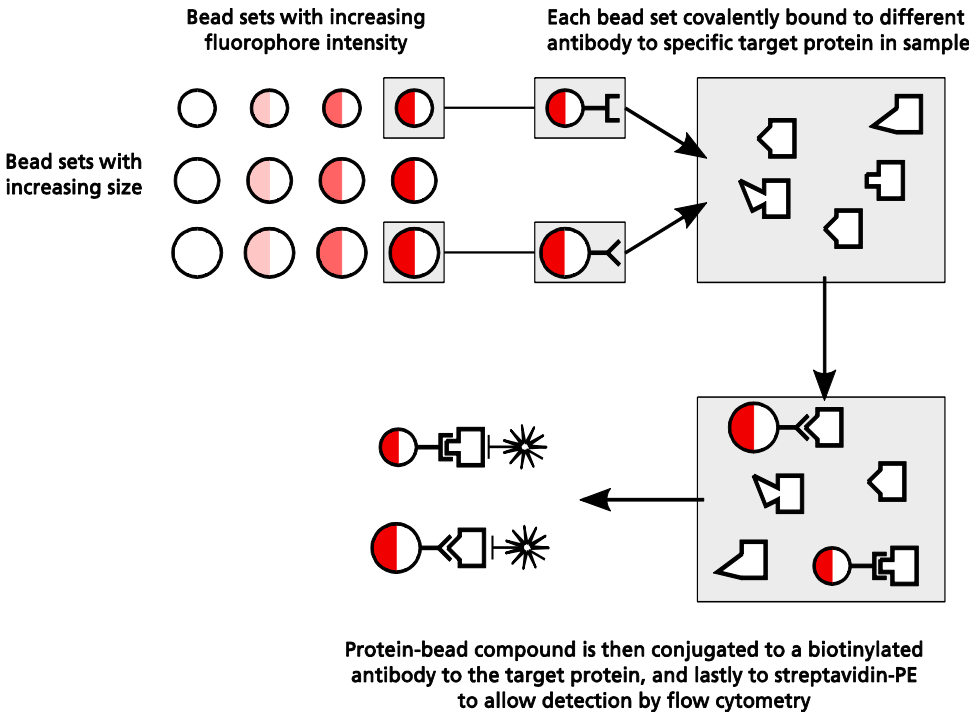

Bead analytes are recognised according to intensity of primary flurophore label and bead size. The signal from PE flurophore is read by a second laser. Concentrations are determined accoridng to a standard curve generated using purified, standardised cytokines

2.16.2 Protocol

A panel of cytokines were tested using a kit from R&D systems according to the manufacturer's instructions. Analytes were chosen in order to reflect the profile of inflammatory and anti-inflammatory cytokines, and specifically those thought to be regulated by the redox environment of the cell. Results were reported uncorrected for multiple comparisons; such corrections in this case are too conservative given that behaviour of individual cytokines are highly likely to be related[367].

For a full justification of the choice of analytes, and further details see 5.3.1.

2.17 Determination of lipid peroxides by high pressure liquid chromatography (HPLC)

The principle of HPLC is that the hydrophobic and molecular weight properties of molecules may be used to separate components of a mixture in solution. Samples are dissolved in a solvent and injected under high pressure into a sealed porous column. The time taken to pass through this column depends on the polar characteristics of the substances being analysed and those of the solvent, the molecular weight and the properties of the column. By measuring absorbance or fluorescence properties of the eluted fluid at specific time points, the molecular composition of the sample may be quantified[368].

Lipid peroxides are formed within polyunsaturated fatty acid residues as a result of reactive oxygen species, particularly the hydroxyl ion. This is commonly formed by the Fenton reaction of molecular iron with hydrogen peroxide and may be initiated in the presence of haem groups[369]. The resultant result of the loss of hydrogen atom from CH_2 groups destabilises the molecule which rearranges to a conjugated diene[370]. Propagation of lipid peroxidation may occur along the fatty acid chain by the reaction of oxygen with the diene forming a peroxyl radical[142]. Ultimately, the lipid hydroperoxides may generate secondary products which can lead to further cellular damage. Malondialdehyde (MDA) is one such substance which may be determined by the thiobarbituric acid reacting substances (TBARS) assay.

Some criticism of this method is made in that there are other sources of malondialdehyde from within cells including the production of prostaglandins. However the vast majority of cellular MDA relates to oxidative damage to lipids: as a measure of the effect of reactive oxygen species it is well validated[371]. A second criticism levelled at this assay is that it is non-specific, and other adducts of

thiobarbituric acid may be formed during the assay reaction. However, by using reverse phase high pressure liquid chromatography (HPLC), those formed with MDA may be separated and individually quantified[372].

In this method, an HPLC column composed of octodecyl carbon chain (C18) is used with a pore diameter of 5nm. The solvent is 20% acetonitrile, run at 1mL/minute. MDA:TBARS adducts pass through the column in around 4.8 minutes. Older methods have used absorption measurement at 533nm as an endpoint. However fluorescence detection after HPLC has increased the sensitivity and specificity of the assay[372]. Here an excitation wavelength of 515 nm was used while monitoring fluorometrically emission at 553nm.

2.17.1 Materials and reagents

- HPLC column (Sphereclone 5μm ODS 1 250x4.6mm, Phenomenex, Macclesfield, UK)
- Autosampler (Gynkotech Gina 50, Macclesfield, UK)
- Fluorescence detector (Gilson model 121 fluorometer, Gilson, Middleton, USA)
- 2M sodium acetate pH 3.5: made by titration of 2M glacial acetic acid (Mw = 60.05, Sigma, UK. Cat #320099) with 2M sodium acetate trihydrate ($NaC_2H_3O_2.3H_2O$, Mw = 136.08, Sigma, UK. Cat #71188)
- 2% w/v 2-thiobarbituric acid: 40mg ($C_4H_4N_2O_2S$, Mw = 144.15. Sigma, UK. Cat #T5500) in 2M acetate buffer
- 5% w/v butylated hydroxytoluene (BHT, $[(CH_3)_3C]_2C_6H_2(CH_3)OH$, Mw = 220.35. Sigma, UK. Cat #W218405) in ethanol
- 4.4M 1,1,3,3,-tetraethoxypropane (TEP, density 0.919 g/mL at 25°C, Mw = 220.31. Sigma, UK. Cat # T9889)
- 20% acetonitrile (CH_3CN, density 0.786 g/mL at 25°C, Mw = 41.05. Sigma, UK. Cat# 34967) in water

- Butan-1-ol ($CH_3(CH_2)_3OH$, density 0.81g/mL at 25°C, Mw = 74.12. Sigma, UK. Cat # 34867)

2.17.2 Protocol

Pilot experiments informed the dilution range of clinical samples. Using 2M acetate buffer (pH 3.5), urine was diluted 1 part in 9 parts buffer; serum was diluted 1 part in 10 parts buffer; cell suspension from bronchoalveolar lavage was diluted 1 part in 9 parts buffer

In order to form TBA adducts, 20µL 2% TBA and 3µL 5% BHT were added to 200µL of each sample and standard. This reaction was performed at 95°C for 1hour, after which samples were kept on ice. To each mixture 100µL butanol was added for extraction. After vigorous vortexing, samples and standards were centrifuged at 20000g for 5 minutes, and the resulting top butanol layer transferred carefully into glass HPLC vials without contamination with the aqueous layer.

HPLC detection was performed in a mobile phase of 20% v/v acetonitrile in water. Sample volumes of 20µL were introduced to the HPLC column running at 1mL/min. Detection by fluorescence (excitation=530nm emission=553nm) demonstrated peaks at between 4.5 to 5 minutes; signal area and peak height of all samples and standards were recorded from the detector. Sample concentrations are calculated from the resulting standard curve.

2.18 Manufacture of beads for measurement of intraphagosomal oxidative burst and proteolysis

2.18.1 Principle

Internalisation of particles by macrophages may occur by a number of pathways depending on the particle size and characteristics, and the receptor engaged (see section 1.1.4.1). Other stimuli may direct a less inflammatory process of phagosome

destruction[373]. For example, apoptotic cells have alternative and poorly delineated pathways for recognition and removal which are distinct from those used for microbial and other non-self particulate matter[374].

Russell and colleagues have developed assays of this intraphagosomal bacterial killing capacity[375]. These assays measure the maximal capacity of macrophages to produce oxidative burst and proteolytic activity within the phagolysosome. The method involves challenge of adherent macrophages with silica beads which are coated with the reporter molecule which acts as a substrate for either the oxidative burst pathway (Oxyburst fluorochrome), or the proteolytic pathway (DQ Green BSA conjugate). The increase in fluorescence of the reporter substances is a quantitative measure of phagosomal activity which may be detected using flow cytometric or plate-based fluorometric readers.

Figure 2-5 Diagram of Oxyburst / DQ Proteolysis beads.

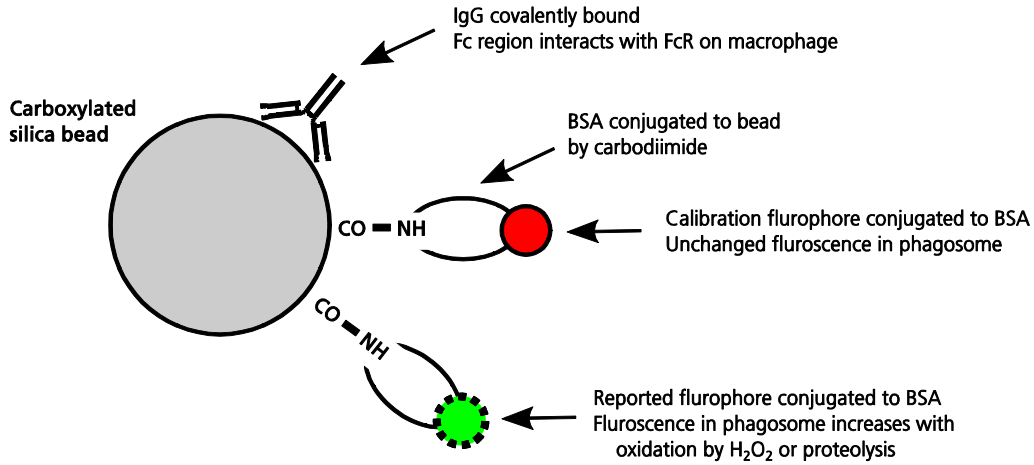

Carboxylated silica beads are conjugated to immunoglobulin, reporter fluorochrome and calibrator fluorochrome. The ratio of calibration and reporter fluorochrome is constant and allows the use of fluoresence ratios as a metric of the degree to which the reporter fluorochome chnages.

In order to enhance uptake into the macrophage and to direct beads to the phagosome, the silica beads are coated in immunoglobulin (IgG). Co-labelling with a second fluorophore which is unchanged by phagosomal reactions allowed

calibration of the system, and the use of ratios to define activity. Reporter fluorochromes are excited at 488nm, whereas calibration fluorophore may be chosen to excite best at 405nm or 633nm.

Conjugation is accomplished using carbodiimides which allow cross-linking of carboxyl groups[376] on the silica beads to primary amines within the BSA.

2.18.2 Materials and reagents

- Carboxymethylated silica beads of 3µm diameter (Kisker Biotech, Germany)
- Dimethylsulfoxide (DMSO) (Sigma, UK. Cat#D2650)
- OxyBurst Green succinimidyl ester (H2DCFDA-SE, Invitrogen, UK. Cat#D2935) dissolved to 25mg/mL in DMSO
- DQ-BSA Green conjugate (3x1mg) (Invitrogen, UK. Cat#D12050)
- Alexa 405 succinimidyl ester (Invitrogen, UK. Cat#A30000) dissolved to 5mg/mL in DMSO
- Human IgG 10mg/mL (Sigma, UK. Cat#I4506)
- N,N'-dicyclohexylcarbodiimide (Sigma, UK. Cat#36650)
- Bovine serum albumin (BSA) defatted and low endotoxin 10 mg/mL (Sigma, UK. Cat#A8806)
- Sodium borate 0.1M buffer at pH 8.0
- Sodium azide (Sigma, UK. Cat#S8032)

2.18.3 Preparation of beads - method

250µL of silica beads were washed twice in phosphate buffered saline using a 10 second quick spin at 5000 rpm to precipitate out the beads after each wash. Beads were re-suspended in 1 mL phosphate-buffered saline, and added to 20 mg of N,N'-dicyclohexylcarbodiimide. The mixture was incubated for 20 minutes at room temperature on a rotational mixer. Three further washes in phosphate-buffered saline were performed to remove excess carbodiimide. From this point, all

manipulations of the beads were performed quickly in lowlight conditions, and incubations performed on a rotational mixer at room temperature while protected from light.

In order to conjugate to DQ substrate, the bead pellet was re-suspended in 1mL coupling buffer, 10μL IgG and 3mg of DQ-BSA. Incubation for 12 hours is allowed for this conjugation to take place.

For conjugation to Oxyburst substrate the method differs: to the bead pellet, a mixture of 900μL coupling buffer, 100μL of defatted BSA and 10μL of IgG was added. After an incubation of 12 hours followed by three washes in coupling buffer, the beads were incubated in 5μL Oxyburst-SE and 95 mL of DMSO for 60 minutes. The beads were rinsed once in coupling buffer and the Oxyburst labelling step repeated once.

From this point, both DQ and Oxyburst label beads were treated similarly in order to couple to the calibration fluorochrome. After two washes in coupling buffer, the beads were re-suspended in 1mL coupling buffer with 5μL Alexa 405 and incubated for 60 minutes at room temperature. To further washes in coupling buffer and one wash in PBS were performed to remove excess unconjugated calibration fluorochrome. The prepared beads were stored in 500μL PBS with sodium azide 0.02% at 4^{o}C in the dark.

2.19 Measuring intraphagosomal capacity for oxidative burst and proteolysis

For mechanism of labelling and detection, see 2.18. Macrophages ex-vivo were plated at 1x10^{6} per well in a 24 well plate and allowed to adhere for at least two hours. Cells were washed once with RPMI1640 with 5% FCS. For each well to be tested, 1.5μL of pre-prepared detection beads (see 2.18) were washed three times in

RPMI1640 with 5% FCS before being added to the plate to a total well volume of 500µL. At 10 minutes, excess beads were washed off in PBS, and the medium replaced. For cell removal, the wells were filled with cold citric saline solution (0.015M sodium citrate, 0.135M potassium chloride) to effect detachment of the cells. After five minutes incubation, cell suspensions were removed, centrifuged at 450g for 5 minutes and suspended in PBS with 1% formaldehyde for flow cytometry analysis.

For each volunteer, a number of controls were used (see Table 2-4 and section 3.8).

Table 2-4 Oxyburst and proteolysis bead assay – controls and samples

Cells	**Beads**	**Time of harvest**	**Post harvest addition**	**Reason**
No	Oxyburst	N/A	None	Comparator for fluorescence of cells
No	Oxyburst	N/A	8.5µL 30% H_2O_2	Check that Oxyburst beads are sensitive to oxidation
No	DQ	N/A	None	Comparator for fluorescence of cells
Yes	None	60	None	Baseline control for cell fluorescence
Yes	Oxyburst	10	17µL 30% H_2O_2	Check that Oxyburst beads are sensitive to oxidation
Yes	Oxyburst	60	None	Measurement of Oxyburst capacity
Yes	DQ	180	None	Measurement of proteolytic capacity

Flow cytometry was performed using a Beckman Coulter Cyan system. Detection of the reporter fluorochromes used 488nm excitation, 520nm emission, and calibrator fluorochromes were detected through 405nm excitation, and 420nm emission. Strict analytical procedures were followed in order that bias was minimised. Steps are illustrated by flow cytometry output summarised below, and illustrated in Figure 2-6.

1. Bead and cell samples were captured using the same detector voltages. A "cell gate" was set on macrophages to exclude unbound beads using forward scatter (FSC) and side scatter (SSC) parameters
2. The "cell gate" was adjusted if necessary using the FITC channel fluorescence of unlabelled cells to identify macrophage autofluorescence and to minimise the inclusion of cell debris
3. A bifurcating gate was set within the cell gate at the 98th centile of 405/420nm channel of unlabelled cells. This was applied to all bead-challenged cells and enabled consistency in identifying macrophages with and without associated beads

Activity indices of Oxyburst and proteolysis detecting beads were calculated according to *Equation 12, Equation 13* and *Equation 14*.

Equation 12: $$MFI\ ratio_{cells} = \frac{Reporter\ MFI\ of\ cells\ containing\ beads}{Calibrator\ MFI\ of\ cells\ containing\ beads}$$

Equation 13: $$MFI\ ratio_{beads} = \frac{Reporter\ MFI\ of\ beads}{Calibrator\ MFI\ of\ beads}$$

Equation 14: $$Activity\ index = \frac{MFI\ ratio_{cells}}{MFI\ ratio_{beads}}$$

Figure 2-6 *Gating strategy for analysis of phagosomal bead assay*

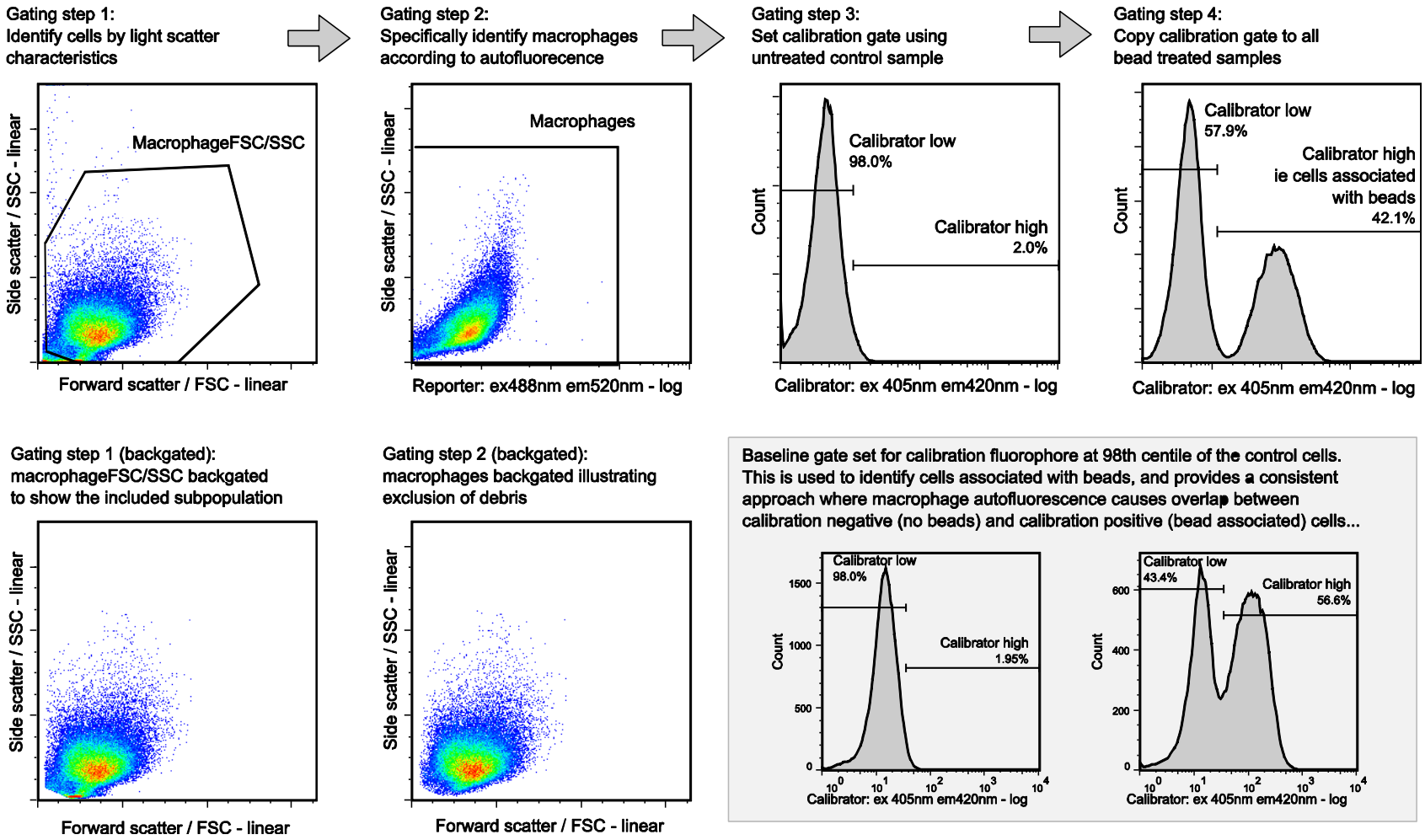

2.20 Relative quantification of nuclear factor [erythroid-derived 2]-like 2 (Nrf2) by Western blotting

2.20.1 Background

Nrf2 is a protein with a short cytoplasmic half-life due to its continual degradation by the proteasome[377]. Under the action of electrophilic attack or oxidative stress however, this destructive pathway is slowed resulting in increased cytoplasmic concentrations of unbound Nrf2[293]. Concomitant translocation to the nucleus occurs[378] where Nrf2 has a role as transcription factor for genes associated with the antioxidant response element (ARE). Downstream effects of this transcription factor include translation of a number of cytoprotective proteins including those for glutathione and thioredoxin homeostasis, antioxidant enzymes (GPx, GR, TrxR), NADPH regenerating enzymes[379].

Western blotting allows specific detection of this Nrf2 and other proteins or peptide fragments in solution. Prior fractionation of cellular components may be performed in order to specifically measure cytoplasmic or nuclear Nrf2. In this project, whole cell concentrations of Nrf2 are reported unless otherwise stated. This assumes that cytoplasmic concentrations are proportional to those in the nucleus, and therefore to the expected increase in ARE transcription activity[380].

The process involves denaturation of proteins, followed by their electrophoretic separation on an SDS-PAGE gel according to their relative properties of size and electrical charge. This is followed by transfer of these separated proteins onto a membrane in order that they may be probed by specific (primary) antibodies. Detection systems vary, but in this case a secondary antibody conjugated to horseradish peroxidase (HRP) was used to detect the antibody-antibody-antigen conjugate. This uses light produced by the HRP catalysed oxidation of luminol by

hydrogen peroxide: the light emitted is detected by photographic film or by charge-coupled device.

2.20.2 Materials and reagents

- NuPAGE sample buffer (Life Technologies, UK. Cat#NP0007)
- NuPAGE sample reducing agent (Life Technologies, UK. Cat#NP0009)
- NuPAGE 4-12% Bis-Tris gel 1.5mm 15 well (Life Technologies, UK. Cat#NP0336)
- 3-(N-morpholino)propanesulfonic acid buffer (MOPS buffer, 20x)
- 209.2g MOPS (Sigma, UK. Cat#M1254); 121.2g Tris base (Sigma, UK. Cat#T1503); 20g SDS (Sigma, UK. Cat#L4390); 6g EDTA (Sigma, UK. Cat#E9884) in water
- Transfer buffer (10x)
- 150.2g glycine (Sigma, UK. Cat#G8898); 30.3g Tris base (Sigma, UK. Cat#T1503) in 1:2:7 ration of 10x transfer buffer: methanol: water
- Bio-Rad Kaleidoscope molecular weight markers (Bio-Rad, UK. Cat#161-0375)
- Nitrocellulose membrane 0.45µm – GE Hybond HCl (GE, UK. Cat#RPN303D)
- Bio-Rad blotting grade blocker (Bio-Rad, UK. Cat#170-6404)
- TBS buffer (20x)
- 175.2g sodium chloride (Sigma, UK. Cat#S9888); 4.48g potassium chloride (Sigma, UK. Cat#P9541); 60.6g Tris base (Sigma, UK. Cat#T1503)at pH 7
- TBS-Tween buffer (TBST)
- TBS buffer as above with 1% Tween 20 (Sigma, UK. Cat#P7949)
- Detection system – Western Lightning Plus ECL (Perkin Elmer, MA, USA. Cat# NEL104001EA)
- Hyperfilm ECL X-ray film (GE Amersham, UK. Cat#ST03-B004)
- Rabbit anti-human Nrf2 antibody (Abcam, US. Cat#ab62352)
- Mouse anti-beta actin antibody AC-15 (Abcam, US. Cat#ab6276)

- Anti-rabbit secondary antibody (Sigma, UK. Cat#A9169)
- Anti-mouse secondary antibody (Sigma, UK. Cat#A9044)

2.20.3 Protocol

Cells were lysed in RIPA buffer with 0.5% protease inhibitor and frozen at -80°C until analysis. Typically, 200µL of buffer was used per 10^6 cells. Samples were volume corrected to give standardised protein concentrations for each lane. This was determined by Bradford protein assay (see 2.15) with correction to an estimated 20µg in 10µL of buffer (1x sample buffer, 1x reducing buffer). Each sample was denatured by incubation at 80°C for 6 minutes before loading onto precast electrophoresis gels. Molecular weight markers (4µL) were run concurrently. SDS-PAGE gels were immersed in MOPS buffer, and subjected to 90V for 10 minutes followed by 170V for 60 minutes in order to give adequate protein separation. Transfer to the nitrocellulose membrane was performed in cold MOPS buffer at 230mA for 65 minutes. The gel was separated between 66kDa (Nrf2) and 42kDa (beta actin) in order to stain with separate primary antibodies, before overnight blocking in 2% milk powder at 4°C to minimise non-specific binding. After three washes in TBS-Tween buffer (TBST), gels were incubated at room temperature with primary antibody in TBST with 2% milk powder. Three hour incubation was used with anti-human Nrf2 (1:400 dilution), and 30minute incubation with anti-beta actin (1:10000). After six washes in TBST on a rocking platform, each of 10 minutes, secondary antibodies were introduced in TBST with 2% milk powder. Secondary antibodies (1:10000 anti-rabbit for Nrf2 and 1:10000 anti-mouse for beta actin) were incubated for a further 1 hour at room temperature before six final 10minute washes were performed. The gels exposed to the ECL detection mixture as per manufacturer's guidelines. Gels were aligned within an X-ray cassette and exposed

to X-ray film under dark room conditions. Relative quantification of Nrf2 signal was standardised to beta actin signal.

2.21 Isolation and culture of peripherally derived mononuclear cells

2.21.1 Background

During cell culture, monocytes undergo a phenotypic and morphological change towards macrophage type behaviour and appearance. Peripheral blood mononuclear cells may therefore be used to produce monocyte derived macrophages, which are a model for alveolar macrophages.

Whole blood centrifugation leads to a Buffy coat layer which contains most leucocytes and platelets. To enhance extraction of mononuclear cells, density centrifugation may be refined using a Ficoll-hypaque interface which has a density of 1.077 g/mL[381] which does not allow monocytes or lymphocytes to penetrate, and enhances coagulation of erythrocytes, and sedimentation of neutrophils. Mononuclear cells appear as a cloudy layer at the Ficoll interface; approximately 20% of these are monocytes[382]. After removal the cells are introduced to cell culture plates allowing enrichment of monocytes concentrations by adherence and relative loss of lymphocytes[383].

2.21.2 Materials and reagents

- Neubauer Haemocytometer (Sigma, UK. Cat#Z359629)
- Lymphoprep (Ficoll-Hypaque) (Axis-Shield, UK)
- RPMI1640 culture medium (Sigma, UK. Cat R 8758)
- Fetal calf serum (Sigma, UK. Cat#F7524)
- EDTA 0.5M (Mw = 336.21.Sigma, UK. Cat# E7889)

2.21.3 Protocol

Anti-coagulated blood (4.5mM final concentration of EDTA) was carefully pipetted into a 50mL centrifuge tube. This was slowly overlaid with half volume of lymphoprep in order to generate a clean blood-Lymphoprep interface. This was then centrifuged at 800g for 20 minutes at room temperature. The mononuclear cell layer was removed with Pasteur pipette, and the cells washed twice in large volumes PBS with pelleting first at 450g then 250g. The final cell pellet was re-suspended in RPMI1640 for counting and haemocytometer. Mononuclear cells were pipetted into 24 well plates (Greiner BioOne, UK)at $2x10^6$ per well for overnight adherence. The next day, culture media was entirely replaced, and subsequently changed every three days.

2.22 Glutathione peroxidase assay

Glutathione peroxidase (GPx) activity was measured by spectrophotometry using a method described by Paglia and Valentine (1967). The catalysed reaction uses cumene hydroperoxide to oxidise glutathione as per Equation 15

Equation 15: $$ROOH + 2\,GSH \xrightarrow[GPx]{} ROH + GSSG + H_2O$$

Sodium azide is used to reduce the competitive catalase activity of other substances. GSH is kept at constant concentration during the assay by using an excess of glutathione reductase to recycle the GSSG (Equation 16).

Equation 16: $$GSSG + NADPH + H^+ \xrightarrow[GR]{} 2\,GSH + NADP^+$$

As NADPH is oxidised, its absorbance at 340nm decreases; monitoring this change photometrically after addition of cumene hydroperoxide to a sample allows calculation of enzyme activity.

Glutathione peroxidase activity was determined by this method using a kit (Ransel, Randox UK, Cat#RS504) using a Randox RX Imola auto-analyser, by Randox

laboratories, UK. One unit of GPx activity catalyses the oxidation of 1µmol of reduced glutathione per minute at pH 7.0 at 25°C (see Equation 17).

Equation 17: $$GPx\ Units/ml = 2\frac{(\Delta A340_{test} - \Delta A340_{blank})}{6.22}\frac{vol_{reaction}}{vol_{enzyme}}$$

ΔA340 =the rate of change of absorbance at 340nm
2 = correction for 2µmol GSH per 1µmol NADPH
6.22 = millimolar extinction coefficient of NADPH at 340nm
0.05 = volume of enzyme used (mL)
$vol_{reaction}$ = volume of reaction (mL)
vol_{enzyme}= volume of enzyme used (mL)

2.23 Data management and storage

Clinical information was collected and recorded for three purposes:

- To allow appropriate interpretation of research findings
- To allow healthcare professionals seeing the subject after the bronchoscopy to know what has been done *e.g.* if the patient suffers complications
- To allow tracing of the patient if abnormal findings are detected at bronchoscopy or in later laboratory observation

True anonymisation was therefore neither desirable nor possible in maintaining the safety of participants. Research data was therefore pseudo-anonymised by the unique study number.

Laboratory measurements were requested and reported using the unique study number. Demographic and questionnaire data was collected on a paper Clinical Report Form (CRF), and double entered into an SQL database maintained by the Data Department of Malawi-Liverpool-Wellcome (MLW) Clinical Research Laboratories. Front end access to this was provided by a REDCap[384] (Vanderbilt University, US) system hosted locally. Pseudo-anonymised paper CRFs were kept in

a locked room, and in a separate location tracing information contained details of participants' names, addresses and contact details cross referenced to study number. Only the research nurse and the principle investigator had access to this tracing information.

On closure of the study, the database was directly exported to Stata v12 (StataCorp, US) for data analysis. Haematology and biochemistry results from the MLW laboratory were incorporated at this stage by first exporting to CSV format, and merging records according to unique study identifier. Where direct electronic transfer was not possible, data were entered and verified on two separate occasions.

2.24 Statistics

Statistical methods and choice of significance tests are described in the methods sections associated with each results chapter.

3 Methods development

All methods used in this project appear in previously published research, as cited. However, some optimisation was required for cell type. For assays where there was significant change to published protocols, precision estimates have been given, quoting coefficient of variation (CV) values as shown in Equation 18.

Equation 18 $$CV = \frac{\sigma}{\mu} = \frac{standard\ deviation}{mean}$$

3.1 Glutathione assay development

3.2 Glutathione in HAM

The recycling assay for glutathione (see 2.6) is sensitive and known to work on a variety of sources. In order to optimise the protocol for human alveolar macrophages and number of experiments were run, and are described below.

3.2.1 Using an HK-2 cell line model

Initial assay optimisation used an adherent HK-2 cell line seeded in Dulbecco's Modified Eagle's Medium (DMEM. Sigma, UK. Cat: # D5796) at $2x10^4$/well and grown to 90% confluence in 6 well plates. After pre-exposure to N-acetylcysteine for 1 hour in DMEM, 600µL 1% 5-sulfasalicylic acid was added to each well. Glutathione was assayed as described in the methods using DTNB was used at a concentration of 1.1mM in line with previous protocols.

Figure 3-1 Standard curve of glutathione concentration vs rate of change in absorbance

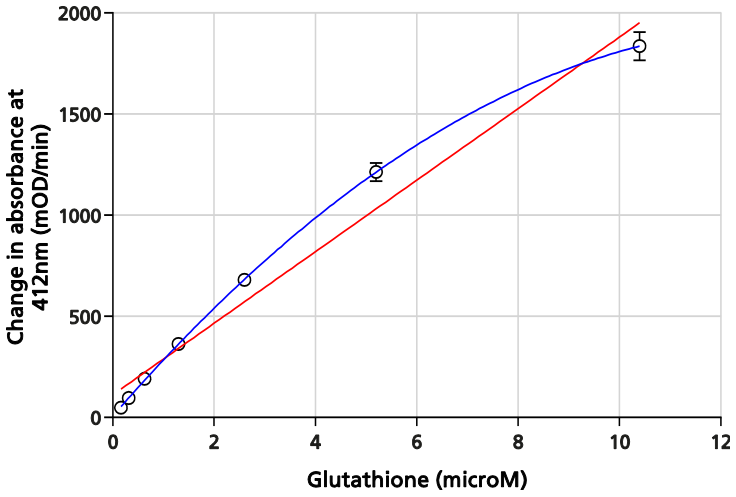

The absorbance was measured here at 412nm for the first two minutes after addition of glutathione reductase. Two fitting equations are drawn: linear (red), and 2nd polynomial (blue).

Figure 3-1 shows the standard curve generated. Although the lower five standards are approximately linear, there is considerable deviation at higher concentrations, suggesting that the enzyme catalysed kinetics are becoming limited by a reactant other than glutathione. This is seen to happen if the reaction is monitored for longer periods (see Figure 3-2). However, if this occurs earlier (in the time period over which kinetic measurements are taken), it is a violation of the method's principle that all reactants should be present in excess, and therefore makes the assay unreliable. Such limitations may be due to a relative shortage of DTNB, glutathione reductase or NADPH. Increasing the DTNB concentration to 6mM improved the linearity (see Figure 3-3) and the reaction proceeded more slowly associated with minor improvements in accuracy and precision (see Table 3-1). Despite these advantages, the blank reaction appeared to proceed faster than the lowest three standards, as evidenced by the blank corrected absorbance change in Figure 3-3.

Figure 3-2 Glutathione assay reaction becoming saturated when observed for long periods

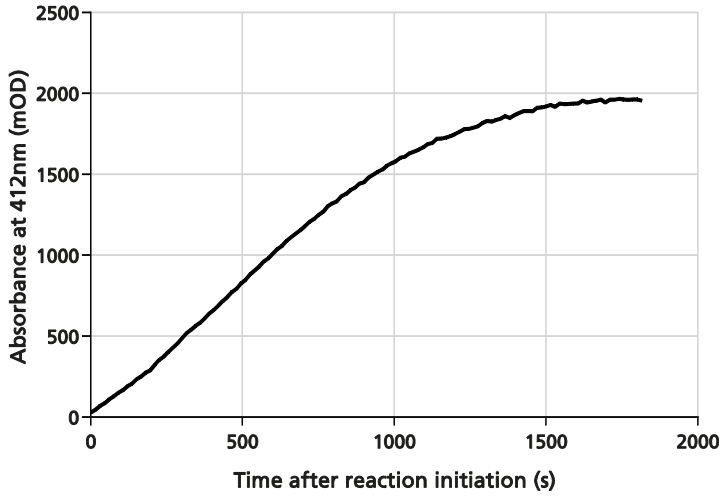

In this example, after 900 seconds, it is likely DTNB has become maximally oxidised. Similar patterns occur where NADPH availability becomes limited

Figure 3-3 Standard curve of glutathione concentration – improved linearity

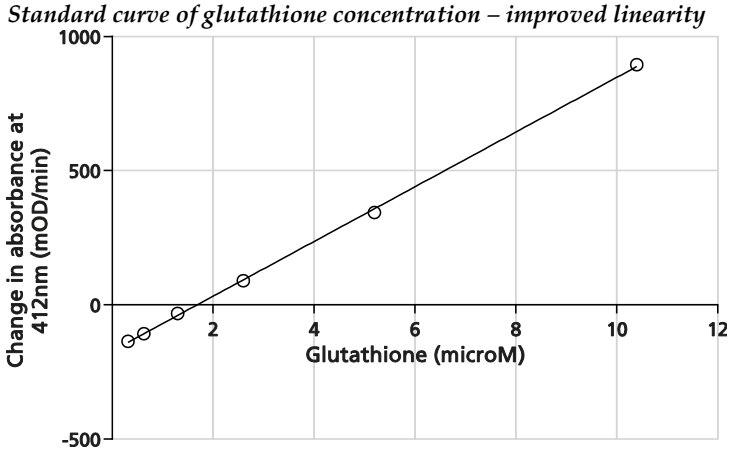

Absorbance was measured here at 412nm for the first eight minutes after addition of glutathione reductase. Blank corrected absorbance values are used. A linear fitting equation is added

Table 3-1 Accuracy and precision of glutathione assay – comparison of the assay performed with DTNB at 1.1mM and 6mM

Standard (μM)	**Inaccuracy (%)**	
	1.1mM	6mM
10.4	3.1	0.6
5.2	10.1	2.7
2.6	12.3	1.0
1.3	1.2	5.8
0.65	33.4	2.2
0.325	114.2	14.9

Unknown	**Precision (CV)**	
	1.1mM	6mM
1	5.5	6.6
2	6.6	3.2
3	6.1	5.1
4	4.2	3.2
5	5.4	4.5
6	8.6	8.6
Mean	6.0	5.2

Left table: Accuracy determined according to known concentrations of total glutathione (mean of n=2) Right table: Precision as determined by variability of calculated concentrations from samples representative of range (0.625 – 10.4μM). n=4

When the absorbance over time was examined, the reaction kinetics showed a concave upwards appearance or "lag" phase (see Figure 3-4). By pre-warming the reaction mixture, this artefact improved, and the blank reaction rate fell below that of all of the standards (see Figure 3-5).

Figure 3-4 *Reaction kinetics of glutathione standards followed over time*

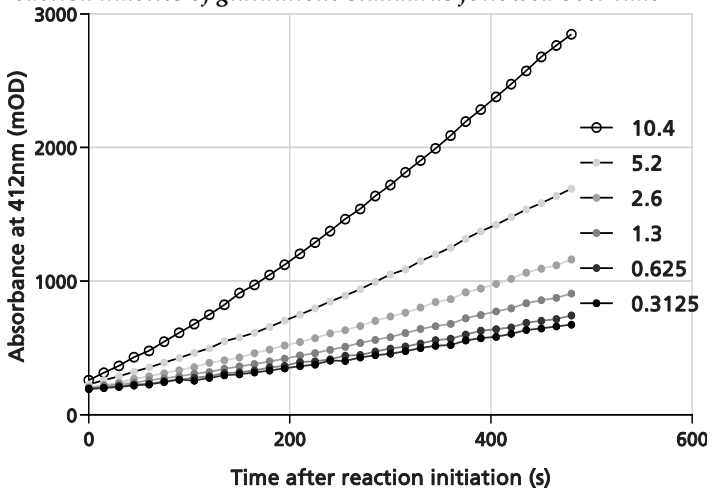

Points represent the absorbance at 412nm as measured every 15 seconds

Figure 3-5 *Reaction kinetics of glutathione standards over time after pre-warming of reaction mixture*

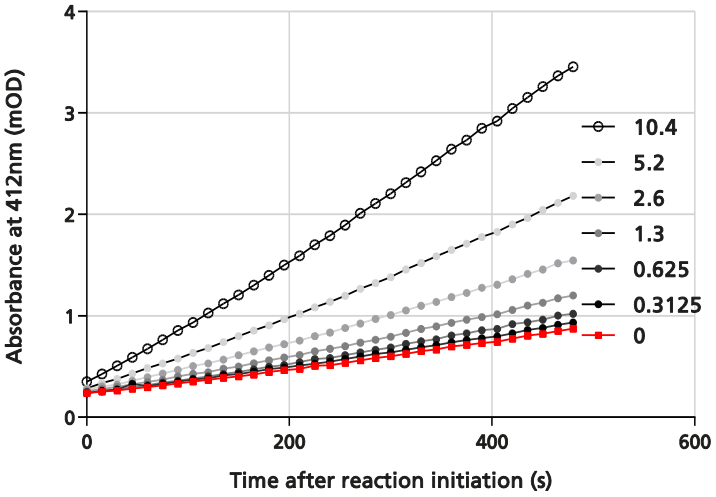

Points represent absorbance at 412nm as measured every 15 seconds. Blank reaction is shown in red.

Some other possibilities which improve sensitivity were considered but discounted where they significantly added complexity or time to the assay method. Such examples, from Brehe[385] are: removing the ammonium sulphate preservative from glutathione reductase to increase activity; the addition of bovine serum albumin to increase GR stability (Brehe); buffering the reaction in imidazole to increase NADPH stability. Other acids may be used instead of 5-SSA, for example

hydrochloric acid[386]. For consistency with previously stored samples, this change was not adopted.

3.2.2 Concentrations and CVs in the glutathione assay

Relatively low numbers of cells are expected from bronchoalveolar lavage; BAL volumes used in the assay, and their cell concentration was optimised for precision and practicability. Decisions regarding methods were made early in the project and based on a small number of samples; those decisions relating to CVs and accuracy tended to be conservative *i.e.* to be biased towards improving reproducibility at the expense of increased sample use.

Changes in the concentration of DTNB improved the precision of estimates in the lower reference range (see Table 3-2). Further work determined the number of cells required, using PBMC as a model.

Cell numbers and glutathione concentration

Making the assumption that oxidised glutathione represents 1 to 5% of the total, total concentrations should therefore exceed 32.5μM in order that measured GSSG should exceed the lower limit of detection (0.325μM). PBMC were seeded in 24 well tissue culture plates (Greiner BioOne, UK) at a density of $1.5x10^6$ per well and used on day 10 to 14 of adherent culture. Multiple experiments were carried out varying both the cell number and volume of 5-SSA. Due to the variable proportion of monocytes in PBMC preparations (usually 10-20%) and inconsistent adherence to culture plates, absolute cell numbers were difficult to determine. However, four wells of PBMC in 200μl 5% 5-sulfasalicylic acid gave total GSH concentrations of between 42.3 and 94.6μM in the assay *i.e.* adequate concentrations for measuring GSSG even at the lower estimate of relative concentration. Estimation of required cell numbers was done as follows:

Equation 19: $$Cell\ number \approx [wells\ used]\ x\ [cells\ seeded\ per\ well]\ x\ [proportion\ monocytes] = 4x1.5x10^6x0.15 = 0.9x10^6$$

This informed the standardised protocol for *ex vivo* glutathione measurement. From previous data, approximately 8 million alveolar macrophages are isolated following bronchoalveolar lavage in a volume of 120mL. From this estimation, 15mL of whole BAL would contain $1x10^6$ cells, and was therefore incorporated into the protocol. After ten BAL procedures, cell numbers were consistently lower ($8.6x10^5$ estimated in the glutathione sample), although the proportion of GSSG was higher (5.2%). In one sample the GSSG was below the limit of detection. Future glutathione measurements on BAL were performed on 30mL to reduce the likelihood of this recurring.

Precision and accuracy of glutathione measurement

PBMC were seeded in 24 well plates at a density of $1.5x10^6$ per well and used on day 12 of adherent culture. Parallel estimation of total glutathione and the oxidised form was done as described in section 2.6 using 4 wells of PBMC for each condition in a total of 200µL 5% 5-SSA. Oxidised glutathione was measured from only one derivitivisation, run in duplicate (see Table 3-2).

Table 3-2 Precision of the oxidised glutathione assay.

Standard	Precision of standards pre-optimisation - CV%	Precision of standards from first 10 runs - CV%
5.2	-	0.9
3.9	14.2	-
2.6	7.8	4.0
1.95	10.3	-
1.3	15.2	7.0
0.975	9.1	-
0.65	34.3	12.2
0.325	42.1	23.2
Samples	25.8 (15-40)	20.0 (4 – 40)

Precision as determined by variability of calculated standards and samples, CV for samples represents the variability within multiple measurements of the same sample (before optimisation using PBMCs [n=2 for each sample] and after optimisation using ex vivo alveolar macrophages [n=6 for each sample]). Values in parentheses for samples are the range of CV values obtained from these 10 samples.

On the basis of imprecision (optimally less than 15%), particularly at lower concentrations, samples were subsequently derivitivized in triplicates, and each derivitivized sample run in duplicates within the plate. The standard range for GSSG was increased to include a higher top standard. Retrospective data from the first 10 volunteers are given in this table for comparison; these are likely to reflect precision of the final results. Here, CVs indicate the within sample variation of the derivitivisation and measurement process *i.e.* the precision of the 6 measurements for each sample.

3.3 Lowry protein estimation protocol optimisation

Glutathione and other assays used in this project require normalisation against protein content. This is partly because bronchoalveolar lavage gives a variable

sample in terms of cell number. It is also known that macrophage size varies with particulate exposure (cigarette smoke)[387]. Moreover, macrophage turnover is likely to change the average size as (smaller) monocyte influx is in part responsible for replenishing AM populations[388]. Cell number is therefore not an ideal method where a denominator is required for assay results *e.g.* glutathione is better expressed as *μmol per milligram of cellular protein* compared with *μmol per 10^6 cells*.

The Lowry method (see 2.14) was chosen for its relative advantages in alkaline solution. Early tests showed significant non-linearity of the higher part of the standard curve (see Figure 3-6). It has been noted that some non-linearity is to be expected, therefore the standard range was truncated 0-400μg/mL to improve performance. Samples were therefore diluted as required. This had other benefits in terms of reducing the problem of precipitation within the Lowry reagent, presumably by decreasing the concentration of potassium ions[389].

Figure 3-6 Linearity of the Lowry assay

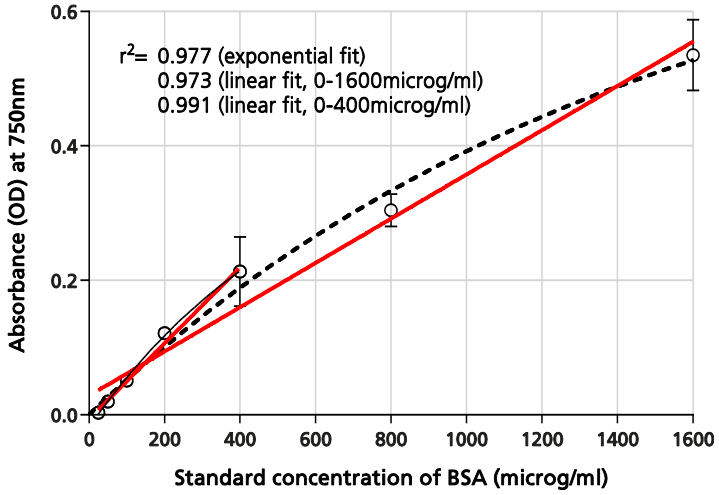

The absorbance at 750nm for each standard concentration of BSA is shown. Linear model fitting is shown by the red lines; one for the entire range (0-1600µg/mL) and the other for 0-400µg/mL). An exponential fit is also shown (dotted, black line)

Colour development has been noted to continue until approximately 2 hours after addition of the Folin–Ciocalteu reagent, and that accuracy tends to improve over this time[366]. This was repeated using high and low standards, with colour development assessed as light absorbance at 660nm and 750nm (see Figure 3-7). These wavelengths represent the lower and upper boundaries usually tested for determining concentrations by the Lowry method. This experiment does not compare enough values to give adequate estimates of precision. However, minimal change in absorbance occurred after 2 hours, and in line with previously published recommendations, this time point was used in any further assays.

Coefficient of variation (CV) of all the standards and 20 unknown samples was calculated based on concentrations derived from absorbance measurements at 120minutes (see Equation 18). There was no difference in CV of results from 660nm absorbance measurement (10.34%) vs. that from 750nm (10.43%) p=0.96 by t-test. Therefore 750nm was chosen as the wavelength to measure, as at this wavelength there are fewer likely interfering substances.

Figure 3-7 Colour development of the Lowry assay

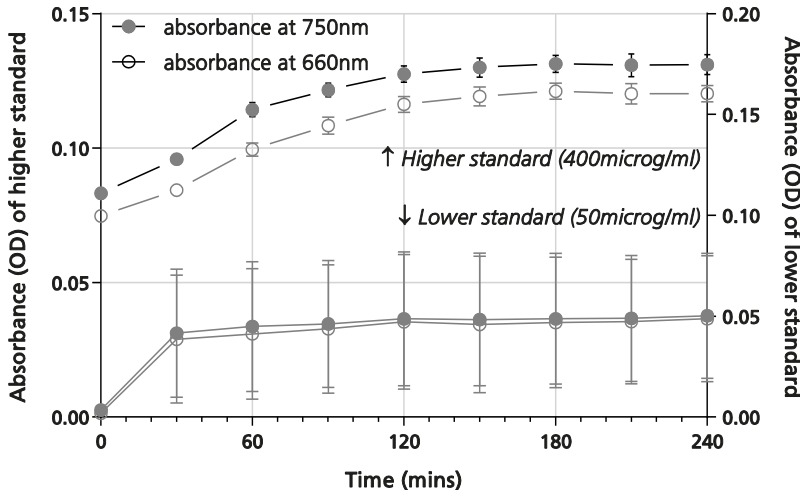

Absorbance of light at 660nm and 750nm by a developing Lowry assay. Each point represents duplicate standards of bovine serum albumin. Data for higher (400µg/mL) and lower (50µg/mL) standards are shown.

3.4 Recovery of cells from 24 well plates for flow cytometry

In order to compare the intraphagosomal function of ex-vivo human alveolar macrophages with other measurements (such as particulate density or redox balance), smaller scale assays of the former method were required. Previously, 6 well plates were used, and cells were removed mechanically by scraping. In order to use fewer cells (in either 96 or 24 well plate format), and alternative mechanism was required. The requirements for a new method were that it would be:

- fast (less than 10 minutes in order that the time-dependent functional assays remained meaningful);
- non-oxidant (to prevent oxidation of reporter fluorochromes before analysis)
- associated with low rates of cell lysis (to prevent systematic errors in interpretation of phagocytosis);
- usable in combination with other flow cytometry based assays for surface marker phenotyping

A number of methods were trialled, as detailed below. These used both PBMC and HAM models according to their availability at the time of experiment.

3.4.1 Trypsin-EDTA

Trypsin-EDTA is commonly used during the passage of adherent immortalised cell lines. As a serine protease, the trypsin cleaves extracellular proteins, some of which are responsible for cell attachment. EDTA chelates calcium and magnesium ions which otherwise inhibit enzymatic proteolysis.

PBMC at day 11 of adherent culture (see 2.21) were washed twice in Ca^{2+} and Mg^{2+} free PBS before being incubated at 37°C with 1x trypsin (Sigma, UK. Cat#T4549) in RPMI-1640 medium according to the manufacturer's protocol. Macroscopic appearance was judged every 5-10 minutes. Using this technique, 10 minutes of incubation time was required for all cells to be removed even with vigorous pipetting: this method was therefore abandoned.

3.4.2 Lignocaine EDTA

Peripherally derived mononuclear cells at day 12 of maturation, initially plated at $1.5x10^6$ total PBMC per well, were gently washed twice with 1mL PBS. Lignocaine-EDTA buffer (1mL/well of lignocaine hydrochloride 15mM, EDTA 10mM in PBS) was added with incubation at 37°C. Observation by light microscopy showed approximately one third of cells had become detached at 5 minutes but the majority remained irregular and adherent. Even with exposure times to detachment buffer of up to half hour, the remaining cells could not be detached without vigorous pipetting. Previous literature suggested that a late stage of tissue culture, the cells cannot be effectively removed without significant degree of destruction[390]. This approach was therefore not used.

3.4.3 Citric saline

Citric saline was chosen for testing as an alternative to trypsin which can cause oxidative stress in cells[391]. As with previous trials, plated cells were washed twice with PBS before exposure to 500µL/well of sterilised removal buffer (here: 5g potassium chloride; 2.2g sodium citrate in 500mL water). Alveolar macrophages were used in this evaluation as they were available. After 5 minutes at 37°C, minor pipetting removed all cells from the plate. Microscopically, minimal fragmentation was noted. This method was used hereafter for detachment of HAM.

3.5 Real time measurements of oxidative stress

3.5.1 Lipid peroxide

A real time marker of oxidative stress would be highly valued, and one candidate is the degree to which cellular lipids have undergone peroxidation (for a single point in time measure, see 2.17). This would allow tracking of rates of peroxidation, and the potential for spatial analysis by confocal microscopy.

We tested the viability of using the oxidation sensitive lipid probe C11-BODIPY(581/591). While in principle useful due to its spectral properties, stability, good signal-to-noise ratio and lipophilic tendency even once oxidised[392], it has not been fully tested in macrophages. C11-BODIPY when loaded into the cells becomes incorporated to lipid membranes. It has two emission peaks of 520 nm and 590 nm; on becoming oxidised, emission at 590 lessons while at 520 increases.

3.5.1.1 Principle of BODIPY use- cell free system

Concentration for loading cells

In a cell free system, C11-BODIPY (Invitrogen, UK. Cat#D3861) was reconstituted in ethanol, and introduced to 96 well plates at concentration range 0 to 200 µmol. Cumene hydroperoxide ($C_9H_{12}O_2$. Sigma, UK. Cat #C0524) was used at

concentration of 10mM in order to induce oxidation. Fluorescence emission was measured using a fluorescence plate reader (BMG Omega, excitation 484 nm, emission 520 and 590 nm band-pass filters).

Concentrations of transition metal ions in the presence of hydrogen peroxide promote Fenton reactions (see section), and are expected to increase the rate of lipid peroxidation. This was tested using copper (40nM) as the sulphate ion in the presence of C11-BODIPY 581/591 with hydrogen peroxide as the oxidising agent. Equal volumes of solution were tested for detectable evidence of oxidised C11-BODIPY in 96 well plates at baseline, 60 minutes and 120 minutes (see Figure 3-8).

Figure 3-8 Effect of oxidising C11-BODIPY 581/591 in an acellular environment

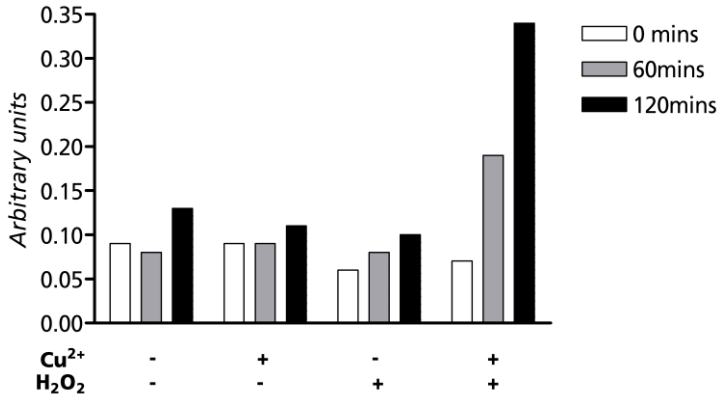

Ordinate reports the ratio of fluoroscence emissions (exλ488nm emλ520nm to exλ544nm emλ590nm) as an average of two wells. Conditions are the presence of copper ions (40nM) and hydrogen peroxide (200μM)

In the presence of an oxidising agent alone, C11-BODIPY 581/591 does not exhibit any changes indicating oxidation. Only after the addition of transition metal ions in this cell free system does the emλ520 increase relative to emλ590, in line with previous observations[393].

3.5.1.2 Optimal BODIPY loading in cellular system

PBMC were used at day 14 of adherent cell culture in 96 well tissue culture plate (Greiner Bio-One, UK) from an initial seeding density of $1x10^5$/well. These cells were loaded with 5μM C11-BODIPY 581/591 in RPMI-1640 medium without FBS for 30 minutes at 37°C. Serum was omitted in order to prevent absorption of the fluorochrome onto soluble protein. Wells were washed three times, and then incubated with combinations of control (phenol red free RPMI-1640 media only), copper sulphate and hydrogen peroxide. Fluorescence was measured using equivalent settings to the cell-free trial; results are shown in Figure 3-9.

Loading at this dose appeared to be successful: while fluorescence at exλ485nm emλ520nm stayed constant, that at exλ544nm emλ590nm increased approximately six fold in the control wells. A systematic effect of the presence of copper ions could be seen throughout as a reduction in the exλ485nm emλ520nm channel , presumably due to direct absorption. It was expected that hydrogen peroxide would initiate oxidation resulting in an increased ratio of these fluorescence measurement. However, no immediate effect was seen, and both absolute and relative fluorescence intensities were unchanged when followed for 3 hours (data not shown). A further identical experiment using the more lipid soluble cumene hydroperoxide (Sigma, UK. Cat#247502) at 200μM gave similar results.

Figure 3-9 The fluorescence of C11-BODIPY 581/591 in a cellular system

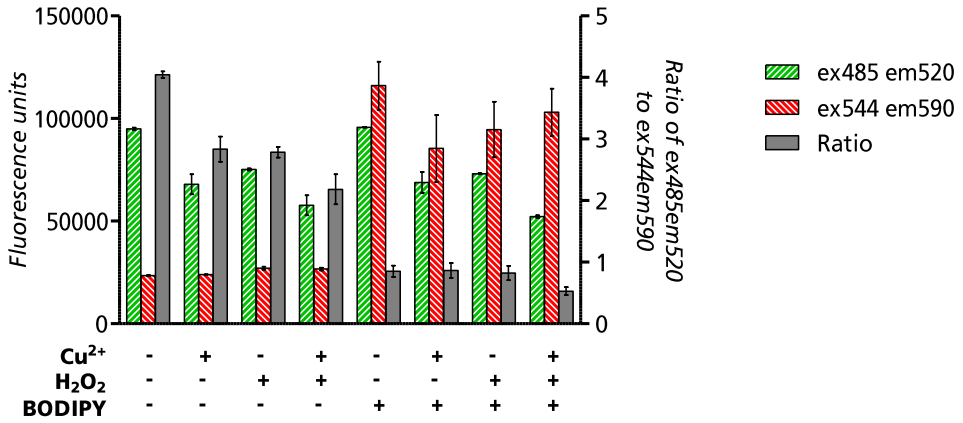

PBMC loaded with 5μM BODIPY immediately after addition of hydrogen peroxide (200μM) and copper sulphate (40nM). Bars represent the relative fluorescence from a) exλ485nm emλ520nm and b) exλ544nm emλ590nm and c) the calculated ratio of a:b. Four replicates per condition are shown: error bars represent SD.

3.5.2 Improving the positive control in the cellular BODIPY system

As both H_2O_2 and cumene hydroperoxide are substrates for glutathione peroxidase, and this enzyme is present in macrophages, the experimental design was extended to study the effects of endogenously produced oxidants. As previously (section 3.5.1.2), PBMC at 14 days were loaded with C11-BODIPY 581/591. Cells were incubated in the plate reader with: vehicle only (DMSO 0.4%, Sigma, UK. Cat# D2650); cumene hydroperoxide 200μM as a direct oxidant; apocynin 300μM (4′-Hydroxy-3′-methoxyacetophenone. Sigma, UK. Cat#55539) as a direct stimulant of NADPH oxidase (see Figure 3-16); fMLP (formyl-methionyl-leucyl-phenylalanine. Sigma, UK. Cat# F3506) as a stimulant of oxidative burst. Figure 3-10 shows these results. Good loading of the fluorophore is confirmed by the increase in exλ544nm emλ590nm fluorescence in vehicle treated compared with unloaded cells. Again, throughout the conditions, minimal change is seen in either fluorescence channel suggesting that lipid peroxidation is not occurring at a detectable level or that the C11-BODIPY 581/591 is a relatively insensitive reporter. Further examination of this

compound was not undertaken; elsewhere in this work, lipid peroxidation has been measured by the thiobarbituric acid reducing substances (TBARS) assay coupled to HPLC fluorescence detection (see section 2.17).

Figure 3-10 Oxidation of C11-BODIPY 581/591 in a cellular system with endogenous oxidant production.

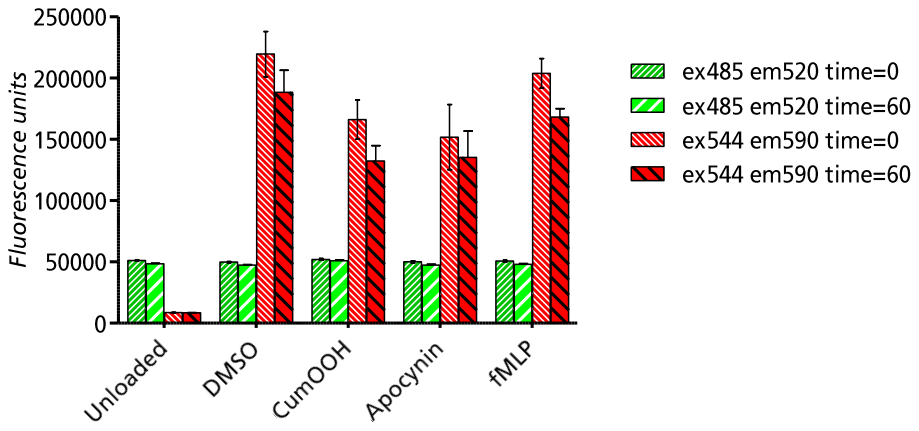

PBMC loaded with 5μM BODIPY (except the "unloaded" control). Bars represent the relative fluorescence from exλ485nm emλ520nm (green, upwards hatch) and exλ544nm emλ590nm (red, downwards hatch) shown immediately after addition of the stimulus, and at 60 minutes. DMSO was used as a negative control, as it is the vehicle for other conditions. CumOOH = cumene hydroperoxide. Apocynin used at 300μM. fMLP (formyl-methionyl-leucyl-phenylalanine) used at 10mciroM. Four replicates per condition are shown: error bars represent SD.

3.6 Measurement of intracellular oxidant production

A number of experiments were planned to investigate the relationship between levels of oxidative stress in macrophages, and their ability to produce reactive oxygen species by NADPH oxidase (oxidative burst activity). This was postulated as a mechanism which would explain the epidemiological association between high levels of particulate exposure in the home (from the burning of biomass fuels) and the incidence of pneumonia.

In order trial methods for ROS detection, we used monocytes and macrophages in adherent cell culture, and confined investigation to fluorescent reporter molecules. A number of such compounds exist, each with distinct profiles (see Table 3-3).

Carboxydichlorofluorescein diacetate (carboxy-H_2DCFDA, Invitrogen. Cat#C400) was chosen for evaluation due to its relative advantages: relatively cell permanent; broad sensitivity; low toxicity; previous successful use of this class of indicator in alveolar macrophages[394, 395].

Table 3-3 Characteristics of commonly used fluorescence probes for detection of reactive oxygen and nitrogen species in phagocytes[395]

Compound	Detection	Characteristics
Dichlorofluorescein diacetate (DCFH)	H_2O_2 Peroxidases Lipid peroxides[396] Peroxynitrite[397] 495/520nm	Oxidised DCF product has enhanced fluorescence Increased cellular retention due to acetate groups. Require catalytic presence of peroxidase, iron, catalase xanthine oxidase which are all present in macrophages Reduced extracellular background "leeching from cells" allowing more accurate measurement over time. Carboxylated form improves cell permanency. Auto-oxidation can lead to "run away" oxidation once initiated Relies on intracellular esterases to convert the diacetate form (DCFH-DA) to oxidant sensitive DCFH which may be limiting in some mononuclear cells[398] Non-specifically oxidised, but can be used in mitochondrial blocking experiments to estimate cellular production[399]
Dihydroethidium (DHE)	O^{2}-[400] H_2O_2 (only in the presence of peroxidase) 510/595nm	May be localised to mitochondria – useful for imaging. Oxidised product fluorescent but enhanced by binding to mitochondrial and nuclear DNA: fluorescence not directly proportional to concentration due to variable DNA enhancement. Subject to spontaneous oxidation[401]
Dihydrorhodamine 123 (DHR)	Peroxynitrite[402] 505/534nm	Affinity for mitochondria and cell membranes Sensitive and low background[403]

3.6.1.1 Optimal cell loading concentration of carboxy-H_2DCF

Optimal cell loading concentrations for carboxy-DCF were determined. Briefly, monocyte derived macrophages at day 5 of adherent cell culture were washed in PBS, then incubated in RPMI-1640 medium without phenol red, with carboxy-DCF (0-100μM) for 30 minutes at 37°C. Initial incubation time was consistent with similar work reported for alveolar macrophages in the literature[399]. Excess media and probe were removed by three further washes, and fluorescence measured using a plate reader. Additional hydrogen peroxide was injected to each well to final concentrations of 0-100μM. Figure 3-11 shows the relative fluorescence of the well contents at 60 minutes after addition of H_2O_2: good loading was noted in terms of signal: background ratio *i.e.* comparing the fluorescence of the control (control well to that of the treatment well with 100μM H_2O_2); the best ratio was noted at maximal dose of reporter fluorophore. However, concerns over toxicity to cells, or the altered behaviour or phenotype in the presence of carboxy-H_2DCFDA led to the lower doses being used in further experiments.

Figure 3-11 Optimising loading of PBMCs with carboxy-H2DCFDA

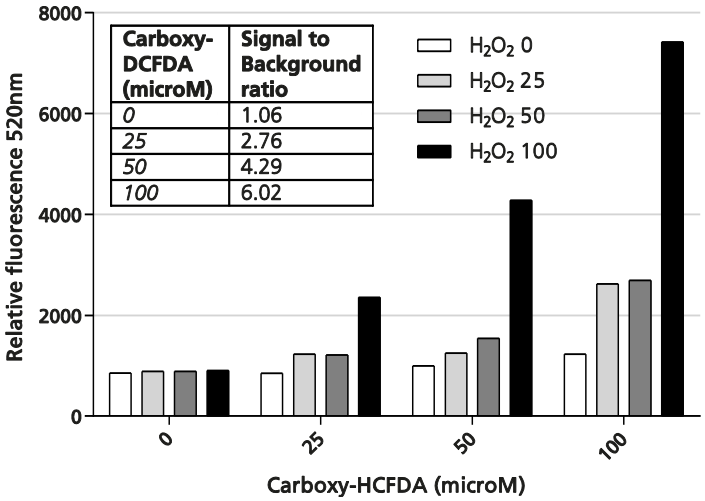

After 30 minutes of incubation with the reporter compound, cells were washed and incubated with culture medium with varying concentrations of hydrogen peroxide. Relative fluorescence at 520nm was measured from all wells at 60 minutes. Each condition is a mean of duplicate wells with blank correction (to wells containing media only).
Inset: Table of signal:background ratio for each concentration of carboxy-H2DCFDA (fluorescence[H2O2 100μM] / fluorescence[H2O2 0mM])

3.6.1.2 Optimal time course of carboxy-H_2DCFDA

The development of fluorescence was followed according to the method in section 0. Figure 3-12 shows this over the hour following addition of hydrogen peroxide. It would be expected that the oxidant effect of H_2O_2 be short lived due to intracellular cellular glutathione peroxidase and catalase. However, increased in fluorescence seemed to be exponential at all doses of carboxy-H2DCFDA. This indicated auto-oxidation, or an initiation of oxidative burst by the monocyte/macrophage cells, or photo-oxidation as a result of repeated interrogation within the plate reader.

Figure 3-12 Increasing oxidation of carboxy-H2DCFDA over time

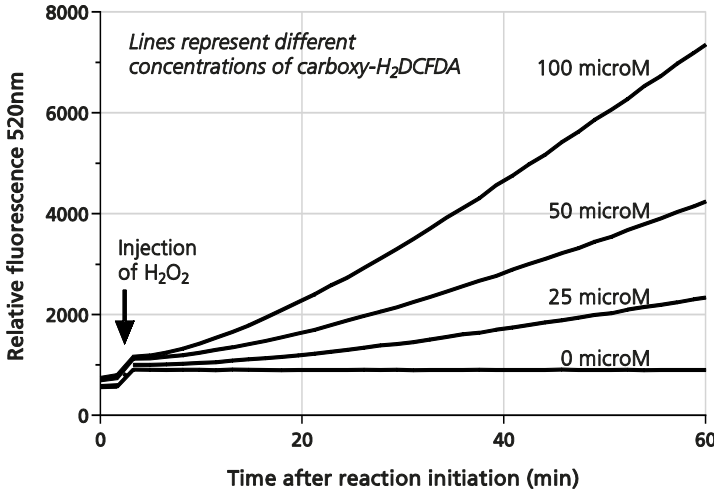

After 30 minutes of incubation with varying concentrations of the the reporter compound, cells were washed and incubated with culture medium with 100μM hydrogen peroxide. Relative fluorescence at 520nm was measured from all wells over 60 minutes. Each condition is a mean of duplicate wells, with blank correction (to wells containing medium only).

3.6.1.3 Optimal concentration of hydrogen peroxide for positive control

Using a constant concentration of carboxy-H2DCFDA for cell loading, and the same protocol as section 0, the relative signal from different concentrations of hydrogen peroxide was followed in order to establish the dose to be used as a positive control.

Figure 3-13 Optimising the dose of hydrogen peroxide as a positive control

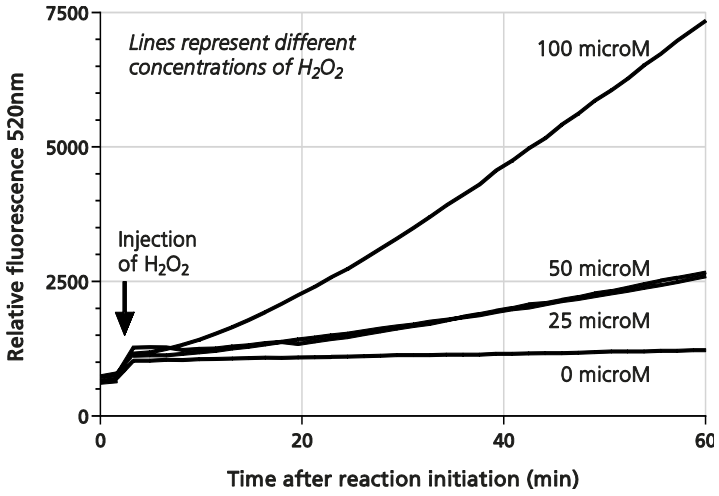

After 30 minutes of incubation with 100μM of the reporter compound, cells were washed and incubated with culture medium with varying concentrations of hydrogen peroxide. Relative fluorescence at 520nm was measured from all wells over 60 minutes. Each condition is a mean of duplicate wells, with blank correction (to wells containing medium only).

Figure 3-13 shows clearly that 100μM hydrogen peroxide gave the highest fluorescence signal. However 25 and 50μM solutions did not differ significantly; in both the 100μM H_2O_2 resulted in between 3 and 4 times higher fluorescence after 15 minutes when corrected for the baseline of untreated cells. We have subsequently used 100μM of H_2O_2 as positive control.

3.6.1.4 Optimal concentration for mediation of H_2DCF oxidation by N-acetylcysteine

Within *in vitro* experiments, extrinsically manipulating the antioxidant content of cells is useful. Decreasing glutathione concentration is dealt with in Section 0. In order to investigate the potential for increasing antioxidant buffering, N-acetylcysteine (Sigma, UK. Cat#A9165) was used. PBMC from NHS Buffy coats seeded at $4x10^4$/well in 96 well plates, at day 8 of adherent cell culture were incubated for 18 hours with varying concentrations of N-acetylcysteine (0-50mM). Cells were then washed three times, incubated with 25μM carboxy-H_2DCFDA for 60 minutes and washed again. Hydrogen peroxide (final concentration 100μM) was

added and the fluorescence at 520nm recorded using a plate reader (BMG Omega) over 60 minutes. Another condition was treated similarly to the control (no NAC loading), but had 50mM NAC within the media at the time of adding H_2O_2.

As shown in Figure 3-14, N-acetylcysteine reduced oxidation of the reporter at 5mM and 50mM, and was not demonstrably dose dependent in this experiment. As expected, using NAC in the media at the time of H_2O_2 introduction entirely buffered the oxidant effect.

Figure 3-14 The effect of N-acetylcysteine on carboxy-H_2DCFDA fluorescence in monocyte derived macrophages after addition of H_2O_2

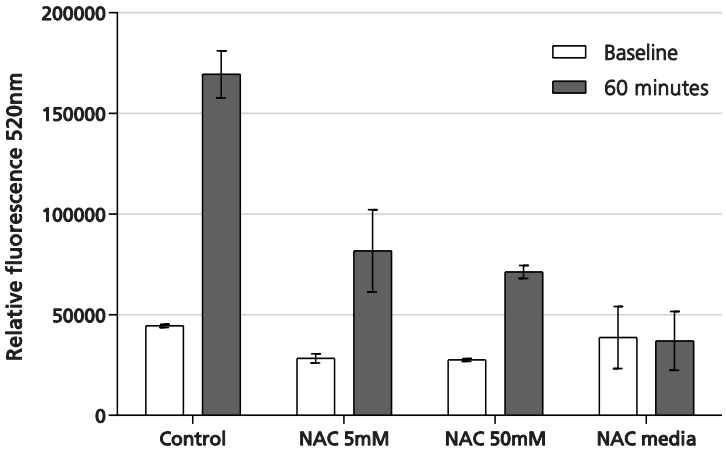

Prior loading of cells with NAC (5 or 50mM) or media only (control) for 18 hours as indicated. Cells were loaded with 25μM carboxy-H_2DCFDA, washed and hydrogen peroxide added to all wells (final concentration 100μM). NAC media represents wells which were not loaded with NAC, but had this added concurrently with H_2O_2. Fluorescence values are not blank corrected. Error bars represent SD of duplicate wells (n=2).

3.6.1.5 Improving positive control of H_2DCF with Fe^{2+}

The formation of oxidative species may be affected by the presence of transition metals, as discussed elsewhere. Most commonly, in terms of exposure of alveolar macrophages, this will be ferrous iron. Under these circumstances, hydroxyl ions might be expected to generate earlier or stronger oxidation responses, and might form the basis for augmenting the positive control signal.

This was investigated using monocyte derived macrophages in day 5 of adherent cell culture in black walled 96 well tissue culture plates (Greiner Bio-One, UK). These cells were loaded with carboxy-H_2DCFDA as in 0, washed 3 times in PBS, and fluorescence at 520nm monitored over 1 hour after the addition of H_2O_2 (final concentration 100μM), with varying concentrations of ferrous sulphate (0-2000μM).

Figure 3-15 shows two representations of the same data. The top panel indicates that the highest concentration of ferrous iron results in an early and significant increases in fluorescence of the reporter although this effect tailed off after 10 minutes, and overall oxidation was less than control at the end of 1 hour. This concentration is likely to be supra-physiological under most circumstances. However, the error bars (SD around the mean for the triplicate wells) are extremely wide. When further examined, it seemed that the ultimate fluorescence for each well depended largely on the starting conditions; early small differences within each replicate were compounded over time leading to the large final variation. This is seen more obviously in the bottom panel, where values are calculated as fold increase over the starting fluorescence of each well. Here, error bars are much narrower.

This illustrates a difficulty of using this assay; relative and absolute changes may be interpreted differently. Early signals becoming amplified suggest that auto-oxidation is a significant problem here; this problem is shared by many of the DCF based reporter compounds. Initial differences may be related to variations in cell numbers; in adherent cell culture there is inevitable loss of cells during changes of media.

If interpretable at all, these data suggest that small amounts of ferrous iron make no difference to carboxy-H_2DCFDA oxidation, although high concentrations may have an early effect.

Figure 3-15 The additional effect of ferrous iron on oxidation of carboxy-H2DCFDA in monocyte derived macrophages

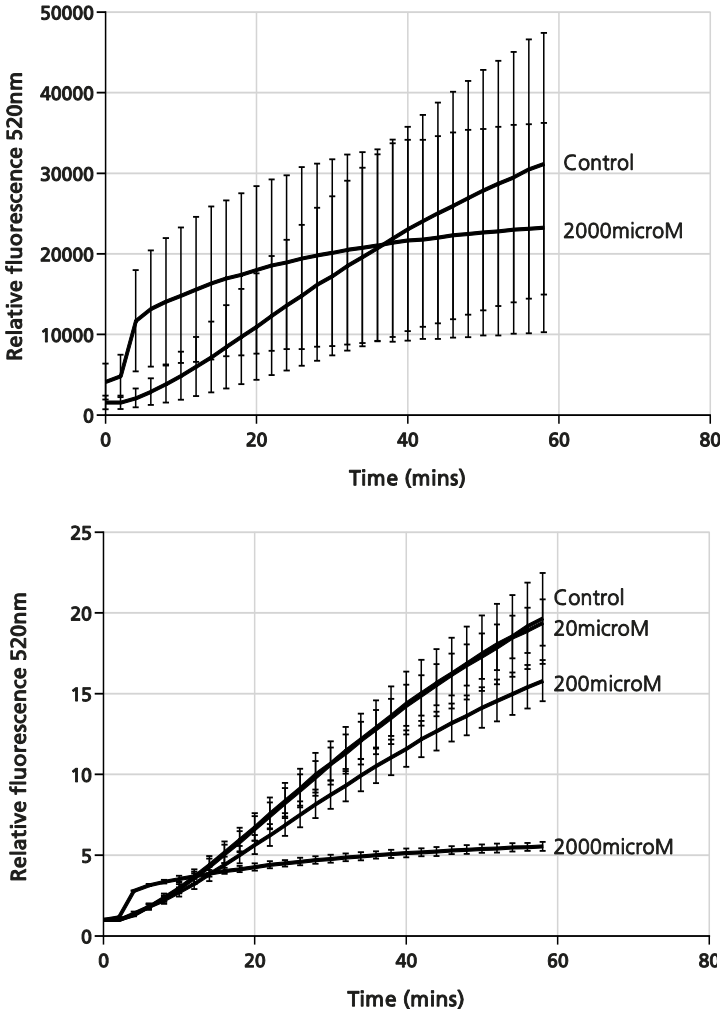

Top panel: Absolute blank corrected increase in fluorescence. Intermediate concentrations of ferrous sulphate (20 and 200μM) are excluded for clarity
Bottom panel: Blank corrected increase in fluorescence proportional to the starting fluorescence of each condition
Lines represent the mean of triplicate wells for each condition. Error bars show SD.

3.6.1.6 NADPH oxidase positive control

Physiological controls for the intracellular oxidation assay would be improved by a more physiological positive control. In monocytes and macrophages, stimulation of the NADPH oxidase mechanism would provide this. A number of compounds are known to cause assembly and activation of NADPH oxidase. Three were investigated: phorbol myristate acetate (PMA. Sigma, UK. Cat#P1585); apocynin (acetovanillone. Sigma, UK. Cat#A10809); N-Formyl-Met-Leu-Phe (fMLP. Sigma, UK . Cat# F3506). PMA is an non-specific activator of protein kinase C, with wide ranging effects including phagosome-lysosome fusion. fMLP is a peptide known to induce chemotaxis and activate macrophages. Apocynin is a vanillin, and acts as a selective inhibitor of NADPH oxidase derived from plant sources.

PBMCs were loaded with 25μM carboxy-H_2DCFDAas detailed in section 0. This experiment was performed using PBMCs in suspension *i.e.* before adherence in order to test the hypothesis that cell number variation due to cell culture caused the wide margins of error around the mean seen in section 3.6.1.5, and to select which positive controls were most promising. After loading, cells were washed three times in PBS and loaded into 96 well plates at $8x10^4$ cells/well, and fluorescence of the reporter fluorophore measured over 60 minutes.

Figure 3-16 shows an insignificant rise in oxidant production of cells exposed to vehicle (DMSO) compared to control. fMLP at 1μM appears to give rise to oxidant response, but less than the heretofore used hydrogen peroxide positive control. PMA was superior to H_2O_2. Standard deviations around the mean values were considerably tighter than experiment 3.6.1.5.

Figure 3-16 Oxidation of carboxy-H_2DCFDA in PBMCs: evaluation of cellular positive controls

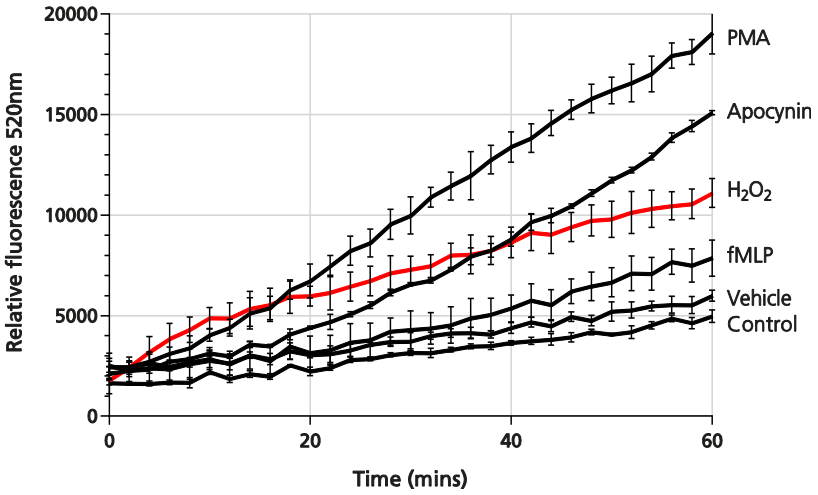

PBMCs in suspension were loaded with 25μM carboxy-H_2DCFDA, washed and incubated with various stimuli. Fluorescence was tracked over one hour. Lines represent the mean of triplicate wells. Error bars are SD. Final concentrations of stimuli are: control (media only); vehicle (DMSO, 0.2%); fMLP 10μM; PMA 2μM; Apocynin 300μM.

Apocynin was, surprisingly for a documented inhibitor of NADPH oxidase subunit assembly[404], associated with significant fluorescence increases. These data are consist with published literature which suggests that phagocytes and non-phagocytes respond differently to apocynin; although in both fibroblasts and macrophages there is initial stimulation of reactive oxygen species, in fibroblasts this continues. In macrophages, perhaps due to the presence of peroxidases, apocynin is postulated to be converted into an inhibitor of NADPH oxidase[405, 406]. Due to the issues of auto-oxidation described above, any early increase in ROS production might feed forward to a strong positive fluorescence signal despite later changes in apocynin behaviour in the cell.

These findings were replicated in alveolar macrophages in adherent cell culture (day 3 after isolation from BAL); results are shown in Figure 3-17. In this cell type, fMLP and DMSO caused small but non-significant increases in oxidation. PMA and apocynin approximated the effect of H_2O_2. These data are consistent with findings

that PMA is not as robust a positive control in alveolar macrophages compared with its use in monocytes and neutrophils[396]. Future use of positive controls used both PMA and apocynin.

Figure 3-17 Oxidation of carboxy-H2DCFDA in AMs: evaluation of cellular positive controls

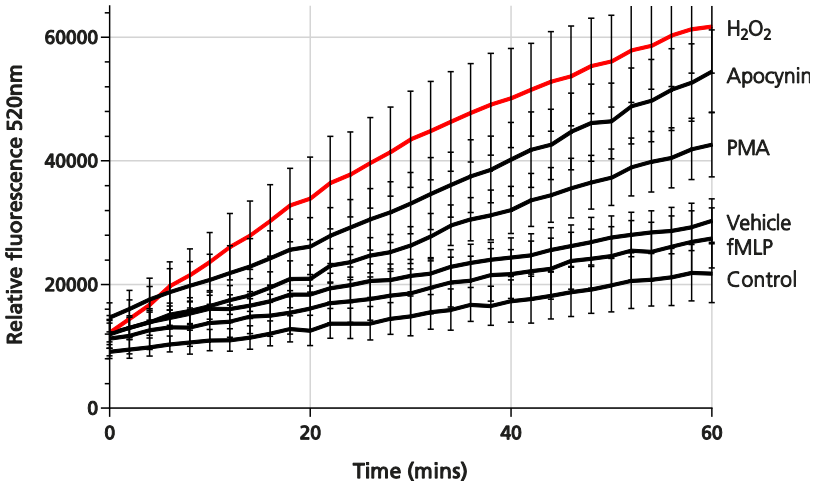

AMs in adherent cell culture were loaded with 25μM carboxy-H2DCFDA, washed and incubated with various stimuli. Fluorescence was tracked over one hour. Lines represent the mean of triplicate wells. Error bars are SD. Final concentrations of stimuli are: control (media only); vehicle (DMSO, 0.2%); fMLP 10μM; PMA 2μM; Apocynin 300μM.

3.6.1.7 Inhibition of glutathione peroxidase – enhancing intracellular oxidation

In addition to a robust positive control, inclusion of a condition which decreased cellular antioxidant capacity would be useful. The effect of buthionine sulfoximine (BSO) is reported in section 0. Here, an inhibitor of glutathione peroxidase, mercaptosuccinate (Sigma, UK. Cat#M6182) underwent preliminary testing in a similar dose range to other experiments involving alveolar macrophages[407]. Alveolar macrophages on day 2 of adherent cell culture after isolation were pre-incubated with mercaptosuccinate 0-1500μM in culture medium for 1 hour. After a single wash, media were replaced with 25μM carboxy-H2DCFDA for a further hour. Each well was washed three times replaced with RPMI-1640 without phenol red, and positive controls added (PMA 2μM, H_2O_2 100μM, Apocynin 300μM final

concentrations). Fluorescence was recorded at 60 minutes; results are shown in Figure 3-18. Contrary to the expected result (that mercaptosuccinate would increase oxidation effect), there appeared to be a dose dependent decrease in fluorescence of the reporter, especially notable with apocynin as the stimulant. Explanations for this might include: deterioration in cell function *i.e.* toxicity of the mercaptosuccinate; rapid increase (over 2 hours) in the intracellular concentrations of other antioxidant as a result of mercaptosuccinate *e.g.* glutathione synthesis. Despite its introduction to a buffered solution, mercaptosuccinate altered the pH of cell medium as observed by the yellowing of phenol red. This suggests the former explanation is more likely. In view of the likely toxicity, mercaptosuccinate was not used in further experiments.

Figure 3-18 ***The effect of a glutathione peroxidase antagonist on intracellular oxidation of carboxy-H_2DCFDA in alveolar macrophages.***

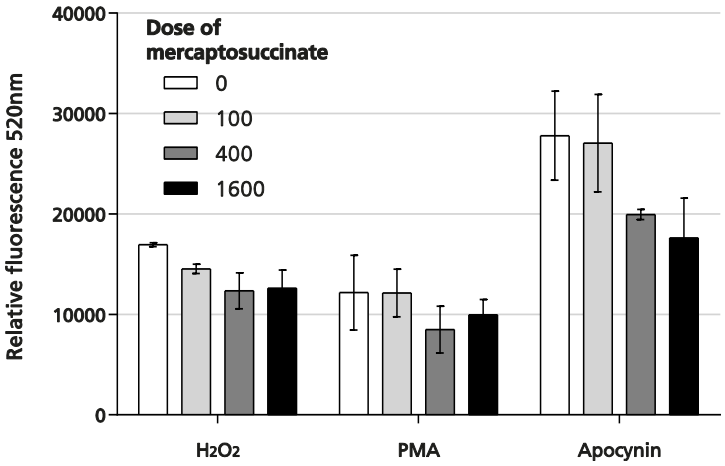

Cells at 5x10⁴/well were preincubated with varying doses of mercaptosuccinate (0-1600μM) for 1 hour, followed by washing and loading for 1 hour with carboxy-H_2DCFDA 25μM. After 3 further washes, positive controls were added, and fluorescence at 520nm measured over 1 hour. Bars represent mean values of triplicate wells, with error bars indicating SDs.

3.6.1.8 Oxidation as measured by carboxy-H_2DCFDA – concluding remarks

Using DCFH, previous work has described that when comparing different phagocytes, polymorphonuclear cells had the greatest capacity to produce oxidants, with monocytes less capable, and alveolar macrophages the least oxidant producing cell type of the three[197]. However, although this data probably accurately describes propensity to oxidative stress (within the cytoplasm), this does not necessarily correlate with local concentration of superoxide and hydrogen peroxide within the phagosome *i.e.* that response which is antibacterial. As a result of preliminary investigation detailed here, cytoplasmic reporter methods were dropped in favour of a more targeted method using reporter beads taken into the phagosomal compartment (see 3.8), which have the following benefits:

- Specifically report the intraphagosomal rather than cytoplasmic conditions and therefore reflect more accurately antibacterial capacity
- Are not susceptible to variation relating to cell loading and cytoplasmic retention of the fluorescent reporter

3.7 BSO toxicity – dosing

We sought a method for causing glutathione depletion in monocytes and macrophages which could be used as a probe for the effect of oxidative stress.

Buthionine sulfoximine is a specific inhibitor of γ-glutamylcysteine synthetase and has been shown to alter macrophage behaviour and function by causing intracellular glutathione depletion, and a relatively more oxidising environment. Specifically, BSO can reduce activation and iNOS activity[408], although in other studies enhances inflammatory cytokine production in human alveolar macrophages[304]. Doses used in preliminary experiments were taken from previous macrophage studies[409].

Initial studies were undertaken to optimise the dose, and to confirm a reasonable time frame for BSO treatment of ex-vivo alveolar macrophages. Specific concerns were:

1. To identify the degree of glutathione change after BSO treatment (see 3.7.1)
2. To check that this did not lead to significant short term cell toxicity which might affect experimental results due to loss of adherence of cells in culture

3.7.1 BSO effect on glutathione

The effect of BSO on intracellular glutathione concentration was assessed in *ex vivo* human alveolar macrophages. On the day of isolation, these were plated at $3x10^6$/well, and rested overnight in RPMI-1640 medium with 10% FCS. The next day, and for 24 hours, the macrophages were incubated with medium with and without additional BSO (0.2mM and 0.5mM). At this point, the adherent cells were washed twice in PBS. 500μL of 5% 5-sulfasalicylic acid was added, and the

suspension used according to the glutathione assay method detailed in section 2.6. Concentrations of both reduced and oxidised forms were calculated from the recycling assay (see Figure 3-19 and Figure 3-20). Maximal reduction in glutathione appeared to require 0.5mM (55% reduction from baseline after 24 hours, although 0.2mM produced a 51% reduction. HAMs from one individual appeared unaffected by BSO. Although numbers in this preliminary study were few, both doses of BSO were concluded to have a significant reduction in total glutathione.

Levels of oxidised glutathione were, generally, concomitantly reduced. This is seen in Figure 3-20, where although total glutathione availability was reduced on average to 30.4% of original values, the proportion of oxidised glutathione showed no consistent pattern, and in all four volunteers remained under 5%. Based on the mechanism of action of BSO *i.e.* reducing the intracellular synthesis of glutathione, these patterns might be expected, provided the mechanisms for recycling oxidised glutathione to reduced glutathione were intact. The data supports this in that total glutathione was reduced, but oxidised glutathione was unchanged as a proportion of the total.

Figure 3-19 Effect of buthionine sulfoximine on intracellular total concentration of glutathione in ex vivo alveolar macrophages.

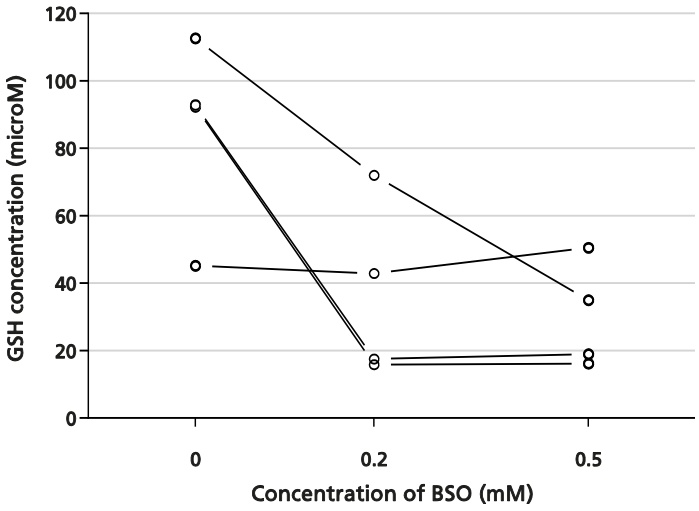

HAMs exposed to BSO in culture medium for 24 hours. Glutathione concentration is not normalised to protein due to the comparable cell numbers in each condition ($3x10^6$ macrophages per condition).

Figure 3-20 Effect of buthionine sulfoximine on the proportion of intracellular glutathione in oxidised form in ex vivo alveolar macrophages.

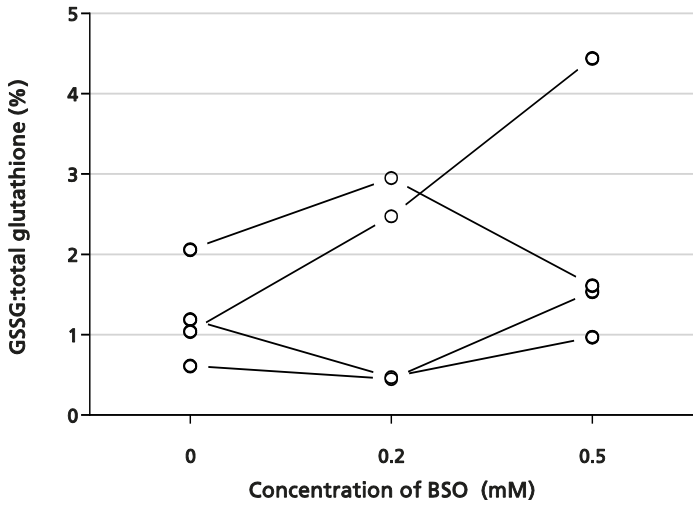

HAMs exposed to BSO in culture medium for 24 hours.

3.7.2 BSO toxicity

Toxicity to cells was assessed by the degree to which intracellular lactate dehydrogenase was lost into culture medium. One widely used method uses as a primary reaction the reduction of NAD by LDH (see Equation 20)

Equation 20: $$NAD^+ + lactate \xrightarrow[lactate\ dehydrogenase]{} NADH + H^+ + pyruvate$$

Subsequent catalytic reduction of a yellow tetrazolium salt by NADH results is a blue formazan product (see Equation 21)

Equation 21: $$NADH + iodonitrotetrazolium \xrightarrow[diaphorase]{} NAD^+ + formazan$$

Absorbance maximum of formazan is 492nm – over a fixed time, the increase in absorption at this wavelength is proportional to the initial LDH concentration, and by implication the number of cells with disrupted plasma membranes[410].

Alveolar macrophages were incubated on the day if isolation in RPMI-1640 medium with 10% FBS at 10^6/well, and with varying concentrations of BSO in triplicates. After 24 hours, culture supernatants were removed and frozen for later testing. Alveolar macrophages which had been cultured in RPMI-1640 medium with 10% FBS only were lysed in water with 1% Triton-X. The resulting lysate was vortexed vigorously, spun at 10000g for 5 minutes in a microcentrifuge (Hereus, UK) and the supernatant used as a positive control. Relative LDH concentrations were measured by a kit according to the manufacturer's instructions (Sigma, UK. Cat#TOX7). There was no increased release of LDH in either BSO 0.2mM or BSO 0.5mM compared with control (p=0.70 and p=0.50 respectively by paired t-test). There was increasing variation in LDH response as BSO dose increases which might represent the uncertainty around the estimate of treatment effect, or suggest a dose response. As a result of these data, and the similar efficacies of both doses of BSO in reducing glutathione concentration, the dose of 0.2mM was chosen for future experiments.

Figure 3-21 Toxicity of butathionine sulfoximine to alveolar macrophages.

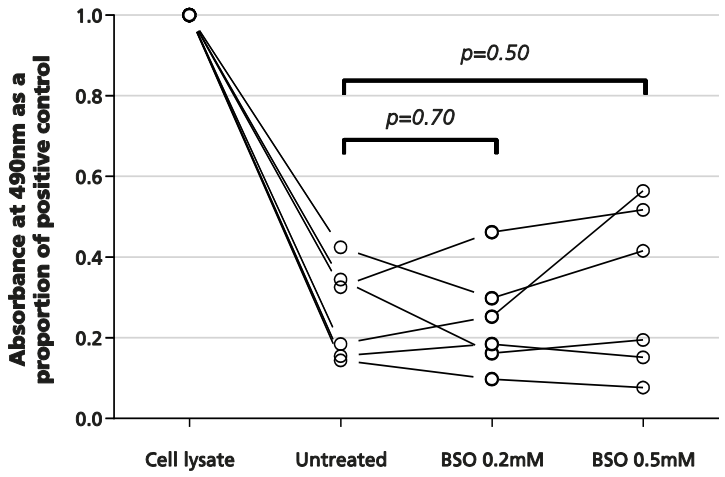

LDH content of culture supernatant after 24 hour exposure of alveolar macrophages to BSO (n=6). p values represent paired t-test results.

3.8 Intraphagosomal oxidative burst measurement

Methods for assessing intraphagosomal function have been developed by Prof Russell's group[375]. As described, of 2',7'-dichlorodihydrofluorescein diacetate succinimidyl ester (H_2DFCDA-SE), is used as a reporter for oxidation.

A number of issues were addressed in order to improve the appropriateness of the published method to the small numbers of alveolar macrophages:

Table 3-4 Method development issues with the use of intraphagosomal reporter beads

Issue	Explanation	Refer to
Cell removal	Small number of cells are available, which should remain intact after removal from adherent culture in order that indices of phagocytosis might be correctly interpreted	Section 3.4
Positive control or bead QA	Oxidation sensitive substances are expected to degrade over time, introducing systematic errors. Beads should be checked as viable at the time of use to ensure consistency	Section 3.8.3.1
Interference of black carbon	Where an output is dependent on light emission, confounding of results might occur if cells from different individuals have inherently different light transmissions e.g. due to carbon or particulate content	Section 3.8.1

3.8.1 Particulate effect on light transmission

Alveolar macrophages when examined by transmission light microscopy, or by digital image analysis (see section 2.10) show heterogeneity in terms of particulate content; this is both between and within volunteer samples. Any method which uses light absorption or emission to probe the character or function of these cells might necessarily be affected by the presence and concentration of these particulates.

The relative effect of various particles on light absorption was tested by generating serial dilutions in RPMI medium without phenol red. Particles were vortexed and sonicated prior to each dilution, and before introduction to 96 well plates for absorbance measurement in a plate reader (BMG Omega). Absorption at 485nm was recorded, and is shown in Figure 3-22. Wood smoke was used as the most relevant particulate to the Malawi *in vivo* exposures. Specific particulates were: fine carbon black (as Huber 990, Haeffner & Co Ltd, Chepstow, UK, donated by Dr R Duffin, University of Edinburgh), mean diameter 260.3nm, surface area 7.9m^3/g; ultrafine carbon black (as Printex 90, donated by Degussa GmBH, Germany) as a

standardised microparticle, mean diameter 14.3nm, surface area 253.9m^3/g; wood smoke as described in section 2.11.

As expected with high surface area to volume ratio, the absorption was higher per unit weight for ultrafine carbon black compared with other particulates. [411]. Wood smoke was more similar to fine carbon black (less than one quarter of wood smoke particles have a diameter of <100nm even under smouldering conditions[412]; fine carbon black is a better approximation of wood particulates by this measure). The linear relationship between concentration and absorption for all three groups was expected, and this provided evidence that particulate suspension generation according to the devised method produced a relatively homogenous particle distribution with minimal clumping.

However, significant light absorption by the particles has the potential to cause error or bias in methods which use fluorescence reporting systems. Further work was therefore done to assess the likelihood of this interference, and is detailed below.

Figure 3-22 Absorbance at 485nm of particulate suspensions.

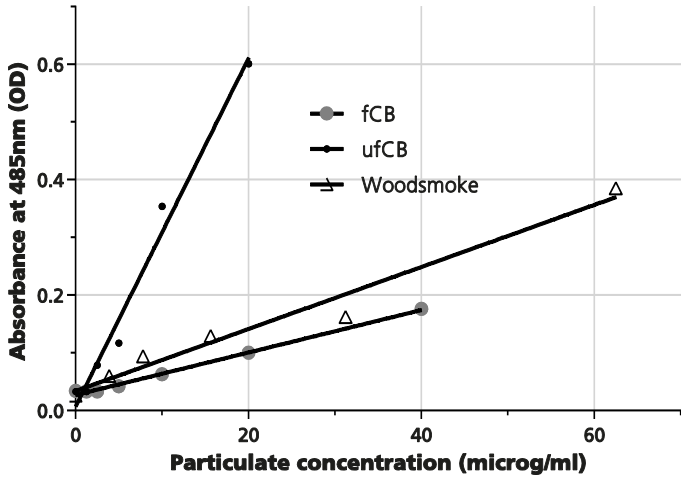

fCB = fine carbon black; ufCB = ultrafine carbon black. Solid black lines represent linear regression line.

3.8.2 Particulate effect on fluorescence measurements

In terms of light absorption, within the scope of this project, the most likely assay to be affected would be the tests of intraphagosomal function. In order to assess this, wood smoke particulates in at a concentration of 50µg/mL in aqueous suspension were introduced to clear 96 well plates. Absorption of light at 10nm intervals between 350 and 650nm were recorded using a plate reader (BMG Omega). These data are represented in Figure 3-23, overlaid on information on the absorbance and emission spectra of the relevant fluorochromes.

Wood smoke might interfere with fluorescence signals by absorbing electromagnetic spectrum radiation between the excitation source and fluorophore, or between the fluorophore and detector. Due to these multiple interactions, deduction of actual effect is complex. However, the intraphagosomal activity assays use as a metric the ratio of fluorescence of AF405 to DCF, and an estimate of effect may be made thus:

- The excitation wavelengths within the flow cytometer are 405nm and 488nm
- The absorbance of wood smoke at these wavelengths is taken from the experiment as 0.2915 and 0.2340 respectively
- The detection filter bandwidths are 450/50 and 530/40
- The mean absorbance of wood smoke in these bands (425-475nm and 510-550nm) is calculated from the experiment as 0.2596 and 0.2418 respectively
- The change in ratio of DCF to AF405 fluorescence as a direct result of wood smoke is likely to lie between 0.2596/0.2418 = 1.07 times and 0.2915/0.2340 = 1.25 times.

The effect of wood smoke is likely to be to increase the relative fluorescence of DCF compared with AF405. The estimate of effect given here is highly cautious: this acellular model exceeds considerably, by visual appearances, the most densely loaded macrophages. It is concluded that the effects of differential electromagnetic spectrum absorption are unlikely to have material effects on the results or interpretation of further experiments.

Figure 3-23 Absorption spectrum of wood smoke particulates relative to Alexa Fluor 405 (AF405) and dichlorofluoroscein (DCF)

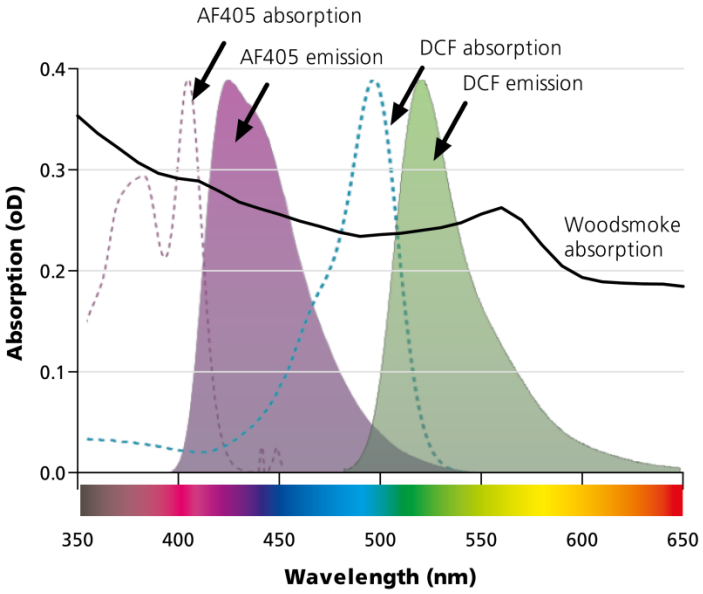

Solid black line indicates the absorbance of woodsmoke particles. Dotted lines represent the absorption spectra of AF405 and DCF. Shaded areas represent emission spectra of AF405 and DCF. Data for AF405 and DCF taken from BD website[413]. Absorption values are only relevant to woodsmoke.

3.8.3 Pre-oxidising H_2DCFDA-SE beads for positive control

One of the difficulties of positive controls when using these beads is that the fluorophore is esterified to improve cellular retention of the fluorescent product. This structure makes the fluorophore initially relatively insensitive to oxidation which has benefits in terms of the shelf life of reagent and improving artefact due to prolonged storage. In macrophages, after internalisation, the action of intracellular esterases exposes the oxidation site of the fluorophore, allowing the oxidation dependent increase in fluorescence to take place.

In order to maximally oxidise the Oxyburst fluorophore, either chemical or enzymatic removal of the two acetate groups should be followed by continuous exposure to hydrogen peroxide or another oxidant for a period of time. The latter might be maintained at a constant concentration by the action of glucose oxidase[414]. However, as a daily method for testing oxidation sensitivity this is not pragmatic,

and bolus addition of hydrogen peroxide was chosen as the oxidant delivery method as in previously published methods[375]. Preliminary tests of bead oxidation following both chemical and biological methods for de-esterification were performed with the intention of trying to improve the existing practice for checking bead activity *i.e.* adding 1% hydrogen peroxide directly to untreated H_2DCFDA-SE coated beads. Both chemical and biological means were examined as alternatives using hydroxylamine treatment and exposure to leucocyte lysate respectively.

3.8.3.1 Chemical de-esterification with hydroxylamine

Hydrolysis with hydroxylamine was done by incubation of bead suspension in 0.15M hydroxylamine hydrochloride ($NH_2OH.HCl$ Sigma, UK. Cat#55459) in aqueous solution at pH 8.5 for 1 hour at room temperature[415]. Each condition was performed in duplicate in a 96 well plate with 1µL of beads per well. A single bolus of hydrogen peroxide (250mM final concentration) was added to each well in either water or citric saline. The latter was to test the hypothesis that it would protect beads from further oxidation after cells were removed from culture plates (see 3.4.3). At all times, reagents were protected from light. Fluorescence of the beads was measured using a plate reader (BMG Omega) with excitation wavelength of 488nm and emission of 520nm (see Figure 3-24).

Untreated beads, were relatively resistant to oxidation: fluorescence increased to 1.48x baseline after treatment with hydrogen peroxide: Both sets of de-esterified beads were, at baseline, more fluorescent that untreated beads (2.14x in water and 2.59x in citrate buffer). In pure aqueous solution, H_2O_2 caused de-esterified beads' fluorescence to increase to 5.63x baseline compared with 2.61x where citrate was present. This experiment demonstrated that: 1) following de-esterification, beads became more sensitive to oxidation; 3) the presence of citrate protected beads in suspension from oxidation.

Figure 3-24 Fluorescence of H_2DCFDA-SE coated beads in a cell free system - the effect of oxidation on untreated and chemically de-esterified beads

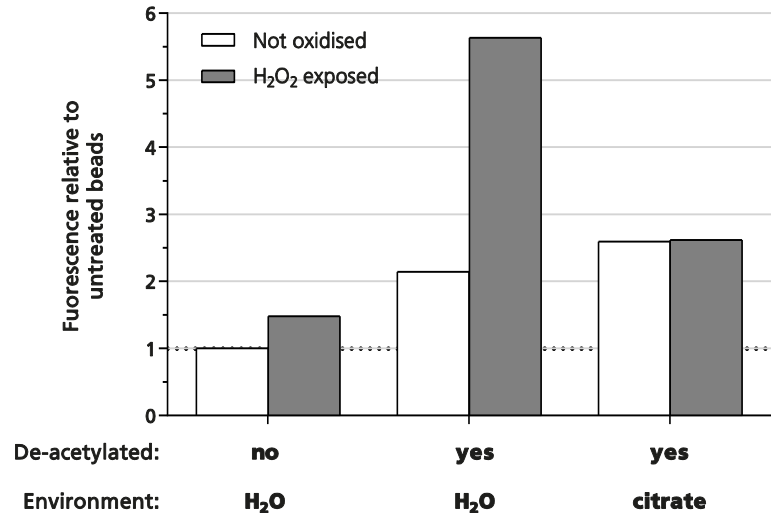

De-esterified beads were incubated with 0.15M hydroxylamine. Bars show an average fluorescence of 3 wells normalised to control (esterified, without H_2O_2). Oxidation was performed with a bolus of 250mM hydrogen peroxide.

3.8.3.2 Biological / enzymatic de-esterification

PBMCs were derived from 20mL fresh whole blood by density centrifugation (see 2.21). This cell suspension was lysed in 2mL PBS by vigorous repeated passage through a 22G needle in the presence of 0.1% Tween 20 (Sigma, UK. Cat#P2287). The supernatant was removed following centrifugation at 10000rpm for 5 minutes. Thereafter 5µL of beads were added to 100µL supernatant for 30minutes at 37°C. The pH of the suspension was 6.6. Control beads were similarly treated except by substitution of PBS for cell lysate supernatant. Beads were washed twice in PBS before 1% hydrogen peroxide (final concentration) was added. Fluorescence of both reporter and calibrator were measured by flow cytometry using a Cyan ADP machine (see Figure 3-25). Similarly experiments were performed using beads exposed to hydrogen peroxide but without prior incubation with cell lysate supernatant.

Figure 3-25 Flow cytometry plot of reporter beads before and after de-esterification and oxidation

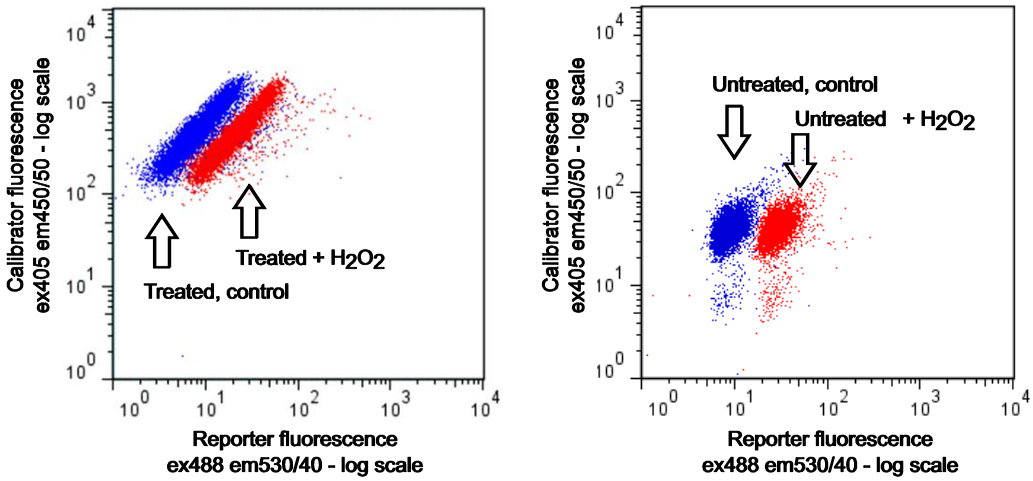

Left panel: Latex beads coated with both H2DCFDA-SE (reporter fluorophore) and Alexa 405 (calibrator fluorophore) were incubated either in PBS (control, displayed blue) or PBMC extract (a source of intracellular esterases, displayed red). Rightward shift represents increased oxidation of H2DCFDA-SE Right panel: Beads similarly treated with control or hydrogen peroxide, but without de-esterification. NB: Dissimilar acquisition settings do not allow direct comparison of left and right panels.

Where de-esterification had been attempted with cell lysate supernatant, the fluorescence of the calibrator compound changed as a result of hydrogen peroxide treatment (reduction of 5.8%, $p<0.0001$ by t-test) presumably due to degradation of Alexa 405. However the magnitude of this change is very small compared with that induced in the reporter (increase of 2.4 fold over control, $p<0.0001$ by t-test). Thus the use of calibrator fluorescence as a denominator in the activity index calculations is justified (see 2.19). Where de-esterification was not attempted, the beads behaved similarly with respect to reporter (3.1 fold increase, $p<0.0001$) but changes in calibrator fluorescence were not significant (1% fall, $p=31$ by t-test). It was concluded firstly that exposure to cell lysates rather than oxidation *per se* degraded the calibrator. Secondly, although oxidant response of the reporter is blunted without de-esterification (see Figure 3-24), direct addition of hydrogen peroxide produced a slightly superior effect when beads had not been exposed to cell lysates. There may be a number of possible explanations. Firstly, monocytes have limited

esterase activity compared with macrophages[398], although still sufficient for significant hydrolysis[416]. Secondly, that this protocol released insufficient non-specific esterases, or that esterase inhibitors in addition to esterases were released; these hypotheses have not been tested.

Positive controls for bead activity in further experiments therefore used hydrogen peroxide treatment alone.

3.8.4 Additional effect of H_2O_2 after de-esterification in macrophages

Although de-esterification was relatively unsuccessful using cell lysates, it was expected that within phagosomes it would be maximal. The effect of hydrogen peroxide on beads thus exposed was tested in order to determine if the positive control might be improved.

Ex vivo alveolar macrophages were used on the day of bronchoscopy. Reporter beads with H2DCFDA-SE were used according to the method given in section 2.19. Synthesis of the flow cytometry data from one individual is given in Figure 3-26. Compared with either cells or beads alone, a rightward shift in the reporter fluorescence histogram is noted in the 60 minute exposed beads and further in 60 minute exposed beads subsequently treated with 1% hydrogen peroxide. This graph suggests that: intraphagosomal oxidation is taking place, because there is a rightward shift in the fluorescence of cells containing beads compared to unexposed cells and beads alone; the beads response to oxidation is not saturated in this individual because further oxidation is possible with H_2O_2; there is a heterogeneous oxidant response within the macrophage population, because the peaks are broad and irregular compared with controls. Compared with beads alone, there was a 3.31 fold increase in mean reporter fluorescence of cells with beads, and 7.11 fold increase in cells with beads treated with hydrogen peroxide. On this basis, future

positive controls contained (where cell numbers allowed) cells exposed to beads followed by H_2O_2. As shown in section 0 however, there is reason to suspect that the degree of additional chemical oxidation by H_2O_2 may be strongly altered by the presence of cellular antioxidant, which shows considerable interpersonal variation. Its use as a control is therefore limited, although it does provide reassurance that beads remain responsive to oxidation after some time in storage.

Figure 3-26 Fluorescence of reporter beads in alveolar macrophages.

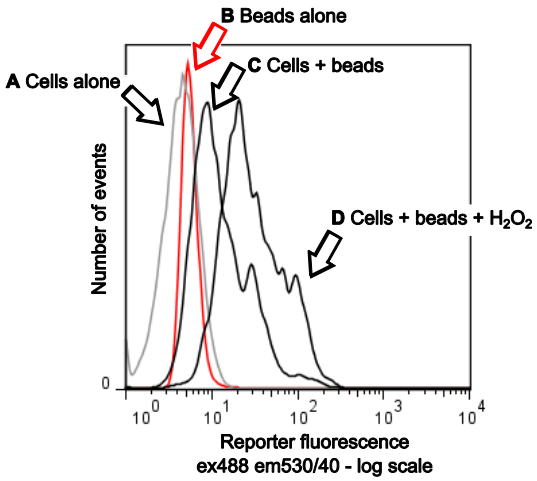

Data from flow cytometry are represented in four overlaid histogram plots of H_2DCFDA band fluorescence.
A Cells alone, gated on macrophages according to FSC and SSC properties
B Beads alone, no gating
C Beads incubated with cells for 60 minutes using macrophage gate in A and child gating on calibration^{high} population
D Beads incubated with cells for 60 minutes, with subsequent addition of 1% H_2O_2, gated as C

3.9 Dose response of wood smoke

Data from this section (3.9) was experimentally derived and analysed by Dr Fullerton. It is presented here to provide background information to the *in vitro* work done in this study.

Wood smoke extract is used throughout this study for ex vivo challenge of HAM and MDM. In order to inform on the appropriate concentration to be used, particulate loading experiments were performed using MDMs (see Figure 3-27).

Monocyte derived macrophages were derived from Buffy coat blood (UK Blood Transfusion Service). This was diluted 1:1 in normal saline, layered onto Lymphoprep® gradient separation (Axis-Shield UK) and centrifuged according to the manufacturer's directions. Cells were seeded in a 24-well plate in RPMI 1640 supplemented with 10% FBS and 2mM L-glutamine. Cells were cultured on borosilicate glass coverslips at 37ºC in 5% CO2 for 10 days. Media was changed after 24 hours and every 3 days to remove non-adherent cells leaving MDMs adherent to the coverslips in each well. Wood smoke particles (see section 2.11) were added in fresh media after 10 days of adherent cell culture at doses of 5, 10, 50 and 100μg/mL. After 5 hours, the coverslips were washed twice in PBS, fixed, permeabilised and stained. Staining and subsequent analysis of particulate density was performed as described in section 2.10.

There was a dose dependent uptake of particulate matter after challenge with wood smoke extract, from 1.5% with 5μg/mL to 16.2% with 100μg/mL. Unpublished data from our group demonstrate a similarity of response between MDM and HAM in terms of particulate density after in vitro challenge.

There is a dose dependent relationship in MDMs between the concentration of wood smoke particles added to culture medium, and the resulting cellular particulate density. Fifty micrograms per mL was chosen as the dose to be used subsequently, based on the observation that this produced particulate densities similar to those seen in the highest exposed Malawian HAMs (around 10%) and for consistency with previous work in our group.

Figure 3-27 Dose dependent effect of wood smoke concentration on particulate density in monocyte derived macrophages

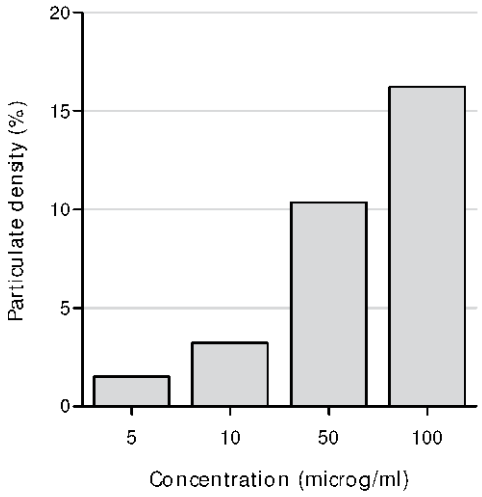

Monocyte derived macrophages at day 10 challenged for five hours with varying concentrations of wood smoke extract (n=5).

3.10 *In vitro* effect of wood smoke particles, LPS and bacterial culture supernatants on glutathione

Ex vivo alveolar macrophages were used to investigate the effect of particulates and inflammatory stimuli on redox balance as measured by relative oxidised glutathione levels. Wood smoke extract used throughout this project derives from the same batch of filters, processed at the same time using the same equipment. In order to test the hypothesis that this particulate suspension could cause oxidative stress, ex vivo alveolar macrophages were exposed at 50μg/mL. Cells were harvested, processed and plated into 6 well plates at $3x10^6$/well. After 18 hours of adherent culture, cells were washed in warm culture medium (RPMI-1640) and then incubated at 37°C with medium only, or 50μg/mL re-suspended wood smoke particles (see section 2.11 for preparation). After 20 minutes, cells were scraped into ice cold 5% sulfasalicylic acid and assayed for oxidised and reduced glutathione, and total protein as previously described in section 2.6. Change in oxidised glutathione was tested using paired t-tests.

Figure 3-28 Effect of wood smoke and inflammatory stimuli on intracellular oxidised glutathione concentrations in ex vivo alveolar macrophages

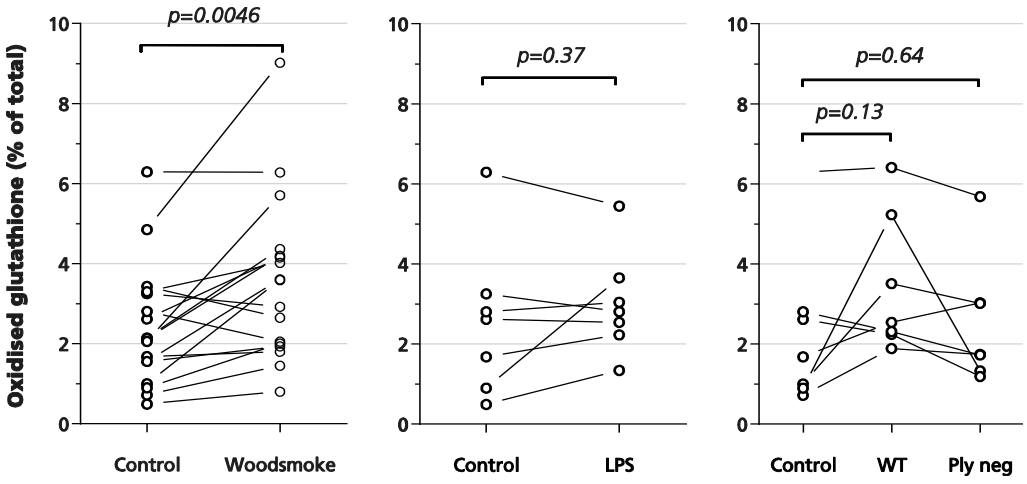

Statistics: Paired t-test used for comparisons. n=7 for LPS and pneumococcal analyses. n=17 for wood smoke analysis. Abbreviations: LPS lipopolysaccharide; WT and Ply neg culture supernatant from Streptococcus pneumoniae sertoptype D39 wildtype and pneumolysin deficient respectively.

As seen from Figure 3-28, at 20 minutes the proportion of oxidised glutathione had increased from a baseline mean of 2.40% to 3.56% (p=0.0046). There was no change in those cells exposed to LPS (mean 2.57% to 3.01%, p=0.37). Exposure to supernatants of both wild type *Streptococcus pneumoniae* and that of the pneumolysin deficient strain did not affect the proportion of oxidised glutathione.

This established *in vitro* evidence that relevant particulate exposure (*i.e.* respirable wood smoke particles) can produce redox responses in human alveolar macrophages, and that this is likely to be independent of the effect of bacterial endotoxin (as seen from the inconsistent response to LPS).

4 Redox balance in the human alveolar macrophage

4.1 Introduction

The redox state of a cell has broad implications for its behaviour and function, as described in section 1.2. It has been well described in disease states (cigarette smoking[417], asthma[418], pulmonary vascular disease[419], cystic fibrosis[420], ventilator associated pneumonia[326], Farmer's lung[421] and HIV[422]), and in a number of specific exposures (ozone[423], glass dust exposure[424]). No such study has been undertaken within a population of healthy people *at risk* of redox alterations due to high levels of environmental particulates.

This section examines such individuals, in the context of exposure to household air pollution from the combustion of biomass fuels. Comparison is made with unexposed individuals, and with cigarette smokers who are known to exhibit both oxidative stress and compensatory upregulation of antioxidant systems. The study has been performed in the UK and in Malawi.

4.1.1 *In vivo* studies of alveolar redox balance

In vitro studies of particulate exposure lead to the expectation that individuals exposed to wood smoke and other products of biomass fuel combustion are likely to demonstrate relatively high levels of alveolar oxidative stress[76, 82, 84, 134, 425, 426]. In healthy individuals, the effect of *in vivo* wood smoke exposure has been studied in controlled environments. Barregard et al subjected individuals in a chamber to four sessions of wood smoke exposure at a $PM_{2.5}$ concentration of 240-280μ/m^3. After hour long exposures, lipid peroxidation and exhaled nitric oxide levels were raised compared with air exposed controls[91]. Bronchoscopic studies are few, but demonstrated that after 3 hours, 224$\mu g/m^3$ wood smoke causes increase in epithelial

lining fluid glutathione, suggestive of mobilisation of antioxidant as a protective mechanism against local oxidative stress.

A study of atopic individuals thought to be more prone to airway oxidative stress have shown no increase in exhaled nitric oxide or short term pulmonary function after 3 hours of 400μg/m^3 wood smoke[427]. Another 3 hour 354microg/m^3 exposure study failed to demonstrate evidence of oxidative stress or inflammatory response in peripheral leucocytes[428]. Responses to other particulates including concentrated ambient particles and diesel exhaust particulates are detailed in Table 1-2. At lower particulate concentrations, these exposures demonstrate airway antioxidant upregulation[429, 430], and glutathione mobilisation to the airway[120] with measurable airway inflammation[120] and systemic inflammatory responses[431].

These controlled exposure studies in humans have carefully defined acute exposure to particulates. However, practical limitations of the wood smoke experiments limit the generalizability to chronic "natural" exposures seen from human populations using biomass fuel in the home:

1. Indoor air particulate concentrations have mean PM_{10} concentrations 300μg/m^3 to 3000μg/m^3, and peaks reaching 30000μg/m^3[9]. Such high exposures are difficult to model in the laboratory and might cause concern regarding harm to the research volunteers
2. Chronic exposures behave differently to acute ones, particularly with respect to redox balance. Acute exposures and disease processes tend to reduce alveolar concentrations of glutathione and enzymatic antioxidants GPx and catalase (such as pneumonia[326] and acute cigarette smoke exposure[417]). Generally, chronic exposures potentiate upregulation mechanisms, resulting in higher levels than unexposed individuals (chronic cigarette smoke exposure[417]), although reach a point in disease progression after which a decline occurs (asthma[194], COPD[432]).
3. The distinction between intracellular and extracellular redox balance in *ex vivo* studies cannot always be defined, for example where exhaled breath concentrations are measured. Bronchoscopic studies have often used whole BAL as an indicator or airway redox balance. This mixture of extracellular fluid (predominantly formed by epithelial cells) and intracellular fluid (predominantly macrophages) gives an overview, but is insufficient to explain the effect of redox balance on innate immunity. Extracellular glutathione has been extensively studied in humans[185], but intracellular glutathione studies have been mostly limited to animal and cell line models, and to cigarette smokers.

Ex vivo study of human exposure, although difficult, is therefore required to complement the current literature.

4.1.2 Tissue culture models of alveolar redox balance

In examining the issues of redox balance with respect to cellular compartment, cell type and acute vs chronic exposure, tissue culture models of alveolar macrophages have some advantages in improving homogeneity, reducing complexity and avoiding the research need for bronchoscopy and bronchoalveolar lavage. One such model is monocyte derived macrophages (MDM) which are peripheral blood mononuclear cells in prolonged (7-14 days) of adherent culture. It is expected that in maturing from peripheral monocytes to adherent MDMs, cells move towards a macrophage phenotype, and this can be enhanced by the presence of GM-CSF in the culture medium. While AM are known to proliferate within the lung, contributing to the slow turnover kinetics[433], repopulation by monocytes has a role in replenishing numbers[434]. Alveolar macrophages are noted to have high antioxidant buffering capacity, and relative insensitivity to oxidants compared with monocytes[210]. Tissue culture models of macrophages often use PBMCs after extended adherent culture; the degree of similarity to primary tissue macrophages is investigated here.

4.1.3 Hypotheses

This chapter presents results relating to the following hypotheses:

1. Monocyte derived macrophages represent an adequate model of alveolar macrophages with respect to redox balance
2. Chronic alveolar redox balance may be described by a universal stress response *i.e.* high levels of oxidative stress is associated with a co-ordinated response leading to:
    a. Up-regulated intracellular and extracellular glutathione levels
    b. High proportions of total glutathione existing in oxidised form
    c. Up-regulated intracellular antioxidant enzyme activity (specifically glutathione peroxidase and superoxide dismutase)
    d. High levels of cellular lipid peroxidation
3. Enzymatic stress responses (glutathione peroxidase) are confined to the lung
4. Individuals living in Malawi have higher levels of oxidative stress than those in the UK due to higher levels of particulate exposure from domestic biomass fuel use

Within hypothesis 2, determinants of the degree of glutathione derangement and enzymatic upregulation are investigated.

4.2 Methods

4.2.1 Volunteers and recruitment

Healthy adults were recruited to this study in two sites; Liverpool, UK and Blantyre, Malawi. Potential volunteers were screened by medical interview and examination, spirometry and HIV testing as described in section 0.

Volunteers from Malawi underwent specific questioning relating to their socioeconomic status as this is likely to impact on their exposure to smoke from biomass fuel combustion[435], discussed in sections 1.1.4.2 and Table 4-2. Markers of socioeconomic status were chosen for compatibility with previous research projects

in Malawi, including items from the principle components analysis used by the Malawian Ministry of Health for resource allocation[436].

In order to improve the external validity of comparisons between UK and Malawi cohorts, in addition to healthy non-smokers, comparison was also made with UK cigarette smokers. This gives "positive control" individuals who are known to have alterations in their redox balance[437]. These individuals were screened identically to non-smokers, and were recruited if they smoked more than 10 cigarettes per day.

4.2.2 Spirometry

Spirometry was performed according to American Thoracic Society guidelines[438] using an ndd EasyOne World spirometer (ndd, Switzerland). Data for FEV_1 and FVC are presented as percentage of predicted rather than raw values. The use of z-scores, which have some advantages over percentage predicted values[439], has not been adopted here for two reasons: 1) there will be no longitudinal comparisons; 2) the lack of a local reference range for Malawians considerably lessens the advantages of z-scores. The same predicted ranges were used for all cohorts, but the ERS/ECCS normal reference range used takes into account age, sex and height with a correction factor of 0.88 for FEV_1 and FVC in black individuals.

4.2.3 Laboratory assays

Laboratory assays were carried out as described in section 2. For specific details, please see the following sections: glutathione (2.6); glutathione peroxidase (2.22); superoxide dismutase (2.22); protein concentration (2.14 and 2.15); plasma selenium (2.8); cellular particulate burden (2.10); lipid peroxidation (2.17).

GPx and SOD and haemoglobin were measured by Randox laboratories, UK. Plasma selenium was measured in the Royal Liverpool University Hospital, UK. All other assays were performed by the author.

Initially, oxidised glutathione was measured in the extracellular compartment of BAL. However, absolute levels were consistently below the limit of detection of the assay (results not shown).

4.2.4 Peripheral blood mononuclear cells and monocyte derived macrophage maturation

Peripheral blood mononuclear cells (PBMCs) were isolated from citrate anti-coagulated blood by density centrifugation as detailed in section 2.21, and cultured in 6 well plates at $6x10^6$ per well. At days 0 (2 hours), 1, 3, 5 and 7 after the initial adherence step, the contents of one well were scraped into 250μL phosphate buffered saline, and frozen at -80°C pending analysis. Cell culture medium from remaining wells was removed and replaced with fresh medium (RPMI 1640 + 10% FCS).

4.2.5 Bronchoscopy

Bronchoscopy was performed as described in section 2.5. Extracellular samples analyses for glutathione are reported as uncorrected results. For consistency with previous published literature, intracellular glutathione is here corrected to total protein of the sample as determined by the Lowry method.

4.2.5.1 Justification for presenting uncorrected glutathione results in extracellular samples

As bronchoalveolar lavage returns variable quantities of fluid, various devices are used to correct raw results. These include protein (for cellular samples) and urea (for extracellular samples). Extracellular samples were reported as raw results only, despite some authors using the urea method. This correction technique assumes that after instillation of the fluid, urea in the bronchoalveolar lining fluid is diluted, and that the extent of that dilution is proportional to the BAL to serum urea ratio. However, due to concentration gradient after fluid instillation, urea crosses the

capillary membrane into the alveolar space thereby violating the underlying assumption of a fixed ratio[440].

4.2.6 Statistical analysis

All analyses were performed using Stata v12 (StatCorp, USA).

MDM maturation glutathione and antioxidant enzyme levels are shown as connected dot plots for each individual donor. For comparison, a box blot is given to indicate levels found within human alveolar macrophages (from the Malawi cohort). Changes in levels over time in maturing MDMs are compared with Kruskal-Wallis one way analysis of variance. The usefulness of monocytes and MDMs as a model for redox balance in HAM is assessed by comparison of day 0 and day 7 MDMs with HAM using Mann-Whitney U test at α=0.05 significance level.

For comparisons of the human cohorts, t-tests and one way analysis of variance (ANOVA) is used to compare baseline characteristics where described by normally distributed continuous data. Where data do not follow normal distributions, Mann-Whitney U and Kruskal Wallis tests are employed. Categorical data are compared using Fisher's exact test.

One non-normally distributed variable (particulate loading) was normalised by log transformation for the purposes of all analyses in order that parametric tests could be used. In all other cases, such transformation did not improve the normality of distribution, and variables were therefore analysed using non-parametric tests.

Univariate analyses of predictors of glutathione, GPx and SOD were performed using linear regression against continuous variables and ordinal categorical variables. No correction for multiple analyses was made. A significance level of

p<0.1 was used to identify candidate associated variables. A model was then fitted using these variables, and refined by backward elimination, where variables were removed singularly based on Wald statistics using a cut-point of p=0.05.

Correlation of antioxidant enzyme activities in blood and urine were compared with linear regression with analysis of covariance (ANCOVA) testing for differences between groups. Cohorts from the UK and Malawi were compared with respect to glutathione peroxidase and lipid peroxides by t-test.

4.3 Results

4.3.1 Antioxidant systems in maturing monocyte derived macrophages

Representative images of the maturing cells are shown in Figure 4-1 showing the increase in size and irregularity of PBMCs over time indicating a transition towards the morphological appearances of macrophages.

Figure 4-1 Representative polarised light microscopy images of PBMC maturation in adherent culture

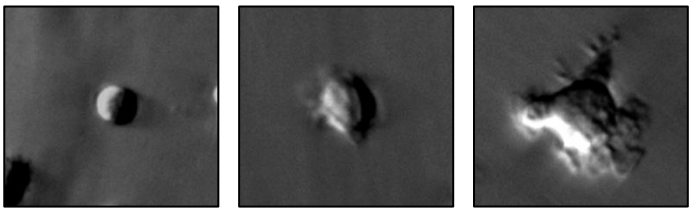

Day 1 *Day 3* *Day 7*

Images are taken at x40 magnification in all cases.

Cellular glutathione levels are shown in Figure 4-2. Median concentrations, when corrected for total protein, were 10.71nmol/mg (range 2.7 to 23.1) in the adherent monocytes day 0 compared with 20.09nmol/mg (IQR 11.58 to 27.19) in HAM, although this difference did not reach statistical significance (p=0.051). Significant variation was observed in PBMC glutathione content as previously reported: a

study of healthy volunteers found concentrations of 16.1nmol/mg ±SD 5.2)[441]. This may represent differing cell viabilities during culture, or variations in the proportion of monocytes within collected PBMCs. Over the first 24 hours, glutathione levels dropped in every sample, although five out of six showed subsequent increase from day 1 to day 7. However, among these six samples, there was no statistically significant change over time (p=0.25). By day 7, MDM had reached cellular glutathione levels in the range see in HAM (p=0.91) with median levels of 18.6nmol/mg (IQR 11.98 – 25.38) in MDM vs. 20.09nmol/mg (IQR 11.58 to 27.19) in HAMs.

Figure 4-2 Glutathione concentrations of PBMCs in adherent culture over time

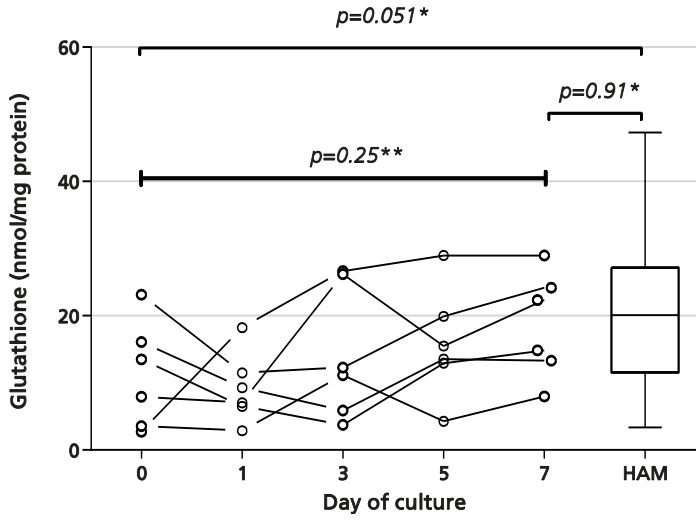

*Glutathione is corrected to total protein for MDM (n=6). Levels for human alveolar macrophagesfrom Malawian volunteers (HAMs) are given for comparison (n=42). Box plot represents: centiles 2.5, 25, 50, 75, 97.5. * Mann-Whitney U test comparing monocyte/MDM with HAM. ** Kruskal-Wallis one way analysis of variance for difference within the groups*

Data for antioxidant enzyme levels are shown in Figure 4-3. Glutathione peroxidase tends to decrease during cell culture, and changes significantly over time (p=0.0075). At baseline, median GPx activity was 77.1U/mg protein (IQR 51.9 to 123.4). At day 7, median activity had fallen to 29.3U/mg (IQR 19.7 to 37.9), and was significantly

lower than HAM at both time points (p=0.001 and p=0.0002 respectively). Indeed, prolonged tissue culture seems to exacerbate the differences.

For superoxide dismutase, median activity at baseline was 1.41U/mg (IQR 0.60 to 2.02), and 1.3U/mg (IQR 1.87 to 2.70) by day 7. Overall there was no difference during maturation (p=0.72). Baseline levels were significantly lower than HAM (p=0.0068), although at day 7, this difference was non-significant (p=0.17).

Figure 4-3 Glutathione peroxidase and superoxide dismutase levels of PBMCs in adherent culture over time

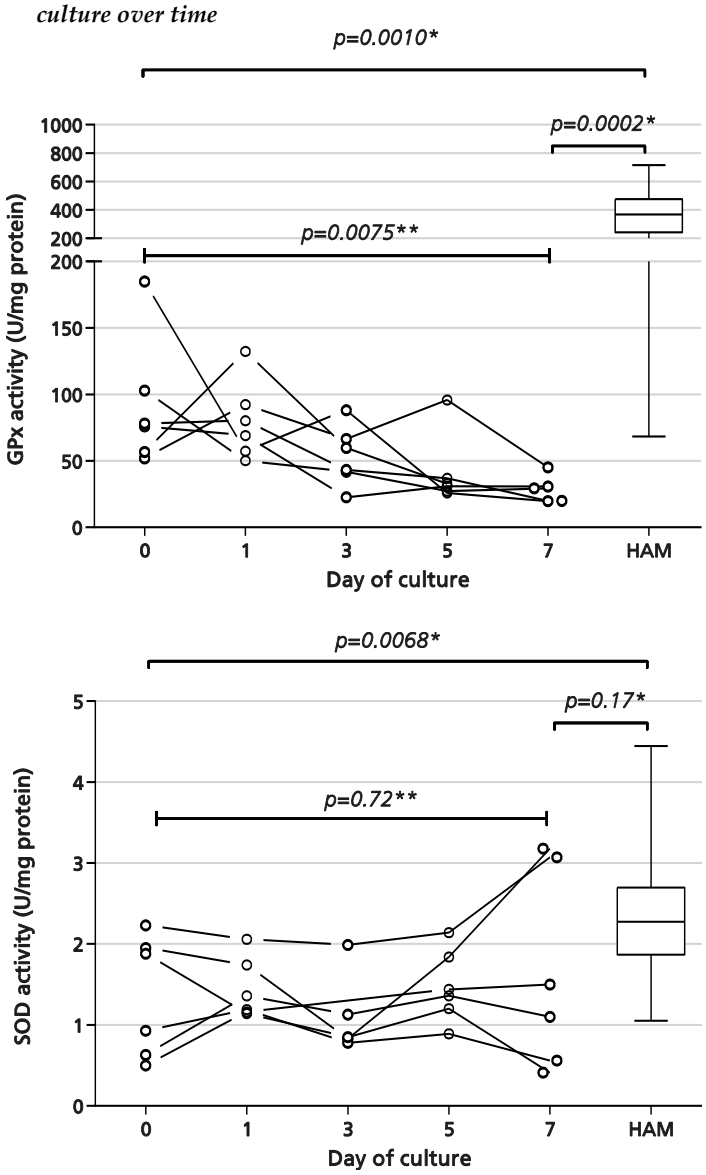

*GPx and SOD activities are reported as Units/mL corrected to total protein (n=6). Levels for human alveolar macrophages (HAMs) are given for comparison (n=42). * Mann-Whitney U test comparing monocyte/MDM with HAM. ** Kruskal-Wallis one way analysis of variance for difference within the groups*

4.3.2 Antioxidant balance *in vivo* - description of cohorts

4.3.2.1 Demographics

In order to support comparison between groups, it is necessary to demonstrate baseline similarities. Table 4-1 gives a summary of key demographic findings of the three cohorts from which *ex vivo* data on redox balance and alveolar macrophage

behaviour are drawn: UK non-smokers, UK smokers and Malawian non-smokers. Of those comparisons within Table 4-1, no differences were seen by sex or body mass index (BMI). Malawian volunteers were on average older (mean age 30.6 years compared with 24.2 in the UK volunteers as a whole). As expected, Malawians were significantly shorter at 1.62m ($p<0.0001$ across all groups). No differences were found between UK non-smokers and Malawian non-smokers in terms of exposure to second hand cigarette smoke in the home ($p=027$), previous smoking history ($p=0.29$ for "ever smoker" and $p=0.13$ for pack years smoked).

Summary statistics of socioeconomic status of the Malawian volunteers are given in Table 4-2. These are presented to inform on the generalizability of results to the wider Malawian and sub-Saharan African population. Where national statistics were available from the National Statistical Office survey[442] for urban populations, the recruited volunteers were similar to these in terms of household goods and size and type of water supply. Recruited individuals were better educated than urban averages (56.8% completed primary education compared with 26%), but had less access to transport (car availability 1.6% vs. 8.0%, and bicycle 14.0% vs. 34.5%).

Use of biomass fuel in for cooking and lighting amongst the Malawian cohort is described in Table 4-3. Most individuals cooked inside the home (77, 60.6%), and 119 (93%) used open wood fire or charcoal as the main fuel. Even for lighting, a minority used electricity (31, 24.4%). The remaining volunteers reported use of paraffin or candle lighting (35.4% and 37% respectively). Overall, the use of biomass fuel in the home for heating or lighting was nearly universal; only 9 individuals (7%) used electricity for both purposes.

Table 4-1 Demographic summary for Malawian volunteers

	UK non-smokers	UK smokers	Malawian non-smokers	Difference
n	14	14	128	n/a
Age (years)	24.4 (5.1)	23.9 (4.5)	30.6 (7.7)	p = 0.0009
Sex (% female)	7 (50%)	6 (43%)	57 (44%)	p = 0.98
Height (m)	1.73 (0.11)	1.74 (0.094)	1.62 (0.073)	p < 0.0001
Body Mass Index	23.9 (4.7)	23.9 (4.1)	22.5 (3.8)	p = 0.27
Ethnicity	African: 0 (0%) White: 12 (86%) Asian: 2 (14%)	African: 0 (0%) White: 14 (100%)	African: 129 (100%)	n/a
Ever smoked	4 (10%)	14 (100%)	22 (14%)	0.29*
Pack years smoked	0.33 (0.82)	3.86 (4.23)	0.37 (2.09)	0.13*
Passive cigarette smoke exposure	0 (0%)	n/a	23 (18%)	p = 0.27

*Summary statistics given as mean (SD) unless otherwise indicated. Continuous data tested for significant disparity using ANOVA test. Categorical data were tested using Fisher's exact test. "n/a" denotes a comparison which was not tested due to pre-selected groups where bias was intentionally introduced i.e. in the selected smokers, "ever smoker" must by definition be universal. * indicates only UK non-smokers and Malawian non-smokers were compared.*

Table 4-2 Socioeconomic summary for Malawian volunteers

	n	(%)	National statistics[442]	
			Overall	Urban
Education level (cumulative)				
Enrolled at primary level	12	97.6	79	
Enrolled at secondary level	71	56.8	26	
Completed university	10	8.0		
Incomplete data	3			
Household				
*Total household size**	4.5		4.6	4.4
Animals sleep in same room as people	22	17.2		
Indicators of socioeconomic status				
Bicycle in household	18	14.0	48.1	34.5
Car in household	2	1.6	2.1	8.0
Fridge in household	16	12.5	4.3	18.5
Mobile phone in household	105	82.0	41.4	75.6
Livestock in household	37	29.1	64.3	30.8
Roofing				
Corrugated metal	120	93.8		
Grass	8	6.2		
Windows				
Glass	119	93.0		
None	9	7.0		
Water				
Piped to property	49	38.6	6.6	32.0
Piped to communal area	61	48.0	15.1	43.7
Bore hole	17	13.4	51.8	12.8
Incomplete data	1			

Study data and national statistics are given as percentages (n=128). National statistics labelled "Overall" are representative of the wider Malawi population, including rural areas.

Table 4-3 Use of biomass fuel amongst Malawian volunteers

	n	(%)	National statistics[442]	
			Overall	Urban
Cooking (main source)				
Open wood fire	43	33.6	86.4	40.7
Charcoal stove	76	59.4	10.4	49.4
Electricity	9	7.0	1.6	8.9
Cooking location				
Inside the house	77	60.6	51.2	70.4
Outside	50	39.4	46.6	29.6
Lighting (main source)				
Paraffin	45	35.4		
Candle	47	37.0		
Electricity	31	24.4	9.1	36.8
Flaming torch	4	3.2		
Incomplete data	1			

n=127. Study data and national statistics are given as percentages (n=128). National statistics labelled "Overall" are representative of the wider Malawi population, including rural areas.

4.3.2.2 Lung function

Spirometry was performed on all volunteers. Overall, 87.7% of traces were acceptable: 2 (14.3%) were excluded each from the UK non-smoker and smoker groups; 16 (12.7%) were omitted from the Malawi group. Figure 4-4 summarises the results across each group with respect to FEV_1, FVC and FEV_1/FVC ratio. There were no statistical differences between non-smoking cohorts in the UK and Malawi. UK smokers had higher mean FEV_1 as percentage of predicted value than their non-smoking UK counterparts (116.2% vs. 99.1%, p=0.0086). FVC was also disproportionately increased in smokers (123.1% predicted vs. 99.2%, p=0.0005) leading to a lower FEV1/FVC (80.5% vs. 86.0%, p=0.046).

Figure 4-4 Spirometric indices from volunteers in UK and Malawi

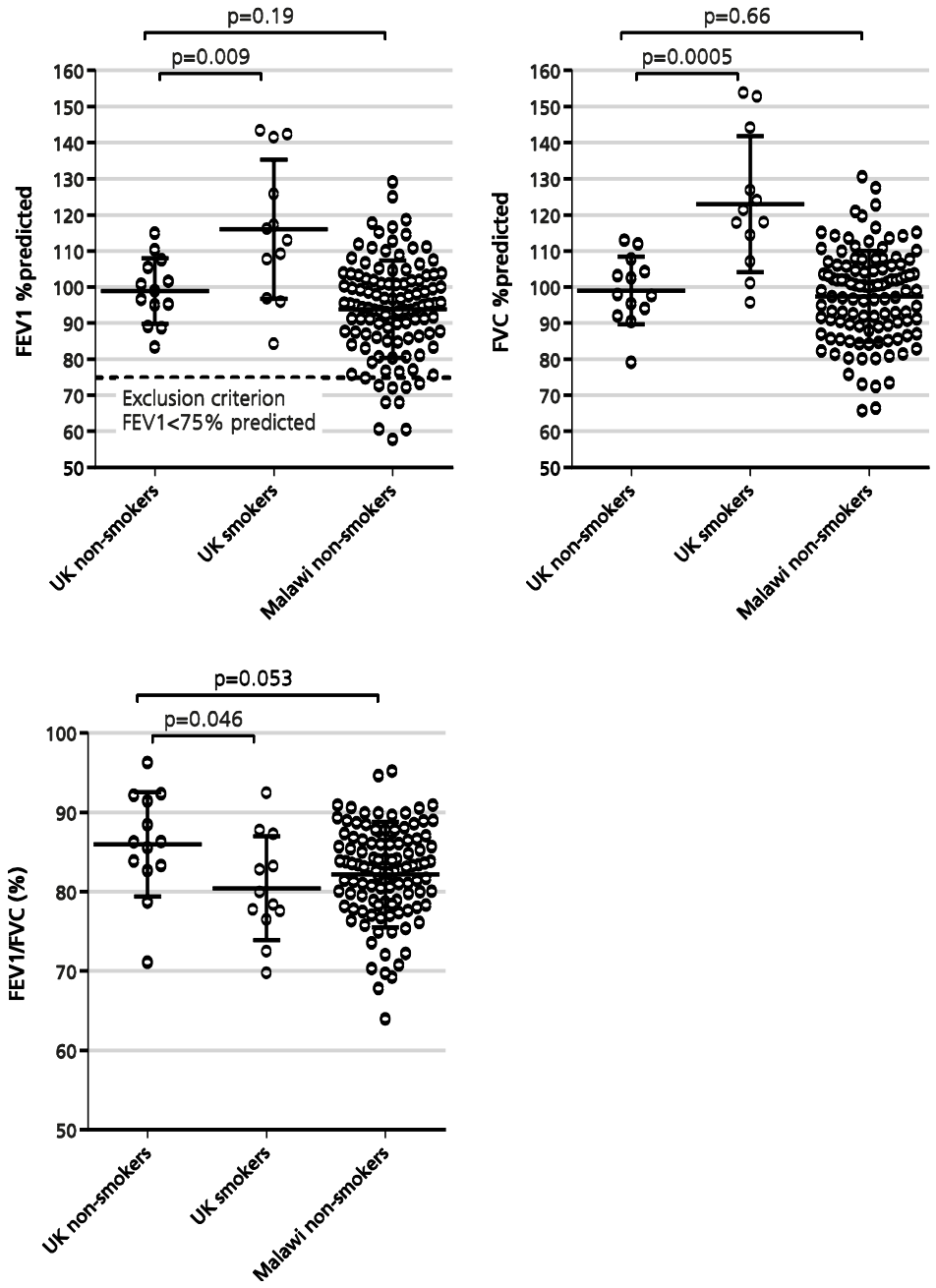

Only volunteers producing adequate traces are included here (n=13 for UK non-smokers, n=12 for UK smokers, n=110 for Malawi non-smokers). Comparisons are made between UK non-smokers and UK smokers, and between UK non-smokers and Malawi non-smokers using t-tests.

As a result of spirometry, ten individuals were stopped from further participation in the research project as their FEV_1 did not meet the minimum requirement for

bronchoscopy (this level of 75% predicted was established before recruitment commenced, and designed to increase safety of the bronchoscopy).

4.3.2.3 Bronchoscopy

Table 4-4 summarises the results of all blood tests and bronchoscopies from the study volunteers. Volunteers across all three groups were similar in terms of haemoglobin and mean red cell volume and platelets. As expected, total white cell counts were lower in the Malawi group ($p<0.0001$).

Trace element levels are pertinent to this analysis as a number of antioxidant enzymes contain copper, zinc and selenium at their active site (see section 1.2.3). Of these, the latter two show no significant differences across groups (Table 4-4). The copper levels are lower in the non-smoking UK cohort (mean 13.72µmol/L [SD 1.80] , $p=0.020$). No differences were noted in BAL fluid returned, or the proportion of macrophages in the fluid. Variability of BAL cell differential counts is small across the three cohorts: the median macrophage content as a proportion of total cells in the returned fluid is 96.2%, with IQR of 93.7% to 98%.

Macrophage particulate content was lower in the UK non-smokers compared with Malawians (0.13% vs. 0.81%, $p=0.0035$). Variability in the latter group was much greater with interquartile range 0.20 to 0.95 compared with 0.0 to 0.30

Table 4-4 Details of blood tests and bronchoscopies in the three cohorts

	UK non-smokers	UK smokers	Malawian	p
n	14	14	128	n/a
Hb (g/dL)	14.08 (1.59)	13.89 (1.04)	14.29 (1.87)	0.79
MCV (fL)	88.99 (6.69)	89.33 (3.16)	85.70 (8.79)	0.28
Platelets ($x10^9$/mL)	221.4 (41.4)	218.1 (24.1)	203.4 (67.9)	0.99
WCC total ($x10^9$/mL)	6.47 (1.96)	6.99 (1.49)	4.75 (1.26)	<0.0001
Neutrophils (%)	59.8 (7.3)	63.4 (9.8)	46.1 (13.8)	0.76
Lymphocytes (%)	29.1 (8.0)	28.3 (8.9)	41.0 (10.9)	0.24
Monocytes (%)	7.7 (2.5)	5.3 (1.4)	7.3 (4.7)	0.99
Eosinophils (%)	2.7 (1.7)	2.2 (1.5)	4.9 (5.6)	0.09
Serum urea (mmol/L)	4.31 (1.42)	4.78 (1.72)	3.09 (0.88)	<0.0001
Serum trace elements				
Copper (µmol/L)	13.72 (1.80)	16.66 (4.50)	18.99 (4.10)	0.02
Zinc (µmol/L)	11.03 (1.13)	11.32 (1.71)	11.83 (2.21)	0.81
Selenium (µmol/L)	1.05 (0.18)	1.07 (0.14)	1.14 (0.22)	0.99
*BAL return (mL)**	125 (105-140)	120 (85-135)	130 (112-140)	0.66
*BAL % macrophages**	95.8 (94.5-96.9)	95.7 (93.3-98.1)	96.3 (93.7-98.1)	0.94
*Macrophage viability (%)**	94.4 (88.0-98.4)	data missing	97.0 (95.0-99.0)	0.05
*Macrophage particulate content (%)**	0.13 (0.0 – 0.3)	not assayed	0.81 (0.20 – 0.95)	0.0035

*Summary statistics given as mean (SD) unless indicated with *, where median and IQR are used due to skewed distribution. Continuous data tested for significant disparity using ANOVA test, except for those marked with * = skewed distribution and Kruskal-Wallis test used. Summary statistics are reported to one more significant figure than the source data.Multiple statistical comparisons have been performed; these are given to inform on potential covariates and confounding and are therefore presented uncorrected[443].Data for macrophage viability were not fully recorded for the UK smokers cohort, and are therefore omitted from this table. BAL return is after instillation of 200mL of normal saline.*

4.3.3 Glutathione in BAL

The following section compares all three cohorts with respect to glutathione in intracellular and extracellular compartments of bronchoalveolar lavage fluid. The Malawi cohort is examined for evidence of *in vivo* determinants of glutathione status.

4.3.3.1 Absolute glutathione levels in cellular bronchoalveolar lavage fluid

Figure 4-5 shows glutathione levels in the cellular component of bronchoalveolar lavage fluid from three cohorts *i.e.* the cells remaining after centrifugation of BAL. These are 96% alveolar macrophages (Table 4-4).

Uncorrected glutathione levels are similar across all groups. There are, however, lower median corrected glutathione levels in the UK smokers compared with non-smokers (13.1nmol/μg protein vs. 27.7, p=0.037), but no statistical differences were found comparing non-smokers from the UK and Malawi (13.1nmol/μg protein vs. 20.1, p=0.055).

Figure 4-5 Total glutathione concentration in cellular component of BAL – raw and corrected results

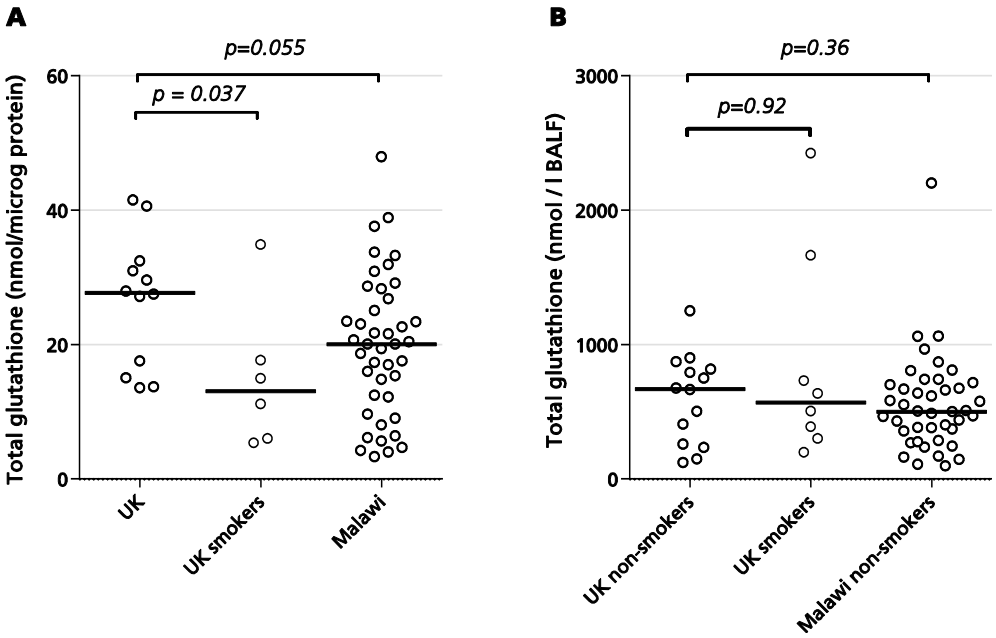

Panel A: glutathione levels in ex vivo BAL cells when corrected for total protein
Panel B: glutathione levels without protein correction
Lines represent median values. Comparisons were made using Mann-Whitney U tests as distributions were not normal.

4.3.3.2 Glutathione in extracellular bronchoalveolar lavage fluid

Results for the three cohorts are shown in Figure 4-6.

Compared with the UK non-smoking group, concentrations of extracellular glutathione are higher in the UK smokers (p=0.0033), and amongst the Malawian non-smokers (p=0.0046). Median values are 1.18μM (IQR 0 to 1.27), 3.84μM (IQR 2.66 to 4.59) and 2.05μM (IQR 1.25 to 3.22) respectively.

Figure 4-6 Extracellular total glutathione in bronchoalveolar lavage fuid

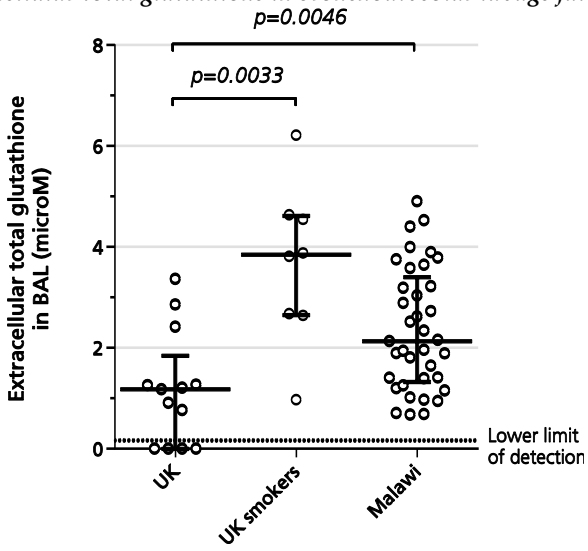

Horizontal lines indicate median values with IQR. Groups compared using Mann-Whitney U test. Four data points in the UK non-smoking group lie below the lower limit of detection.

4.3.3.3 Ratio of oxidised to total glutathione

As discussed in section 1.2.1.1, the ratio of oxidised to total glutathione is a measure of the redox balance. Cellular redox balance in bronchoalveolar lavage is summarised in Figure 4-7.

UK non –smokers have a median cellular ratio of 4.74% compared with 10.70% in UK smokers and 2.98% in Malawian non-smokers. Means (SD) are considerably different, especially in Malawian non-smokers 4.41% (2.83), 11.80% (6.34), 4.26% (3.28) respectively, demonstrating a non-normal distribution. Median values for UK non-smokers differ from UK smokers (p=0.0055), but do not significantly differ from Malawian non-smokers (p=0.49).

Examination of Figure 4-7, however, reveals a considerably positively skewed distribution amongst Malawian non-smokers (skewness 1.61, p<0.0001 by Shapiro-Wilk test). Figure 4-8 shows that the UK non-smoker and Malawian non-smoker populations appear differently distributed with respect to oxidised glutathione proportion in the cellular compartment. Cumulative proportion histograms are

preferred to "ordinary" histograms due to their more precise depiction of the small UK dataset. For orientation, a probability histogram of the Malawi group is also shown in Figure 4-8. While the UK group approximates a normal distribution, observations within the Malawian cohort appear bimodally distributed.

Due to the relatively small numbers of observations from which to draw conclusions, mathematical models were created using a number of potential scenarios which might describe the data. This modelling was done by Prof Diggle at Lancaster University, UK using R[444]. The script for this analysis has been annotated by JR, and appears in full in section 7.1.1.

We evaluated the following hypotheses:

Null hypothesis 1: Oxidised glutathione in the Malawian non-smokers is described no better by a bimodal (*i.e.* two normally distributed sub-populations) model than a single normal distribution

Null hypothesis 2: Under the assumption that the UK is a homogenous (normally distributed) group and Malawi a mix of two different (normally distributed) subgroups, one of the Malawian subgroups the same as the Liverpool group

For each hypothesis, a null model and alternative model were created and fitted to the original data. Maximum likelihood estimation was to generate the most likely parameters for each model. The log-likelihood for each model was recorded, which is a measure of goodness of fit. Models were then compared to each using the log-likelihood ratio *i.e.* how much more likely the first model is to describe the data compared to the second model. From log-likelihood ratios, p values are determined as a measure of statistical significance[445].

Null hypothesis 1 was rejected: log likelihood ratio was 11.64 in favour of the bimodal model, translating to $p<0.0001$. Maximum likelihood estimation suggested two subpopulations of mean 2.75% and 8.55% with standard deviations of 1.05 and 3.33 respectively. The smaller subgroup (with higher levels of oxidised glutathione) was estimated to account for 26.8% of the overall population. The fit of the model is shown visually in Figure 4-9.

Null hypothesis 2 was similarly rejected ($p=0.003$). Neither the "low" nor the "high" peaks amongst the Malawi data corresponded to the UK single peak.

Figure 4-7 Proportion of cellular BAL glutathione in oxidised form

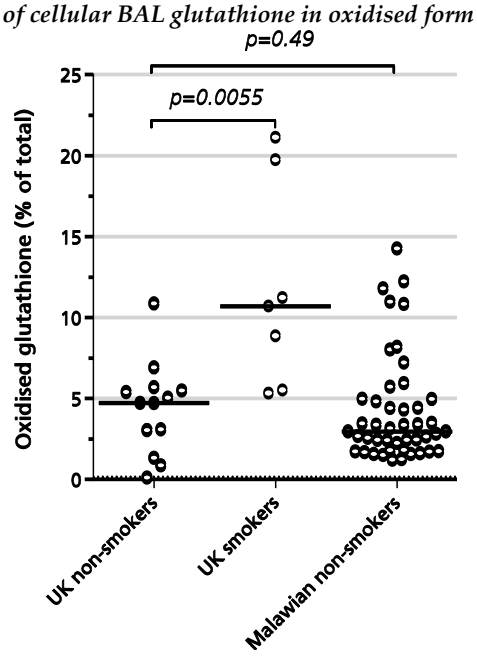

Horizontal lines are medians. Comparisons use Mann-Whitney U test as data are not normally distributed.

Figure 4-8 Histograms of cellular BAL glutathione in oxidised form

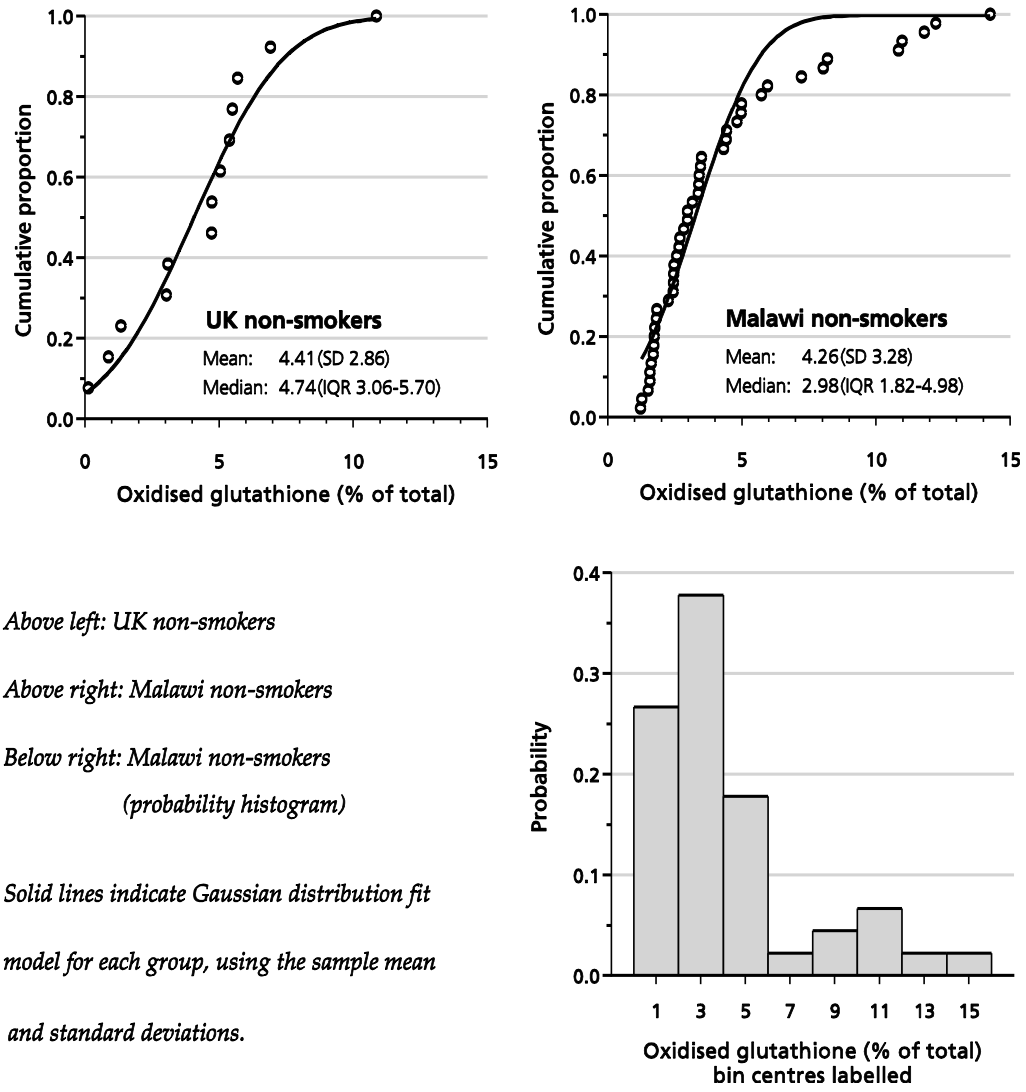

Above left: UK non-smokers

Above right: Malawi non-smokers

Below right: Malawi non-smokers (probability histogram)

Solid lines indicate Gaussian distribution fit model for each group, using the sample mean and standard deviations.

Figure 4-9 Fitted model of the "two normally distributed subgroups" compared with observed results – cumulative proportional histogram

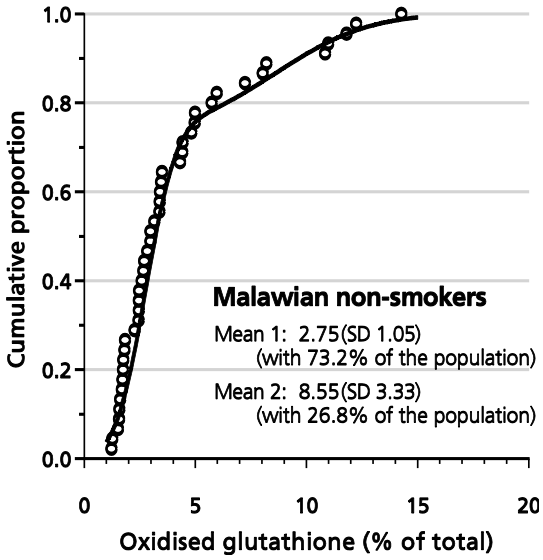

Model fitted from maximum likelihood estimation of the statistical model given in 7.1.1.

4.3.3.4 Predictors of high relative levels of oxidised glutathione in Malawians - univariate analysis

We undertook an investigation of the predictive factors for oxidised to total glutathione ratios. This would identity variables which determined or associated with high levels of oxidative stress in the alveolar macrophage.

Variables included in the analysis were: 1) those relating to the primary hypothesis (that particulate exposure causes oxidative stress); 2) antioxidant enzymes which share a common physiological purpose and are therefore likely to be confounders); 3) basic physiological parameters; 4) indicators of cell type and viability within the lavage fluid. This univariate analysis is shown in Table 4-5.

Oxidised glutathione ratio was significantly negatively associated with total glutathione, glutathione peroxidase activity and lighting with an open paraffin lamp ($p<0.1$). No other predictors were found. In multivariate analysis, all of these

remained significantly negatively associated with oxidised glutathione at p<0.05 (see Table 4-6).

Table 4-5 Associations of oxidised glutathione within the cellular component of bronchoalveolar lavage fluid – univariate analysis

Factor	**Odds ratio**	**95% CI**	**p**
Sex (female)	-0.45	-1.63 – 2.53	0.67
Age (years)	0.019	-0.14 – 0.18	0.81
Passive smoker	-0.20	-3.13 – 2.74	0.89
Cooking fuel (compared with wood)			
Wood and charcoal	0.99	-1.65 – 3.64	0.45
Charcoal	-0.95	-4.70 – 2.79	0.61
Electricity	2.67	-1.08 – 6.41	0.16
Lighting fuel (compared with electricity)			
Candle	-1.26	-3.71 – 1.19	0.31
Paraffin (no glass)	-2.41	-5.14 – 0.32	0.083
Paraffin (glass)	-2.02	-5.46 – 1.41	0.24
Bronchoscopy operator	-0.83	-2.81 – 1.15	0.40
*Bronchoscopy list position**	0.98	-0.28 – 2.24	0.12
BAL volume returned (mL)	-0.014	-0.055 – 0.027	0.50
Cell viability (%)	-0.15	-0.46 – 0.16	0.33
Macrophage proportion (%)	-0.10	-0.35 – 0.15	0.41
Cell particulate (%, log transformed)	-0.28	-1.24 – 0.68	0.56
Total glutathione (nmol/mg protein)	-0.18	-0.26 - -0.98	<0.001
Glutathione peroxidase activity (U/mg protein)	-0.0098	-0.015 - -0.0049	<0.001
Superoxide dismutase activity (U/mg protein)	-1.24	-2.99 – 0.52	0.16

** where the position of a volunteer on the bronchoscopy list might impact on time to processing the sample. Comparator group for cooking fuel was those who used wood: this was chosen in order to give a greater precision of the estimate as only a small number of individuals used electricity. Lighting comparator group was those using electricity as greater numbers were available for comparison.*

Table 4-6 Associations of oxidised glutathione within the cellular component of bronchoalveolar lavage fluid – multivariate analysis

Factor	Odds ratio	95% CI	p
Lighting with paraffin (uncovered wick)	-2.58	-4.75 – 0.41	0.021
Total glutathione (nmol/mg protein)	-0.14	-0.24 - -0.34	0.011
Glutathione peroxidase activity (U/mg protein)	-0.0098	-0.012 - -0.00066	0.030

4.3.4 Glutathione peroxidase and superoxide dismutase

4.3.4.1 Predictors of BAL cellular antioxidant enzymes – univariate analysis

Data on 93 individuals were available for univariate analysis of determinants of glutathione peroxidase and superoxide dismutase levels. Table 4-7 shows this analysis. No correction for multiple comparisons has been made here.

Criteria for univariate analysis were as specified in 4.3.3.3. Associated with GPx at a significance of <0.1 were: age; cell viability; glutathione concentration; SOD activity; serum copper. When introduced to the multivariate model (see Table 4-8), only glutathione and SOD activity remained in the model at $p<0.05$. Of note, particulate load in the alveolar macrophage was not associated with GPx activity.

Superoxide dismutase levels were associated with: age; volume of bronchoalveolar lavage returned; glutathione; GPx activity; lighting the house with candles. In the multivariate model (Table 4-9), only GPx activity and total glutathione remained significant. Particulate load was not associated with SOD activity.

Table 4-7 Associations of glutathione peroxidase and superoxide dismutase activity in the cellular compartment of bronchoalveolar lavage fluid – univariate analysis

Factor	GPx effect	95% CI	p	SOD effect	95% CI	p
Sex (female)	-40.4	-114.6 – 33.8	0.28	0.11	-0.24 – 0.46	0.53
Age (years)	-4.7	-10.7 - -1.2	0.015	-0.03	-0.05 – 0.01	0.007
Passive smoker	-39.1	-132.9 – 54.8	0.41	0.29	-0.66 – 0.08	0.12
Cooking fuel (compared with wood)						
Wood and charcoal	76.0	-55-3 – 207.4	0.26	0.25	-0.17 – 0.68	0.24
Charcoal	60.2	-46.1 – 166.6	0.25	0.05	-0.48 – 0.58	0.85
Electricity	-22.9	-182.7 – 137.0	0.77	0.05	-0.59 – 0.70	0.87
Lighting fuel (compared with electricity)						
Candle	-11.1	-106.0 – 83.7	0.82	-0.02	-0.40 – 0.37	0.09
Paraffin (no glass)	-8.4	-119.7 – 103.0	0.88	-0.14	-0.59 – 0.31	0.63
Paraffin (glass)	16.8	-114.6 – 148.3	0.80	-0.10	-0.63 – 0.43	0.37
BAL volume (mL)	1.10	-0.54 – 2.73	0.19	0.01	0.00 – 0.02	0.027
Cell viability (%)	19.9	3.6 – 36.2	0.017	0.01	-0.05 – 0.07	0.74
Macrophages (%)	1.66	-5.77 – 9.11	0.66	-0.02	-0.05 – 0.02	0.32
Cell particulate (%, log transformed)	6.7	-38.1 – 51.5	0.77	0.09	-0.10 – 0.27	0.35
Total glutathione (nmol/mg protein)	10.6	6.4 – 14.9	<0.001	0.030	0.011 – 0.050	0.003
GPx (U/mg protein)	-	-	-	0.0030	0.0022 – 0.0037	<0.001
SOD (U/mg protein)	136.1	101.5 – 170.6	<0.001	-	-	-
Selenium (µM)	-11.6	-195.6 – 172.4	0.90	-0.10	-1.00 – 0.76	0.82
Copper (µM)	-7.06	-15.27 – 1.16	0.09	-0.0064	-0.046 – 0.033	0.75
Zinc (µM)	5.08	-13.44 – 23.60	0.59	-0.019	-0.11 – 0.067	0.66

Although cell viability is strongly negatively skewed, linear regression modelling has been used as the residuals do *follow normal dsitributions. No correction has been made here for multiple comparisons*

Table 4-8 Determinants of glutathione peroxidase activity in the cellular compartment of bronchoalveolar lavage fluid – multivariate analysis

Factor	Odds ratio	95% CI	p
Age	-0.33	-9.30 – 8.64	0.94
Cell viability (%)	6.91	-15.33 – 29.15	0.53
Total glutathione (nmol/mg protein)	8.78	4.11 - 13.44	0.001
Superoxide dismutase activity (U/mg protein)	152.28	41.87 – 262.70	0.008
Copper (µM)	-4.91	-15.16 – 5.34	0.34

Table 4-9 Determinants of superoxide dismutase activity in the cellular compartment of bronchoalveolar lavage fluid – multivariate analysis

Factor	Odds ratio	95% CI	p
Age	-0.024	-0.049 – 0.000	0.05
BAL volume returned (mL)	-0.0030	-0.0098 – 0.0037	0.36
Total glutathione (nmol/mg protein)	0.14	0.24 - 0.34	0.011
Glutathione peroxidase activity (U/mg protein)	0.0098	0.012 - 0.00066	0.030
Lighting with paraffin (uncovered wick)	0.091	-0.24 – 0.42	0.57

4.3.5 Compartmentalisation of antioxidant enzyme response

Glutathione peroxidase is positively correlated with plasma selenium levels, increasing proportionally with selenium to around 1.3µmol/l[446]. This is due to dose dependent incorporation of selenocysteine residues, increased stability of GPx mRNA at higher Se concentrations, and probably the requirements of other tissues for selenoenzymes[447]. At higher levels, this relationship is less well pronounced. The use of plasma or serum selenium as a biomarker for whole body selenium status is well accepted, although no "gold standard" test exists[448].

As a major determinant of red cell and plasma glutathione peroxidase, selenium was specifically examined in terms of its relationship to alveolar macrophage GPx. Figure 4-10 shows data from 89 Malawi volunteers for whom these parameters were available. As a major determinant of red cell and plasma glutathione peroxidase, selenium was specifically examined in terms of its relationship to alveolar macrophage GPx. There is no evidence of a linear relationship between HAM GPx activity and plasma selenium (p=0.90). Similarly, there was no correlation between glutathione peroxidase activity in the alveolar macrophage and in whole blood (see Figure 4-11).

Figure 4-10 Relationship between alveolar macrophage glutathione peroxidase activity and serum selenium concentration

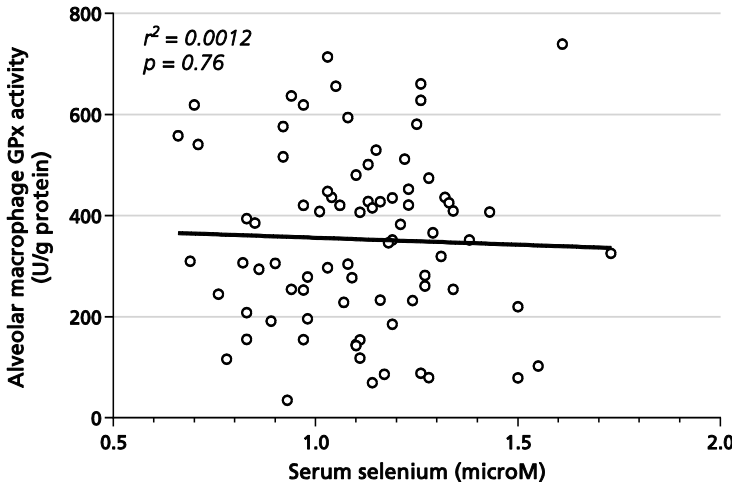

Alveolar macrophage GPx is corrected to total protein. Solid black line represents linear regression model. p-value represents the probablity that the line of linear regression is horizontal.

Data from the UK and Malawi are shown in Figure 4-12. Both cohorts show a statistically significant correlation when fitted to the linear model. Analysis of co-variance (ANCOVA) testing compared the degree of selenium-GPx relationship. Results do not refute the null hypothesis that the groups are significantly different in slope (p=0.35) despite a higher correlation coefficient in the UK group (0.29 vs. 0.074).

Overall, no differences were seen in whole blood glutathione peroxidase levels when comparing UK non-smokers, smokers and Malawi subjects (see Figure 4-13).

Figure 4-11 Relationship between alveolar macrophage glutathione peroxidase and whole blood glutathione peroxidase activity

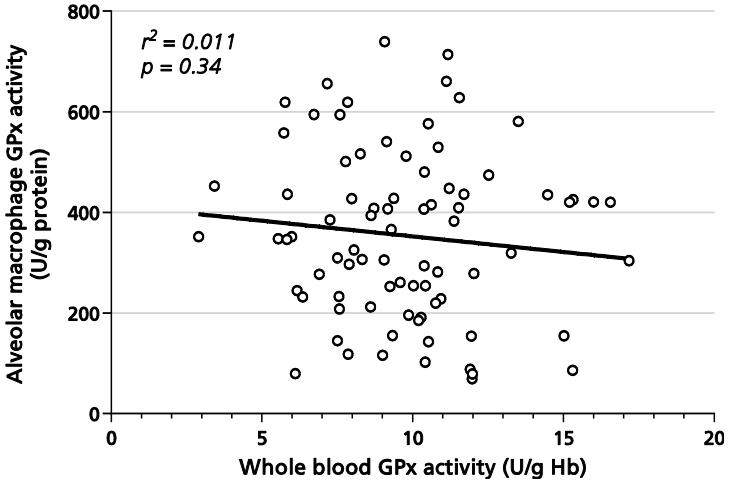

Whole blood GPx is corrected to haemoglobin concentration. Alveolar macrophage GPx is corrected to total protein. Solid black line represents linear regression model. p-value represents the probablity that the line of linear regression is horizontal.

Figure 4-12 Relationship between whole blood glutathione peroxidase activity and serum selenium concentration in Malawian(top) and UK (bottom) volunteers

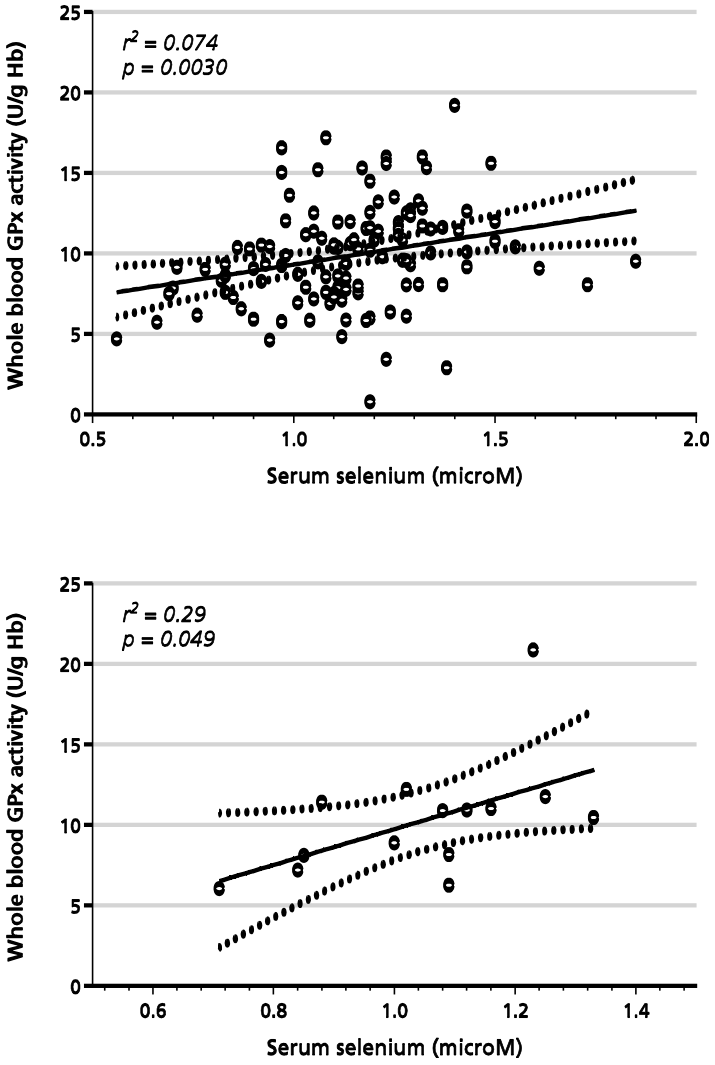

Whole blood glutathione peroxidase is corrected to haemoglobin concentration. Solid black line represents linear regression model with 95% confidence intervals indicated by dashed line. p-value represents the probablity that the line of linear regression is horizontal. Data are shown for Malawi (top graph) and UK (bottom graph).

Figure 4-13 Whole blood glutathione peroxidase activity in UK non-smokers, UK smokers and Malawi non-smoking cohorts

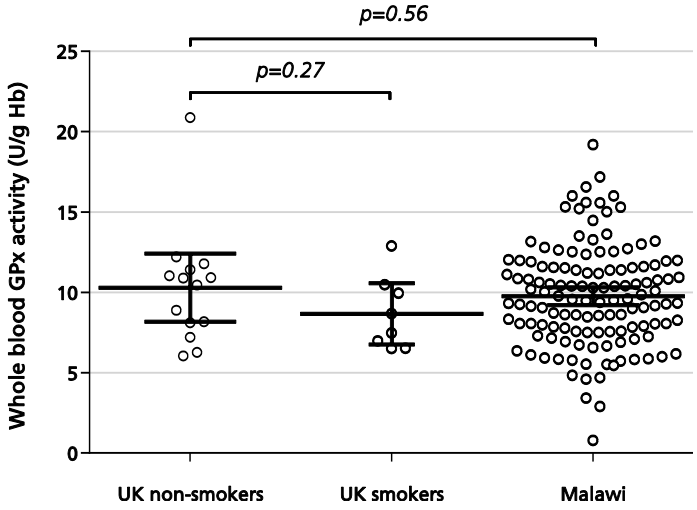

Whole blood glutathione peroxidase is corrected to haemoglobin concentration.Horizontal lines represent mean and 95% confidence intervals.

4.3.6 Lipid peroxidation

As a downstream maker of oxidative stress in the cellular compartment, lipid peroxides from BAL derived cells were measured. Results are shown in Figure 4-14, normalised to total protein levels. These data are normally distributed, and demonstrate a significantly higher mean level of malondialdehyde in the Malawian cohort compared with UK volunteers (5.79nmol/mg protein vs. 3.36nmol/mg, p=0.026).

Figure 4-14 Cellular peroxidation in bronchoalveolar lavage from UK and Malawi non-smokers

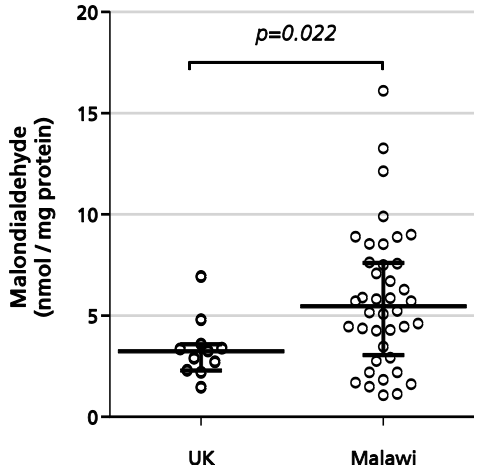

Malondialdehyde measured by TBARS reaction with fluorescence detection of the MDA:TBA adduct using HPLC.Groups compared using t-test.Total protein measured using the Bradford method.

4.4 Discussion

4.4.1 Mature MDMs do not well represent HAM in terms of cellular redox balance.

Decreasing glutathione peroxidase activity over time in MDMs runs counter to the expected three fold rise given the hypothesis that PBMCs mature towards HAM-like cells (termed monocyte derived macrophages). Similarly, although not reaching statistical significance, superoxide dismutase levels were lower in MDMs than HAM.

Initial falls in the glutathione concentration after adherent culture might represent a fall in cellular viability. As lower glutathione availability predisposes to apoptosis[315] this may be a cause of increased cell death, perhaps due to availability of substrate for synthesis in the medium, or initially increased oxidative stress *in vitro*. However, cell concentrations of glutathione fall during apoptosis as an effect of multiple processes, and results here more likely reflect this. At the end of seven days of tissue culture, glutathione levels were not significantly different from HAM.

Given these data, examination of antioxidant enzyme levels in MDM models are likely to be misleading, and further investigation using the primary HAM is strongly supported. Our phenotypic data is supported by cDNA microarray analysis which finds significant differences between MDMs and HAMs[449]. Interpretation of existing data which uses MDM models in assays of oxidative stress should not be generalised to HAMs.

Other culture conditions are likely to impact on *ex vivo* studies for both HAM and MDM models. For example, bovine serum albumin varies in selenium content, and this may alter GPx availability. For the purposes of this project, BSA from the same batch was used, and culture medium from a single manufacturer was used throughout.

4.4.2 *Ex vivo* data on alveolar redox balance

In this section, the validity of making comparisons between the UK and Malawian groups in terms of their baseline characteristics is considered (section 4.4.2.1). There follows discussion of the interpretation of results concerning redox balance in the lung.

4.4.2.1 Baseline characteristics are similar between UK and Malawi groups

Direct comparisons of the three cohorts in terms of lifestyle are complicated by living conditions, educational level and other socioeconomic variables. Ethnicity may also be an independent predictor of some endpoints within this study, although there are no published data on the effect of ethnicity on these biochemical measures of redox balance.

Malawian volunteers were older than those from the UK. Decreasing availability of antioxidant capacity is documented in animal models of aging[450], but not well documented in human lungs[451]. While statistically significant here, the small

absolute difference seems unlikely to contribute to biochemical differences; data from human plasma samples shows no significant change in glutathione between these two age groups[452].

4.4.2.2 Malawian volunteers represent the urban population of Malawi

Malawian volunteers seem to represent the wider urban population in terms of markers of socioeconomic status, household water, cooking and lighting use and number of people in the household. On average, volunteers were better educated than the national average, although no urban data comparison was available from national statistics. These data help to define the studied population, and to confirm that biomass smoke exposure is likely. To support this, 33.6% used wood as the main fuel for cooking, and 60.6% cooked indoors. Furthermore electricity was used as the main source of lighting only by a quarter; the remaining volunteers tended to use paraffin (35.4%) or candles (37%). Together, this burning of biomass fuel in the home is known to cause both alveolar macrophage particulate loading[347], and symptoms and signs of respiratory disease[453].

4.4.2.3 Spirometry results are similar between UK and Malawian non-smokers

It was hypothesised that the Malawi cohort would have lower FEV_1 and FVC than the UK group as a result of suboptimal nutrition in early life and exposure to indoor air pollution[454] amongst other factors. These data do not support this conclusion; spirometric values as a proportion of predicted are similar in UK and Malawi cohorts. Absolute values for FEV_1 and FVC are, as expected, significantly lower in the Malawi non-smokers ($p<0.0001$ for both) due to relative stunting in the Malawian cohort. The FEV1/FVC ratios do not differ.

Generalisation from these data is precluded as they are not randomly selected from the wider population, but based on opportunistic sampling. Such sampling bias may explain the statistical significantly higher FEV_1 and FVC in UK smokers compared with their non-smoking counterparts. FEV_1 was 116.2% predicted in smokers vs. 99.1% in non-smokers. (p=0.0086) and FVC 123.1% predicted vs. 99.2% respectively (p=0.0005). Young people taking up smoking may self-select based on respiratory symptoms and therefore initially have higher FEV_1 than non-smoking counterparts (as previously reported)[455]. Lastly, the number of individuals in each UK cohort is small and therefore susceptible to bias resulting from the exclusion of "poor quality traces" from analysis. If such individuals among the smoking group tended to have poorer lung function, then the mean values for the remaining volunteers would be artificially elevated.

4.4.2.4 Baseline biochemical results show minor variation between UK and Malawian non-smokers

Lower white cell counts in Malawians are consistent with previously observed racial differences, and which is unlikely to significantly impact the interpretation of the study as this is not thought to be clinically significant[456]. Multiple factors might explain the lower urea in the Malawian cohort; machine calibration; differences in hydration; lower consumption of red meat or protein; renal disease. The differences are unlikely to represent clinical differences as all volunteers underwent health screening.

Trace metal concentrations showed significant variation only in copper between UK non-smoker and Malawi cohorts. However, serum copper levels are noted to be higher in smokers[457], and are generally correlate with dietary intake, sex, inflammatory indices such as CRP and caeruloplasmin and serum lipid levels (specifically HDL-C)[458]. As laboratory analyses were identical in all groups, it seems

likely that any differences result from multiple factors, most likely dietary and possibly higher inflammatory responses in the smokers and Malawian groups. These issues are not further pursued here.

4.4.2.5 Glutathione

Cellular glutathione in bronchoalveolar lavage compares reasonably with another study of healthy volunteers from Germany[459], which reported mean levels of 12.4nmol/mg protein in non-smokers (in this Malawian cohort, 19.8nmol/mg). Similarly in this study, smokers were reported to have lower intracellular levels of glutathione than never smokers despite high levels in the epithelial lining fluid, which is reflected in our results. This may be due to impairment of the glutamate-cysteine ligase enzyme which is rate limiting in glutathione synthesis, or an inflammatory phenotype which causes reduction in the activity of the Nrf2 pathway, hence restricting anti-oxidant supply at the point of transcription[460]. High levels of oxidation can also oxidise glutathione, and cause reduction in its availability and from data presented in section 3.10, *in vitro* evidence for this exists in alveolar macrophages treated with wood smoke particles. Finally, in the absence of an influx of inflammatory cells within the BAL fluid (see Table 4-4), these results might represent greater numbers of less mature macrophages.

The relatively high levels of extracellular glutathione in both smokers and Malawian non-smokers are highly suggestive of oxidative stress resulting in higher levels of extracellular antioxidant capacity. Such augmentation of glutathione in the epithelial lining fluid is well documented in animal models after an initial fall following smoke exposure. Human studies confirm the chronically higher levels of extracellular glutathione in smokers[170], and upregulation in people experimentally exposed to wood smoke[228].

Oxidised glutathione ratio

In terms of oxidised glutathione ratio mean and median levels between the UK and Malawian non-smoker cohorts were not dissimilar. However, due to the observed differences in distribution between the two groups, we performed mathematical modelling which showed strong evidence against a normal distribution in the Malawian non-smokers, and against the hypothesis that the Malawian cohort represented a population similar to the UK non-smokers. This evidence suggests that compared with the UK cohort, the majority of Malawian non-smokers have lower proportions of oxidised glutathione within the cellular component of bronchoalveolar lavage fluid. A subpopulation, however, have higher levels than those volunteers from the UK. If considered as a measure of susceptibility to oxidative stress, higher GSSG to total glutathione levels suggest lower antioxidant capacity, and vice versa. This population distribution suggests, among Malawians but not those from the UK, a bimodal distribution of exposure to oxidants or a bimodal distribution of response to oxidants.

The exploratory analysis of determinants of oxidised glutathione, as might be expected, showed potential antioxidants had a statistically significant negative association with oxidised glutathione ratio. These included total glutathione, glutathione peroxidase and superoxide dismutase activity. This suggests that individuals with higher levels of antioxidant buffering capacity have lower levels of oxidised glutathione, or conversely that increased oxidative stress reduces the capacity of cells to buffer against it. In a physiologically stable system, considering the feedback mechanisms available to up-regulate cellular antioxidants, the former scenario is most likely.

These results are prone to the type 1 error due to the multiple statistical testing. However, the plausibility and consistency of association gives confidence in the

laboratory assays and in the conclusions. As no other predictors were found within those factors tested, an association with antioxidant activity does not ultimately explain the relative levels of oxidised glutathione. This may only reflect an antioxidant feedback mechanism *i.e.* is likely to mask the effect of underlying chronic stressors due to the physiological response.

A number of explanations are possible, including methodological variation. However, as all samples were processed by the same team according to standard operating procedures in a single laboratory, this seems unlikely. Other possibilities have not been testable within the limitations of this study, including:

- A genotypic difference which limits availability of antioxidants in a sub-population *e.g.* relative inability to up-regulate or produce effective glutamate cysteine ligase[461], hence lower glutathione availability
- The influence of a strong environmental insult in a sub-population which was unmeasured or unmeasurable *e.g.* differences in particulate exposure in terms of concentration, time course or particle content which are not well reflected by the proxy measure of macrophage particulate burden.

4.4.2.6 Glutathione peroxidase and superoxide dismutase

Overall, glutathione, GPx and SOD are strong co-variates. This is unsurprising as they are all up-regulated by common pathways including Nrf2 in response to oxidative stress[462]. This is the most consistent finding throughout the multivariate models. There is further strong evidence for a higher level of oxidative stress in the alveolar macrophages of the Malawian cohort.

Univariate analysis identified that GPx was negatively associated with cell viability, which might represent reduction in GPx and other proteins during apoptosis and cell death. However, its absence from the multivariate model suggests co-variation with another variable as the explanation.

The association of superoxide dismutase levels with BAL volumes in univariate analysis might be explained by with small returns representing fluid from more proximally in the bronchial tree, and therefore is not representative of alveolar conditions. Indeed, higher BAL returns are significantly, but weakly associated, with higher macrophage viabilities ($r^2 = 0.11$, $p<0.0001$). In this way, dead and apoptotic alveolar macrophages are better represented in the more proximal washings as they are removed by the mucociliary escalator. However, this association is not important in the final multivariate model.

Positive correlations between selenium levels in serum and blood glutathione peroxidase activities are well documented (see section 1.2.3.2). We hypothesised that such a relationship would also occur in alveolar macrophage GPx activity. The data presented here demonstrate no such relationship, and we could find no published data with which to compare our findings. Different types of glutathione peroxidase are present depending on location; within alveolar macrophages, GPx1 (the cytoplasmic form) is likely to predominate, although these cells are known to secrete GPx3 (the plasma form)[204]. Each GPx behaves differently at suboptimal selenium status resulting in uneven usage both within and between tissue types[463]. For example, the reduction in GPx4 (the phospholipid, monomeric form) as a result of selenium deficiency is less pronounced in the lung than that of GPx1, but levels of both in brain are preferentially preserved compared with liver and kidneys[208]. Total levels of GPx in lung are high relative to other organs[463], and high concentrations are particularly important in alveolar macrophages in order to prevent excessive redox signalling[210]. It is possible that this absence of relationship with plasma selenium is an indicator of preferential selenium use by HAMs. Alternatively, as an inducible enzyme, such compensatory mechanisms might dwarf a relatively weak relationship with selenium concentration. To test these hypotheses would require

intervention studies in an animal model to demonstrate changes during selenium depletion and repletion.

It was postulated that Malawians would have higher levels of glutathione peroxidase in the cellular component of bronchoalveolar lavage due to this enzyme's importance in protecting the alveolar macrophage from oxidative stress[204], and the hypothesised higher levels of oxidative stress from inhaled particulate matter.

4.4.2.7 Particulate effects on oxidative stress

Neither fuel types for lighting and cooking nor particulate density were consistently found to associate with measures of oxidative stress. There is no evidence that, according to the proxy measurements of personal exposure presented here, particulate inhalation causes a measurable upregulation in antioxidant capacity, nor oxidative stress. Limited evidence from controlled human studies demonstrate signs of oxidative stress in the first day after wood smoke exposure[91] as measured by nitric oxide and malondialdehyde in exhaled breath condensate. *In vitro* studies consistently show the potential for oxidative stress induced by wood smoke particles.

That we did not demonstrate this in our cohort of individuals might have a number of explanations. Firstly, in a stable physiological system, compensation mechanisms such as Nrf2 related translation of GPx and SOD are likely to mask the primary measure of oxidative stress (GSSG:GSH). However, this would also be expected to produce a differential upregulation of these antioxidant enzymes relating to particulate levels. We found no strong evidence to support this hypothesis, although the high levels of extracellular glutathione and lipid peroxidation in the Malawi cohort are suggestive of chronic, compensated oxidative stress. These

cohorts have potentially many other differences than their exposure to airborne particulates, and confounding is likely. Despite this, the observation of such broad variation between healthy human populations has not previously been described.

Secondly, although the use of particulate area within macrophages is widely accepted, this single measure is unlikely to fully represent the inhaled oxidant load from indoor air pollution. This is due to the diverse range of fuels used, and their variable combustion products: elemental carbon, trace metals, carbon monoxide, nitrous oxide, and multiple complex organic molecules are differentially present and depend on the completeness of combustion and the type and state of fuel[9].

Thirdly, it is uncertain to what degree the macrophage particulate measure responds to intensity of exposure. We did not perform individual air quality monitoring, but a previous study in the same geographical area showed short, high intensity particulate exposures in the home[361]. Oxidative stress resulting from such exposures might be expected to reflect changes in particulate exposure *i.e.* large derangements of short duration. It is possible, if macrophage phagocytosis was saturated during high exposure periods, that particulate levels in the cells do not correlate with physiochemical effect on them.

Finally, the volunteers recruited to this study had relatively lower levels of particulate within the macrophages than in other studies[464]. This may represent methodological differences, or generally lower exposures relating to the recruitment and selection criteria used. This is discussed below.

4.4.2.8 Other limitations of the study

Opportunistic sampling may be flawed where there it introduced systematic bias *i.e.* the recruits do not represent the population from which they are drawn. However, due to the relatively invasive research methods employed (*i.e.* bronchoscopy), using healthy volunteers, such sampling is the only method which does not infringe the ethical principle of autonomy. It is likely that the Malawian group represent their urban counterparts based on the available socioeconomic data. However, data will not be generalizable to rural populations. This limits the generalizability, particularly as rural populations differ considerably in type and amount of biomass fuels used, and therefore the particulate exposure[348]. Relative comparisons within the recruited population are likely to remain valid in terms of the effect of particulate on biochemical behaviour and function.

Bias may arise as a result of exclusion of individuals from bronchoscopy due to poor lung function. Given the inverse relationship of lung function and biomass smoke exposure[454], these ten individuals are likely to have had higher particulate densities. The effect of exclusion is to reduce the relative differences amongst the group, and to decrease the chances of finding real associations between particulate exposure and other parameters.

We have demonstrated high levels of oxidative stress in a healthy Malawian population which in many aspects of antioxidant balance reflects changes seen in cigarette smokers. Despite methodological consistency, epidemiological differences between the groups make causative factors difficult to infer. However, the groups are well balanced in terms of basic demographics, trace element levels and lung function. Macrophage particulate content is considerably different between the UK and Malawi cohorts and at least circumstantially implicates environmental particulates.

The novel description of bimodal distribution of intracellular glutathione oxidation state requires further work to test the hypothesis that a genetic determinant may underlie this. Of a number of candidate polymorphisms, the population frequency of GSTM1 null and GSTP1 AA (Ile105Val; AA → AG/GG) genotypes are similar to the proportion of "highly oxidised" subgroup from this cohort (around one quarter)[465, 466]. Both genotypic variations are likely to alter propensity to the effects of oxidative stress, and the GSTP1 AA genotype appears to have an influence on lung function measures after exposure to particulate matter[466].

As has been discussed in section 1.3, oxidative stress and antioxidant buffering has the potential to alter cell phenotype and response to infection. Specifically, antioxidants *in vitro* reduce the inflammatory response and promote cell survival. Given the considerable variation in oxidative stress between populations, and within the Malawi cohort, such results of variation in the redox environment might be expected to be measurable *ex vivo*.

5 Effect of particulate matter on alveolar macrophage function

5.1 Introduction

Epidemiological evidence consistently demonstrates an association between all-cause mortality and particulate matter (PM) in ambient air[467, 468]. The dose-response relationship extends even to the lowest PM concentrations[469]. The relative effect of PM on death is greater for respiratory than for cardiovascular causes[470, 471], and is particularly strong in the elderly[472] and in those under five years[473, 474]. In developed countries the number of attributed deaths are greater for cardiovascular causes[475] due their relatively high prevalence. Low income countries differ considerably from higher income countries: lower respiratory tract infection is the most common cause of death[80] and smoke from domestic biomass fuel use is the greatest source of PM exposure[476]. Biomass fuel use increases the risk of childhood pneumonia by 1.8 times[477], and attributable risk fractions suggest this translates to 900000 deaths per year in children under 5 years[478]. The most commonly isolated bacterial respiratory pathogen is *Streptococcus pneumoniae*[479].

Mechanisms to explain the relationship between particulate exposure and failure of pulmonary immunity against infection have been described extensively in animal models. As the primary tissue phagocyte, the alveolar macrophage is widely assumed to have a central role in this association. As described in section 1.1.4, the AM must maintain a fine balance between appropriate inflammatory responses, for example against bacterial infection, and the suppression of excessive inflammation caused by inhalation of particulate matter. Both antibacterial and inflammatory responses can be altered by redox balance (see section 1.2.3.5), and failure of either function is detrimental to the host.

Competent alveolar macrophages, faced with infection by *Streptococcus pneumoniae* are able to internalise the organism[480], initiate killing responses by NADPH oxidase activation[40] and manage recruitment of other components of the immune system through cytokine signalling[481]. Defects in these behaviours cause detriment to the host. Failure of bacterial killing is seen in chronic granulomatous disease, where an inherited defect of NADPH oxidase activity is associated with recurrent infections[482].

The situation is complex, however: NADPH oxidase activity and (redox) cytokine signalling are connected (see Figure 1-3). Reactive oxygen species signalling in alveolar macrophages (from NADPH oxidase or extrinsic sources such as particulates) induces inflammatory responses though diverse pathways including NF-κB and AP1 associated transcription[150, 483], calcium signalling[255], redox sensitive MAPK cascades[79, 484] and histone de-acetylation[258]. Failure of AM to provide adequate anti-inflammatory cytokine responses [485] or to dampen inflammatory signalling through apoptosis[66], increase the mortality in animal models of pneumococcal pneumonia. Conversely, some anti-inflammatory signals, such as that from prostaglandin E2, can impair AM bacterial killing responses by inhibiting NADPH oxidase[486]. Aberrations in any of these signalling pathways might conceivably alter outcomes from bacterial infection through either insufficient or excessive responses.

In knockout mouse models, gp91$^{phox-/-}$ mutations for NADPH oxidase have been used to investigate the relationship between ROS and antibacterial function. Such mice when challenged with *Streptococcus pneumoniae* exhibit better microbial killing with increased neutrophil influx and activation and higher levels of inflammatory cytokines including IL-6 and TNFα[62]. However, the same mouse model have

generally lower inflammatory cytokine responses (including IL-6) when challenged with concentrated ambient particulate matter[487]. It is consistently shown that exaggerated responses to these particles in wild type mice cause inflammatory and oxidative stress effects which are detrimental to AM *S. pneumoniae* phagocytosis and survival from streptococcal pneumonia[98 488].

Prior exposure to ultrafine particles (those with diameter less than 100nm), however, confers survival benefit in a model of overwhelming pneumococcal infection, and is associated with lower inflammatory cytokine responses[139]. These responses are contrary to the increase found *in vitro*[100, 102]. The apparent contradiction might be due to the prior recruitment of neutrophils into the airway thus altering the kinetics of early infection.

Overall, studies of alveolar macrophages suggest that acute particulate exposure causes exaggerated cytokine responses, reduced phagosomal killing, and altered susceptibility to pneumonia. These studies are consistent with data from cigarette smoke toxicity models where phagocytosis and killing of *S. pneumoniae* by AM is impaired. In these studies there are high levels of pulmonary inflammatory cytokine[489]. Alterations in these responses might be mediated through, or exaggerated by, oxidative stress, although the extent to which this occurs is unclear.

Acute exposures to particulates from many sources are well studied in terms of their effect on redox balance, and cytokine response (see Table 1-2, Table 1-6 and Table 1-7). Certainly, models of one-off exposure to wood smoke report increased inflammation and increased NF-κB activity in macrophages[110] in part mediated through TLR4 receptors[257]. Chronic exposure to wood smoke shows a different effect in animal models. Rats after 70 days of wood smoke exposure have minimal changes in BAL concentrations of cytokines, and lower levels IL-1β than controls[113].

Cigarette smoking causes a hypo-responsive state in the *ex vivo* human alveolar macrophage, with blunted pro-inflammatory cytokine responses[490]; analogous data for other particulates is not available. Transcriptional profiling of smokers' macrophages reveals "deactivated" phenotypes with less capacity for pro-inflammatory response[360]. Analogous data for ambient particles is not available.

Table 5-1 Selecting cytokine panel for analysis in alveolar macrophage stimulation experiments

	Action	Association[491]	Reason
IL-1β	Pro-inflammatory cytokine, precursor	NF-κB regulated ↑ cell proliferation, differentiation, apoptosis and ROS and RNS production	Oxidising environment promotes secretion[492]. Nrf2 activity counteracts LPS induced secretion[493].
IL-8	Chemokine (CXCL8)	NF-κB regulated ↑ neutrophil and T cell influx, and neutrophil activation with $p47^{phox}$ translocation[494]	Antioxidants moderate release in alveolar macrophages[495] Prominent cytokine in particulate exposure.
TNFα	Pro-inflammatory cytokine	NF-κB regulated	Synthesis after LPS stimulation promoted by oxidising environment[496]
IL-6	Pro-inflammatory cytokine	NF-κB regulated Also ↑ IL-10 and IL-1ra	Prominent cytokine in particulate exposure.
IL-10	Anti-inflammatory cytokine	↓ IL-1, IL-6 and TNFα in LPS treated macrophages ↓ MHC2 expression on macrophages ↓ ROS production[497]	Redox related: LPS induced production reduced by NAC[498]
IL-1ra	Antagonistic to IL-1 β	Competitively inhibits binding of IL-1 β	Potential for significant interaction with IL-1β
MCP-1	Chemokine (CCL2)	↑ recruitment of monocytes and dendritic cells	Chemokine effect reduced by thioredoxin in monocytes[499], and oxidising environments promote expression of MCP-1[500]
RANTES	Chemokine (CCL5)	↑ recruitment of T cells, eosinophils and basophils	Redox regulation demonstrated in bronchial epithelial cells[501]: BSO increases production, and NAC reduces it

NF-κB pathways and ROS production are commonly connected – see section 1.2.3.6

Based on these experimental findings, and firm associations with redox regulation, a panel of cytokines were chosen for examination. The justification for each is detailed in Table 5-1.

5.1.1 Hypotheses

The results presented in this chapter examine hypotheses which address the effect of chronic particulate exposure on alveolar macrophage behaviour. Current understanding of chronic exposures have been detailed in section 1.2.3.5.

1) Cytokine production in response to particulate challenge
    a) Lipopolysaccharide and wood smoke extract induce inflammatory cytokine release in *ex vivo* alveolar macrophages; these responses are enhanced in cells depleted of glutathione
    b) Alveolar macrophages previously exposed *in vivo* to high particulate burdens will have a less inflammatory cytokine release profile when stimulated with wood smoke extract *ex vivo* than AM with low *in vivo* exposure. *i.e.* negative feedback due to chronic exposure exists.
2) Intraphagosomal function. Particulate burden in the alveolar macrophage is inversely associated with capacity to produce effective phagocytosis, oxidative burst and proteolytic function
3) Alveolar macrophage surface marker phenotype may be polarised towards inflammatory /M1 type by exposure to LPS or by oxidative stress *i.e.* demonstrating increased CD86, HLA-DR, CCR7, CD11b and reduced CD206

Further exploratory work is presented examining the effect of particulate within the alveolar macrophage on Nrf2 signalling. This was done to help understand if *in vivo* exposure to particulates was associated with upregulation of antioxidant response element related genes.

5.2 Methods

5.2.1 Cytokine release

For cytokine experiments, human alveolar macrophages (isolated from non-smoking Malawians, see section 2.5) were incubated for 18 hours in RPMI-1640 with 10% FCS at $1x10^6$/well of a 24 well plate (Greiner Bio-One, UK). Where indicated in

the results, this media was supplemented with buthionine sulfoximine 0.2mM (BSO, Sigma, UK) or BSO 0.2mM and N-acetylcysteine 2mM (Sigma, UK) in order to test for the effect of depletion of glutathione. Cells were then washed twice in media. Media was replaced fresh, with additional wood smoke extract 50μg/mL (see section 2.11 for preparation) or LPS 100ng/mL (Sigma, UK) as dictated by the exposure condition. After six hours, supernatants were removed and centrifuged at 450g for 5 minutes to remove cellular debris. Supernatants were then stored at -80°C prior to analysis. Fresh media with identical additives was added to each well, and supernatants were similarly processed after 24 hours incubation. Concentrations of cytokine were determined by the fluorokine multianalyte profiling (MAP) platform using a Bio-Plex 200 machine (BioRad Laboratories). Cytokines were chosen due to represent chemokine and cytokine activities (pro and anti-inflammatory cytokines were both measured). Where multiple candidates for testing were obvious those with known or putative redox regulation[86] were chosen (see Table 5-1). Six hour time points were used to define TNFα, IL-6, IL-1ra and IL-8 concentrations. Twenty-four hour time points were used for RANTES, MCP-1 and IL-1β. These were based on preliminary data examining the optimum signal to background ratio for each cytokine at these time points (data not shown).

5.2.2 Particulate loading

The particulate burden of *ex vivo* alveolar macrophages was measured as described in section 2.10.

5.2.3 Oxidative burst and proteolysis

The method for determining intraphagosomal capacity for oxidative burst and proteolytic function is described in section 2.19 with optimisation experiments detailed in section 3.8. Peripheral blood derived mononuclear cells were isolated by density centrifugation (see section 2.21). Cells were plated into 24 well plates at

1.5x10^6/well and washed after 4 hours with fresh RPMI culture medium with 10% FCS. Medium was replaced with and without LPS 100ng/mL (test and control). Cells were analysed for oxidative burst capacity according to the protocol used for alveolar macrophages.

5.2.4 Surface marker phenotyping

Surface phenotypes in terms of M1/M2 polarisation were determined in *ex vivo* alveolar macrophages according to the protocol described in section 2.9. Data were acquired using an ADP CyAn flow cytometer with single fluorophore stained conditions in order to provide colour compensation data (for final method, see section 2.9). A minimum of 50000 events were acquired. For blocking experiments, 10^6 cells in 1mL in in flow cytometry tubes were incubated with 3mg/mL mouse IgG (Caltag, Cat#10400) or control (PBS) for 30 minutes on ice and washed twice in PBS before the addition of phenotyping antibodies.

For polarisation experiments, alveolar macrophages were plated into 24 well tissue culture plates (Greiner Bio-One, UK) at 10^6/well in 1mL of RPMI 1640 with 10% FCS. Where indicated. In test wells, LPS (100ng/mL) was added to culture medium in order to effect polarisation towards an M1 phenotype[502]. Cells were removed from the plate after 24 hours using citric saline as outlined in section 3.4.3. Thereafter, they were washed twice in PBS before re-suspension in flow cytometer sheath fluid for analysis.

5.2.5 Western blotting

Western blotting was carried out as described in section 2.20. For experiments measuring the effect of wood smoke and LPS, *ex vivo* alveolar macrophages were used within 24 hours of isolation in adherent cell culture in RPMI 1640 + 10% FCS at a density of at 10^6 cells per well. LPS (100ng/mL) or wood smoke extract (50µg/mL)

was added in media for six hours. At the end of incubation, cells were washed twice in PBS and then separated into cytoplasmic and nuclear fractions using the NE-PER nuclear extraction kit (Pierce, UK. Cat#78833) according to manufacturer's instructions. Lysates were stored in RIPA buffer (Sigma, UK. Cat#R0278) with 0.5% protease inhibitor cocktail (Sigma, UK. Cat# P8340) at -80^{o}C prior to analysis.

Positive and negative controls for Nrf2 expression were obtained from Dr Ian Copple, University of Liverpool. Positive controls were RIPA buffer lysed HeLa cells which had been exposed to proteasome inhibitor MG132 for two hours at 10μM. Negative controls were similarly treated with vehicle only (DMSO 0.1%). Protein concentrations within the samples were measured by Bradford assay (see section 2.15) in order to produce consistent loading of wells prior to electrophoresis. Macrophage lysate was used at 20μg per well, and controls at 10 μg/well. Molecular weight markers were used to confirm the presence of bound Nrf2 at 66kDa[503]. Densitometry was performed using the BioRad GS-800 scanner (BioRad, UK) and Quantify One v4.6.1 software (BioRad, UK).

5.2.6 Analysis

Cytokine concentrations were normalised by log transformation prior to analysis. This allowed baseline concentrations to be compared using one way ANOVA. Comparisons of wood smoke and LPS stimulated cells were compared to control values using paired t-tests of log transformed data.

Log increases in cytokine concentration were tested for equal variances between groups using Bartlett's test. In all cases for *in vivo* particulate exposure strata, variances were not equal by Bartlett's test ($p<0.01$). This phenomenon (heteroscedasticity) is a violation of one of the assumptions of the ANOVA test, and therefore a non-parametric test was used for comparison of cytokine increases

between particulate groups (*i.e.* low, medium and high carbon loaded macrophages).

Data examining the relationship between particulate burden and intraphagosomal function, are described by scatterplots and goodness of fit to a linear regression model. For intraphagosomal function, pre-treatment effects on alveolar macrophages were assessed by paired t-test of log transformed data.

For surface marker phenotyping, macrophages were identified by their forward and side scatter characteristics. Phenotypes were reported by log change in mean fluorescence intensities (MFI, using the geometric mean) or by the percentage of cells expressing a specific marker. Cells were defined as expressing a marker if their fluorescence in that channel exceeded the 98th centile of fluorescence in a paired but unstained sample. The latter measure was used when comparing phenotypes within the cohort of volunteers as this provided an internal comparator for each individual where between individual autofluorescence was variable.

Nrf2 densitometry results were normalised to β-actin from the same blot. Values for individuals were reported as a proportion of the normalised negative control signal. For other experiments, treatment effects are reported as the proportion of normalised paired control value.

Particulate burdens were log transformed in order to improve the normality of distribution. Correlations were then tested by fitting linear regression models with the exception of Nrf2. For Nrf2, three individuals had particulate burdens of zero: as log transformation was therefore not possible, the data were analysed by Spearman-Rank test.

5.3 Results

5.3.1 Cytokine response of HAM to LPS and wood smoke extract

Cytokine release from *ex vivo* alveolar macrophages stimulated with lipopolysaccharide (LPS) and wood smoke (WS) extract is summarised in Table 5-2. Results are also represented in graphs for clarity (Figure 5-2 and Figure 5-3). Significant increases in all cytokines were observed after LPS exposure. Wood smoke extract caused increased release of TNFα (p=0.012), IL-6 (p=0.034) and IL-8 (p=0.0085), but no significant change in IL-1ra, IL-1β, RANTES or MCP-1.

5.3.2 Cytokine release of HAM – the effect of redox balance

Data for alveolar macrophage cytokine response according to redox balance are shown in Table 5-3 (LPS stimulation) and Table 5-4 (wood smoke extract stimulation). Results are also represented in Figure 5-2 and Figure 5-3. A consistent feature of both LPS and wood smoke treated macrophages was a reduction in MCP-1 production after treatment with BSO (6780pg/mL compared with baseline 9910pg/mL for LPS [p=0.0023] and 905pg/mL compared with baseline 1590pg/mL for wood smoke treatment [p=0.012]). This effect due to LPS was partly offset by co-treatment with N-acetylcysteine. There were no other observed effects of glutathione depletion.

Toxicity of treatments might explain a lack of observed effect. However, BSO has been shown in section 0 to cause no increased release of lactate dehydrogenase when used as described here. It was observed microscopically that there was some cell detachment after LPS and BSO treatment. To test if this was disproportionately affecting treatment compared with control wells, culture medium was removed from the treatment wells at six hours and, as previously, centrifuged. After removal of the supernatant, the remaining pellet was tested for total protein content using

the Bradford test. Results of this are shown in Figure 5-1. There was no difference in protein by treatment group (p=0.63).

Figure 5-1 Total protein removed with culture medium in cytokine release experiments

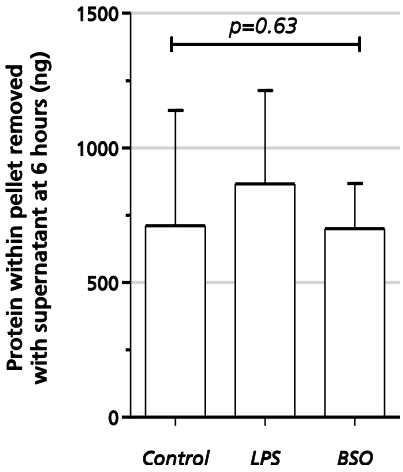

Bars represent mean and 95% confidence interval. n=6 for each condition.Statistical comparison used one way ANOVA.

5.3.2.1 Cytokine release and prior particulate exposure

Data for twenty five individuals were available to compare cytokine responses to wood smoke extract according to *in vivo* particulate exposure. Results for cytokine release from their *ex vivo* alveolar macrophages treated with control (media only), wood smoke extract (50µg/mL) and lipopolysaccharide (100ng/mL) are shown in Figure 5-4.

No significant differences were found in the production of any cytokine / chemokine according to the pre-existing particulate burden of the macrophages.

Table 5-2 Cytokine release from alveolar macrophages stimulated ex vivo with LPS and wood smoke extract

Cytokine	**Control**		**Wood smoke**			**LPS**		
	Geometric mean (pg/mL)	95% CI	Geometric mean (pg/mL)	95% CI	*p*	Geometric mean (pg/mL)	95% CI	*p*
TNFα	150	103.6 – 216.6	353	205.2 – 608.6	*0.012*	104000	83420 - 130400	*<0.0001*
IL-6	358	239.3 – 536.8	712	441.8 – 1148	*0.034*	122000	92290 - 161100	*<0.0001*
IL-8	70100	48240 - 102000	115000	86920 - 150800	*0.0085*	597000	299400 - 1189000	*<0.0001*
IL-1ra	67800	47500 - 96800	73300	53530 – 100040	*0.48*	145000	103600 - 203700	*0.0092*
*IL-1β**	15.6	6.39 – 38.41	21.9	12.56 – 38.33	*0.23*	588	314.6 – 1100.5	*0.0002*
*RANTES**	138	85.7 – 223.7	231	110.3 – 482.0	*0.13*	14900	11490 - 19510	*<0.0001*
*MCP-1**	1400	880 - 2240	1595	1029 - 2472	*0.51*	9910	5855 - 16770	*0.022*

*Alveolar macrophages treated with media only (control), lipopolysacchraide (100ng/mL) or wood smoke particulates (50μg/mL). Geometric means given with 95% confidence intervals. p values represent results of paired t-tests comparing the given group with control values. n=25 for control and wood smoke conditions. n=8 forLPS. Cytokines were analysed at 6 hours except where marked * - here 24 hour stimulation was used. Cytokine concentrations given to 3 significant digits.*

Table 5-3 Effect of redox manipulation on cytokine release from HAM stimulated with LPS

Cytokine	**Control**		**BSO**			**BSO + NAC**		
	Geometric mean (pg/mL)	95% CI	Geometric mean (pg/mL)	95% CI	*p*	Geometric mean (pg/mL)	95% CI	*p*
TNFα	104000	83420 - 130400	114000	91380 - 142800	*0.23*	114000	91890 – 140200	*0.10*
IL-6	122000	92290 - 161100	133000	106600 - 165900	*0.26*	138000	112600 - 168300	*0.075*
IL-8	59700	299400 - 118900	908000	767700 - 107300	*0.19*	681000	463200 - 1001000	*0.76*
IL-1ra	145000	103600 - 203700	155000	106400 - 225300	*0.46*	146000	101400 - 210200	*0.94*
*IL-1β**	588	314.6 – 1100.5	551	283.6 – 1071.2	*0.41*	569	304.8 – 1063.7	*0.65*
*RANTES**	14900	11400 - 19510	14100	10500 - 19040	*0.18*	15000	11450 – 19540	*0.91*
*MCP-1**	9910	5855 – 16770	6780	3733 - 12310	*0.0023*	8140	4672 - 14170	*0.027*

*Alveolar macrophages stimulated with lipopolysacchraide (100ng/mL) following 18h pretreatment with control (media only), 0.2mM buthionine sulfoximine (BSO) or 0.2mM BSO and 1mM N-acetylcysteine (NAC). Data represent n=8 independent observations for each condition. Geometric means given with 95% confidence intervals. p values represent results of paired t-tests comparing the given group with control values. Cytokines were analysed at 6 hours except where marked * - here 24 hour stimulation was used. Cytokine concentrations given to 3 significant digits.*

Table 5-4 Effect of redox manipulation on cytokine release from HAM stimulated with wood smoke extract

Cytokine	**Control**		**BSO**			**BSO + NAC**		
	Geometric mean (pg/mL)	95% CI	Geometric mean (pg/mL)	95% CI	*p*	Geometric mean (pg/mL)	95% CI	*p*
TNFα	353	205.2 – 608.6	352	97.4 - 1271.9	*0.72*	176	59.3 – 524.9	*0.37*
IL-6	712	441.8 – 1148.7	772	243.0 – 2453.8	*0.53*	404	146.3 – 1117.0	*0.38*
IL-8	114000	86920 - 150800	182000	100400 - 330400	*0.19*	103000	55830 - 188300	*0.76*
IL-1ra	73200	53520 - 100400	70600	36060 - 138400	*0.51*	45700	19480 - 107100	*0.67*
*IL-1β**	21.9	12.56 – 38.33	22.2	6.42 – 76.93	*0.49*	10.10	6.30 – 16.18	*0.27*
*RANTES**	231	110.3 – 482.0	190	105.3 – 341.7	*0.59*	154	103.1 – 230.0	*0.15*
*MCP-1**	1590	1028.6 – 2472.0	905	269.3 – 3041.5	*0.012*	847	321.8 – 2229.9	*0.0004*

*Alveolar macrophages stimulated with wood smoke extract (50micog/mL) following 18h pretreatment with control (media only), 0.2mM buthionine sulfoximine (BSO) or 0.2mM BSO and 1mM N-acetylcysteine (NAC). Data represent n=8 independent observations for each condition. Geometric means given with 95% confidence intervals. p values represent results of paired t-tests comparing the given group with control values. Cytokines were analysed at 6 hours except where marked * - here 24 hour stimulation was used. Cytokine concentrations given to 3 significant digits.*

Figure 5-2 Effect of in vitro wood smoke particles and LPS on cytokine release from alveolar macrophages according to redox balance (TNFα, IL-6, IL-8, IL-1ra)

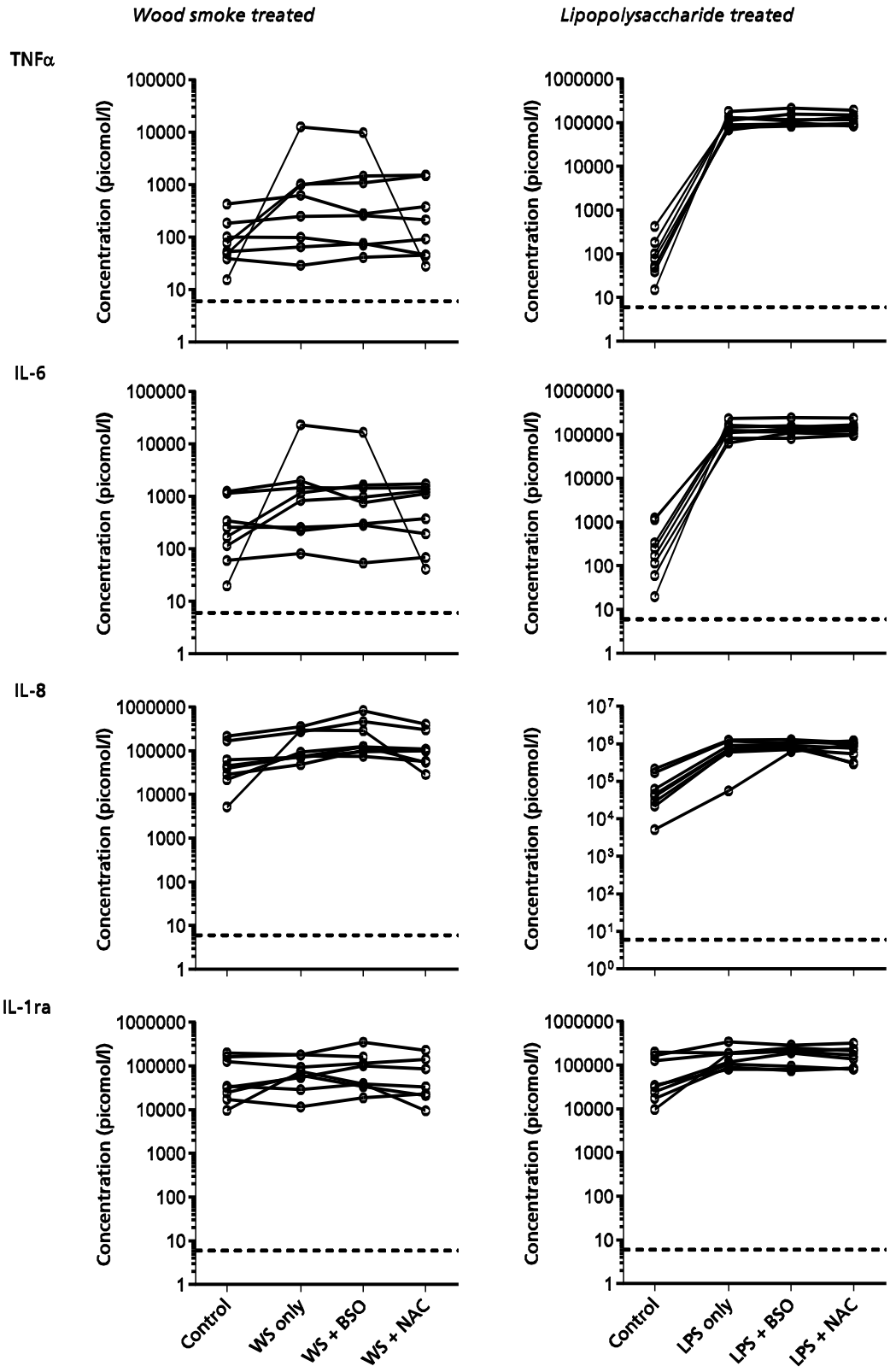

Left panels: Wood smoke treated AM. Right panels: LPS treated AM

Figure 5-3 Effect of in vitro wood smoke particles and LPS on cytokine release from alveolar macrophages according to redox balance (IL-1β, RANTES, MCP-1)

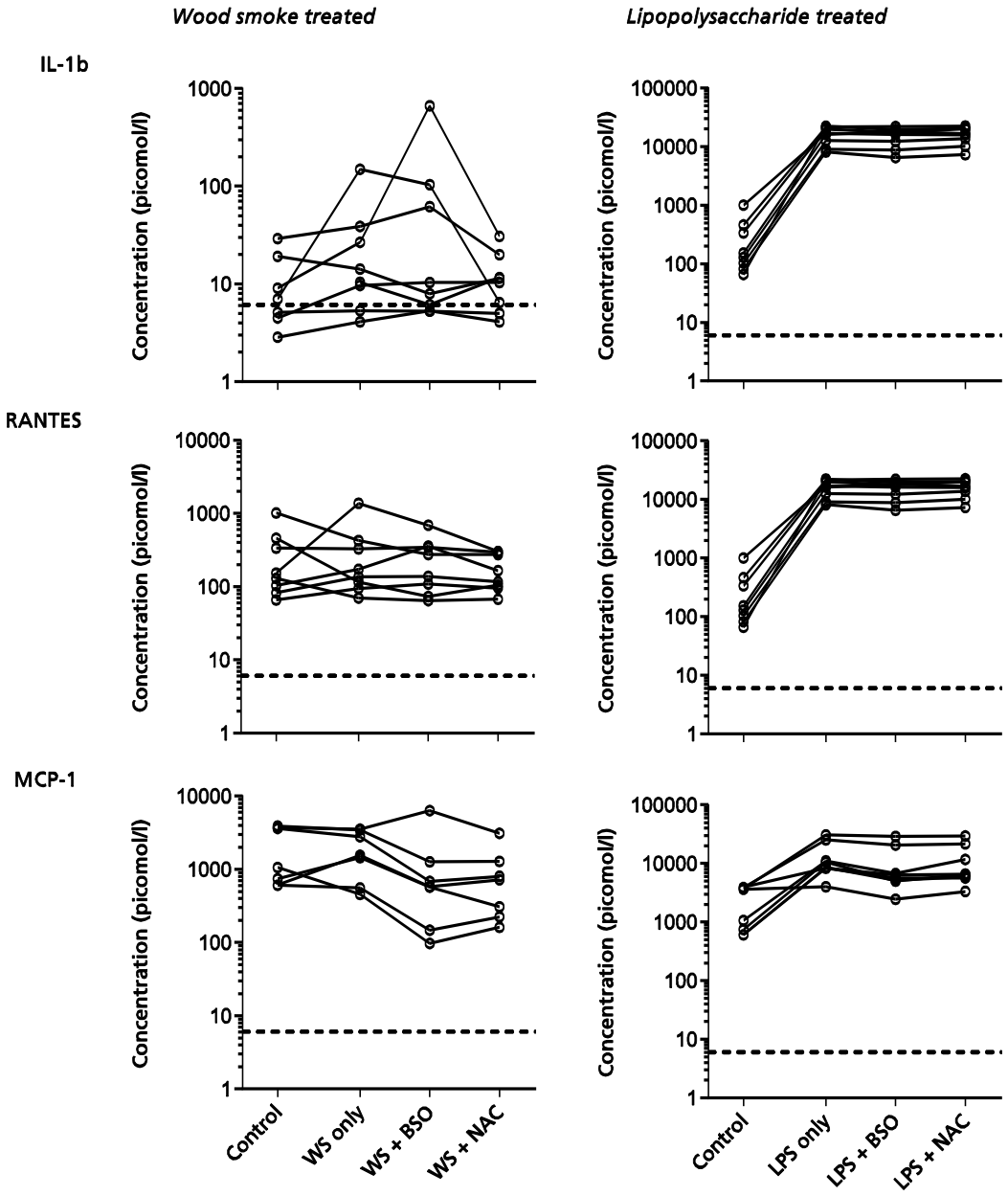

Left panels: Wood smoke treated AM. Right panels: LPS treated AM

Figure 5-4 Effect of in vitro wood smoke particles on cytokine release from alveolar macrophages according to varying in vivo particulate exposure

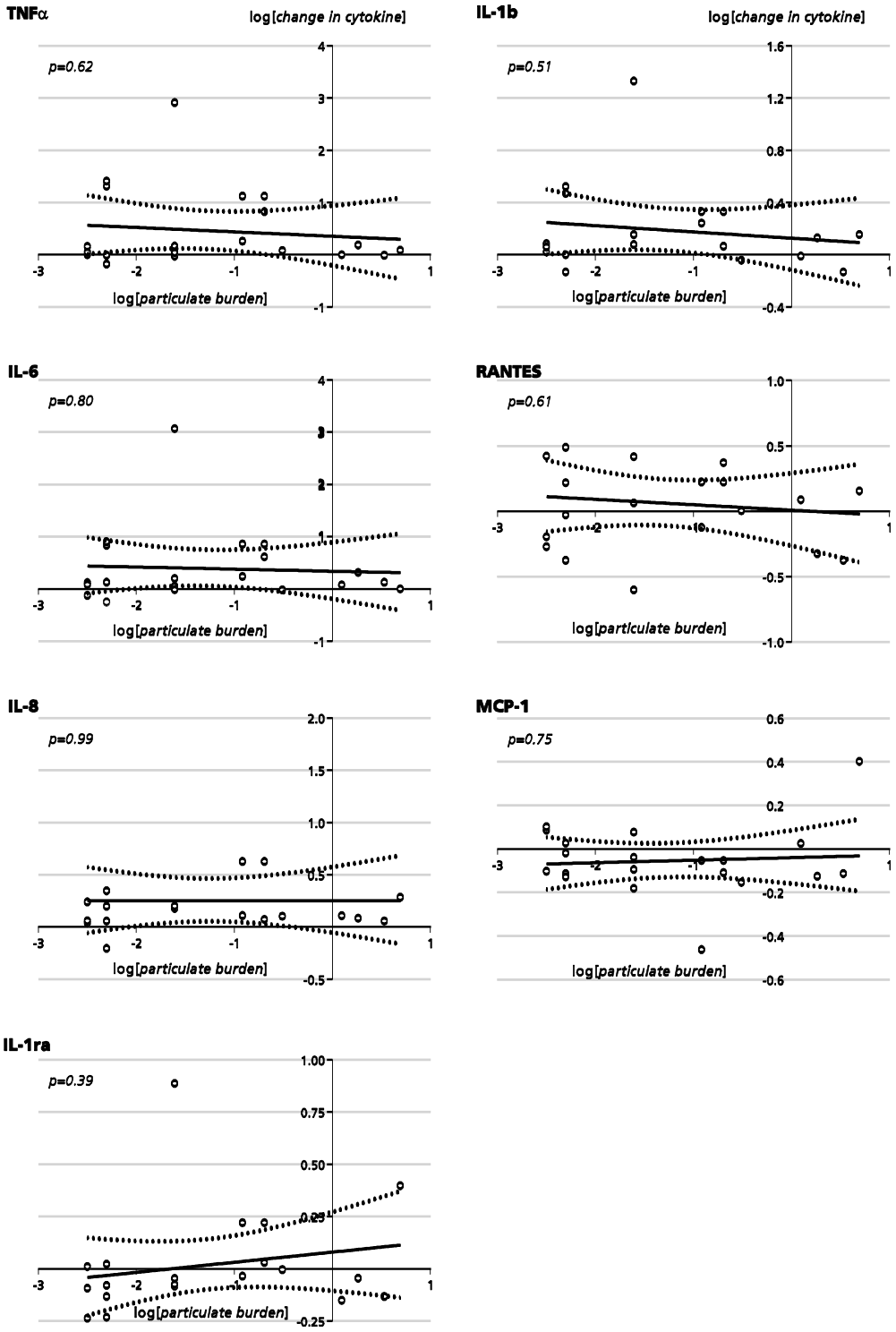

Particulate burden of the alveolar macrophages has been logarithmically transformed to improve linearity. Cytokine changes are reported as log10-change in concencentration between control and treatment conditions.
p-value indicates the probability that the slope of the linear regression model is horizontal i.e. *there is no signnificant slope*

5.3.3 Effect of particulate burden on phagocytosis and intraphagosomal function

For twenty-nine volunteers, data were available on intraphagosomal function and phagocytosis. These are presented in Figure 5-5. There was no relationship between particulate burden and phagocytosis rates, or proteolytic function. There was a significant negative correlation between particulate burden and oxidative burst capacity ($p=0.024$, $r^2 = 0.18$).

Figure 5-5 Phagocytosis and intraphagosomal function in ex vivo alveolar macrophages according to prior particulate burden

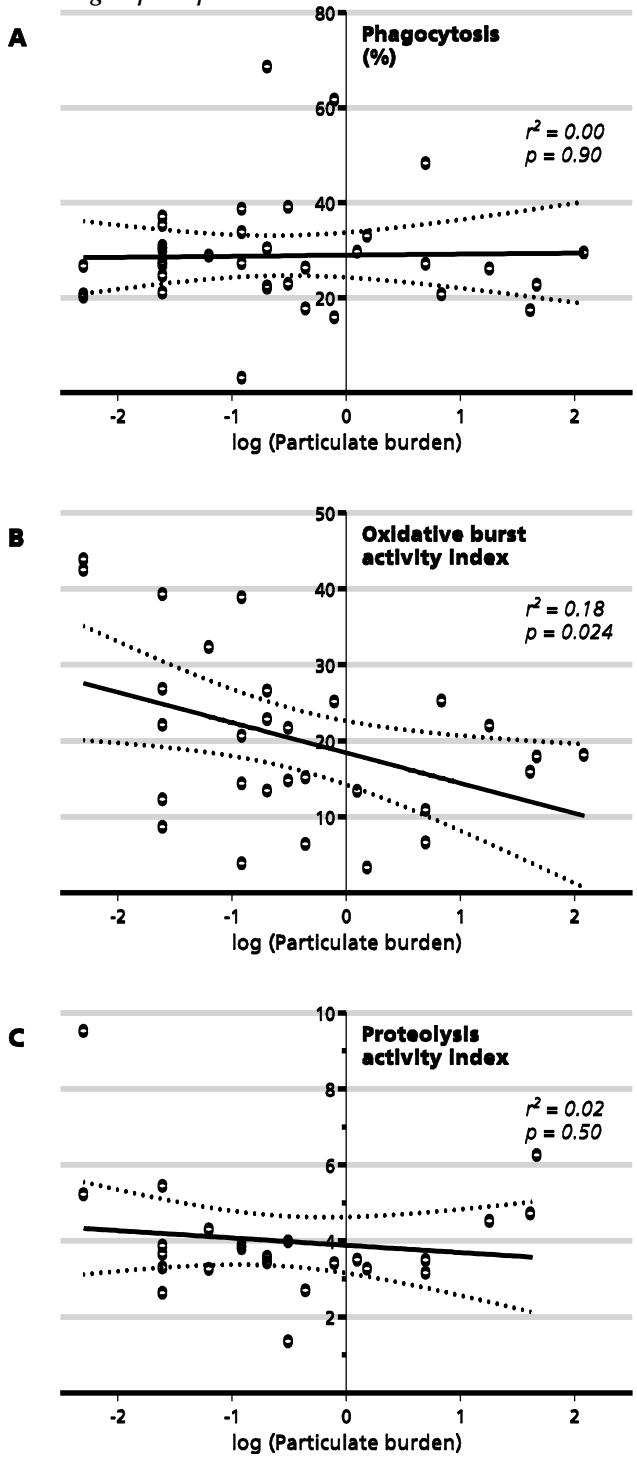

(A) Phagocytosis is proportion of AM associated with silica bead as measured by flow cytometry (B) Oxidative burst activity index is the proportional increase in fluorescence of reporter fluor (H_2DFF) compared with calibrator fluor [Alexa 405]. (C) Proteolytic activity index is similarly reported with DQ-BSA reporter fluor. Particulate burden is logarithmically transformed, representing proportion of cytoplasm occupied by particulate matter as measured by digital image analysis. n=29. Linear regression model fitting is reported as the coefficient of determination (r^2), and p value from Pearson's correlation testing.

5.3.3.1 Effect of LPS pre-treatment

Particulates from biomass fuel combustion contain levels of endotoxin two orders of magnitude higher that those known to cause childhood respiratory disease[83, 218]. In view of the observation of lower oxidative burst in particulate laden macrophages, we hypothesised that on-going stimulation of the cells *in vivo* by such endotoxin might negatively impact phagosomal function. Such attenuated TLR responses have been shown in vitro with LPS induced cytokine response in PBMCs[504]. Similarly, in animal models of post-influenza infection, NF-κB mediated inflammatory response of alveolar macrophages is blunted, and neutrophil recruitment reduced without loss of cell viability[505].

To test the effect on oxidative burst, *ex vivo* alveolar macrophages were incubated for 20 hours with media alone (RPMI 1640 + 10% FCS), or with additional lipopolysaccharide 100ng/mL. Phagosomal function (phagocytosis and oxidative burst) was measured by flow cytometry as before. Results are shown in Figure 5-6. Both phagocytosis and oxidative burst were reduced by LPS pre-treatment ($p=0.0035$ and $p=0.029$ respectively). Adherent peripheral derived mononuclear cells treated identically showed a significant increase in oxidative burst ($p=0.013$), thus validating the method and reagent activity. For a single volunteer, enough cells were available for a time course experiment: *ex vivo* alveolar macrophages were treated with LPS in adherent cell culture for 0, 4, 8 or 20 hours. Oxidative burst activity indices were measured at each time point, and results shown in Figure 5-7.

Figure 5-6 Phagosomal function in the alveolar macrophage after pre-stimulation with lipopolysaccharide

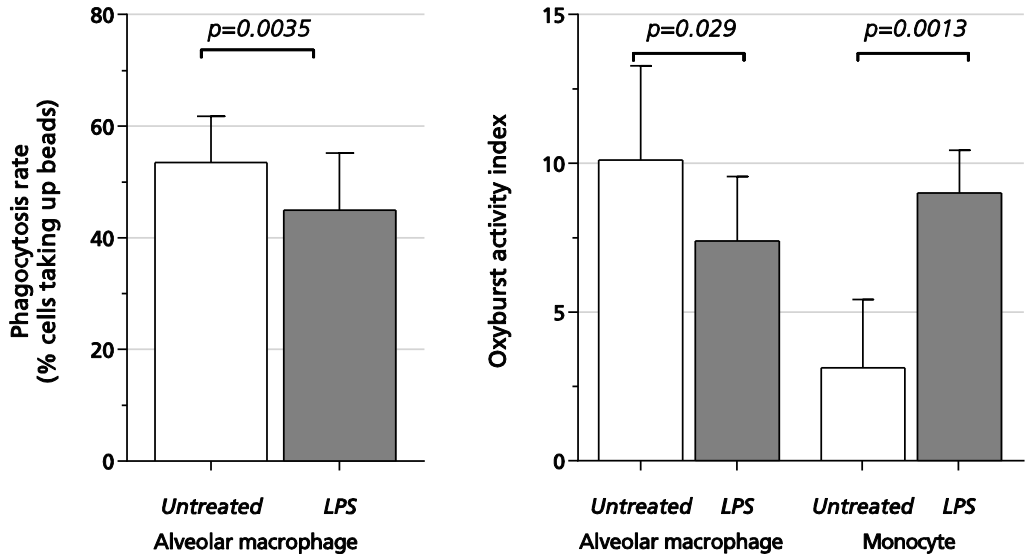

Left panel: Phagocytosis rates in alveolar macrophages pretreated for 20 hours with media alone (open bars) or LPS (grey bars). Phagocytosis is expressed as a proportion of cells taking up silica beads)
Right panel: Oxidative burst activity index with and without LPS pre-treatment. Monocyte treatment effect(positive control) performed under the same conditions using adherent peripheral blood mononuclear cells.
Bars represent means with 95% confidence intervals. Statistical comparisons paired t-tests. n=12 for alveolar macrophage groups. n=3 for monocytes.

Figure 5-7 Oxidative burst activity in ex vivo alveolar macrophages – the time course effect of LPS stimulation (exploratory analysis)

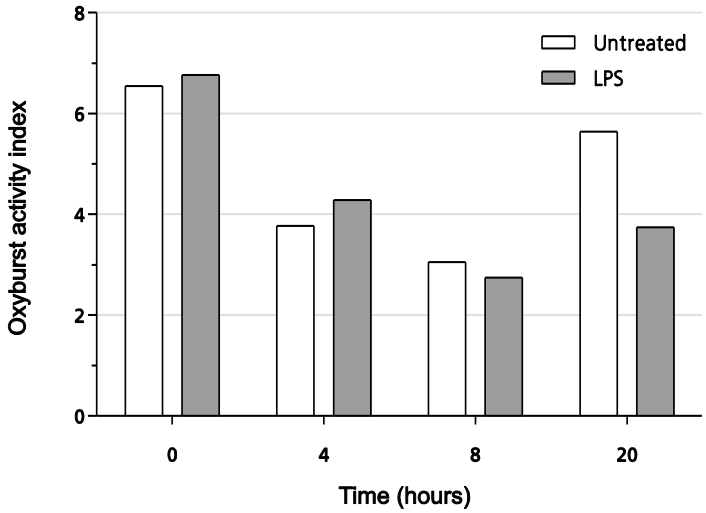

n=1. Ex vivo alveolar macrophages were pre-treated with LPS for 0, 4, 8 or 20 hours with media alone (untreated, open bars) orLPS (solid bars). Oxidative burst was measured as previously at each time point. Further replicates of this experiment were not possible with primary cells due to insufficient cell numbers.

5.3.4 Phenotyping of alveolar macrophage

Redox equilibrium in cells may cause alterations in phenotype, as described in section 1.2.4. In order to test the hypothesis that activation status in human alveolar macrophages might be measured by surface markers, *ex vivo* alveolar macrophages in adherent cell culture were treated with control (media only) or with additional lipopolysaccharide (100ng/mL) for 24 hours. In all cases, expression of surface antigen as measured by flow cytometry followed a unimodal peak as shown by representative fluorescence histograms in Figure 5-9. Non-specific binding was not significant; after blocking with IgG no significant decrease in MFI was seen compared with paired, unblocked samples (see Figure 5-8). As illustrated here, significant autofluorescence in the detection channels was noted, especially using the 488nm excitation laser, and notably in the 520/40nm ("FITC") and 575/26nm ("PE") detection channels.

Phenotype data for six independent experiments are shown in Figure 5-10, comparing that from LPS treated cells with control treated.

In order to illustrate the changing phenotype of alveolar macrophages as a response to tissue culture, for a single volunteer, phenotyping was performed immediately after isolation of the cells (baseline), and after 6 and 24 hours of tissue culture (see Figure 5-11). These results are reported as exploratory analyses; data are available for only one volunteer, and statistical tests are not appropriate here.

Down regulation of CD86, CD11b and HLA-DR is noted with upregulation of CCR7 when comparing tissue cultured cells with those not grown in adherent *ex vivo* conditions. By contrast, and in keeping with data in Figure 5-10, the change in surface expression induced by LPS is minimal for all antigens tested.

Figure 5-8 Effect of blocking non-specific binding sites on phenotype measurement in ex vivo alveolar macrophages

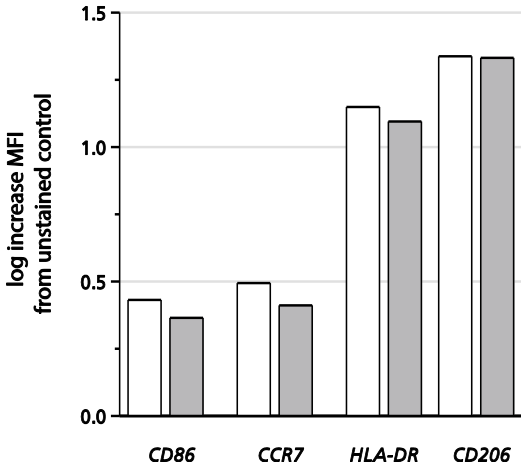

Each bar represents paired samples treated with 3mg/mL of mouse IgG (shaded bars) or PBS control open bars) before phenotyping. n=1

Figure 5-9 Representative histograms of flow cytometry measured cell fluorescence illustrating differential signal:background ratio according to fluorophore

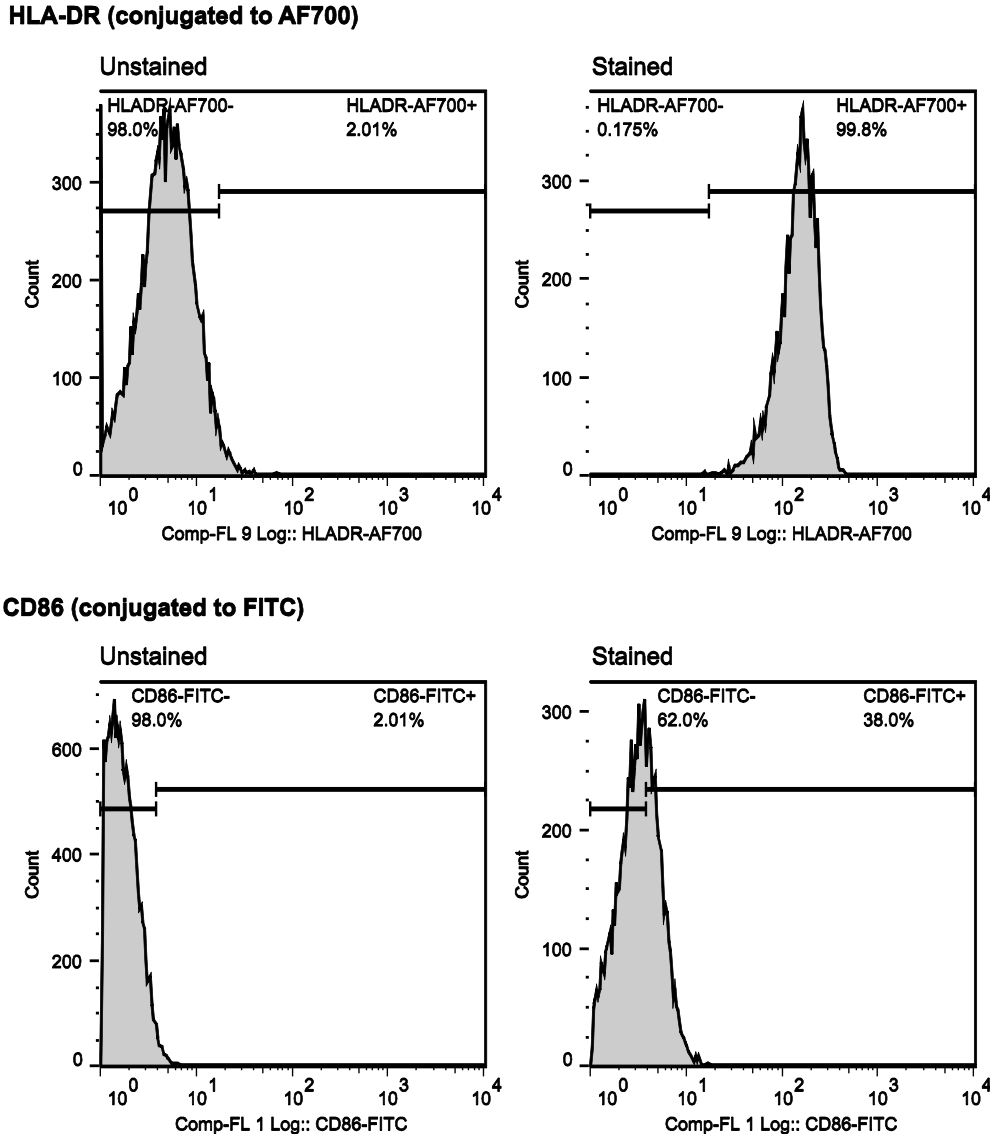

Top: Ex vivo alveolar macrophages unstained (left) and stained with anti-HLA-DR antibody conjugated to AF700 (right)
Bottom: Ex vivo alveolar macrophages unstained (left) and stained with anti-CD86 antibody conjugated to FITC
These data show the difficulty of low signal:noise ratio in the FITC channel, due to cellular autofluorescence.

Figure 5-10 Lipopolysaccharide induced changes in surface antigen expression of ex vivo alveolar macrophages

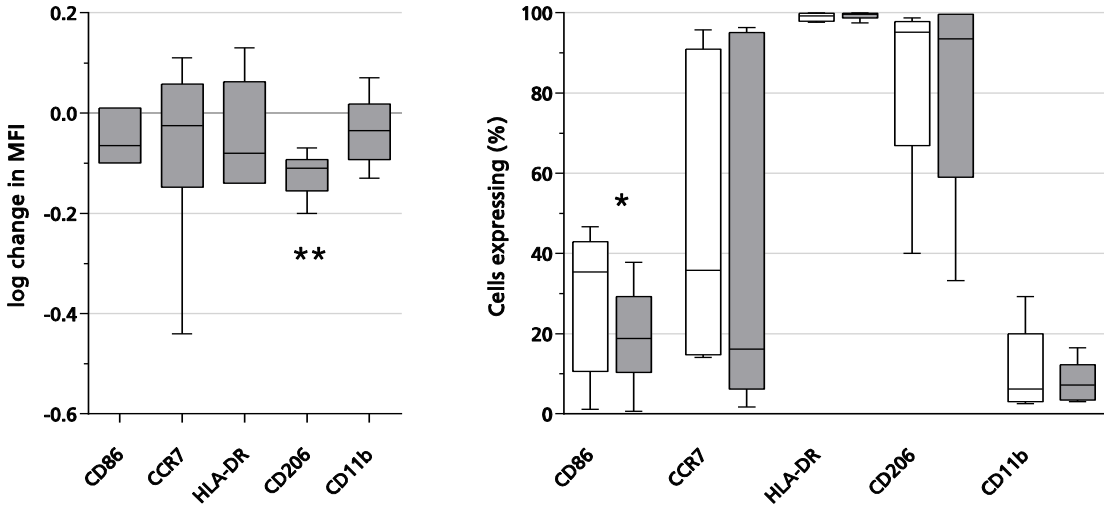

*Left: Log change in geometric mean fluorescence intensity of alveolar macrophages treated with lipopolysaccharide (100ng/mL for 24 hours) comapred with antibody stained, untreated control.** = significantly differs from 0 by Wilcoxon matched pairs test (p<0.05)*
*Right: Percentage cells expressing given antigen in stained, untreated control cells (open bars) and stained, LPS treated cells (grey bars). * = control and LPS values differ significantly by Wilcoxon matched pairs test (p<0.05)*
Bars represent median and whiskers 95% confidence intervals. n=6 for each comparison.

Figure 5-11 Tissue culture induced changes in surface antigen expression of ex vivo alveolar macrophages

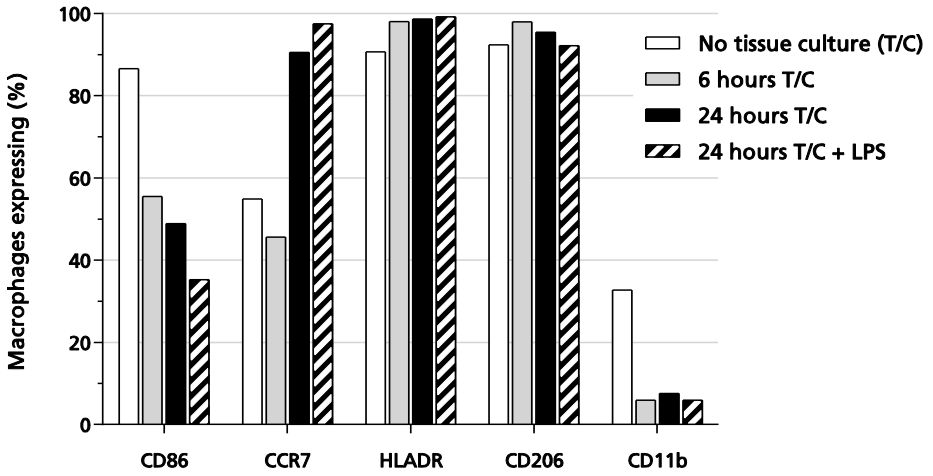

Ex vivo alveolar macrophages underwent surface phenotype staining either directly after isolation from the voluntee (clear bars), or after 6hours (grey bars) or 24 hours (solid black bars) in tissue culture. At 24 hours, phenotype was measured in both cells cultured in standard medium (solid black bars) and medium with addition LPS 100ng/mL (striped bars). n=1

5.3.4.1 Surface marker phenotype – association with particulate loading

Macrophages from eighteen non-smoking Malawian volunteers were available for phenotyping. These were quantified after 2 hours of adherent cell culture according to the protocols set out in sections 3.4.3 and 2.9 for detachment and staining respectively. The association between surface phenotype and carbon loading is illustrated in Figure 5-12.

No statistical differences or trends were observed between categories of particulate loading in terms of CD86, CCR7, HLA-DR and CD206 expression. Considerable variation in expression was seen for CD86 and CCR7 and CD11b, although HLA-DR and CD206 were highly expressed in all volunteers; with only two exceptions these were expressed on more than 90% of all macrophages.

Figure 5-12 Variation of surface antigen expression on alveolar macrophages according to particulate loading

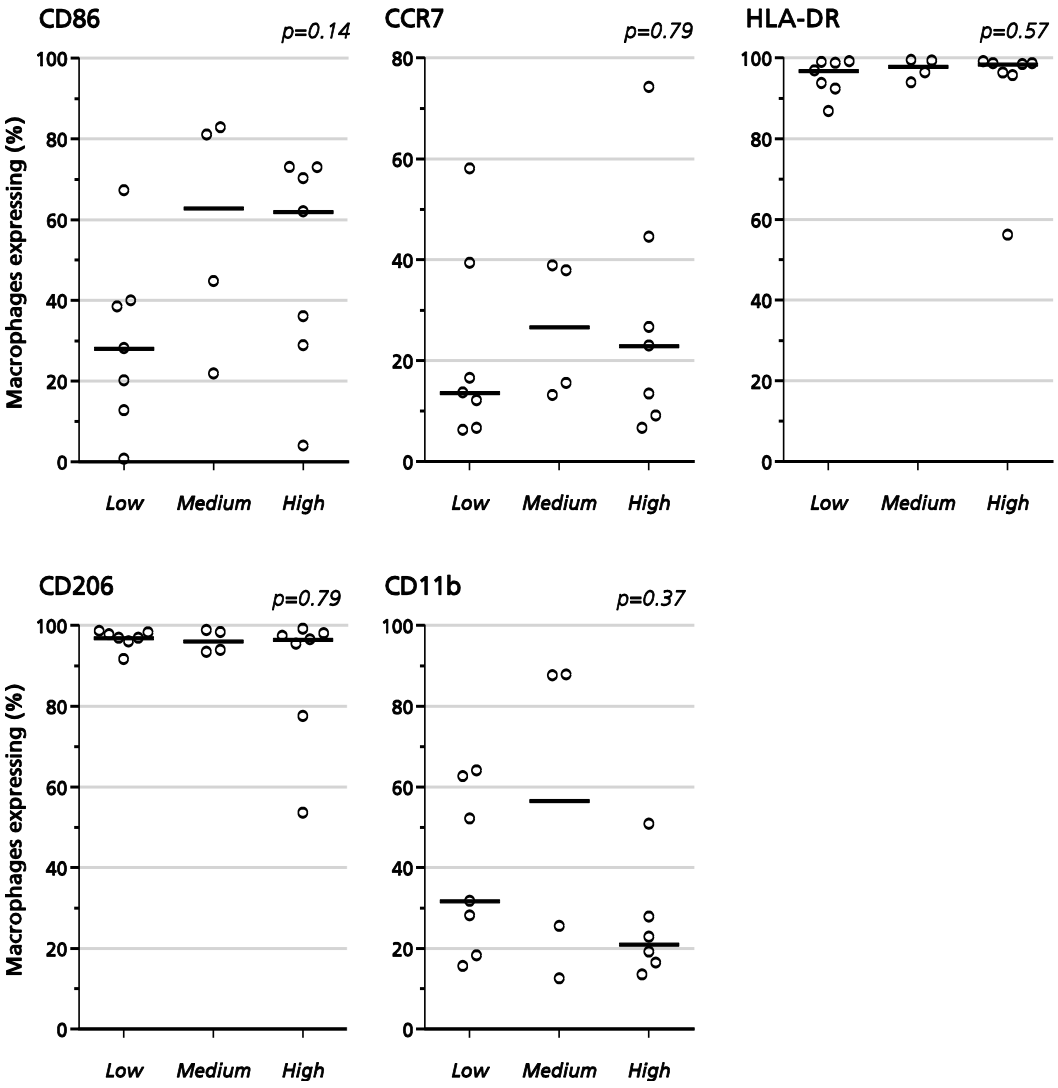

Bars represent median values. n=18 available for comparison. These are displayed by tertile of particulate density; groups are not equally represented because these tertiles are calcualted only once for the entire project in order to give some validity between assay types: n=7 (low); n=4 (medium); n=7 (high). p values are results of Kruskal Wallis tests.

5.3.5 Nrf2 pathway

5.3.5.1 Western blot of Nrf2 post stimulation with WS / LPS

Ex vivo stimulation of alveolar macrophages for relative Nrf2 quantification was done on three individuals. A representative Western blot is shown in Figure 5-13.

No further samples were available for analysis (Western blotting was performed in the UK after recruitment completed in Malawi). No statistical tests were done due to the low number of samples. Nrf2 levels in the nuclear fraction increased after treatment of cells with wood smoke extract, but not after LPS treatment. No such pattern was observed with cytoplasmic Nrf2 detection (see Figure 5-14).

Figure 5-13 Western blot of Nrf2 in alveolar macrophages treated with LPS and wood smoke

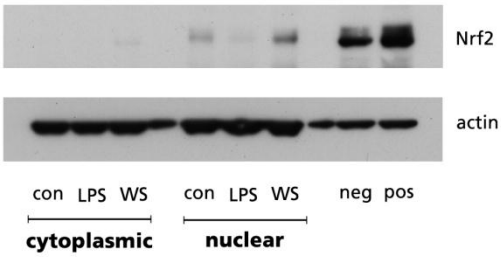

Ex vivo alveolar macrophages were treated for 6 hours with control (medium only), LPS (100ng/mL) or wood smoke extract (50μg/mL). Cells were fractionated into cytoplasmic and nuclear extracts Positive and negative controls were whole cell HeLa cell lysate with and without protesome inhibitor treatment respectively. In order to demonstrate Nrf2 presence, large loading volumes have been required especially for nuclear lysate; this has resulted in spill-over to blank lanes.

5.3.5.2 Total cellular Nrf2 – association with particulate matter

Using Western blot to quantify total cellular Nrf2 was done for 24 non-selected consecutive volunteers; one blot is shown in Figure 5-15 for illustration. Adequate loading of cellular protein is demonstrated by blots of β-actin which derived stronger signal than from the controls. However, Nrf2 was considerably lower than in the control cell lysate, although was detectable in most lanes at the illustrated exposure. At longer exposures, non-specific bands appeared in the developed film. Densitometry was performed, with results normalised to the negative control. The

relationship between total cellular Nrf2 within alveolar macrophages, and particulate loading is shown in Figure 5-16. There is a significant correlation between these two measurements (p=0.013). Further optimisation of the blotting was not possible due to limited sample volume: protein loading into the wells, and detection of Nrf-2 after electrophoresis is therefore suboptimal. These findings therefore require further corroboration. Detection of other Nrf-2 related products would be an ideal approach, but would require new samples.

Figure 5-14 Densitometry of Nrf2 signal from ex vivo alveolar macrophages treated with LPS and wood smoke extract

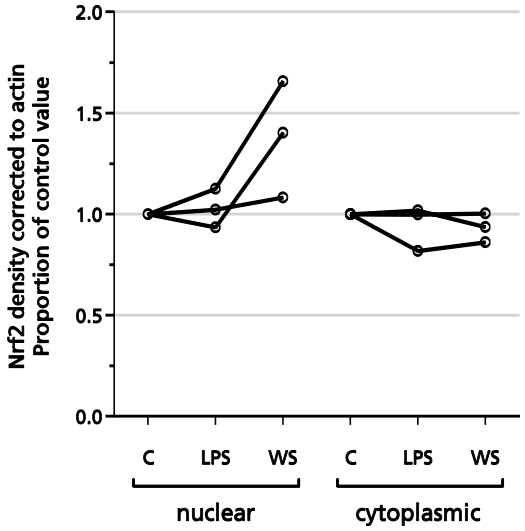

Ex vivo alveolar macrophages were treated for 6 hours with control (medium only), LPS (100ng/mL) or wood smoke extract (50μg/mL). Cells were fractionated into cytoplasmic and nuclear extracts. Data are reported as the density ratio of Nrf2 blot relative to β-actin. For each individual, LPS and WS signals are given as a proportion of the control value.

Figure 5-15 Total cellular Nrf2 in ex vivo alveolar macrophages – variation and low expression

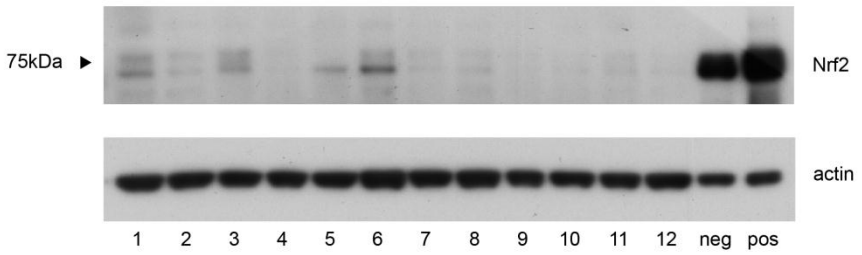

Ex vivo alveolar macrophages were lysed in RIPA buffer with protease inhibitor. Western blots were carried out for 12 volunteers (labelled 1-12). Positive and negative controls were whole cell HeLa cell lysate with and without protesome inhibitor treatment respectively.Marker shows the molecular weight marker at 75kDa – Nrf2 is expected at around 66kDa

Figure 5-16 Total cellular Nrf2 in ex vivo alveolar macrophages – relationship with particulate loading

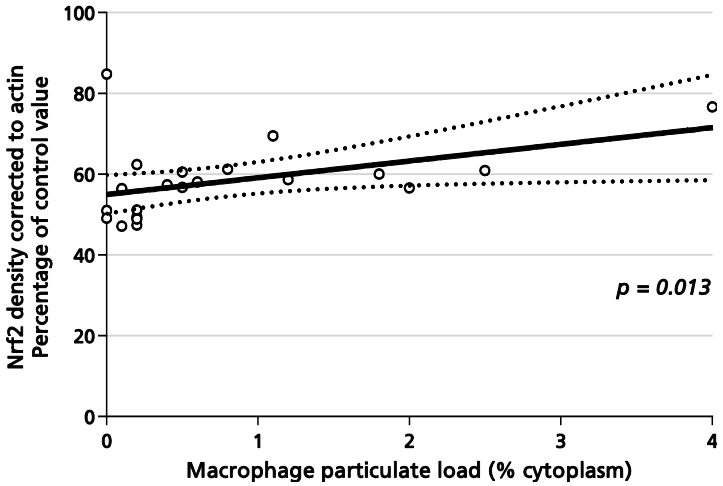

Ex vivo alveolar macrophages were lysed in RIPA buffer with protease inhibitor. p value is for Spearman-Rank tes. n=24.

5.4 Conclusions

5.4.1 Wood smoke extract and LPS elicit an inflammatory cytokine response in *ex vivo* alveolar macrophages

We noted increased TNFα, IL-6 and IL-8 after wood smoke extract exposure. This is a similar inflammatory profile in alveolar macrophages as in the THP-1 monocyte cell line[82], although that study noted increased IL-1β in addition to TNFα and IL-8. Similar increases in IL-6 and IL-8 have been noted in A549 (epithelial) cell lines[426]

and in serum after *in vivo* exposures to wood smoke amongst firefighters[506]. Results of environmental particulates using the same *ex vivo* stimulation methods and human cells also show increased IL-6, TNFα, IL-8. Notably, and in keeping with results here, IL-1β was unchanged although MCP-1 did rise[97].

The pattern of cytokine release strongly implicates NF-κB or AP-1 transcriptional activation. TNFα release is associated with NF-κB activation[110] in laboratory study of wood smoke. Investigation of diesel particulates showed NF-κB or AP-1 activity mediated IL-8 increases depending on the particulate concentration (lower concentrations were NF-κB independent)[507]. IL-6 is also NF-κB dependent in ambient particulate studies[508] and in endotoxin/LPS treatment[219]. However, differential effects are well known depending on particle source, type and composition [509]: a consistent NF-κB related pathway would also produce rises in RANTES[510] which were not observed here.

5.4.2 Redox regulation of cytokine response is evident for MCP-1, but not for other cytokines

In alveolar macrophages stimulated with either LPS or wood smoke extract, reducing glutathione availability with BSO was consistently associated with reduced MCP-1 concentration. For LPS treated cells, N-acetylcysteine partially corrected this towards control values. There is no evidence of increased cell toxicity or cell detachment with LPS or BSO treatment. This suggests that redox regulation has a role In MCP-1 release.

MCP-1 is implicated by knockout models in protection against oxidative stress related damage associated with activated alveolar macrophages[511]. In pulmonary alveolar macrophages its release into supernatant follows acute inflammatory lung injury[512]. It has the potential to inhibit pro-inflammatory cytokine production,

although due to its recruitment of monocytes (and, to a lesser extent neutrophils) it is pro-inflammatory in LPS induced lung inflammation[513]. Reduced MCP-1 concentrations during oxidative stress may prevent lung injury caused by excessive inflammatory cell recruitment.

Work reported here shows that wood smoke extract is capable of perturbing redox balance in *ex vivo* alveolar macrophages (see section 3.10). Despite the relatively high oxidative potential compared with LPS, wood smoke treatment does not have an additional effect on cytokine production. This is surprising, particularly IL6, IL-8 and TNFα, for which in murine studies N-acetylcysteine has a mediating effect on LPS induced cytokine concentration in bronchoalveolar lavage fluid[303, 514]. The production of IL-8 in particular is strongly influenced by oxygen metabolites[219, 303].

In this study, glutathione levels after BSO treatment fell to 30.4% of control values (see Figure 3-20) which might be expected to exert a physiological effect. Gosset et al[304] report more profound decreases (to 10% of control) associated with an increase in IL-8 and TNFα release. While the effectiveness of BSO in depleting glutathione might explain our observed lack of redox effect, Gosset et al note increases in IL-8 after only 3 hour BSO treatment (with mean reduction in glutathione to 54.8% of control). These relative differences in intracellular glutathione concentration are similar to those noted between cigarette smokers and non-smokers (see 4.3.3.1), and represent physiologically relevant levels of oxidative stress. The lack of BSO effect on cytokine production observed here might therefore suggest a lack of relevance to the behaviour of the alveolar macrophage. Alternatively, in cells which are highly buffered against oxidative stress by enzymatic antioxidants such as glutathione peroxidase, it is possible that more profound derangements of redox balance

(particularly an increase in oxidised glutathione) are necessary to elicit any effect on behaviour.

Lastly, the experimental model is necessarily simplistic and cannot distinguish cell to cell variation in responses. It has been observed that uptake of particulates is highly heterogeneous: other macrophage responses, such as cytokine release, might be expected to vary considerably.

5.4.3 Particulate burden in the alveolar macrophage is not associated with cytokine response to wood smoke

We provide evidence against the hypothesis that the inflammatory response of alveolar macrophages is dampened by chronic particulate exposure: despite inducing an acute inflammatory response in alveolar macrophages, the released cytokine concentrations are unaffected by pre-exposure cell particulate burden.

Chronic responses in humans to particulates from indoor air pollution include DNA damage due to oxidative stress.[515], but inflammatory changes are not well documented outside of disease processes such as COPD[516]. In rabbits, after four weeks of daily PM10 exposure, there is increased airway cellularity and AM activation although no inflammatory cell influx[517]. In the same study, IL-6 concentrations showed an initial increase but were insignificantly different from baseline by 3 weeks. This suggests a restorative mechanism to protect against chronic airway inflammation, although such evidence is not available for human exposures. A recent literature review on these effects in cigarette smoke suggested that even for this well investigated exposure "there exists no consensus, and no emerging trend line, of the reproducible effect(s) of cigarette smoke"[86].

Such *in vitro* challenge models are necessarily removed from real-world effects. However, here we used respirable fraction particles at concentrations which

mimicked cellular appearances of *in vivo* exposure macrophages. These smoke particles were also produced from the same firewood sources as used by the exposed population, thus providing a relevant exposure model. Volunteers who provided bronchoalveolar lavage specimens had their indoor particulate exposures defined by questionnaire study; most had mixed exposure in the home to charcoal and wood burning stoves, and to paraffin lamps. As such, the origins of the particulate matter within the alveolar macrophages are variable and not defined by personal exposure monitoring. However, using particulate burden as a proxy measure of exposure is well accepted[518].

5.4.4 Particulate burden in the alveolar macrophage is associated with reduced oxidative burst

There is a specific defect in phagosomal function associated with increasing particulate loading of alveolar macrophages: oxidative burst capacity decreases, but proteolytic and phagocytic functions are preserved. Despite known physiological crosstalk between oxidative burst and proteolysis (NADPH oxidase inhibits macrophage proteolysis by creating an environment in which to reduce disulfide bonds[519]), the effect of particulate appears to be independently associated with the oxidative burst. This data here contradicts mouse models of chronic $PM_{2.5}$ exposure which found increasing NADPH oxidase activity due to infiltration of bone marrow derived monocytes[520].

From these data, we are unable to define the biochemical mechanism behind this reduction in oxidative burst. There are several possibilities:

1. It is possible that oxidative stress or upregulation of specific antioxidants might cause this. Neutrophil oxidative burst capacity is known to be reduced by chronic oxidative stress[521].
2. Changes in modifiers of NAPDH oxidase activity are also associated with particulate exposure. For example, NADPH oxidase assembly can be reduced by surfactant protein C in epithelial lining fluid which coats particulates prior to phagocytosis[394]. In cigarette smoke models, surfactants tend to be decreased[522]. If this is true for other particulates, the dampening effect on NADPH activity would be lost at higher exposures.
3. Upregulation of cellular antioxidants may also inhibit NADPH oxidase activity but not abundance in phagocytes. For example, upregulation of detoxifying enzyme heme oxygenase 1 (HO-1) causes concentrations of its end product, bilirubin, to rise. This bilirubin mediates the impairment of NADPH activity at concentrations considerably below those where it acts as a direct antioxidant[523].

Methodological issues might explain our observations:

1. Disproportionate light absorption by particulate are dealt with in section 3.8.1, and are unlikely to have a strong enough effect to be measurable
2. Culture makes AM more prone to produce oxidative burst[524], and so each sample was assayed on the day of bronchoscopy, and is unlikely to explain the effect
3. The falling oxidative burst in high particulate loads is an epiphenomenon resulting from lower intraphagosomal pH (DCFH fluorescence drops off below pH 6.0[525]). While this is physiologically possible in the early phagosome[526], most oxidation is completed before the phagosomal pH falls this low[45]. The alternative hypothesis, that particulate laden cells have lower

phagosomal pH also seems unlikely, and this suggests an enhanced function not in keeping with *in vitro* exposure experiments[527].

A reduction in oxidative burst capacity would suggest less robust bacterial killing mechanisms; such processes are key to pulmonary innate defence in the early stages of infection. NADPH oxidase is important in both killing responses, but also in limiting inflammatory responses. In mouse models, NADPH oxidase activity is required in order to limit NF-κB activity, and to cap the effect of LPS on pro-inflammatory cascades; this protective response is in part mediated through upregulation of Nrf2[63]. Our data provides novel evidence that innate pulmonary immunity is specifically impaired by *in vivo* particulate exposure. Significantly, this mechanism is consistent with epidemiological associations of increased pulmonary infection and indoor air pollution. Further work would be useful in examining the role of inflammatory and anti-inflammatory signalling pathways in those individuals highly exposed to particulates. We found no evidence of differences in cytokine release, but alteration in Nrf2 mediated antioxidant protection is possible (see section 5.4.7).

5.4.5 Endotoxin exposure can reduce phagosomal function in *ex vivo* alveolar macrophages

Pre-treatment of alveolar macrophages with lipopolysaccharide reduced both oxidative burst and phagocytosis. Our preliminary data suggest that the effect of LPS on *ex vivo* alveolar macrophage oxidative burst changes over time; shorter treatments have an enhancing effect whereas longer time courses become detrimental to function. Previous studies have used lipopolysaccharide as a stimulus for oxidative burst, and short (2-6 hour) pre-treatment enhances superoxide production and phagocytosis[528, 529], although a human challenge model has shown a negative effect of low dose inhaled LPS on granulocyte oxidative

burst[530]. Using our model, measuring earlier time points may have been useful in clarifying the relationship between LPS and oxidative burst function; we were unable to do this due to low cell numbers.

The non-specific effect on both phagocytosis and oxidative burst might represent a generalised toxic effect on cells in culture. While we did not measure this, other studies report no difference on macrophage viability at the same dose and time interval[531]. Our method for determining oxidative burst measures responses from cells taking up beads only, which is less likely to be altered by a general toxic effect.

It is possible that more chronic LPS exposure has dampening effects on inflammatory response and therefore might explain our results. Observations on cell culture may not well reflect *in vivo* effects. Human challenge models might use natural exposure, which would be difficult to quantify and complex to control. Experimental human exposure to LPS has been performed in other contexts, but serial challenge presents a significant danger of severe pulmonary inflammatory response and controlled human data is unlikely to be safely obtainable[530]. Animal studies might provide a method for more rigorously testing this hypothesis.

5.4.6 Cell surface antigen expression

After *ex vivo* treatment with LPS, only CD206 on alveolar macrophages was seen to change in terms of median fluorescence intensity. There was no change in percentage of cells expressing CD206, although a fall in CD86 expression was noted. Interpreting the results of surface phenotyping work presented here is complicated. LPS should act as a strong stimulus towards M1 (classically activated) phenotypes[360], although our data show a lack of consistent effect. It would be expected that expression of CD206 decreases, and that of CD86, CCR7, HLA-DR and CD11b increases. Notably, previous study of human monocyte cells demonstrated

upregulation of HLA-DR after particulate carbon exposure[532]. This was postulated as an explanation for increased allergic sensitisation caused by some particulates; we found no evidence to support that in our study. That such consistent changes are not seen in our data suggests a number of explanations: the stimulus has been too weak; measurement was flawed; an external antagonistic influence was stronger than the LPS or that human macrophages *ex vivo* do not fit the current model of M1/M2 polarisation.

The dose and time course used here is same throughout the project, and is similar to that used in other published work[533]. The additional use of IFNγ has been used by other groups[534] when differentiating M1 macrophages from monocyte precursors, but this was not considered here. Exploratory work in Figure 5-11 suggests that tissue culture has a larger effect than LPS on the surface phenotype as measured by our panel. This produces a tendency away from M1 type activation as evidenced by lower CD86 and CD11b (traditionally M1 markers) and unchanged CD206. This effect might be anticipated although it is not well described in the literature. This is perhaps because use of human primary macrophage use is uncommon; researchers tend to focus on *in vivo* animal models where no tissue culture is required, or in *in vitro* models requiring the prior differentiation of macrophage precursors in the laboratory. Widely accepted M1 and M2 phenotypic markers used in murine studies have been found to be not useful in human research[534].

Significant problems in phenotyping human alveolar macrophages may have resulted from autofluorescence. This intrinsic cellular fluorescence is most obvious in the emission range 450-550nm and is due to upregulation of NADPH, lipofucins , flavins, protoporphyrins and ceroid pigments[535]. This phenomenon increases after cigarette smoke exposure, and is evident within 4 hours. For these data, the most

likely to be affected was CD86 antigen (emission filter 530nm with 40nm tolerance). Unlike other phenotypic markers used for lymphocytes (such as CD4), the selected macrophage antigens represent more homogenous populations; this is seen as unimodal peaks for fluorescence histograms. For phenotyping purposes, and especially for those antigens conjugated to fluorophores affected by autofluorescence backgrounds, the antigens would ideally be highly expressed and the antibodies conjugated to a highly fluorescent product. The power to detect differences in M1 and M2 type cells was therefore limited by fluorophore choice. Data presented here for HLA-DR, CD11b and CD206 are more robust than for CD86 and CCR7 due to their higher intensity of staining, but still do not consistently demonstrate M1 skewing after LPS treatment. The use of unlabelled primary antibody, and conjugation to a secondary antibody emitting light far outside the autofluorescence spectrum might mitigate against this problem. However, the number of antigens which can then by simultaneously labelled is reduced. More recently, arginase 1 has been suggested as an M2 phenotype marker, where changes in CD11b have also been noted in *ex vivo* human studies of cigarette smoke exposed alveolar macrophages[536].

5.4.7 Nrf2 expression in alveolar macrophages

We found that wood smoke extract increased the nuclear concentration of Nrf2 compared with control, although samples were too few for statistical comparison. This observation is consistent with hypothesis of Nrf2 upregulation after administration with a known oxidant (wood smoke). Few papers have examined the effect of particulates in this context, and these focus on the relationship between Nrf2 genotype and propensity to develop particulate driven asthma[247, 537]. Nrf2 upregulation is detectable in alveolar macrophages in mice models of cigarette smoke exposure. It protects against oxidative stress and the inflammatory and

architectural changes[538]. This is likely to be mediated through IL-8 and other inflammatory cytokine responses; Nrf2 negatively influences these[539]. Nrf2 is also important in protecting against genotoxicity from organic carcinogens known to be present in wood smoke (*e.g.* benzo[a]pyrene)[540].Knockout models are highly prone to emphysema, and heterologous bone marrow replacement with Nrf2 positive cells causes influx of new alveolar macrophages and a prevention of emphysema[295] suggesting a key role for the macrophage.

In studies of sepsis, Nrf2 protects against excessive pulmonary inflammation and limits alveolar macrophage NF-κB and TNFα responses[541], and enhances glutathione availability resulting in an overall survival benefit[296]. It seems likely that Nrf2 in alveolar macrophages is protective against acute inflammatory insults, and promotes successful anti-infective responses. Where there is prior oxidative stress, Nrf2 is protective against pulmonary bacterial infection, and this is partly mediated through glutathione upregulation[542].

If Nrf2 were to vary in human populations according to prior particulate exposure, this might have implications for innate immune defence in the lung. Genotypic polymorphisms in humans have been identified which express lower activity, and are associated with poorer outcomes from acute lung injury[543]. Studies relating exposure-related variation have not been done.

Our data show an association of Nrf2 concentration with particulate burden in the macrophage; mechanistically, this is both plausible and fitting with the hypothesis that alveolar macrophages have levels of oxidative stress partially dependent on their particulate exposure. The *in vitro* evidence for this considerable (see section 1.2.3.5 for a summary of the literature, and section 3.10 for results from this project). These, however, are the first *in vivo* data to show this association.

In human models alveolar macrophages, Nrf2 has only been examined in relation to disease processes. Western blot and mRNA studies have shown decreasing levels in chronic cigarette smoke exposure[544]. This is the converse of our findings in which highly exposed macrophages had higher levels. The populations were, however, different: we have investigated healthy individuals. Bronchoscopic studies of the respiratory epithelium have documented increased Nrf2 translocation in "healthy" cigarette smokers[545]. Acute exposure to oxidants, including cigarette smoke[544], cause increasing activation of Nrf2 in macrophages in the absence of disease. This feeds through to increases in antioxidant levels of thioredoxin reductase and other Nrf2 modulated genes[545].

Relatively low levels of Nrf2 in alveolar macrophages were present in the samples taken, this is commonly seen compared with cell line studies, although alveolar macrophages and respiratory epithelium have relatively high Nrf2 levels compared with other parts of the lung *in vivo*[546]. An alternative and complementary approach, such as the use of real time PCR would allow more accurate quantification, and would not suffer from the problems of non-specific binding seen in Western blots during prolonged exposures. Ideally, this would be done in the same samples to increase confidence in the results.

Nrf2 is controlled at multiple levels, including phosphorylation events which enhance its activity and nuclear translocation[503]. Whole cell measurement of Nrf2 is a simplified assay which does not take into account nuclear translocation and binding to the ARE, but is a reasonable summary measure of overall activity[380]. Protein stripping from existing Western blots could be done, with the membranes re-probed for downstream markers of Nrf2 activation including glutathione-S-transferases, (GST), NAD(P)H quinone oxidoreductase (NQO1), and heme-

oxygenase 1 (HO-1) products[547]. This would confirm the functional consequence of Nrf2 activation.

In summary, we have demonstrated an association in *ex vivo* alveolar macrophages between particulate exposure and a) reduced oxidative burst capacity and b) increased cellular Nrf2. In a stable state of exposure, chronic upregulation of antioxidants might impair NADPH oxidase activity as described above. We propose that while established as a mechanism to protect the self against excessive oxidative stress, this has potential detrimental effects on host defence in terms of bacterial killing. This hypothesis is summarized in Figure 5-17.

Figure 5-17 Hypothesised pathway relating particulate induced antioxidant upregulation to reduction in NADPH oxidase activity

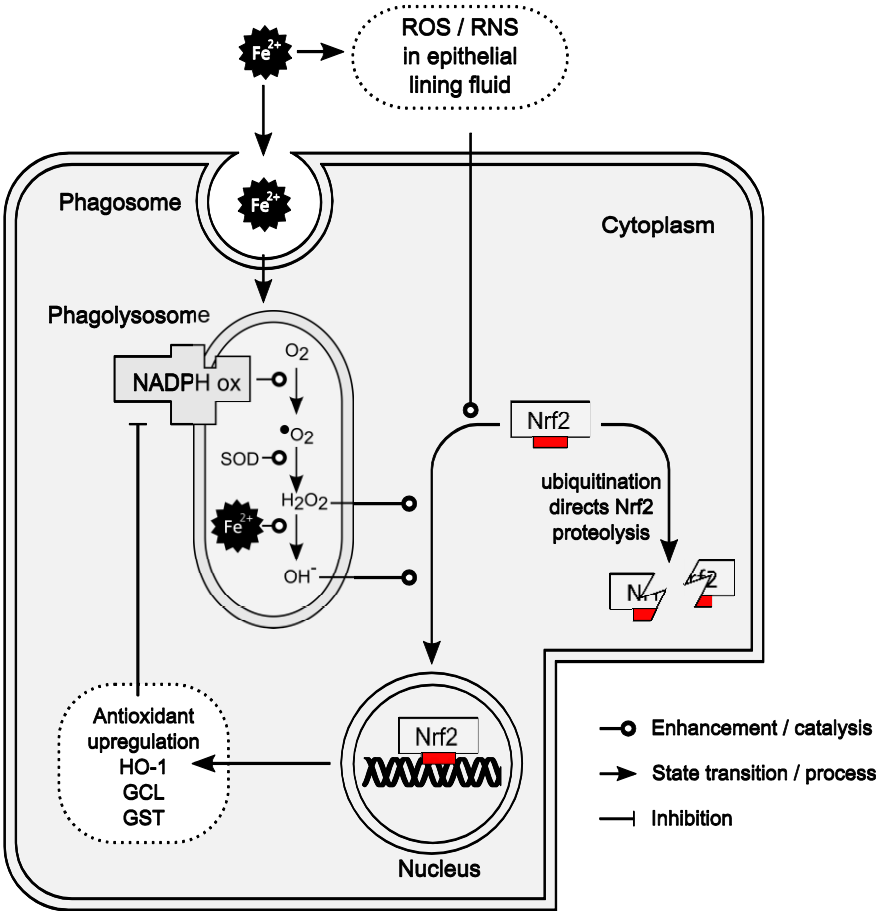

1 Particulate material in the airway is known to directly cause release of ROS and RNS from epithelium
2 Phagocytosis initates assembly and activation of NADPH oxidase
3 Ferrous material also promotes hydroxyl radical (OH-) formation from hydrogen peroxide
4 Both H_2O_2 and OH- leak from the phagolysosome and promote Nrf2 translocation to the nucleus
5 Nrf2 enhances transcription of genes associated with the Antioxidant Response Element (ARE)
6 HO-1 is known to inhibit NADPH oxidase activity

6 Conclusions and suggestions for further work

We have addressed three overarching hypotheses within this project.

1. Particulate exposure is associated with altered redox balance in the lung in both intracellular and extracellular compartments
2. Redox balance in the alveolar macrophage alters innate immune function
3. Particulate exposure is detrimental to alveolar macrophage function

Summary of the findings in context

Alveolar macrophages may undergo considerable changes to their phenotype depending on the redox balance. This in turn is dependent on intracellular endogenous production of reactive oxygen and nitrogen species and their release in response to exogenous sources, such as inhaled particulates.

6.1.1 Alveolar macrophages and monocytes have different redox balance

We have confirmed earlier studies which show that the redox balance in monocytes and alveolar macrophages are considerably different. Both glutathione peroxidase and superoxide dismutase levels are lower in monocytes. The results of our study agree with previous work: comparison of AM and monocytes demonstrated higher SOD in the former, predominantly due to cytoplasmic forms[192]. Glutathione peroxidase is also more highly expressed in AM[210]. Total glutathione in monocytes[198] and human alveolar macrophages[459] closely agreed with previous estimates. Taken together these results suggest that alveolar macrophages, being considerably larger than monocytes (4990μm^3 vs 332-380 μm^3),[548, 549] have a higher concentration of intracellular glutathione. Our results are compatible with this: we noted a non-significant difference between monocytes and HAM (10.71nmol/mg vs. 20.09nmol/mg).

The differences between monocytes and AM suggest that the upregulation of enzymatic antioxidants is necessary for HAM to function in the microenvironment of the lung. When numbers of alveolar macrophages are depleted due to infection, or particulate induced cell death, they are replenished both from parenchymal lung macrophages, and from influx of circulating monocytes. In the latter, this is likely to mean that the lung supports a population of "early" tissue phagocytes which have different (and less) buffering against oxidative stress.

6.1.2 Baseline redox balance in the lung

We have defined the redox balance of alveolar macrophages in three human cohorts. Previous comparisons have included non-smokers and those exposed to cigarette smoke, but this is the first study to establish differences in two non-smoking, healthy human populations.

In our study, intracellular glutathione concentrations were significantly lower in smokers compared with non-smokers in the UK, in agreement with previous work[459]. In a Malawian population highly exposed to inhalable particulates from biomass fuels, levels were non-significantly lower than UK non-smokers. Extracellular glutathione was raised in both the UK smokers and Malawian non-smokers. This was a consistent antioxidant response in the Malawi group, as evidenced by higher rates of lipid peroxidation in HAM.

Glutathione levels in smokers have been previously shown to be lower in AM and higher in acellular epithelial lining fluid than non-smokers[459]. In that study, expression of the glutamate cysteine ligase modulatory unit was decreased suggesting that *de* novo synthesis of glutathione was impaired by smoking, and that extracellular glutathione had an alternative (non AM) source.

Our findings concur with these observations. Furthermore, we note that Malawians have a pattern of GSH both inside and outside the cell which is similar to cigarette smokers. Although circumstantial, the difference between Malawian and UK volunteers redox status in terms of glutathione and lipid peroxidation provides evidence that lifestyle and environmental influences can alter redox balance in the lung. It is likely, given the profound differences in particulate exposures, that indoor air pollution plays a contributory role in this. These are the first data to show significant variation in redox balance and oxidative damage *in vivo* between two populations of healthy humans.

Our finding of *ex vivo* derangement of glutathione balance in human alveolar macrophages exposed to wood smoke extract provides a demonstration of plausible biological effect. We used wood smoke derived from the same source as that which is used by the local population, and endeavoured to control the dose in order that *ex vivo* and *in vivo* cytoplasmic particulate burdens were similar. We did not, however, demonstrate a dose response relationship between *in vivo* measures of glutathione and particulate burden in the alveolar macrophage. This may be explained by data from questionnaire study which showed that exposure to biomass fuel burning in the home was close to universal. It is possible that the exposure in Malawians may be sufficient to cause redox changes in nearly all volunteers. A similar low threshold has been seen in intervention trials: the RESPIRE study installed cleaner cook stoves and demonstrated a reduction in pneumonia, but this was most evident only with substantial reductions from the baseline exposure[11]. Another potential explanation for this is the relatively low exposure gradient seen in our volunteers compared with previous cohorts recruited from similar environs of Blantyre, Malawi[361]. It might be expected that studies requiring volunteers for BAL might suffer from this problem, and therefore misrepresent the population in general. It is also recognised

that the measurement of AM cytoplasmic particulate is not necessarily a direct measurement of exposure: different combustion sources affect this independent of dose and in particular, kerosene smoke causes relatively more macrophage particulate "blackening" [Unpublished data from our group].

6.1.3 Marker redox changes in a subgroup of volunteers

We measured the proportion of total glutathione in HAM which was in the oxidised form. Despite a small total number of volunteers, within the Malawian group there is strong evidence of a subgroup of individuals with high GSSG to GSH ratios. Using a modelling approach, we have provided evidence that this is not simply artefact, but is likely to represent a real observed difference. Specifically: 1) that this measure in Malawians is more likely to be represented by a bimodal than a unimodal distribution and 2) there is no statistical evidence for the same distribution in the UK cohort. Multivariate analysis suggests a strong relationship between high oxidised glutathione and low total glutathione and glutathione peroxidase levels.

The subgroup we have described will be predisposed to oxidative stress due to low antioxidant (GSH and GPx) capacity and therefore these individuals will have a higher risk of oxidative damage to HAM, and will also tend towards a pro-inflammatory phenotype. This subgroup has not been previously described in humans, and should be investigated further. The three variables remaining in the multivariate model as predictors of GSSG to GSH ratio were: lighting with paraffin (negatively associated with high ratio); total glutathione (negatively associated); glutathione peroxidase (negatively associated). In interpreting these findings, we assume that the process of retrieving cells by bronchoscopy and lavage, is in itself a stressor and likely to cause short term changes in the glutathione *i.e.* that this output

is a measurement of the propensity to oxidative stress within the HAM. Furthermore, the relationship of GSH, GSSG:GSH and GPx strongly suggests a consistent lack of antioxidant upregulation in the high GSSG:GSH subgroup. Our interpretation of these findings, assuming that none are subject to type 1 error, might be one of the following:

1. That paraffin lighting prevents high GSSG to GSH ratio through upregulation of other antioxidants, perhaps through chronic oxidative stress in the lung leading to Nrf2 activation
2. That alternative fuels cause relatively less upregulation than paraffin, or cause damage to GSH and GPx activity, leaving the cells less buffered against oxidative stress. This occurs in cigarette smokers, with whom the non-smoking Malawians have some common redox responses
3. That another unmeasured factor within the Malawian population predisposes to oxidative stress in the macrophage. In this context, with a bimodal peak likely to represent reality, a genetic polymorphism or deletion might provide an explanation. Examples are GSTM1 and GSTT1 which are involved in conjugation of glutathione with toxic substances. Upon challenge with biomass fuels except paraffin, differences in these enzyme activities are unmasked and measurable as GSSG to GSH. Other metabolic steps which could conceivably be altered in this way are shown in Figure 6-1. Specifically, γ-glutamyl-transferase which alters intracellular availability of glutathione subunits, and glutamate-cysteine-ligase which is the rate limiting step in glutathione formation. Measurement of a number of genetic polymorphisms might provide some useful information. For future studies, the implications of our findings are that, when subjected to measures to reduce levels of oxidative stress in the lung (for example by providing advanced cook stoves), individuals within a population are likely to show considerable heterogeneity of response.

Figure 6-1 Glutathione metabolic pathways

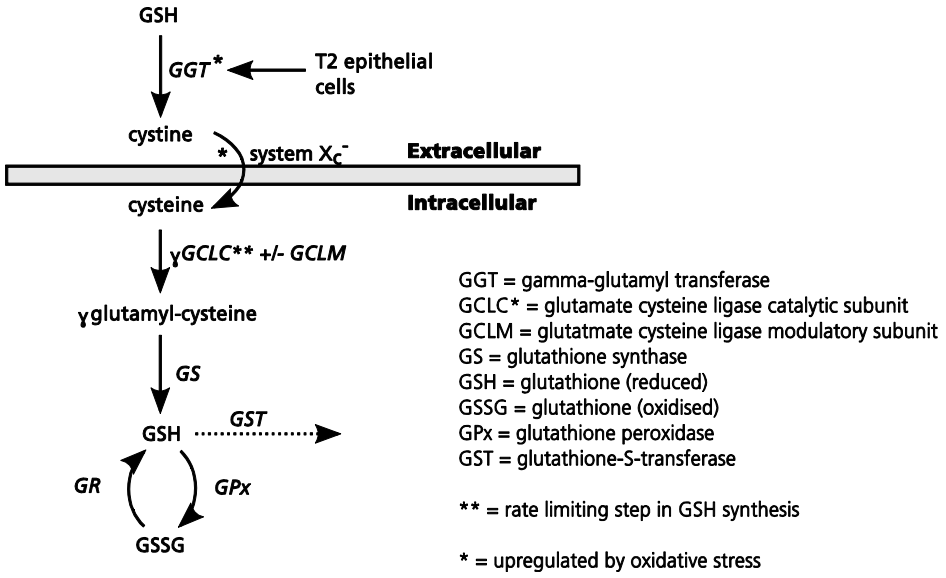

Simplified diagram of the metabolic pathways in the synthesis and use of glutathione. This describes enzymatic steps which might explain the observed bimodal peak of oxidised glutathione in human alveolar macrophages. See text for details.

6.1.4 Selenium and glutathione peroxidase relationship

We found that selenium is positively associated with whole blood glutathione peroxidase activity. This is consistent with previous reports[446]. In our cohorts, the association was stronger in UK volunteers than in the Malawian group despite very similar mean plasma selenium concentrations. It is known that GPx activity is regulated at multiple points including: the effects of the Sec insertion sequence (SECIS, which is required in the mRNA of selenoproteins for full expression of selenocysteine residues); post-transcription methylation of tRNA; alteration of mRNA stability by adenosine; tyrosine kinase pathways; homocysteine levels. Oxidative stress and homocysteine may reduce SECIS effect[250]. This multi-point regulation allows for wide ranging stimuli to alter GPx activity, and makes single factor differences between the two populations very difficult to identify. The lack of relationship between selenium and GPx in HAM is likely to represent this

phenomenon, and also a difference in proportions of GPx forms in these two compartments.

From these results we can infer that interventions to increase GPx levels *in vivo* (by providing dietary selenium supplementation) will not succeed in elevating such levels in the lung.

6.1.5 Phagosomal function and particulate

Our observation that intraphagosomal oxidative burst is reduced in macrophages with high particulate burden is novel. It appears that this abnormality is isolated to a specific pathway, as phagocytosis and proteolysis are unaffected. Furthermore, where LPS pre-stimulation usually increases oxidative burst in monocytes and monocyte derived macrophages, it may impair NADPH oxidase activity in HAM.

Hypotheses to explain this phenomenon in a mechanistic context are laid out in 5.4.4. The NADPH oxidase pathway might be affected at a number of points: altered trafficking and assembly of the NADPH oxidase subunits at the phagosome; reduced phosphorylation of the complex; reduced availability of the p40 subunit. The availability of antioxidants might influence NADPH oxidase activity. Although we found no direct evidence for this in terms of GPx and SOD levels in highly smoke exposed individuals, the increased Nrf2 in this subpopulation suggests upregulation.

In vitro models might not be useful, as the phenomenon we have observed seems peculiar to *in vivo* exposure in humans. Using primary macrophages is difficult due to low numbers of cells, but a mouse model will only be useful if *in vivo* exposures can adequately reproduce the phenomena which we have observed. Further experiments would then usefully include comparison of smoke exposed and unexposed mice, examining:

- Co-localisation of NADPH oxidase subunits and the phagosomal membrane, for example using fluorescent labelled antibodies to $p47^{phox}$ and LAMP to visualise the structures under confocal microscopy
- The use of existing Nrf2 knockout murine models. It should be expected that the effect of smoke exposure would be relatively reduced in such mice, although the background NADPH oxidase activity would increase
- *Ex vivo* manipulation of antioxidant concentrations, for example using specific enzyme blockers. However, these studies are difficult as the effect must be great enough to measure above background heterogeneity, but low enough to avoid significant toxicity. Our experience using BSO to reduce glutathione was that although reductions in availability were possible without such toxicity, downstream effects were difficult to measure

The major finding, however, is that particulate exposure *in vivo* has been directly associated with impaired antibacterial action. Although our study was performed in adults, we propose that the cellular observations will be similar in children. In this age group, reduced macrophage function could plausibly explain the association of particulates with pneumonia and death[6].

Interventions to reduce indoor particulate exposure have recently been given greater political prominence, with organisations such as the Global Alliance for Clean Cookstoves (http://www.cleancookstoves.org/the-alliance/) campaigning for action, citing multiple advantages to improving cooking and lighting emissions: decreased deforestation with positive effects on the local ecosystem; combating climate change; decreasing costs to consumers by improving efficiency; empowerment of women; improving morbidity and mortality. Our data provide the first *in vivo* description of how such health benefits might occur, and highlight the on-going risk of disease in those 2.4 billion people exposed. While intervention studies are keenly needed to identify the most effective and cost-efficient means of

decreasing emissions from domestic lighting and cooking appliances, it is clear that public health interventions will be needed on a massive scale. This study provides data on biological plausibility, and strengthens the case for action.

6.1.6 HAM phenotype measurement and polarisation

We found phenotypes of human alveolar macrophages to be relatively unresponsive to LPS treatment. There was also no relationship with particulate load. Changes in surface antigens could be detected more easily during the first 24 hours of adherent cell culture. This suggests that, where *ex vivo* phenotypes are measured, this should be done without intermediate *in vitro* cell culture.

Our observations also serve to highlight several difficulties of working with human alveolar macrophages: autofluorescence and a relative lack of data on phenotype compared with mouse models. These experiments could be extended by using interferon-γ in addition to LPS in order to increase the strength of stimulus. However, where "natural" exposures in healthy populations are being compared, our stimuli exceeded the likely *in vivo* stimuli. Measurable alterations in the phenotype according to the M1/M2 paradigm are possible in disease processes, but their success in explaining variation in a healthy population will require more sophisticated approaches, and the additional measurement of intracellular functional parameters.

6.1.7 Nrf2 increases with high levels of particulates

In preliminary observations of intracellular Nrf2, we noted a positive correlation between Nrf2 concentrations and *in vivo* particulate exposure. This is expected from *in vitro* studies of concentrated ambient particles[115] which showed both an upregulation response and a protective effect of Nrf2 in macrophages. In humans, these data represent novel confirmation of the relevance of this to alveolar

macrophages. Confirmation of these observations should be performed, with measurements of ARE associated gene products. This would support Nrf2 data with downstream measurements of effect on the cell biology *e.g.* HO-1 or GCLC upregulation. These products are measurable using Western blot techniques; their cytoplasmic concentrations and stability are higher than Nrf2.

If the findings are replicable, these data show that, unlike cigarette smoking which impairs Nrf2 activity[544], the level of particulates inhaled by our volunteers caused an upregulation of protective responses. Nrf2 is implicated in protection from oxidative stress in animal studies, where it is key in minimising susceptibility to lung damage from cigarettes[235]. Functional polymorphisms in humans are also linked with increased risk of acute lung injury[543]. Our study shows that Nrf2 is likely to be a relevant area of study in understanding susceptibility to the effect of particulate exposure.

6.1.8 Cytokine effects

Alveolar macrophages release selected cytokines after exposure to wood smoke particles at a dose which replicates a typical *in vivo* particulate burden. This includes rises in TNFα, IL-6 and IL-8. Prior *in vivo* exposures did not alter the LPS or wood smoke induced responses. Redox manipulation, by reducing intracellular glutathione, did not alter responses other than MCP-1, for which release was reduced. We did not replicate the only previous study of HAMs which showed, after glutathione depletion, increased production of TNFα and IL-8 in response to LPS[304].

We expected that recurrent *in vivo* challenge events with particulates would down-regulate subsequent responses and therefore reduce the potential for pulmonary damage as a result of chronic low level inflammation. We did not observe this effect.

There are no human studies with which to compare our results. Chronic exposure to $PM_{2.5}$ in mice has shown exaggerated inflammatory profiles from monocytes, which are in part mediated through the effect of lipid peroxidation on TLR4 and NADPH oxidase pathways[520]. In this study, there was an increase in lung MCP-1 associated with NADPH $p47^{phox}$ phosphorylation which the authors hypothesised led to pulmonary influx of monocytes. The effect on alveolar macrophages was not recorded: to reconcile our results with this study requires that other (endothelial and epithelial) cells play a greater role in cytokine production than AM, and that AM have somewhat down-regulated NADPH oxidase activity as a compensatory measure. In another model however, rabbits exposed to repeated tracheal instillation of urban PM_{10} had raised systemic inflammatory responses after six weeks of exposure[517]: IL-6 correlated with the proportion of AMs containing particulate matter.

While systemic inflammatory effects of pulmonary particulate exposure are not in doubt, the source of inflammatory mediators is not yet clear. In the context of the limited literature, it seems from our data that AM have dampened NADPH oxidase responses to chronic particulate exposure, but behave similarly in acute and chronic exposures with respect to cytokine release. This may represent a specific blunting of the pro-inflammatory response expected after repeated exposure.

6.2 Possibility of future human studies

Intervention with antioxidants in human populations has been studied in the context of both prevention and treatment of pneumonia. These arise from the observation of whole body depletion of some antioxidants during infection, and the subsequent suggestion that replacement might have a normalising (therefore beneficial) effect. Results have tended to be disappointing, including a detrimental

effect in some subgroups (for example, vitamin E supplementation in smokers). As described in section 1.2.4, oxidative stress leads to signalling changes, and an upregulation of pathways such as Nrf2 which buffer against cellular damage. Assuming that delivery of antioxidants to the necessary compartments is possible, altering the cellular redox balance with antioxidants is likely to have results which are difficult to predict. Desensitisation of pathways relating to inflammation and apoptosis can occur; while this will reduce oxidative stress, the overall functional effect on the AM might be detrimental. This may be a reason why interventions to manipulate of intracellular thiols have been ineffective. There is some suggestion that a more targeted approach may be more successful. For example Nrf2 agonism in mouse models of COPD and in *ex vivo* HAM improves bacterial clearance[317], but no studies on humans have been done.

Given the public health importance of both exposure (biomass smoke combustion) and effect (decreased innate immune function), human studies in the context of exposure reduction interventions would be most fruitful. Before and after comparisons of individuals taking part in, for example cook stove interventions, would test the relevance of our findings with respect to plausible improvements in particulate levels.

7 Appendices

7.1 Mathematical modelling of oxidised glutathione content of human alveolar macrophages

7.1.1 Script for creating the models in R

```
# Script and mathematical modelling by Prof Peter Diggle (25 September 2011)
# Comments by Peter Diggle preceded by PD:
# All other annotation of script by Jamie Rylance, and preceeded by JR:


# JR: Read data from CSV file
# JR: contains two columns: [1] Site (integer       1= Liverpool non-smokers
# JR:                                               2=Malawians)
# JR:                       [2] GSH ratio (floating point)

data<-read.csv("GSHdata_cleaned.csv",header=T)
names(data)
data<-data[!is.na(data$gshratio),]
dim(data)
gshrange<-range(data$gshratio)


# JR: Set up plot for cumulative distribution scatter plots for both cohorts

plot(gshrange,c(0,1),type="n",xlab="Oxidised glutathione ratio (%)",ylab="cumulative
proportion")


# JR: Separate arrays are created for each group: 'x' for UK non-smokers
# JR:                                             'y' for Malawians

# JR: Variables 'nx' and 'ny' are the number of observations
# JR: in their respective arrays

x<-data$gshratio[data$site==1]
nx<-length(x)

y<-data$gshratio[data$site==2]
ny<-length(y)


# JR: Data are sorted into arrays as above, and plotted in order
# JR: pch 19 = filled circle for UK non-smokers
# JR: pch 21 = open circle for Malawian non-smokers

points(sort(x),(1:nx)/nx, pch=19, col=gray(0))
points(sort(y),(1:ny)/ny, pch=21, col=gray(0))

# PD: cumulative plots - better for small data-sets than histograms because
# PD: no need to choose bin-width

# JR: Variables 'mux' and 'muy' are means of UK non-smokers
# JR: and Malawaian cohorts respectively

# JR: Variables 'sdx' and 'sdy' are their respective standard deviations

mux<-mean(x)
sdx<-sqrt(var(x))
muy<-mean(y)
sdy<-sqrt(var(y))

# JR: Array 'px' is an array of points to be plotted at intervals of 0.1
# JR: along the x axis

# JR: lty=1 = UK group in solid line
# JR: lty=2 = Malawian group in dotted line
# JR: Lines are drawn following a normal distriubution around each
```

```
# JR: cohort mean with given SD

px<-1+0.1*(0:145)
lines(px,pnorm(px,mux,sdx),col=gray(0), lwd=3, lty=1)
lines(px,pnorm(px,muy,sdy),col=gray(0), lwd=3, lty=2)

# JR: UK cohort approximates normal distribution
# JR: Considerable deviation from normal in the Malawi cohort


# PD: define log-likelihood functions for simple Normal and for
# PD: two-component Normal mixture

# JR: f1 is the simple normal distribution
# JR: f2 is the combined function of two normal distributions

        f1<-function(x,mu,sigma) {
                sum(dnorm(x,mu,sigma,log=T))
                }
        f2<-function(x,mu1,sigma1,mu2,sigma2,p) {
                sum(log(p*dnorm(x,mu1,sigma1)+(1-p)*dnorm(x,mu2,sigma2)))
                }

# PD: define various log-likelihood functions that might be of interest
# PD: L1: Malawi is completely different to Liverpool

        L1<-function(x,y,mu1,sigma1,mu2,sigma2,mu3,sigma3,p) {
                f1(x,mu1,sigma1)+f2(y,mu2,sigma2,mu3,sigma3,p)
                }

# PD: L0: Malawi is mix of Liverpool plus something different
        L0<-function(x,y,mu1,sigma1,mu2,sigma2,p) {
                f1(x,mu1,sigma1)+f2(y,mu1,sigma1,mu2,sigma2,p)
                }

# PD: Maximum liklihood estimation for Liverpool
        muhat<-mean(x)
        sigmahat<-sqrt(nx*var(x)/(nx-1))
        maxL.liv<-f1(x,muhat,sigmahat)

# JR: Maximum liklihood for this = -25.81514



# JR: ### MODEL 1 ###

# PD: MLE for Malawi, assuming completely different from UK

        p.init<-0.5

        mu1.init<-muhat
        sigma1.init<-sigmahat

        mu2.init<-mu1.init
        sigma2.init<-sigma1.init

        mu3.init<-(mean(y)-p.init*mu2.init)/(1-p.init)
        sigma3.init<-sigma1.init

param<-log(c(mu1.init,sigma1.init,mu2.init,sigma2.init,mu3.init,sigma3.init,p.init))
        print.progress<-F

        fn1<-function(param) {
                ep<-exp(param)
                mu1<-ep[1]
                sigma1<-ep[2]
                mu2<-ep[3]
                sigma2<-ep[4]
                mu3<-ep[5]
                sigma3<-ep[6]
                p<-ep[7]
                logL<-L1(x,y,mu1,sigma1,mu2,sigma2,mu3,sigma3,p)
                if (print.progress) print(round(c(ep,logL),3))
                -logL
        }

# JR: Iteration continues to refine this model (up to 500 times)
```

```
        result1<-optim(param,fn1,control=list(maxit=500))
        maxL.both<--result1$value

# JR: Maximum liklihood for this = maxL.both = -124.174

        thetahat<-exp(result1$par)
        round(thetahat,3)

# PD: [1] 3.879 2.062 2.747 1.051 8.550 3.331 0.732

# JR: Results of this model 'thetahat' suggest:
# JR:          UK mean  = 3.879
# JR:          UK SD    = 2.062
# JR: and where Malawi group has two normally distributed component 'sub' populations
# JR:          Malawi mean [1] = 2.747
# JR:          Malawi SD   [1] = 1.051
# JR:          Malawi mean [2] = 8.550
# JR:          Malawi SD   [2] = 3.331
# JR:   and that of the overall Malawi group
# JR:          component   [1] represents 0.732 of the total ie. 73.2%


# JR: ### MODEL 2 ###

# PD: for Malawi assuming Normally distributed

        mu2hat<-mean(y)
        sigma2hat<-sqrt(ny*var(y)/(ny-1))
        maxL0.mal<-f1(y,mu2hat,sigma2hat)

# JR: Maximum liklihood for this = maxL0.mal = -116.5128

# JR: Greater Likelihood Ratio Test (GLRT) for Malawi Normal vs Malawi mixture

        dev<-2*(maxL.both-(maxL0.mal+maxL.liv))

# PD: GLRT output = dev = 11.63861

        p<-1-pchisq(dev,3)

# PD: p<0.0001

# JR: Reject the null hypothesis ie. that there is no better fit of the
# JR: Malawi mixture model compared with the normally distributed model



# JR: ### MODEL 3 ###

# PD: for combined data, assuming one component of UK same as Malawi

        fn2<-function(param) {
                ep<-exp(param)
                mu1<-ep[1]
                sigma1<-ep[2]
                mu2<-ep[3]
                sigma2<-ep[4]
                p<-ep[5]
                logL<-L1(x,y,mu1,sigma1,mu1,sigma1,mu2,sigma2,p)
                if (print.progress) print(round(c(ep,logL),3))
                -logL
        }

        mu1.init<-thetahat[1]
        sigma1.init<-thetahat[2]
        mu2.init<-thetahat[3]
        sigma2.init<-thetahat[4]
        p.init<-1-thetahat[7]
        param<-log(c(mu1.init,sigma1.init,mu2.init,sigma2.init,p.init))
        result2<-optim(param,fn2,control=list(maxit=5000))
        thetahat2<-exp(result2$par)
        maxL.both.constrained<--result2$value
        dev<-2*(maxL.both-maxL.both.constrained)

# JR: Model output = dev = 11.63861

        p<-1-pchisq(dev,2)
```

```
# PD: p=0.002969669

# JR: Reject the null hypothesis ie. that there is no difference between
       the UK cohort and one component of the Malawi cohort


# PD: Maximum Likelihood Estimate MLE's for Malawi only
# PD: (since no parameters in common with UK)
       fn3<-function(param) {
              ep<-exp(param)
              mu1<-ep[1]
              sigma1<-ep[2]
              mu2<-ep[3]
              sigma2<-ep[4]
              p<-ep[5]
              logL<-f2(y,mu1,sigma1,mu2,sigma2,p)
              if (print.progress) print(round(c(ep,logL),3))
              -logL
       }
       param<-log(thetahat[3:7])
       result3<-optim(param,fn3,control=list(maxit=5000))
       thetahat3<-exp(result3$par)



# PD: Highly significant evidence for:
# PD:   (a) Malawi is a mixture of two component Normals
# PD:   (b) Neither of the two Malawi component distributions is equal
# PD:       to the UK distribution
#


# JR: Then plot the model against the original data

       x<-0.1*(10:150)
       F.liv<-pnorm(x,3.879,2.062)

       F.mal<-0.732*pnorm(x,2.747,1.0581)+(1-0.732)*pnorm(x,8.550,3.331)

       lines(x,F.liv,lwd=2,col="red", lty=1)
       lines(x,F.mal,lwd=2,col="red", lty=2)

write.csv(x, file="output.csv")
write.csv(F.mal, file="output2.csv")

# JR: Script ends
```

7.2 Nernst equation for redox reactions

Equation 22:

$$aRed_1 + bOx_2 \overset{equilibrium}{\Longleftrightarrow} cOx_1 + dOx_2$$

Equation 23:

(Nernst equation)

$$\Delta E = \Delta E^{\circ} \frac{RT}{nF} ln\left(\frac{[Ox_1]^c[Red_2]^d}{[Red_1]^a[Ox_2]^b}\right)$$

where: R = gas constant

T = temperature

F = Faraday constant

ΔE^0 = standard reduction potential *i.e.* electromotive force

n= number of moles electrons transferred

8 References

1. Rudan I, Boschi-Pinto C, Biloglav Z, Mulholland K, Campbell H. Epidemiology and etiology of childhood pneumonia. *Bull World Health Organ* 2008; **86**(5): 408-16.
2. Jones N, Huebner R, Khoosal M, Crewe-Brown H, Klugman K. The impact of HIV on Streptococcus pneumoniae bacteraemia in a South African population. *AIDS* 1998; **12**(16): 2177-84.
3. Nuorti JP, Butler JC, Farley MM, et al. Cigarette smoking and invasive pneumococcal disease. Active Bacterial Core Surveillance Team. *N Engl J Med* 2000; **342**(10): 681-9.
4. Coles CL, Fraser D, Givon-Lavi N, et al. Nutritional status and diarrheal illness as independent risk factors for alveolar pneumonia. *Am J Epidemiol* 2005; **162**(10): 999-1007.
5. Emmelin A, Wall S. Indoor air pollution: a poverty-related cause of mortality among the children of the world. *Chest* 2007; **132**(5): 1615-23.
6. Dherani M, Pope D, Mascarenhas M, Smith KR, Weber M, Bruce N. Indoor air pollution from unprocessed solid fuel use and pneumonia risk in children aged under five years: a systematic review and meta-analysis. *Bull World Health Organ* 2008; **86**(5): 390-8C.
7. Mulholland K. Perspectives on the burden of pneumonia in children. *Vaccine* 2007; **25**(13): 2394-7.
8. Pope CA, 3rd, Ezzati M, Dockery DW. Fine-particulate air pollution and life expectancy in the United States. *N Engl J Med* 2009; **360**(4): 376-86.
9. Torres-Duque C, Maldonado D, Perez-Padilla R, Ezzati M, Viegi G. Biomass fuels and respiratory diseases: a review of the evidence. *Proc Am Thorac Soc* 2008; **5**(5): 577-90.
10. Ezzati M, Kammen D. Indoor air pollution from biomass combustion and acute respiratory infections in Kenya: an exposure-response study. *Lancet* 2001; **358**(9282): 619-24.
11. Smith KR, McCracken JP, Weber MW, et al. Effect of reduction in household air pollution on childhood pneumonia in Guatemala (RESPIRE): a randomised controlled trial. *Lancet* 2011; **378**(9804): 1717-26.
12. Hoffmann JA, Kafatos FC, Janeway CA, Ezekowitz RA. Phylogenetic perspectives in innate immunity. *Science* 1999; **284**(5418): 1313-8.
13. Delves PJ, Roitt IM. Roitt's essential immunology. 12th ed. Chichester, West Sussex ; Hoboken, NJ: Wiley-Blackwell; 2011.
14. Zwilling BS, Eisenstein TK. Macrophage-pathogen interactions. New York: M. Dekker; 1994.
15. Medzhitov R, Schneider DS, Soares MP. Disease tolerance as a defense strategy. *Science* 2012; **335**(6071): 936-41.
16. Van der Schans CP. Bronchial mucus transport. *Respir Care* 2007; **52**(9): 1150-6; discussion 6-8.
17. Ganz T. Defensins: antimicrobial peptides of innate immunity. *Nat Rev Immunol* 2003; **3**(9): 710-20.
18. Zipfel PF, Skerka C. Complement regulators and inhibitory proteins. *Nat Rev Immunol* 2009; **9**(10): 729-40.
19. Stuart LM, Ezekowitz RA. Phagocytosis and comparative innate immunity: learning on the fly. *Nat Rev Immunol* 2008; **8**(2): 131-41.

20. Underhill DM, Goodridge HS. Information processing during phagocytosis. *Nat Rev Immunol* 2012; **12**(7): 492-502.
21. Soehnlein O, Lindbom L. Phagocyte partnership during the onset and resolution of inflammation. *Nat Rev Immunol* 2010; **10**(6): 427-39.
22. Anjilvel S, Asgharian B. A multiple-path model of particle deposition in the rat lung. *Fundamental and applied toxicology : official journal of the Society of Toxicology* 1995; **28**(1): 41-50.
23. Heyder J. Deposition of inhaled particles in the human respiratory tract and consequences for regional targeting in respiratory drug delivery. *Proc Am Thorac Soc* 2004; **1**(4): 315-20.
24. Gordon SB, Read RC. Macrophage defences against respiratory tract infections. *British medical bulletin* 2002; **61**: 45-61.
25. Karimi R, Tornling G, Grunewald J, Eklund A, Skold CM. Cell recovery in bronchoalveolar lavage fluid in smokers is dependent on cumulative smoking history. *PLoS One* 2012; **7**(3): e34232.
26. Meyer KC, Soergel P. Variation of bronchoalveolar lymphocyte phenotypes with age in the physiologically normal human lung. *Thorax* 1999; **54**(8): 697-700.
27. Burkitt HG, Young B, Heath JW, Wheater PR. Wheater's functional histology : a text and colour atlas. 3rd ed. Edinburgh ; New York: Churchill Livingstone; 1993.
28. Trisolini R, Lazzari Agli L, Cancellieri A, et al. Bronchoalveolar lavage findings in severe community-acquired pneumonia due to Legionella pneumophila serogroup 1. *Respir Med* 2004; **98**(12): 1222-6.
29. Lam JK, Liang W, Chan HK. Pulmonary delivery of therapeutic siRNA. *Adv Drug Deliv Rev* 2012; **64**(1): 1-15.
30. Garcia-Suarez Mdel M, Florez N, Astudillo A, et al. The role of pneumolysin in mediating lung damage in a lethal pneumococcal pneumonia murine model. *Respir Res* 2007; **8**: 3.
31. van der Poll T, Opal SM. Pathogenesis, treatment, and prevention of pneumococcal pneumonia. *Lancet* 2009; **374**(9700): 1543-56.
32. Bogaert D, De Groot R, Hermans PW. Streptococcus pneumoniae colonisation: the key to pneumococcal disease. *Lancet Infect Dis* 2004; **4**(3): 144-54.
33. Bentley SD, Aanensen DM, Mavroidi A, et al. Genetic analysis of the capsular biosynthetic locus from all 90 pneumococcal serotypes. *PLoS genetics* 2006; **2**(3): e31.
34. Hirst RA, Kadioglu A, O'Callaghan C, Andrew PW. The role of pneumolysin in pneumococcal pneumonia and meningitis. *Clin Exp Immunol* 2004; **138**(2): 195-201.
35. Kadioglu A, Weiser JN, Paton JC, Andrew PW. The role of Streptococcus pneumoniae virulence factors in host respiratory colonization and disease. *Nat Rev Microbiol* 2008; **6**(4): 288-301.
36. Davis KM, Nakamura S, Weiser JN. Nod2 sensing of lysozyme-digested peptidoglycan promotes macrophage recruitment and clearance of S. pneumoniae colonization in mice. *J Clin Invest* 2011; **121**(9): 3666-76.
37. Rubins JB. Alveolar macrophages: wielding the double-edged sword of inflammation. *Am J Respir Crit Care Med* 2003; **167**(2): 103-4.
38. Taut K, Winter C, Briles DE, et al. Macrophage Turnover Kinetics in the Lungs of Mice Infected with Streptococcus pneumoniae. *Am J Respir Cell Mol Biol* 2008; **38**(1): 105-13.

39. Flannagan RS, Jaumouille V, Grinstein S. The cell biology of phagocytosis. *Annual review of pathology* 2012; **7**: 61-98.
40. Gordon SB, Irving GR, Lawson RA, Lee ME, Read RC. Intracellular trafficking and killing of Streptococcus pneumoniae by human alveolar macrophages are influenced by opsonins. *Infect Immun* 2000; **68**(4): 2286-93.
41. Taylor PR, Martinez-Pomares L, Stacey M, Lin HH, Brown GD, Gordon S. Macrophage receptors and immune recognition. *Annual review of immunology* 2005; **23**: 901-44.
42. Arredouani MS, Palecanda A, Koziel H, et al. MARCO is the major binding receptor for unopsonized particles and bacteria on human alveolar macrophages. *J Immunol* 2005; **175**(9): 6058-64.
43. Thakur SA, Hamilton RF, Jr., Holian A. Role of scavenger receptor a family in lung inflammation from exposure to environmental particles. *Journal of immunotoxicology* 2008; **5**(2): 151-7.
44. Pluddemann A, Mukhopadhyay S, Gordon S. The interaction of macrophage receptors with bacterial ligands. *Expert reviews in molecular medicine* 2006; **8**(28): 1-25.
45. Vieira OV, Botelho RJ, Grinstein S. Phagosome maturation: aging gracefully. *Biochem J* 2002; **366**(Pt 3): 689-704.
46. Fang FC. Antimicrobial reactive oxygen and nitrogen species: concepts and controversies. *Nat Rev Microbiol* 2004; **2**(10): 820-32.
47. Nauseef WM. Assembly of the phagocyte NADPH oxidase. *Histochem Cell Biol* 2004; **122**(4): 277-91.
48. Cross AR. p40(phox) Participates in the activation of NADPH oxidase by increasing the affinity of p47(phox) for flavocytochrome b(558). *Biochem J* 2000; **349**(Pt 1): 113-7.
49. Flannagan RS, Cosio G, Grinstein S. Antimicrobial mechanisms of phagocytes and bacterial evasion strategies. *Nat Rev Microbiol* 2009; **7**(5): 355-66.
50. Toews GB, Vial WC, Dunn MM, et al. The accessory cell function of human alveolar macrophages in specific T cell proliferation. *J Immunol* 1984; **132**(1): 181-6.
51. Guth AM, Janssen WJ, Bosio CM, Crouch EC, Henson PM, Dow SW. Lung environment determines unique phenotype of alveolar macrophages. *Am J Physiol Lung Cell Mol Physiol* 2009; **296**(6): L936-46.
52. Gong JL, McCarthy KM, Rogers RA, Schneeberger EE. Interstitial lung macrophages interact with dendritic cells to present antigenic peptides derived from particulate antigens to T cells. *Immunology* 1994; **81**(3): 343-51.
53. Opitz B, van Laak V, Eitel J, Suttorp N. Innate immune recognition in infectious and noninfectious diseases of the lung. *Am J Respir Crit Care Med* 2010; **181**(12): 1294-309.
54. Koppe U, Suttorp N, Opitz B. Recognition of Streptococcus pneumoniae by the innate immune system. *Cellular microbiology* 2012; **14**(4): 460-6.
55. Schmeck B, Zahlten J, Moog K, et al. Streptococcus pneumoniae-induced p38 MAPK-dependent phosphorylation of RelA at the interleukin-8 promotor. *J Biol Chem* 2004; **279**(51): 53241-7.
56. Verstak B, Nagpal K, Bottomley SP, Golenbock DT, Hertzog PJ, Mansell A. MyD88 adapter-like (Mal)/TIRAP interaction with TRAF6 is critical for TLR2- and TLR4-mediated NF-kappaB proinflammatory responses. *J Biol Chem* 2009; **284**(36): 24192-203.

57. Malley R, Henneke P, Morse SC, et al. Recognition of pneumolysin by Toll-like receptor 4 confers resistance to pneumococcal infection. *Proc Natl Acad Sci U S A* 2003; **100**(4): 1966-71.
58. Dessing MC, Florquin S, Paton JC, van der Poll T. Toll-like receptor 2 contributes to antibacterial defence against pneumolysin-deficient pneumococci. *Cellular microbiology* 2008; **10**(1): 237-46.
59. Kong X, Thimmulappa R, Kombairaju P, Biswal S. NADPH oxidase-dependent reactive oxygen species mediate amplified TLR4 signaling and sepsis-induced mortality in Nrf2-deficient mice. *J Immunol* 2010; **185**(1): 569-77.
60. Anrather J, Racchumi G, Iadecola C. NF-kappaB regulates phagocytic NADPH oxidase by inducing the expression of gp91phox. *J Biol Chem* 2006; **281**(9): 5657-67.
61. Dewas C, Dang PM, Gougerot-Pocidalo MA, El-Benna J. TNF-alpha induces phosphorylation of p47(phox) in human neutrophils: partial phosphorylation of p47phox is a common event of priming of human neutrophils by TNF-alpha and granulocyte-macrophage colony-stimulating factor. *J Immunol* 2003; **171**(8): 4392-8.
62. Marriott HM, Hellewell PG, Whyte MK, Dockrell DH. Contrasting roles for reactive oxygen species and nitric oxide in the innate response to pulmonary infection with Streptococcus pneumoniae. *Vaccine* 2007; **25**(13): 2485-90.
63. Segal BH, Han W, Bushey JJ, et al. NADPH oxidase limits innate immune responses in the lungs in mice. *PLoS One* 2010; **5**(3): e9631.
64. Jenner RG, Young RA. Insights into host responses against pathogens from transcriptional profiling. *Nat Rev Microbiol* 2005; **3**(4): 281-94.
65. Nau GJ, Richmond JF, Schlesinger A, Jennings EG, Lander ES, Young RA. Human macrophage activation programs induced by bacterial pathogens. *Proc Natl Acad Sci U S A* 2002; **99**(3): 1503-8.
66. Marriott HM, Hellewell PG, Cross SS, Ince PG, Whyte MK, Dockrell DH. Decreased alveolar macrophage apoptosis is associated with increased pulmonary inflammation in a murine model of pneumococcal pneumonia. *J Immunol* 2006; **177**(9): 6480-8.
67. Erwig LP, Henson PM. Immunological consequences of apoptotic cell phagocytosis. *Am J Pathol* 2007; **171**(1): 2-8.
68. Marriott HM, Mitchell TJ, Dockrell DH. Pneumolysin: a double-edged sword during the host-pathogen interaction. *Curr Mol Med* 2008; **8**(6): 497-509.
69. Fadok VA, Bratton DL, Konowal A, Freed PW, Westcott JY, Henson PM. Macrophages that have ingested apoptotic cells in vitro inhibit proinflammatory cytokine production through autocrine/paracrine mechanisms involving TGF-beta, PGE2, and PAF. *J Clin Invest* 1998; **101**(4): 890-8.
70. Dockrell DH, Marriott HM, Prince LR, et al. Alveolar macrophage apoptosis contributes to pneumococcal clearance in a resolving model of pulmonary infection. *J Immunol* 2003; **171**(10): 5380-8.
71. Natarajan S, Kim J, Remick DG. Chronic pulmonary LPS tolerance induces selective immunosuppression while maintaining the neutrophilic response. *Shock* 2010; **33**(2): 162-9.
72. Langenback EG, Bergofsky EH, Halpern JG, Foster WM. Supramicron-sized particle clearance from alveoli: route and kinetics. *J Appl Physiol* 1990; **69**(4): 1302-8.

73. Oberdorster G, Oberdorster E, Oberdorster J. Nanotoxicology: an emerging discipline evolving from studies of ultrafine particles. *Environ Health Perspect* 2005; **113**(7): 823-39.
74. Renwick LC, Brown D, Clouter A, Donaldson K. Increased inflammation and altered macrophage chemotactic responses caused by two ultrafine particle types. *Occup Environ Med* 2004; **61**(5): 442-7.
75. Stoeger T, Reinhard C, Takenaka S, et al. Instillation of Six Different Ultrafine Carbon Particles Indicates a Surface Area Threshold Dose for Acute Lung Inflammation in Mice. *Environ Health Perspect* 2006; **114**(3): 328-33.
76. Beck-Speier I, Dayal N, Karg E, et al. Oxidative stress and lipid mediators induced in alveolar macrophages by ultrafine particles. *Free Radic Biol Med* 2005; **38**(8): 1080-92.
77. Tao F, Gonzalez-Flecha B, Kobzik L. Reactive oxygen species in pulmonary inflammation by ambient particulates. *Free Radic Biol Med* 2003; **35**(4): 327-40.
78. Pinel-Marie ML, Sparfel L, Desmots S, Fardel O. Aryl hydrocarbon receptor-dependent induction of the NADPH oxidase subunit NCF1/p47 phox expression leading to priming of human macrophage oxidative burst. *Free Radic Biol Med* 2009; **47**(6): 825-34.
79. Chin BY, Choi ME, Burdick MD, Strieter RM, Risby TH, Choi AM. Induction of apoptosis by particulate matter: role of TNF-alpha and MAPK. *Am J Physiol* 1998; **275**(5 Pt 1): L942-9.
80. WHO. Global health risks: Mortality and burden of disease attributable to selecte major risks. Geneva: WHO; 2009.
81. Fullerton DG, Bruce N, Gordon SB. Indoor air pollution from biomass fuel smoke is a major health concern in the developing world. *Trans R Soc Trop Med Hyg* 2008; **102**(9): 843-51.
82. Kocbach A, Namork E, Schwarze PE. Pro-inflammatory potential of wood smoke and traffic-derived particles in a monocytic cell line. *Toxicology* 2008; **247**(2-3): 123-32.
83. Semple S, Devakumar D, Fullerton DG, et al. Airborne Endotoxin Concentrations in Homes Burning Biomass Fuel. *Environ Health Perspect* 2010.
84. Imrich A, Ning Y, Lawrence J, et al. Alveolar macrophage cytokine response to air pollution particles: oxidant mechanisms. *Toxicol Appl Pharmacol* 2007; **218**(3): 256-64.
85. Mehta H, Nazzal K, Sadikot RT. Cigarette smoking and innate immunity. *Inflamm Res* 2008; **57**(11): 497-503.
86. Smith LA, Paszkiewicz GM, Hutson AD, Pauly JL. Inflammatory response of lung macrophages and epithelial cells to tobacco smoke: a literature review of ex vivo investigations. *Immunol Res* 2010; **46**(1-3): 94-126.
87. Naeher LP, Brauer M, Lipsett M, et al. Woodsmoke health effects: a review. *Inhal Toxicol* 2007; **19**(1): 67-106.
88. Bitterle E, Karg E, Schroeppel A, et al. Dose-controlled exposure of A549 epithelial cells at the air-liquid interface to airborne ultrafine carbonaceous particles. *Chemosphere* 2006; **65**(10): 1784-90.
89. Rothen-Rutishauser BM, Kiama SG, Gehr P. A three-dimensional cellular model of the human respiratory tract to study the interaction with particles. *Am J Respir Cell Mol Biol* 2005; **32**(4): 281-9.
90. Kocbach A, Herseth JI, Lag M, Refsnes M, Schwarze PE. Particles from wood smoke and traffic induce differential pro-inflammatory response patterns in co-cultures. *Toxicol Appl Pharmacol* 2008.

91. Barregard L, Sallsten G, Andersson L, et al. Experimental exposure to wood smoke: effects on airway inflammation and oxidative stress. *Occup Environ Med* 2008; **65**(5): 319-24.
92. Saksena S, Thompson L, Smith KR. Database of Husehold Air Pollution Studies in Developing Countries, Protection ofthe Human Environment. Geneva: WHO; 2003.
93. Huang YC, Li Z, Harder SD, Soukup JM. Apoptotic and inflammatory effects induced by different particles in human alveolar macrophages. *Inhal Toxicol* 2004; **16**(14): 863-78.
94. Ning Y, Imrich A, Goldsmith CA, Qin G, Kobzik L. Alveolar macrophage cytokine production in response to air particles in vitro: role of endotoxin. *J Toxicol Environ Health A* 2000; **59**(3): 165-80.
95. Becker S, Soukup JM, Gallagher JE. Differential particulate air pollution induced oxidant stress in human granulocytes, monocytes and alveolar macrophages. *Toxicol In Vitro* 2002; **16**(3): 209-18.
96. Urch B, Speck M, Corey P, et al. Concentrated ambient fine particles and not ozone induce a systemic interleukin-6 response in humans. *Inhal Toxicol* 2010; **22**(3): 210-8.
97. Goto Y, Ishii H, Hogg JC, et al. Particulate matter air pollution stimulates monocyte release from the bone marrow. *Am J Respir Crit Care Med* 2004; **170**(8): 891-7.
98. Sigaud S, Goldsmith CA, Zhou H, et al. Air pollution particles diminish bacterial clearance in the primed lungs of mice. *Toxicol Appl Pharmacol* 2007; **223**(1): 1-9.
99. Monn C, Becker S. Cytotoxicity and induction of proinflammatory cytokines from human monocytes exposed to fine (PM2.5) and coarse particles (PM10-2.5) in outdoor and indoor air. *Toxicol Appl Pharmacol* 1999; **155**(3): 245-52.
100. Becker S, Soukup JM, Gilmour MI, Devlin RB. Stimulation of human and rat alveolar macrophages by urban air particulates: effects on oxidant radical generation and cytokine production. *Toxicol Appl Pharmacol* 1996; **141**(2): 637-48.
101. Imrich A, Ning YY, Koziel H, Coull B, Kobzik L. Lipopolysaccharide priming amplifies lung macrophage tumor necrosis factor production in response to air particles. *Toxicol Appl Pharmacol* 1999; **159**(2): 117-24.
102. Imrich A, Ning Y, Kobzik L. Insoluble components of concentrated air particles mediate alveolar macrophage responses in vitro. *Toxicol Appl Pharmacol* 2000; **167**(2): 140-50.
103. Shaw CA, Robertson S, Miller MR, et al. Diesel exhaust particulate--exposed macrophages cause marked endothelial cell activation. *Am J Respir Cell Mol Biol* 2011; **44**(6): 840-51.
104. Pourazar J, Frew AJ, Blomberg A, et al. Diesel exhaust exposure enhances the expression of IL-13 in the bronchial epithelium of healthy subjects. *Respir Med* 2004; **98**(9): 821-5.
105. Fahy O, Senechal S, Pene J, et al. Diesel exposure favors Th2 cell recruitment by mononuclear cells and alveolar macrophages from allergic patients by differentially regulating macrophage-derived chemokine and IFN-gamma-induced protein-10 production. *J Immunol* 2002; **168**(11): 5912-9.
106. Mundandhara SD, Becker S, Madden MC. Effects of diesel exhaust particles on human alveolar macrophage ability to secrete inflammatory mediators in response to lipopolysaccharide. *Toxicol In Vitro* 2006; **20**(5): 614-24.
107. Yin XJ, Dong CC, Ma JY, Roberts JR, Antonini JM, Ma JK. Suppression of phagocytic and bactericidal functions of rat alveolar macrophages by the organic component of diesel exhaust particles. *J Toxicol Environ Health A* 2007; **70**(10): 820-8.

108. Harder V, Gilmour P, Lentner B, et al. Cardiovascular responses in unrestrained WKY rats to inhaled ultrafine carbon particles. *Inhal Toxicol* 2005; **17**(1): 29-42.
109. Li XY, Brown D, Smith S, MacNee W, Donaldson K. Short-term inflammatory responses following intratracheal instillation of fine and ultrafine carbon black in rats. *Inhal Toxicol* 1999; **11**(8): 709-31.
110. Leonard SS, Wang S, Shi X, Jordan BS, Castranova V, Dubick MA. Wood smoke particles generate free radicals and cause lipid peroxidation, DNA damage, NFkappaB activation and TNF-alpha release in macrophages. *Toxicology* 2000; **150**(1-3): 147-57.
111. Samuelsen M, Cecilie Nygaard U, Lovik M. Particles from wood smoke and road traffic differently affect the innate immune system of the lung. *Inhal Toxicol* 2009; **21**(11): 943-51.
112. Seagrave J, McDonald JD, Reed MD, Seilkop SK, Mauderly JL. Responses to subchronic inhalation of low concentrations of diesel exhaust and hardwood smoke measured in rat bronchoalveolar lavage fluid. *Inhal Toxicol* 2005; **17**(12): 657-70.
113. Tesfaigzi Y, McDonald JD, Reed MD, et al. Low-level subchronic exposure to wood smoke exacerbates inflammatory responses in allergic rats. *Toxicol Sci* 2005; **88**(2): 505-13.
114. Shukla A, Timblin C, BeruBe K, et al. Inhaled particulate matter causes expression of nuclear factor (NF)-kappaB-related genes and oxidant-dependent NF-kappaB activation in vitro. *Am J Respir Cell Mol Biol* 2000; **23**(2): 182-7.
115. Li YJ, Takizawa H, Azuma A, et al. Disruption of Nrf2 enhances susceptibility to airway inflammatory responses induced by low-dose diesel exhaust particles in mice. *Clinical immunology* 2008; **128**(3): 366-73.
116. Kafoury RM, Madden MC. Diesel exhaust particles induce the over expression of tumor necrosis factor-alpha (TNF-alpha) gene in alveolar macrophages and failed to induce apoptosis through activation of nuclear factor-kappaB (NF-kappaB). *International journal of environmental research and public health* 2005; **2**(1): 107-13.
117. Zelikoff JT, Chen LC, Cohen MD, et al. Effects of inhaled ambient particulate matter on pulmonary antimicrobial immune defense. *Inhal Toxicol* 2003; **15**(2): 131-50.
118. Bachoual R, Boczkowski J, Goven D, et al. Biological effects of particles from the paris subway system. *Chem Res Toxicol* 2007; **20**(10): 1426-33.
119. Arimoto T, Kadiiska MB, Sato K, Corbett J, Mason RP. Synergistic production of lung free radicals by diesel exhaust particles and endotoxin. *Am J Respir Crit Care Med* 2005; **171**(4): 379-87.
120. Behndig AF, Mudway IS, Brown JL, et al. Airway antioxidant and inflammatory responses to diesel exhaust exposure in healthy humans. *Eur Respir J* 2006; **27**(2): 359-65.
121. Fick RB, Jr., Paul ES, Merrill WW, Reynolds HY, Loke JS. Alterations in the antibacterial properties of rabbit pulmonary macrophages exposed to wood smoke. *Am Rev Respir Dis* 1984; **129**(1): 76-81.
122. Ghio AJ, Soukup JM, Case M, et al. Exposure to wood smoke particles produces inflammation in healthy volunteers. *Occup Environ Med* 2012; **69**(3): 170-5.
123. Lal K, Dutta KK, Vachhrajani KD, Gupta GS, Srivastava AK. Histomorphological changes in lung of rats following exposure to wood smoke. *Indian J Exp Biol* 1993; **31**(9): 761-4.
124. Barlow PG, Brown DM, Donaldson K, MacCallum J, Stone V. Reduced alveolar macrophage migration induced by acute ambient particle (PM10) exposure. *Cell Biol Toxicol* 2008; **24**(3): 243-52.

125. Gillissen A, Becher B, Vacca G, Dueck R, Juergens U. Chemotactic Effects of Diesel Exhaust Particles on the Interaction between Macrophage and Neutrophilic Granulocytes. American Thoracic Society Conference. San Diego; 2009.
126. Demarest GB, Hudson LD, Altman LC. Impaired alveolar macrophage chemotaxis in patients with acute smoke inhalation. *Am Rev Respir Dis* 1979; **119**(2): 279-86.
127. Zhou H, Kobzik L. Effect of concentrated ambient particles on macrophage phagocytosis and killing of Streptococcus pneumoniae. *Am J Respir Cell Mol Biol* 2007; **36**(4): 460-5.
128. Castranova V, Bowman L, Reasor MJ, Lewis T, Tucker J, Miles PR. The response of rat alveolar macrophages to chronic inhalation of coal dust and/or diesel exhaust. *Environ Res* 1985; **36**(2): 405-19.
129. Lundborg M, Johansson A, Lastbom L, Camner P. Ingested aggregates of ultrafine carbon particles and interferon-gamma impair rat alveolar macrophage function. *Environ Res* 1999; **81**(4): 309-15.
130. Lundborg M, Johard U, Lastbom L, Gerde P, Camner P. Human alveolar macrophage phagocytic function is impaired by aggregates of ultrafine carbon particles. *Environ Res* 2001; **86**(3): 244-53.
131. Aljurayyan AN, Fullerton DG, Barrett S, Gordon SB. Human macrophage model of biomass smoke exposure shows impaired ingestion of Streptococcus pneumoniae. British Thoracic Society Winter Meeting. London: BMJ; 2011.
132. Labedzka M, Gulyas H, Gercken G. Zymosan-induced chemiluminescence of alveolar macrophages: depression by inorganic dust constituents. *Arch Environ Contam Toxicol* 1991; **21**(1): 51-7.
133. Sawyer K, Mundandhara S, Ghio AJ, Madden MC. The effects of ambient particulate matter on human alveolar macrophage oxidative and inflammatory responses. *J Toxicol Environ Health A* 2010; **73**(1): 41-57.
134. Beck-Speier I, Dayal N, Karg E, et al. Agglomerates of ultrafine particles of elemental carbon and TiO2 induce generation of lipid mediators in alveolar macrophages. *Environ Health Perspect* 2001; **109 Suppl 4**: 613-8.
135.Zelikoff JT, Chen LC, Cohen MD, Schlesinger RB. The toxicology of inhaled woodsmoke. *J Toxicol Environ Health B Crit Rev* 2002; **5**(3): 269-82.
136. Antonini JM, Roberts JR, Jernigan MR, Yang HM, Ma JY, Clarke RW. Residual oil fly ash increases the susceptibility to infection and severely damages the lungs after pulmonary challenge with a bacterial pathogen. *Toxicol Sci* 2002; **70**(1): 110-9.
137. Lundborg M, Bouhafs R, Gerde P, et al. Aggregates of ultrafine particles modulate lipid peroxidation and bacterial killing by alveolar macrophages. *Environ Res* 2007; **104**(2): 250-7.
138. Jakab GJ. The toxicologic interactions resulting from inhalation of carbon black and acrolein on pulmonary antibacterial and antiviral defenses. *Toxicol Appl Pharmacol* 1993; **121**(2): 167-75.
139. Tellabati A, Fernandes VE, Teichert F, et al. Acute exposure of mice to high-dose ultrafine carbon black decreases susceptibility to pneumococcal pneumonia. *Part Fibre Toxicol* 2010; **7**: 30.

140. Ramos C, Cisneros J, Gonzalez-Avila G, Becerril C, Ruiz V, Montano M. Increase of matrix metalloproteinases in woodsmoke-induced lung emphysema in guinea pigs. *Inhal Toxicol* 2009; **21**(2): 119-32.
141. Danielsen PH, Loft S, Jacobsen NR, et al. Oxidative stress, inflammation, and DNA damage in rats after intratracheal instillation or oral exposure to ambient air and wood smoke particulate matter. *Toxicol Sci* 2010; **118**(2): 574-85.
142. Halliwell B, Gutteridge J. Free Radicals in Biology and Medicine. Oxford: Oxford University Press; 1999.
143. Valko M, Leibfritz D, Moncol J, Cronin MT, Mazur M, Telser J. Free radicals and antioxidants in normal physiological functions and human disease. *Int J Biochem Cell Biol* 2007; **39**(1): 44-84.
144. Rahman I, Yang SR, Biswas SK. Current concepts of redox signaling in the lungs. *Antioxid Redox Signal* 2006; **8**(3-4): 681-9.
145. Mazzoli-Rocha F, Fernandes S, Einicker-Lamas M, Zin WA. Roles of oxidative stress in signaling and inflammation induced by particulate matter. *Cell Biol Toxicol* 2010; **26**(5): 481-98.
146. Iles KE, Forman HJ. Macrophage signaling and respiratory burst. *Immunol Res* 2002; **26**(1-3): 95-105.
147. Kirkham P. Oxidative stress and macrophage function: a failure to resolve the inflammatory response. *Biochem Soc Trans* 2007; **35**(Pt 2): 284-7.
148. Schafer FQ, Buettner GR. Redox environment of the cell as viewed through the redox state of the glutathione disulfide/glutathione couple. *Free Radic Biol Med* 2001; **30**(11): 1191-212.
149. Thannickal VJ, Fanburg BL. Reactive oxygen species in cell signaling. *Am J Physiol Lung Cell Mol Physiol* 2000; **279**(6): L1005-28.
150. Forman HJ, Torres M. Reactive oxygen species and cell signaling: respiratory burst in macrophage signaling. *Am J Respir Crit Care Med* 2002; **166**(12 Pt 2): S4-8.
151. Martinovich GG, Cherenkevich SN, Sauer H. Intracellular redox state: towards quantitative description. *Eur Biophys J* 2005; **34**(7): 937-42.
152. Kelly FJ, Blomberg A, Frew A, Holgate ST, Sandstrom T. Antioxidant kinetics in lung lavage fluid following exposure of humans to nitrogen dioxide. *Am J Respir Crit Care Med* 1996; **154**(6 Pt 1): 1700-5.
153. Kirkinezos IG, Moraes CT. Reactive oxygen species and mitochondrial diseases. *Semin Cell Dev Biol* 2001; **12**(6): 449-57.
154. Hukkanen J, Pelkonen O, Hakkola J, Raunio H. Expression and regulation of xenobiotic-metabolizing cytochrome P450 (CYP) enzymes in human lung. *Crit Rev Toxicol* 2002; **32**(5): 391-411.
155. Test ST, Weiss SJ. Quantitative and temporal characterization of the extracellular H2O2 pool generated by human neutrophils. *J Biol Chem* 1984; **259**(1): 399-405.
156. Chance B, Sies H, Boveris A. Hydroperoxide metabolism in mammalian organs. *Physiol Rev* 1979; **59**(3): 527-605.
157. Pechkovsky DV, Zissel G, Stamme C, et al. Human alveolar epithelial cells induce nitric oxide synthase-2 expression in alveolar macrophages. *Eur Respir J* 2002; **19**(4): 672-83.
158. Antonenkov VD, Grunau S, Ohlmeier S, Hiltunen JK. Peroxisomes are oxidative organelles. *Antioxid Redox Signal* 2010; **13**(4): 525-37.

159. Sheppard FR, Kelher MR, Moore EE, McLaughlin NJ, Banerjee A, Silliman CC. Structural organization of the neutrophil NADPH oxidase: phosphorylation and translocation during priming and activation. *J Leukoc Biol* 2005; **78**(5): 1025-42.
160. Sies H. Strategies of antioxidant defense. *Eur J Biochem* 1993; **215**(2): 213-9.
161. Szabo C, Ischiropoulos H, Radi R. Peroxynitrite: biochemistry, pathophysiology and development of therapeutics. *Nat Rev Drug Discov* 2007; **6**(8): 662-80.
162. Horton JK, Meredith MJ, Bend JR. Glutathione biosynthesis from sulfur-containing amino acids in enriched populations of Clara and type II cells and macrophages freshly isolated from rabbit lung. *J Pharmacol Exp Ther* 1987; **240**(2): 376-80.
163. Vogt MT, Thomas C, Vassallo CL, Basford RE, Gee JB. Glutathione-dependent peroxidative metabolism in the alveolar macrophage. *J Clin Invest* 1971; **50**(2): 401-10.
164. Li N, Wang M, Oberley TD, Sempf JM, Nel AE. Comparison of the pro-oxidative and proinflammatory effects of organic diesel exhaust particle chemicals in bronchial epithelial cells and macrophages. *J Immunol* 2002; **169**(8): 4531-41.
165. Dauletbaev N, Rickmann J, Viel K, Buhl R, Wagner TO, Bargon J. Glutathione in induced sputum of healthy individuals and patients with asthma. *Thorax* 2001; **56**(1): 13-8.
166. Chang J, Jaeschke H, Randerath K. Effect of Ni(II) on tissue hydrogen peroxide content in mice as inferred from glutathione and glutathione disulfide measurements. *Life Sci* 1994; **55**(23): 1789-96.
167. Kumar VH, Patel A, Swartz DD, et al. Exposure to supplemental oxygen and its effects on oxidative stress and antioxidant enzyme activity in term newborn lambs. *Pediatr Res* 2010; **67**(1): 66-71.
168. Comhair SA, Thomassen MJ, Erzurum SC. Differential induction of extracellular glutathione peroxidase and nitric oxide synthase 2 in airways of healthy individuals exposed to 100% O(2) or cigarette smoke. *Am J Respir Cell Mol Biol* 2000; **23**(3): 350-4.
169. Deneke SM, Fanburg BL. Regulation of cellular glutathione. *Am J Physiol* 1989; **257**(4 Pt 1): L163-73.
170. Cantin AM, North SL, Hubbard RC, Crystal RG. Normal alveolar epithelial lining fluid contains high levels of glutathione. *J Appl Physiol* 1987; **63**(1): 152-7.
171. Hanigan MH, Ricketts WA. Extracellular glutathione is a source of cysteine for cells that express gamma-glutamyl transpeptidase. *Biochemistry* 1993; **32**(24): 6302-6.
172. Jean JC, Liu Y, Joyce-Brady M. The importance of gamma-glutamyl transferase in lung glutathione homeostasis and antioxidant defense. *Biofactors* 2003; **17**(1-4): 161-73.
173. Jean JC, Liu Y, Brown LA, Marc RE, Klings E, Joyce-Brady M. Gamma-glutamyl transferase deficiency results in lung oxidant stress in normoxia. *Am J Physiol Lung Cell Mol Physiol* 2002; **283**(4): L766-76.
174. Seres T, Knickelbein RG, Warshaw JB, Johnston RB, Jr. The phagocytosis-associated respiratory burst in human monocytes is associated with increased uptake of glutathione. *J Immunol* 2000; **165**(6): 3333-40.
175. Rouzer CA, Scott WA, Griffith OW, Hamill AL, Cohn ZA. Glutathione metabolism in resting and phagocytizing peritoneal macrophages. *J Biol Chem* 1982; **257**(4): 2002-8.
176. Seelig GF, Simondsen RP, Meister A. Reversible dissociation of gamma-glutamylcysteine synthetase into two subunits. *J Biol Chem* 1984; **259**(15): 9345-7.

177. Comhair SA, Bhathena PR, Farver C, Thunnissen FB, Erzurum SC. Extracellular glutathione peroxidase induction in asthmatic lungs: evidence for redox regulation of expression in human airway epithelial cells. *FASEB J* 2001; **15**(1): 70-8.
178. Rahman I, Smith CA, Lawson MF, Harrison DJ, MacNee W. Induction of gamma-glutamylcysteine synthetase by cigarette smoke is associated with AP-1 in human alveolar epithelial cells. *FEBS Lett* 1996; **396**(1): 21-5.
179. Takahashi Y, Oakes SM, Williams MC, Takahashi S, Miura T, Joyce-Brady M. Nitrogen dioxide exposure activates gamma-glutamyl transferase gene expression in rat lung. *Toxicol Appl Pharmacol* 1997; **143**(2): 388-96.
180. Lieberman MW, Wiseman AL, Shi ZZ, et al. Growth retardation and cysteine deficiency in gamma-glutamyl transpeptidase-deficient mice. *Proc Natl Acad Sci U S A* 1996; **93**(15): 7923-6.
181. Jounblat R, Clark H, Eggleton P, Hawgood S, Andrew PW, Kadioglu A. The role of surfactant protein D in the colonisation of the respiratory tract and onset of bacteraemia during pneumococcal pneumonia. *Respir Res* 2005; **6**: 126.
182. Yang F, Coalson JJ, Bobb HH, Carter JD, Banu J, Ghio AJ. Resistance of hypotransferrinemic mice to hyperoxia-induced lung injury. *Am J Physiol* 1999; **277**(6 Pt 1): L1214-23.
183. Pacht ER, Davis WB. Role of transferrin and ceruloplasmin in antioxidant activity of lung epithelial lining fluid. *J Appl Physiol* 1988; **64**(5): 2092-9.
184. Yang F, Friedrichs WE, deGraffenried L, et al. Cellular expression of ceruloplasmin in baboon and mouse lung during development and inflammation. *Am J Respir Cell Mol Biol* 1996; **14**(2): 161-9.
185. Cantin AM, Fells GA, Hubbard RC, Crystal RG. Antioxidant macromolecules in the epithelial lining fluid of the normal human lower respiratory tract. *J Clin Invest* 1990; **86**(3): 962-71.
186. Skoza L, Snyder A, Kikkawa Y. Ascorbic acid in bronchoalveolar wash. *Lung* 1983; **161**(2): 99-109.
187. Nowak D, Piasecka G, Antczak A, Pietras T. Effect of ascorbic acid on hydroxyl radical generation by chemical, enzymatic and cellular systems. Importance for antioxidant prevention of pulmonary emphysema. *Biomed Biochim Acta* 1991; **50**(3): 265-72.
188. May JM, Huang J, Qu ZC. Macrophage uptake and recycling of ascorbic acid: response to activation by lipopolysaccharide. *Free Radic Biol Med* 2005; **39**(11): 1449-59.
189. Stocker R, Yamamoto Y, McDonagh AF, Glazer AN, Ames BN. Bilirubin is an antioxidant of possible physiological importance. *Science* 1987; **235**(4792): 1043-6.
190. Sun G, Crissman K, Norwood J, Richards J, Slade R, Hatch GE. Oxidative interactions of synthetic lung epithelial lining fluid with metal-containing particulate matter. *Am J Physiol Lung Cell Mol Physiol* 2001; **281**(4): L807-15.
191. Zelko IN, Mariani TJ, Folz RJ. Superoxide dismutase multigene family: a comparison of the CuZn-SOD (SOD1), Mn-SOD (SOD2), and EC-SOD (SOD3) gene structures, evolution, and expression. *Free Radic Biol Med* 2002; **33**(3): 337-49.
192. Rister M, Baehner RL. A comparative study of superoxide dismutase activity in polymorphonuclear leukocytes, monocytes, and alveolar macrophages of the guinea pig. *J Cell Physiol* 1976; **87**(3): 345-55.

193. Kim H, Morimoto Y, Ogami A, et al. Differential expression of EC-SOD, Mn-SOD and CuZn-SOD in rat lung exposed to crystalline silica. *Journal of occupational health* 2007; **49**(3): 242-8.
194. Smith LJ, Shamsuddin M, Sporn PH, Denenberg M, Anderson J. Reduced superoxide dismutase in lung cells of patients with asthma. *Free Radic Biol Med* 1997; **22**(7): 1301-7.
195. Flohe L, Brand I. Kinetics of glutathione peroxidase. *Biochim Biophys Acta* 1969; **191**(3): 541-9.
196. Ogura Y. Catalase activity at high concentration of hydrogen peroxide. *Arch Biochem Biophys* 1955; **57**(2): 288-300.
197. Haugen TS, Skjonsberg OH, Kahler H, Lyberg T. Production of oxidants in alveolar macrophages and blood leukocytes. *Eur Respir J* 1999; **14**(5): 1100-5.
198. Pietarinen-Runtti P, Lakari E, Raivio KO, Kinnula VL. Expression of antioxidant enzymes in human inflammatory cells. *Am J Physiol Cell Physiol* 2000; **278**(1): C118-25.
199. Asayama K, Yokota S, Dobashi K, et al. Immunolocalization of cellular glutathione peroxidase in adult rat lungs and quantitative analysis after postembedding immunogold labeling. *Histochem Cell Biol* 1996; **105**(5): 383-9.
200. Arthur JR. The glutathione peroxidases. *Cellular and molecular life sciences : CMLS* 2000; **57**(13-14): 1825-35.
201. Serfass RE, Ganther HE. Effects of dietary selenium and tocopherol on glutathione peroxidase and superoxide dismutase activities in rat phagocytes. *Life Sci* 1976; **19**(8): 1139-44.
202. Sies H, Sharov VS, Klotz LO, Briviba K. Glutathione peroxidase protects against peroxynitrite-mediated oxidations. A new function for selenoproteins as peroxynitrite reductase. *J Biol Chem* 1997; **272**(44): 27812-7.
203. Chiba N, Imai H, Narashima K, et al. Cellular glutathione peroxidase as a predominant scavenger of hydroperoxyeicosatetraenoic acids in rabbit alveolar macrophages. *Biol Pharm Bull* 1999; **22**(10): 1047-51.
204. Avissar N, Finkelstein JN, Horowitz S, et al. Extracellular glutathione peroxidase in human lung epithelial lining fluid and in lung cells. *Am J Physiol* 1996; **270**(2 Pt 1): L173-82.
205. El-Chemaly S, Salathe M, Baier S, Conner GE, Forteza R. Hydrogen peroxide-scavenging properties of normal human airway secretions. *Am J Respir Crit Care Med* 2003; **167**(3): 425-30.
206. Comhair SA, Erzurum SC. The regulation and role of extracellular glutathione peroxidase. *Antioxid Redox Signal* 2005; **7**(1-2): 72-9.
207. Bjornstedt M, Xue J, Huang W, Akesson B, Holmgren A. The thioredoxin and glutaredoxin systems are efficient electron donors to human plasma glutathione peroxidase. *J Biol Chem* 1994; **269**(47): 29382-4.
208. Lei XG, Evenson JK, Thompson KM, Sunde RA. Glutathione peroxidase and phospholipid hydroperoxide glutathione peroxidase are differentially regulated in rats by dietary selenium. *J Nutr* 1995; **125**(6): 1438-46.
209. Imai H, Nakagawa Y. Biological significance of phospholipid hydroperoxide glutathione peroxidase (PHGPx, GPx4) in mammalian cells. *Free Radic Biol Med* 2003; **34**(2): 145-69.

210. Carter AB, Tephly LA, Venkataraman S, et al. High levels of catalase and glutathione peroxidase activity dampen H2O2 signaling in human alveolar macrophages. *Am J Respir Cell Mol Biol* 2004; **31**(1): 43-53.
211. Watson WH, Yang X, Choi YE, Jones DP, Kehrer JP. Thioredoxin and its role in toxicology. *Toxicol Sci* 2004; **78**(1): 3-14.
212. Maestrelli P, El Messlemani AH, De Fina O, et al. Increased expression of heme oxygenase (HO)-1 in alveolar spaces and HO-2 in alveolar walls of smokers. *Am J Respir Crit Care Med* 2001; **164**(8 Pt 1): 1508-13.
213. Li N, Venkatesan MI, Miguel A, et al. Induction of heme oxygenase-1 expression in macrophages by diesel exhaust particle chemicals and quinones via the antioxidant-responsive element. *J Immunol* 2000; **165**(6): 3393-401.
214. Ferris CD, Jaffrey SR, Sawa A, et al. Haem oxygenase-1 prevents cell death by regulating cellular iron. *Nat Cell Biol* 1999; **1**(3): 152-7.
215. Li N, Sioutas C, Cho A, et al. Ultrafine particulate pollutants induce oxidative stress and mitochondrial damage. *Environ Health Perspect* 2003; **111**(4): 455-60.
216. Schins RP, Lightbody JH, Borm PJ, Shi T, Donaldson K, Stone V. Inflammatory effects of coarse and fine particulate matter in relation to chemical and biological constituents. *Toxicol Appl Pharmacol* 2004; **195**(1): 1-11.
217. Ghio AJ, Suliman HB, Carter JD, Abushamaa AM, Folz RJ. Overexpression of extracellular superoxide dismutase decreases lung injury after exposure to oil fly ash. *Am J Physiol Lung Cell Mol Physiol* 2002; **283**(1): L211-8.
218. Dales R, Miller D, Ruest K, Guay M, Judek S. Airborne endotoxin is associated with respiratory illness in the first 2 years of life. *Environ Health Perspect* 2006; **114**(4): 610-4.
219. Ndengele MM, Muscoli C, Wang ZQ, Doyle TM, Matuschak GM, Salvemini D. Superoxide potentiates NF-kappaB activation and modulates endotoxin-induced cytokine production in alveolar macrophages. *Shock* 2005; **23**(2): 186-93.
220. Li XY, Gilmour PS, Donaldson K, MacNee W. In vivo and in vitro proinflammatory effects of particulate air pollution (PM10). *Environ Health Perspect* 1997; **105 Suppl 5**: 1279-83.
221. Pradhan A, Waseem M, Dogra S, Khanna AK, Kaw JL. Alterations in bronchoalveolar lavage constituents, oxidant/antioxidant status, and lung histology following intratracheal instillation of respirable suspended particulate matter. *J Environ Pathol Toxicol Oncol* 2005; **24**(1): 19-32.
222. Norwood J, Jr., Ledbetter AD, Doerfler DL, Hatch GE. Residual oil fly ash inhalation in guinea pigs: influence of absorbate and glutathione depletion. *Toxicol Sci* 2001; **61**(1): 144-53.
223. Al-Humadi NH, Siegel PD, Lewis DM, et al. Alteration of intracellular cysteine and glutathione levels in alveolar macrophages and lymphocytes by diesel exhaust particle exposure. *Environ Health Perspect* 2002; **110**(4): 349-53.
224. Arif JM, Khan SG, Ahmad I, Joshi LD, Rahman Q. Effect of kerosene and its soot on the chrysotile-mediated toxicity to the rat alveolar macrophages. *Environ Res* 1997; **72**(2): 151-61.
225. Wilson MR, Lightbody JH, Donaldson K, Sales J, Stone V. Interactions between ultrafine particles and transition metals in vivo and in vitro. *Toxicol Appl Pharmacol* 2002; **184**(3): 172-9.

226. Zhong CY, Zhou YM, Smith KR, et al. Oxidative injury in the lungs of neonatal rats following short-term exposure to ultrafine iron and soot particles. *J Toxicol Environ Health A* 2010; **73**(12): 837-47.
227. Zhou YM, Zhong CY, Kennedy IM, Leppert VJ, Pinkerton KE. Oxidative stress and NFkappaB activation in the lungs of rats: a synergistic interaction between soot and iron particles. *Toxicol Appl Pharmacol* 2003; **190**(2): 157-69.
228. Sehlstedt M, Dove R, Boman C, et al. Antioxidant airway responses following experimental exposure to wood smoke in man. *Part Fibre Toxicol* 2010; **7**: 21.
229. Rhoden CR, Ghelfi E, Gonzalez-Flecha B. Pulmonary inflammation by ambient air particles is mediated by superoxide anion. *Inhal Toxicol* 2008; **20**(1): 11-5.
230. Rouse RL, Murphy G, Boudreaux MJ, Paulsen DB, Penn AL. Soot nanoparticles promote biotransformation, oxidative stress, and inflammation in murine lungs. *Am J Respir Cell Mol Biol* 2008; **39**(2): 198-207.
231. Van Winkle LS, Chan JK, Anderson DS, et al. Age specific responses to acute inhalation of diffusion flame soot particles: cellular injury and the airway antioxidant response. *Inhal Toxicol* 2010; **22 Suppl 2**: 70-83.
232. Wallenborn JG, Schladweiler MC, Nyska A, et al. Cardiopulmonary responses of Wistar Kyoto, spontaneously hypertensive, and stroke-prone spontaneously hypertensive rats to particulate matter (PM) exposure. *J Toxicol Environ Health A* 2007; **70**(22): 1912-22.
233. Sagai M, Saito H, Ichinose T, Kodama M, Mori Y. Biological effects of diesel exhaust particles. I. In vitro production of superoxide and in vivo toxicity in mouse. *Free Radic Biol Med* 1993; **14**(1): 37-47.
234. Sunil VR, Patel KJ, Mainelis G, et al. Pulmonary effects of inhaled diesel exhaust in aged mice. *Toxicol Appl Pharmacol* 2009; **241**(3): 283-93.
235. Rengasamy A, Barger MW, Kane E, Ma JK, Castranova V, Ma JY. Diesel exhaust particle-induced alterations of pulmonary phase I and phase II enzymes of rats. *J Toxicol Environ Health A* 2003; **66**(2): 153-67.
236. Olker C, Siese A, Stumpf S, Muller B, Gemsa D, Garn H. Impaired superoxide radical production by bronchoalveolar lavage cells from NO(2)-exposed rats. *Free Radic Biol Med* 2004; **37**(7): 977-87.
237. van Bree L, Rietjens I, Alink GM, Dormans J, Marra M, Rombout P. Biochemical and morphological changes in lung tissue and isolated lung cells of rats induced by short-term nitrogen dioxide exposure. *Hum Exp Toxicol* 2000; **19**(7): 392-401.
238. Danielsen PH, Moller P, Jensen KA, et al. Oxidative stress, DNA damage, and inflammation induced by ambient air and wood smoke particulate matter in human A549 and THP-1 cell lines. *Chem Res Toxicol* 2011; **24**(2): 168-84.
239. Mondal K, Stephen Haskill J, Becker S. Adhesion and pollution particle-induced oxidant generation is neither necessary nor sufficient for cytokine induction in human alveolar macrophages. *Am J Respir Cell Mol Biol* 2000; **22**(2): 200-8.
240. Kaul N, Forman HJ. Activation of NF kappa B by the respiratory burst of macrophages. *Free Radic Biol Med* 1996; **21**(3): 401-5.
241. Rojanasakul Y, Ye J, Chen F, et al. Dependence of NF-kappaB activation and free radical generation on silica-induced TNF-alpha production in macrophages. *Mol Cell Biochem* 1999; **200**(1-2): 119-25.

242. Gozal E, Forman HJ, Torres M. ADP stimulates the respiratory burst without activation of ERK and AKT in rat alveolar macrophages. *Free Radic Biol Med* 2001; **31**(5): 679-87.
243. Kobzik L. Lung macrophage uptake of unopsonized environmental particulates. Role of scavenger-type receptors. *J Immunol* 1995; **155**(1): 367-76.
244. Kobzik L, Godleski JJ, Brain JD. Oxidative metabolism in the alveolar macrophage: analysis by flow cytometry. *J Leukoc Biol* 1990; **47**(4): 295-303.
245. Persson HL, Vainikka LK. TNF-alpha preserves lysosomal stability in macrophages: a potential defense against oxidative lung injury. *Toxicol Lett* 2010; **192**(2): 261-7.
246. Kinnula VL. Focus on antioxidant enzymes and antioxidant strategies in smoking related airway diseases. *Thorax* 2005; **60**(8): 693-700.
247. Li N, Nel AE. Role of the Nrf2-mediated signaling pathway as a negative regulator of inflammation: implications for the impact of particulate pollutants on asthma. *Antioxid Redox Signal* 2006; **8**(1-2): 88-98.
248. Cho HY, Reddy SP, Kleeberger SR. Nrf2 defends the lung from oxidative stress. *Antioxid Redox Signal* 2006; **8**(1-2): 76-87.
249. Lin W, Wu RT, Wu T, Khor TO, Wang H, Kong AN. Sulforaphane suppressed LPS-induced inflammation in mouse peritoneal macrophages through Nrf2 dependent pathway. *Biochem Pharmacol* 2008; **76**(8): 967-73.
250. Lei XG, Cheng WH, McClung JP. Metabolic regulation and function of glutathione peroxidase-1. *Annu Rev Nutr* 2007; **27**: 41-61.
251. Zamamiri-Davis F, Lu Y, Thompson JT, et al. Nuclear factor-kappaB mediates over-expression of cyclooxygenase-2 during activation of RAW 264.7 macrophages in selenium deficiency. *Free Radic Biol Med* 2002; **32**(9): 890-7.
252. Duong C, Seow HJ, Bozinovski S, Crack PJ, Anderson GP, Vlahos R. Glutathione peroxidase-1 protects against cigarette smoke-induced lung inflammation in mice. *Am J Physiol Lung Cell Mol Physiol* 2010; **299**(3): L425-33.
253. Long H, Shi T, Borm PJ, et al. ROS-mediated TNF-alpha and MIP-2 gene expression in alveolar macrophages exposed to pine dust. *Part Fibre Toxicol* 2004; **1**(1): 3.
254. Tollefson AK, Oberley-Deegan RE, Butterfield KT, et al. Endogenous enzymes (NOX and ECSOD) regulate smoke-induced oxidative stress. *Free Radic Biol Med* 2010; **49**(12): 1937-46.
255. Brown DM, Donaldson K, Borm PJ, et al. Calcium and ROS-mediated activation of transcription factors and TNF-alpha cytokine gene expression in macrophages exposed to ultrafine particles. *Am J Physiol Lung Cell Mol Physiol* 2004; **286**(2): L344-53.
256. Brown DM, Hutchison L, Donaldson K, Stone V. The effects of PM10 particles and oxidative stress on macrophages and lung epithelial cells: modulating effects of calcium-signaling antagonists. *Am J Physiol Lung Cell Mol Physiol* 2007; **292**(6): L1444-51.
257. Soukup JM, Becker S. Human alveolar macrophage responses to air pollution particulates are associated with insoluble components of coarse material, including particulate endotoxin. *Toxicol Appl Pharmacol* 2001; **171**(1): 20-6.
258. Donaldson K, Stone V, Borm PJ, et al. Oxidative stress and calcium signaling in the adverse effects of environmental particles (PM10). *Free Radic Biol Med* 2003; **34**(11): 1369-82.
259. Delacourt C, d'Ortho MP, Macquin-Mavier I, et al. Oxidant-antioxidant balance in alveolar macrophages from newborn rats. *Eur Respir J* 1996; **9**(12): 2517-24.

260. Harvey CJ, Thimmulappa RK, Singh A, et al. Nrf2-regulated glutathione recycling independent of biosynthesis is critical for cell survival during oxidative stress. *Free Radic Biol Med* 2009; **46**(4): 443-53.
261. Bass R, Ruddock LW, Klappa P, Freedman RB. A major fraction of endoplasmic reticulum-located glutathione is present as mixed disulfides with protein. *J Biol Chem* 2004; **279**(7): 5257-62.
262. Seres T, Ravichandran V, Moriguchi T, Rokutan K, Thomas JA, Johnston RB, Jr. Protein S-thiolation and dethiolation during the respiratory burst in human monocytes. A reversible post-translational modification with potential for buffering the effects of oxidant stress. *J Immunol* 1996; **156**(5): 1973-80.
263. Pineda-Molina E, Klatt P, Vazquez J, et al. Glutathionylation of the p50 subunit of NF-kappaB: a mechanism for redox-induced inhibition of DNA binding. *Biochemistry* 2001; **40**(47): 14134-42.
264. Klatt P, Molina EP, De Lacoba MG, et al. Redox regulation of c-Jun DNA binding by reversible S-glutathiolation. *FASEB J* 1999; **13**(12): 1481-90.
265. Hoppe G, Chai YC, Crabb JW, Sears J. Protein s-glutathionylation in retinal pigment epithelium converts heat shock protein 70 to an active chaperone. *Exp Eye Res* 2004; **78**(6): 1085-92.
266. Vangheluwe P, Raeymaekers L, Dode L, Wuytack F. Modulating sarco(endo)plasmic reticulum Ca2+ ATPase 2 (SERCA2) activity: cell biological implications. *Cell Calcium* 2005; **38**(3-4): 291-302.
267. Schroeder BO, Wu Z, Nuding S, et al. Reduction of disulphide bonds unmasks potent antimicrobial activity of human beta-defensin 1. *Nature* 2011; **469**(7330): 419-23.
268. Staal FJ, Roederer M, Herzenberg LA. Intracellular thiols regulate activation of nuclear factor kappa B and transcription of human immunodeficiency virus. *Proc Natl Acad Sci U S A* 1990; **87**(24): 9943-7.
269. Yin Z, Ivanov VN, Habelhah H, Tew K, Ronai Z. Glutathione S-transferase p elicits protection against H2O2-induced cell death via coordinated regulation of stress kinases. *Cancer Res* 2000; **60**(15): 4053-7.
270. Reynaert NL, van der Vliet A, Guala AS, et al. Dynamic redox control of NF-kappaB through glutaredoxin-regulated S-glutathionylation of inhibitory kappaB kinase beta. *Proc Natl Acad Sci U S A* 2006; **103**(35): 13086-91.
271. Aesif SW, Kuipers I, Anathy V, et al. Ablation of Glutaredoxin-1 Attenuates Lipopolysaccharide-Induced Lung Inflammation and Alveolar Macrophage Activation. *Am J Respir Cell Mol Biol* 2010.
272. Giustarini D, Rossi R, Milzani A, Colombo R, Dalle-Donne I. S-glutathionylation: from redox regulation of protein functions to human diseases. *J Cell Mol Med* 2004; **8**(2): 201-12.
273. Gallogly MM, Mieyal JJ. Mechanisms of reversible protein glutathionylation in redox signaling and oxidative stress. *Curr Opin Pharmacol* 2007; **7**(4): 381-91.
274. Gloire G, Piette J. Redox regulation of nuclear post-translational modifications during NF-kappaB activation. *Antioxid Redox Signal* 2009; **11**(9): 2209-22.
275. Oliveira-Marques V, Marinho HS, Cyrne L, Antunes F. Role of hydrogen peroxide in NF-kappaB activation: from inducer to modulator. *Antioxid Redox Signal* 2009; **11**(9): 2223-43.

276. Pepperl S, Dorger M, Ringel F, Kupatt C, Krombach F. Hyperoxia upregulates the NO pathway in alveolar macrophages in vitro: role of AP-1 and NF-kappaB. *Am J Physiol Lung Cell Mol Physiol* 2001; **280**(5): L905-13.
277. Monick MM, Carter AB, Hunninghake GW. Human alveolar macrophages are markedly deficient in REF-1 and AP-1 DNA binding activity. *J Biol Chem* 1999; **274**(25): 18075-80.
278. Schenk H, Klein M, Erdbrugger W, Droge W, Schulze-Osthoff K. Distinct effects of thioredoxin and antioxidants on the activation of transcription factors NF-kappa B and AP-1. *Proc Natl Acad Sci U S A* 1994; **91**(5): 1672-6.
279. Suzuki YJ, Forman HJ, Sevanian A. Oxidants as stimulators of signal transduction. *Free Radic Biol Med* 1997; **22**(1-2): 269-85.
280. Liu H, Zhang H, Iles KE, et al. The ADP-stimulated NADPH oxidase activates the ASK-1/MKK4/JNK pathway in alveolar macrophages. *Free Radic Res* 2006; **40**(8): 865-74.
281. Bindoli A, Fukuto JM, Forman HJ. Thiol chemistry in peroxidase catalysis and redox signaling. *Antioxid Redox Signal* 2008; **10**(9): 1549-64.
282. Arner ES, Holmgren A. Physiological functions of thioredoxin and thioredoxin reductase. *Eur J Biochem* 2000; **267**(20): 6102-9.
283. Iversen R, Andersen PA, Jensen KS, Winther JR, Sigurskjold BW. Thiol-disulfide exchange between glutaredoxin and glutathione. *Biochemistry* 2010; **49**(4): 810-20.
284. Peltoniemi M, Kaarteenaho-Wiik R, Saily M, et al. Expression of glutaredoxin is highly cell specific in human lung and is decreased by transforming growth factor-beta in vitro and in interstitial lung diseases in vivo. *Hum Pathol* 2004; **35**(8): 1000-7.
285. Sekhar KR, Rachakonda G, Freeman ML. Cysteine-based regulation of the CUL3 adaptor protein Keap1. *Toxicol Appl Pharmacol* 2010; **244**(1): 21-6.
286. Yamamoto T, Suzuki T, Kobayashi A, et al. Physiological significance of reactive cysteine residues of Keap1 in determining Nrf2 activity. *Mol Cell Biol* 2008; **28**(8): 2758-70.
287. Huang HC, Nguyen T, Pickett CB. Phosphorylation of Nrf2 at Ser-40 by protein kinase C regulates antioxidant response element-mediated transcription. *J Biol Chem* 2002; **277**(45): 42769-74.
288. Cho HY, Reddy SP, Debiase A, Yamamoto M, Kleeberger SR. Gene expression profiling of NRF2-mediated protection against oxidative injury. *Free Radic Biol Med* 2005; **38**(3): 325-43.
289. Erickson AM, Nevarea Z, Gipp JJ, Mulcahy RT. Identification of a variant antioxidant response element in the promoter of the human glutamate-cysteine ligase modifier subunit gene. Revision of the ARE consensus sequence. *J Biol Chem* 2002; **277**(34): 30730-7.
290. Sasaki H, Sato H, Kuriyama-Matsumura K, et al. Electrophile response element-mediated induction of the cystine/glutamate exchange transporter gene expression. *J Biol Chem* 2002; **277**(47): 44765-71.
291. Singh A, Rangasamy T, Thimmulappa RK, et al. Glutathione peroxidase 2, the major cigarette smoke-inducible isoform of GPX in lungs, is regulated by Nrf2. *Am J Respir Cell Mol Biol* 2006; **35**(6): 639-50.
292. Leonard MO, Kieran NE, Howell K, et al. Reoxygenation-specific activation of the antioxidant transcription factor Nrf2 mediates cytoprotective gene expression in ischemia-reperfusion injury. *FASEB J* 2006; **20**(14): 2624-6.

293. Kobayashi M, Yamamoto M. Nrf2-Keap1 regulation of cellular defense mechanisms against electrophiles and reactive oxygen species. *Adv Enzyme Regul* 2006; **46**: 113-40.
294. Cho HY, Jedlicka AE, Reddy SP, et al. Role of NRF2 in protection against hyperoxic lung injury in mice. *Am J Respir Cell Mol Biol* 2002; **26**(2): 175-82.
295. Ishii Y, Itoh K, Morishima Y, et al. Transcription factor Nrf2 plays a pivotal role in protection against elastase-induced pulmonary inflammation and emphysema. *J Immunol* 2005; **175**(10): 6968-75.
296. Thimmulappa RK, Lee H, Rangasamy T, et al. Nrf2 is a critical regulator of the innate immune response and survival during experimental sepsis. *J Clin Invest* 2006; **116**(4): 984-95.
297. Lee HR, Cho JM, Shin DH, et al. Adaptive response to GSH depletion and resistance to L-buthionine-(S,R)-sulfoximine: involvement of Nrf2 activation. *Mol Cell Biochem* 2008; **318**(1-2): 23-31.
298. Harvey CJ, Thimmulappa RK, Sethi S, et al. Nrf2-dependent Immunomodulation By Sulforaphane Improves Bacterial Phagocytosis In COPD Macrophages And Inhibits Bacterial Burden And Inflammation In Cigarette Smoke-exposed Mice. *Am J Respir Crit Care Med* 2010; **181**(1_MeetingAbstracts): A3828-.
299. Yang H, Magilnick N, Lee C, et al. Nrf1 and Nrf2 regulate rat glutamate-cysteine ligase catalytic subunit transcription indirectly via NF-kappaB and AP-1. *Mol Cell Biol* 2005; **25**(14): 5933-46.
300. Goven D, Boutten A, Lecon-Malas V, Boczkowski J, Bonay M. Prolonged cigarette smoke exposure decreases heme oxygenase-1 and alters Nrf2 and Bach1 expression in human macrophages: roles of the MAP kinases ERK(1/2) and JNK. *FEBS Lett* 2009; **583**(21): 3508-18.
301. Muller L, Riediker M, Wick P, Mohr M, Gehr P, Rothen-Rutishauser B. Oxidative stress and inflammation response after nanoparticle exposure: differences between human lung cell monocultures and an advanced three-dimensional model of the human epithelial airways. *J R Soc Interface* 2010; **7 Suppl 1**: S27-40.
302. Victor VM, Rocha M, De la Fuente M. Regulation of macrophage function by the antioxidant N-acetylcysteine in mouse-oxidative stress by endotoxin. *Int Immunopharmacol* 2003; **3**(1): 97-106.
303. Antonicelli F, Brown D, Parmentier M, et al. Regulation of LPS-mediated inflammation in vivo and in vitro by the thiol antioxidant Nacystelyn. *Am J Physiol Lung Cell Mol Physiol* 2004; **286**(6): L1319-27.
304. Gosset P, Wallaert B, Tonnel AB, Fourneau C. Thiol regulation of the production of TNF-alpha, IL-6 and IL-8 by human alveolar macrophages. *Eur Respir J* 1999; **14**(1): 98-105.
305. Xiao GG, Wang M, Li N, Loo JA, Nel AE. Use of proteomics to demonstrate a hierarchical oxidative stress response to diesel exhaust particle chemicals in a macrophage cell line. *J Biol Chem* 2003; **278**(50): 50781-90.
306. Cuschieri J, Maier RV. Oxidative stress, lipid rafts, and macrophage reprogramming. *Antioxid Redox Signal* 2007; **9**(9): 1485-97.
307. Ceylan E, Kocyigit A, Gencer M, Aksoy N, Selek S. Increased DNA damage in patients with chronic obstructive pulmonary disease who had once smoked or been exposed to biomass. *Respir Med* 2006; **100**(7): 1270-6.

308. Erridge C, Kennedy S, Spickett CM, Webb DJ. Oxidized phospholipid inhibition of toll-like receptor (TLR) signaling is restricted to TLR2 and TLR4: roles for CD14, LPS-binding protein, and MD2 as targets for specificity of inhibition. *J Biol Chem* 2008; **283**(36): 24748-59.
309. Kagan VE, Borisenko GG, Serinkan BF, et al. Appetizing rancidity of apoptotic cells for macrophages: oxidation, externalization, and recognition of phosphatidylserine. *Am J Physiol Lung Cell Mol Physiol* 2003; **285**(1): L1-17.
310. Risom L, Moller P, Loft S. Oxidative stress-induced DNA damage by particulate air pollution. *Mutat Res* 2005; **592**(1-2): 119-37.
311. Mehta M, Chen LC, Gordon T, Rom W, Tang MS. Particulate matter inhibits DNA repair and enhances mutagenesis. *Mutat Res* 2008; **657**(2): 116-21.
312. Pittet LA, Quinton LJ, Yamamoto K, et al. Earliest Innate Immune Responses Require Macrophage RelA during Pneumococcal Pneumonia. *Am J Respir Cell Mol Biol* 2011.
313. Drost EM, Skwarski KM, Sauleda J, et al. Oxidative stress and airway inflammation in severe exacerbations of COPD. *Thorax* 2005; **60**(4): 293-300.
314. Kariya C, Chu HW, Huang J, Leitner H, Martin RJ, Day BJ. Mycoplasma pneumoniae infection and environmental tobacco smoke inhibit lung glutathione adaptive responses and increase oxidative stress. *Infect Immun* 2008; **76**(10): 4455-62.
315. Brown LA, Ping XD, Harris FL, Gauthier TW. Glutathione availability modulates alveolar macrophage function in the chronic ethanol-fed rat. *Am J Physiol Lung Cell Mol Physiol* 2007; **292**(4): L824-32.
316. Gutierrez P, Closa D, Piner R, Bulbena O, Menendez R, Torres A. Macrophage activation in exacerbated COPD with and without community-acquired pneumonia. *Eur Respir J* 2010; **36**(2): 285-91.
317. Harvey CJ, Thimmulappa RK, Sethi S, et al. Targeting Nrf2 Signaling Improves Bacterial Clearance by Alveolar Macrophages in Patients with COPD and in a Mouse Model. *Sci Transl Med* 2011; **3**(78): 78ra32.
318. Mushtaq N, Ezzati M, Hall L, et al. Adhesion of Streptococcus pneumoniae to human airway epithelial cells exposed to urban particulate matter. *J Allergy Clin Immunol* 2011; **127**(5): 1236-42 e2.
319. Haegens A, Heeringa P, van Suylen RJ, et al. Myeloperoxidase deficiency attenuates lipopolysaccharide-induced acute lung inflammation and subsequent cytokine and chemokine production. *J Immunol* 2009; **182**(12): 7990-6.
320. Leeper-Woodford SK, Detmer K. Acute hypoxia increases alveolar macrophage tumor necrosis factor activity and alters NF-kappaB expression. *Am J Physiol* 1999; **276**(6 Pt 1): L909-16.
321. Cemek M, Caksen H, Bayiroglu F, Cemek F, Dede S. Oxidative stress and enzymic-non-enzymic antioxidant responses in children with acute pneumonia. *Cell Biochem Funct* 2006; **24**(3): 269-73.
322. Umeki S, Sumi M, Niki Y, Soejima R. Concentrations of superoxide dismutase and superoxide anion in blood of patients with respiratory infections and compromised immune systems. *Clin Chem* 1987; **33**(12): 2230-3.
323. Velasquez-Melendez G, Okani ET, Kiertsman B, Roncada MJ. Vitamin A status in children with pneumonia. *Eur J Clin Nutr* 1995; **49**(5): 379-84.

324. Vijayamalini M, Manoharan S. Lipid peroxidation, vitamins C, E and reduced glutathione levels in patients with pulmonary tuberculosis. *Cell Biochem Funct* 2004; **22**(1): 19-22.
325. Suresh D, Annam V, Pratibha K, Hamsaveena. Immunological correlation of oxidative stress markers in tuberculosis patients. *International Journal of Biological & Medical Research* 2010; **1**(4): 185-7.
326. Duflo F, Debon R, Goudable J, Chassard D, Allaouchiche B. Alveolar and serum oxidative stress in ventilator-associated pneumonia. *Br J Anaesth* 2002; **89**(2): 231-6.
327. Thimmulappa RK, Scollick C, Traore K, et al. Nrf2-dependent protection from LPS induced inflammatory response and mortality by CDDO-Imidazolide. *Biochem Biophys Res Commun* 2006; **351**(4): 883-9.
328. Shi XL, Shi ZH, Huang H, Zhu HG, Zhou P, Ju D. Therapeutic effect of recombinant human catalase on H1N1 influenza-induced pneumonia in mice. *Inflammation* 2010; **33**(3): 166-72.
329. Kagan VE, Gleiss B, Tyurina YY, et al. A role for oxidative stress in apoptosis: oxidation and externalization of phosphatidylserine is required for macrophage clearance of cells undergoing Fas-mediated apoptosis. *J Immunol* 2002; **169**(1): 487-99.
330. Sanmun D, Witasp E, Jitkaew S, et al. Involvement of a functional NADPH oxidase in neutrophils and macrophages during programmed cell clearance: implications for chronic granulomatous disease. *Am J Physiol Cell Physiol* 2009; **297**(3): C621-31.
331. Richens TR, Linderman DJ, Horstmann SA, et al. Cigarette smoke impairs clearance of apoptotic cells through oxidant-dependent activation of RhoA. *Am J Respir Crit Care Med* 2009; **179**(11): 1011-21.
332. Moon C, Lee YJ, Park HJ, Chong YH, Kang JL. N-acetylcysteine inhibits RhoA and promotes apoptotic cell clearance during intense lung inflammation. *Am J Respir Crit Care Med* 2010; **181**(4): 374-87.
333. Roth DE, Richard SA, Black RE. Zinc supplementation for the prevention of acute lower respiratory infection in children in developing countries: meta-analysis and meta-regression of randomized trials. *Int J Epidemiol* 2010; **39**(3): 795-808.
334. Hemila H, Louhiala P. Vitamin C for preventing and treating pneumonia. *Cochrane Database Syst Rev* 2007; (1): CD005532.
335. Ni J, Wei J, Wu T. Vitamin A for non-measles pneumonia in children. *Cochrane Database Syst Rev* 2005; (3): CD003700.
336. Manaseki-Holland S, Maroof Z, Bruce J, et al. Effect on the incidence of pneumonia of vitamin D supplementation by quarterly bolus dose to infants in Kabul: a randomised controlled superiority trial. *Lancet* 2012; **379**(9824): 1419-27.
337. Hemila H, Virtamo J, Albanes D, Kaprio J. Vitamin E and beta-carotene supplementation and hospital-treated pneumonia incidence in male smokers. *Chest* 2004; **125**(2): 557-65.
338. Hemila H, Kaprio J. Vitamin E supplementation may transiently increase tuberculosis risk in males who smoke heavily and have high dietary vitamin C intake. *Br J Nutr* 2008; **100**(4): 896-902.
339. Chao J, Donham P, van Rooijen N, Wood JG, Gonzalez NC. MCP-1/CCL2 Released from Alveolar Macrophages Mediates the Systemic Inflammation of Acute Alveolar Hypoxia. *Am J Respir Cell Mol Biol* 2010.

340. Gonzalez NC, Allen J, Blanco VG, Schmidt EJ, van Rooijen N, Wood JG. Alveolar macrophages are necessary for the systemic inflammation of acute alveolar hypoxia. *J Appl Physiol* 2007; **103**(4): 1386-94.
341. Bunnell E, Pacht ER. Oxidized glutathione is increased in the alveolar fluid of patients with the adult respiratory distress syndrome. *Am Rev Respir Dis* 1993; **148**(5): 1174-8.
342. Imai Y, Kuba K, Neely GG, et al. Identification of oxidative stress and Toll-like receptor 4 signaling as a key pathway of acute lung injury. *Cell* 2008; **133**(2): 235-49.
343. Moradi M, Mojtahedzadeh M, Mandegari A, et al. The role of glutathione-S-transferase polymorphisms on clinical outcome of ALI/ARDS patient treated with N-acetylcysteine. *Respir Med* 2009; **103**(3): 434-41.
344. Nathens AB, Neff MJ, Jurkovich GJ, et al. Randomized, prospective trial of antioxidant supplementation in critically ill surgical patients. *Ann Surg* 2002; **236**(6): 814-22.
345. Berger MM, Eggimann P, Heyland DK, et al. Reduction of nosocomial pneumonia after major burns by trace element supplementation: aggregation of two randomised trials. *Crit Care* 2006; **10**(6): R153.
346. Heavner DL, Morgan WT, Sears SB, Richardson JD, Byrd GD, Ogden MW. Effect of creatinine and specific gravity normalization techniques on xenobiotic biomarkers in smokers' spot and 24-h urines. *J Pharm Biomed Anal* 2006; **40**(4): 928-42.
347. Fullerton DG, Jere K, Jambo K, et al. Domestic smoke exposure is associated with alveolar macrophage particulate load. *Trop Med Int Health* 2009; **14**(3): 349-54.
348. Fullerton DG, Semple S, Kalambo F, et al. Biomass fuel use and indoor air pollution in homes in Malawi. *Occup Environ Med* 2009; **66**(11): 777-83.
349. Jambo KC, Sepako E, Fullerton DG, et al. Bronchoalveolar CD4+ T cell responses to respiratory antigens are impaired in HIV-infected adults. *Thorax* 2011; **66**(5): 375-82.
350. Mwandumba HC, Bertel Squire S, White SA, et al. Association between sputum smear status and local immune responses at the site of disease in HIV-infected patients with pulmonary tuberculosis. *Tuberculosis* 2008; **88**(1): 58-63.
351. British Thoracic Society guidelines on diagnostic flexible bronchoscopy. *Thorax* 2001; **56 Suppl 1**: i1-21.
352. Anderson ME. Determination of glutathione and glutathione disulfide in biological samples. *Methods Enzymol* 1985; **113**: 548-55.
353. Tietze F. Enzymic method for quantitative determination of nanogram amounts of total and oxidized glutathione: applications to mammalian blood and other tissues. *Anal Biochem* 1969; **27**(3): 502-22.
354. Delves HT, Sieniawska CE. Simple Method for the Accurate Determination of Selenium in Serum by Using Inductively Coupled Plasma Mass Spectrometry. *Journal of Analytical Atomic Spectrometry* 1997; **12**(3): 387-9.
355. Sieniawska CM, R. Delves, HT. Determination of total selenium in serum, whole blood and erythrocytes by ICP-MS. *Journal of Analytical Atomic Spectometry* 1999; **14**: 109-12.
356. Rouxel O, Ludden J, Carignan J, Marin L, Fouquet Y. Natural variations of Se isotopic composition determined by hydride generation multiple collector inductively coupled plasma mass spectrometry. *Geochimica et Cosmochimica Acta* 2002; **66**(18): 3191-9.
357. Lolmede K, Campana L, Vezzoli M, et al. Inflammatory and alternatively activated human macrophages attract vessel-associated stem cells, relying on separate HMGB1- and MMP-9-dependent pathways. *J Leukoc Biol* 2009; **85**(5): 779-87.

358. Benoit M, Desnues B, Mege JL. Macrophage polarization in bacterial infections. *J Immunol* 2008; **181**(6): 3733-9.
359. Mantovani A, Sica A, Sozzani S, Allavena P, Vecchi A, Locati M. The chemokine system in diverse forms of macrophage activation and polarization. *Trends Immunol* 2004; **25**(12): 677-86.
360. Shaykhiev R, Krause A, Salit J, et al. Smoking-dependent reprogramming of alveolar macrophage polarization: implication for pathogenesis of chronic obstructive pulmonary disease. *J Immunol* 2009; **183**(4): 2867-83.
361. Fullerton DG. Indoor air pollution from biomass fuel smoke and its effects on respiratory health, in a population at risk of HIV related pneumonia. University of Liverpool: University of Liverpool; 2011.
362. Scott JA, Hall AJ, Muyodi C, et al. Aetiology, outcome, and risk factors for mortality among adults with acute pneumonia in Kenya. *Lancet* 2000; **355**(9211): 1225-30.
363. Berry AM, Ogunniyi AD, Miller DC, Paton JC. Comparative virulence of Streptococcus pneumoniae strains with insertion-duplication, point, and deletion mutations in the pneumolysin gene. *Infect Immun* 1999; **67**(2): 981-5.
364. Miles AA, Misra SS, Irwin JO. The estimation of the bactericidal power of the blood. *The Journal of hygiene* 1938; **38**(6): 732-49.
365. Lowry OH, Rosebrough NJ, Farr AL, Randall RJ. Protein measurement with the Folin phenol reagent. *J Biol Chem* 1951; **193**(1): 265-75.
366. Pomory CM. Color development time of the Lowry protein assay. *Anal Biochem* 2008; **378**(2): 216-7.
367. Saville DJ. Basic statistics and the inconsistency of multiple comparison procedures. *Canadian journal of experimental psychology = Revue canadienne de psychologie experimentale* 2003; **57**(3): 167-75.
368. Corradini D. Handbook of HPLC. 2nd ed. Boca Raton: Taylor & Francis; 2010.
369. Gutteridge JM. Iron promoters of the Fenton reaction and lipid peroxidation can be released from haemoglobin by peroxides. *FEBS Lett* 1986; **201**(2): 291-5.
370. Gutteridge JM. Lipid peroxidation and antioxidants as biomarkers of tissue damage. *Clin Chem* 1995; **41**(12 Pt 2): 1819-28.
371. Fukunaga K, Yoshida M, Nakazono N. A simple, rapid, highly sensitive and reproducible quantification method for plasma malondialdehyde by high-performance liquid chromatography. *Biomedical chromatography : BMC* 1998; **12**(5): 300-3.
372. Chirico S. High-performance liquid chromatography-based thiobarbituric acid tests. *Methods Enzymol* 1994; **233**: 314-8.
373. Underhill C, Goldstein D, Gorbounova VA, et al. A randomized phase II trial of pemetrexed plus irinotecan (ALIRI) versus leucovorin-modulated 5-FU plus irinotecan (FOLFIRI) in first-line treatment of locally advanced or metastatic colorectal cancer. *Oncology* 2007; **73**(1-2): 9-20.
374. Kinchen JM, Ravichandran KS. Phagosome maturation: going through the acid test. *Nature reviews Molecular cell biology* 2008; **9**(10): 781-95.
375. VanderVen BC, Yates RM, Russell DG. Intraphagosomal measurement of the magnitude and duration of the oxidative burst. *Traffic* 2009; **10**(4): 372-8.
376. Hermanson GT. Bioconjugate techniques. San Diego: Academic Press; 1996.

377. Villeneuve NF, Lau A, Zhang DD. Regulation of the Nrf2-Keap1 antioxidant response by the ubiquitin proteasome system: an insight into cullin-ring ubiquitin ligases. *Antioxid Redox Signal* 2010; **13**(11): 1699-712.
378. Theodore M, Kawai Y, Yang J, et al. Multiple nuclear localization signals function in the nuclear import of the transcription factor Nrf2. *J Biol Chem* 2008; **283**(14): 8984-94.
379. Kensler TW, Wakabayashi N, Biswal S. Cell survival responses to environmental stresses via the Keap1-Nrf2-ARE pathway. *Annual review of pharmacology and toxicology* 2007; **47**: 89-116.
380. Copple IM. The keap1-nrf2 cell defense pathway - a promising therapeutic target? *Advances in pharmacology* 2012; **63**: 43-79.
381. Boyum A. Separation of leukocytes from blood and bone marrow. Introduction. *Scandinavian journal of clinical and laboratory investigation Supplementum* 1968; **97**: 7.
382. Yeo C, Saunders N, Locca D, et al. Ficoll-Paque versus Lymphoprep: a comparative study of two density gradient media for therapeutic bone marrow mononuclear cell preparations. *Regenerative medicine* 2009; **4**(5): 689-96.
383. Wahl LM, Wahl SM, Smythies LE, Smith PD. Isolation of human monocyte populations. *Current protocols in immunology / edited by John E Coligan [et al]* 2006; **Chapter 7**: Unit 7 6A.
384. Harris PA, Taylor R, Thielke R, Payne J, Gonzalez N, Conde JG. Research electronic data capture (REDCap)--a metadata-driven methodology and workflow process for providing translational research informatics support. *Journal of biomedical informatics* 2009; **42**(2): 377-81.
385. Brehe JE, Burch HB. Enzymatic assay for glutathione. *Anal Biochem* 1976; **74**(1): 189-97.
386. Monostori P, Wittmann G, Karg E, Turi S. Determination of glutathione and glutathione disulfide in biological samples: an in-depth review. *Journal of chromatography B, Analytical technologies in the biomedical and life sciences* 2009; **877**(28): 3331-46.
387. Pankow W, Neumann K, Ruschoff J, von Wichert P. Human alveolar macrophages: comparison of cell size, autofluorescence, and HLA-DR antigen expression in smokers and nonsmokers. *Cancer detection and prevention* 1995; **19**(3): 268-73.
388. Landsman L, Jung S. Lung macrophages serve as obligatory intermediate between blood monocytes and alveolar macrophages. *J Immunol* 2007; **179**(6): 3488-94.
389. Vallejo CG, Lagunas R. Interferences by sulfhydryl, disulfide reagents and potassium ions on protein determination by Lowry's method. *Anal Biochem* 1970; **36**(1): 207-12.
390. Nielsen H. Isolation and functional activity of human blood monocytes after adherence to plastic surfaces: comparison of different detachment methods. *Acta pathologica, microbiologica, et immunologica Scandinavica Section C, Immunology* 1987; **95**(2): 81-4.
391. Aoshiba K, Yasuda K, Yasui S, Tamaoki J, Nagai A. Serine proteases increase oxidative stress in lung cells. *Am J Physiol Lung Cell Mol Physiol* 2001; **281**(3): L556-64.
392. Drummen GP, van Liebergen LC, Op den Kamp JA, Post JA. C11-BODIPY(581/591), an oxidation-sensitive fluorescent lipid peroxidation probe: (micro)spectroscopic characterization and validation of methodology. *Free Radic Biol Med* 2002; **33**(4): 473-90.
393. MacDonald ML, Murray IV, Axelsen PH. Mass spectrometric analysis demonstrates that BODIPY 581/591 C11 overestimates and inhibits oxidative lipid damage. *Free Radic Biol Med* 2007; **42**(9): 1392-7.

394. Crowther JE, Kutala VK, Kuppusamy P, et al. Pulmonary surfactant protein a inhibits macrophage reactive oxygen intermediate production in response to stimuli by reducing NADPH oxidase activity. *J Immunol* 2004; **172**(11): 6866-74.
395. Wardman P. Fluorescent and luminescent probes for measurement of oxidative and nitrosative species in cells and tissues: progress, pitfalls, and prospects. *Free Radic Biol Med* 2007; **43**(7): 995-1022.
396. Cathcart R, Schwiers E, Ames BN. Detection of picomole levels of hydroperoxides using a fluorescent dichlorofluorescein assay. *Anal Biochem* 1983; **134**(1): 111-6.
397. Kooy NW, Royall JA, Ischiropoulos H. Oxidation of 2',7'-dichlorofluorescin by peroxynitrite. *Free Radic Res* 1997; **27**(3): 245-54.
398. Brubacher JL, Bols NC. Chemically de-acetylated 2',7'-dichlorodihydrofluorescein diacetate as a probe of respiratory burst activity in mononuclear phagocytes. *J Immunol Methods* 2001; **251**(1-2): 81-91.
399. Imrich A, Ning YY, Kobzik L. Intracellular oxidant production and cytokine responses in lung macrophages: evaluation of fluorescent probes. *J Leukoc Biol* 1999; **65**(4): 499-507.
400. Benov L, Sztejnberg L, Fridovich I. Critical evaluation of the use of hydroethidine as a measure of superoxide anion radical. *Free Radic Biol Med* 1998; **25**(7): 826-31.
401. Rothe G, Valet G. Flow cytometric analysis of respiratory burst activity in phagocytes with hydroethidine and 2',7'-dichlorofluorescin. *J Leukoc Biol* 1990; **47**(5): 440-8.
402. Crow JP. Dichlorodihydrofluorescein and dihydrorhodamine 123 are sensitive indicators of peroxynitrite in vitro: implications for intracellular measurement of reactive nitrogen and oxygen species. *Nitric oxide : biology and chemistry / official journal of the Nitric Oxide Society* 1997; **1**(2): 145-57.
403. Elbim C, Lizard G. Flow cytometric investigation of neutrophil oxidative burst and apoptosis in physiological and pathological situations. *Cytometry Part A : the journal of the International Society for Analytical Cytology* 2009; **75**(6): 475-81.
404. Stolk J, Hiltermann TJ, Dijkman JH, Verhoeven AJ. Characteristics of the inhibition of NADPH oxidase activation in neutrophils by apocynin, a methoxy-substituted catechol. *Am J Respir Cell Mol Biol* 1994; **11**(1): 95-102.
405. Vejrazka M, Micek R, Stipek S. Apocynin inhibits NADPH oxidase in phagocytes but stimulates ROS production in non-phagocytic cells. *Biochim Biophys Acta* 2005; **1722**(2): 143-7.
406. Riganti C, Costamagna C, Bosia A, Ghigo D. The NADPH oxidase inhibitor apocynin (acetovanillone) induces oxidative stress. *Toxicol Appl Pharmacol* 2006; **212**(3): 179-87.
407. Patton GW, Paciga JE, Shelley SA. NR8383 alveolar macrophage toxic growth arrest by hydrogen peroxide is associated with induction of growth-arrest and DNA damage-inducible genes GADD45 and GADD153. *Toxicol Appl Pharmacol* 1997; **147**(1): 126-34.
408. Buchmuller-Rouiller Y, Corrandin SB, Smith J, et al. Role of glutathione in macrophage activation: effect of cellular glutathione depletion on nitrite production and leishmanicidal activity. *Cellular immunology* 1995; **164**(1): 73-80.
409. Venketaraman V, Dayaram YK, Talaue MT, Connell ND. Glutathione and nitrosoglutathione in macrophage defense against Mycobacterium tuberculosis. *Infect Immun* 2005; **73**(3): 1886-9.

410. Legrand C, Bour JM, Jacob C, et al. Lactate dehydrogenase (LDH) activity of the cultured eukaryotic cells as marker of the number of dead cells in the medium [corrected]. *J Biotechnol* 1992; **25**(3): 231-43.
411. Maruf Hossain AM, Park S, Kim JS, Park K. Volatility and mixing states of ultrafine particles from biomass burning. *Journal of hazardous materials* 2012; **205-206**: 189-97.
412. Lin CC, Huang KL, Tsai JH, W.J. L, Chen SJ, Lin SK. Characteristics of water-soluble ions and carbon in fine and coarse particles collected near an open burning site. Atmospheric Environment.
413. BD Biosciences. BD Fluorescence Spectrum Viewer. 2012.
414. Antunes F, Cadenas E. Cellular titration of apoptosis with steady state concentrations of H(2)O(2): submicromolar levels of H(2)O(2) induce apoptosis through Fenton chemistry independent of the cellular thiol state. *Free Radic Biol Med* 2001; **30**(9): 1008-18.
415. Molecular Probes. Amine reactive OxyBURST reagents. Molecular Probes,; 2001.
416. Needham LA, Davidson AH, Bawden LJ, et al. Drug targeting to monocytes and macrophages using esterase-sensitive chemical motifs. *J Pharmacol Exp Ther* 2011; **339**(1): 132-42.
417. Rahman I, MacNee W. Lung glutathione and oxidative stress: implications in cigarette smoke-induced airway disease. *Am J Physiol* 1999; **277**(6 Pt 1): L1067-88.
418. Fitzpatrick AM, Teague WG, Burwell L, Brown MS, Brown LA. Glutathione oxidation is associated with airway macrophage functional impairment in children with severe asthma. *Pediatr Res* 2011; **69**(2): 154-9.
419. Masri FA, Comhair SA, Dostanic-Larson I, et al. Deficiency of lung antioxidants in idiopathic pulmonary arterial hypertension. *Clinical and translational science* 2008; **1**(2): 99-106.
420. Dauletbaev N, Viel K, Buhl R, Wagner TO, Bargon J. Glutathione and glutathione peroxidase in sputum samples of adult patients with cystic fibrosis. *Journal of cystic fibrosis : official journal of the European Cystic Fibrosis Society* 2004; **3**(2): 119-24.
421. Behr J, Degenkolb B, Beinert T, Krombach F, Vogelmeier C. Pulmonary glutathione levels in acute episodes of Farmer's lung. *Am J Respir Crit Care Med* 2000; **161**(6): 1968-71.
422. Pacht ER, Diaz P, Clanton T, Hart J, Gadek JE. Alveolar fluid glutathione decreases in asymptomatic HIV-seropositive subjects over time. *Chest* 1997; **112**(3): 785-8.
423. Avissar NE, Reed CK, Cox C, Frampton MW, Finkelstein JN. Ozone, but not nitrogen dioxide, exposure decreases glutathione peroxidases in epithelial lining fluid of human lung. *Am J Respir Crit Care Med* 2000; **162**(4 Pt 1): 1342-7.
424. Abbate C, Giorgianni C, Brecciaroli R, et al. Changes induced by exposure of the human lung to glass fiber-reinforced plastic. *Environ Health Perspect* 2006; **114**(11): 1725-9.
425. Becker S, Mundandhara S, Devlin RB, Madden M. Regulation of cytokine production in human alveolar macrophages and airway epithelial cells in response to ambient air pollution particles: further mechanistic studies. *Toxicol Appl Pharmacol* 2005; **207**(2 Suppl): 269-75.
426. Karlsson HL, Ljungman AG, Lindbom J, Moller L. Comparison of genotoxic and inflammatory effects of particles generated by wood combustion, a road simulator and collected from street and subway. *Toxicol Lett* 2006; **165**(3): 203-11.

427. Riddervold IS, Bonlokke JH, Olin AC, et al. Effects of wood smoke particles from wood-burning stoves on the respiratory health of atopic humans. *Part Fibre Toxicol* 2012; **9**(1): 12.
428. Forchhammer L, Moller P, Riddervold IS, et al. Controlled human wood smoke exposure: oxidative stress, inflammation and microvascular function. *Part Fibre Toxicol* 2012; **9**: 7.
429. Pourazar J, Mudway IS, Samet JM, et al. Diesel exhaust activates redox-sensitive transcription factors and kinases in human airways. *Am J Physiol Lung Cell Mol Physiol* 2005; **289**(5): L724-30.
430. Mudway IS, Stenfors N, Duggan ST, et al. An in vitro and in vivo investigation of the effects of diesel exhaust on human airway lining fluid antioxidants. *Arch Biochem Biophys* 2004; **423**(1): 200-12.
431. Salvi S, Blomberg A, Rudell B, et al. Acute inflammatory responses in the airways and peripheral blood after short-term exposure to diesel exhaust in healthy human volunteers. *Am J Respir Crit Care Med* 1999; **159**(3): 702-9.
432. Malhotra D, Thimmulappa R, Navas-Acien A, et al. Decline in NRF2-regulated antioxidants in chronic obstructive pulmonary disease lungs due to loss of its positive regulator, DJ-1. *Am J Respir Crit Care Med* 2008; **178**(6): 592-604.
433. Golde DW, Byers LA, Finley TN. Proliferative capacity of human alveolar macrophage. *Nature* 1974; **247**(440): 373-5.
434. Nakata K, Gotoh H, Watanabe J, et al. Augmented proliferation of human alveolar macrophages after allogeneic bone marrow transplantation. *Blood* 1999; **93**(2): 667-73.
435. Kurmi OP, Semple S, Simkhada P, Smith WC, Ayres JG. COPD and chronic bronchitis risk of indoor air pollution from solid fuel: a systematic review and meta-analysis. *Thorax* 2010; **65**(3): 221-8.
436. Manthalu G, Nkhoma D, Kuyeli S. Simple versus composite indicators of socioeconomic status in resource allocation formulae: the case of the district resource allocation formula in Malawi. *BMC health services research* 2010; **10**: 6.
437. van der Vaart H, Postma DS, Timens W, ten Hacken NH. Acute effects of cigarette smoke on inflammation and oxidative stress: a review. *Thorax* 2004; **59**(8): 713-21.
438. Miller MR, Hankinson J, Brusasco V, et al. Standardisation of spirometry. *Eur Respir J* 2005; **26**(2): 319-38.
439. Miller MR, Quanjer PH, Swanney MP, Ruppel G, Enright PL. Interpreting lung function data using 80% predicted and fixed thresholds misclassifies more than 20% of patients. *Chest* 2011; **139**(1): 52-9.
440. Ward C, Thien F, Secombe J, Gollant S, Walters EH. Bronchoalveolar lavage fluid urea as a measure of pulmonary permeability in healthy smokers. *Eur Respir J* 2000; **15**(2): 285-90.
441. Barditch-Crovo P, Svobodova V, Lietman P. Apparent deficiency of glutathionine in the PBMC's of people with AIDS depends on method of expression. *J Acquir Immune Defic Syndr Hum Retrovirol* 1995; **8**(3): 313-4.
442. National Statistical Office. Malawi Demographic and Health Survey 2010. Zomba, Malawi.; 2011.
443. Streiner DL, Norman GR. Correction for multiple testing: is there a resolution? *Chest* 2011; **140**(1): 16-8.

444. R Foundation. R: A language and environment for statistical computing and graphics. 2.15.0 ed; 2010.
445. Diggle P, Chetwynd A. Statistics and scientific method : an introduction for students and researchers. New York: Oxford University Press; 2011.
446. Thomson CD, Rea HM, Doesburg VM, Robinson MF. Selenium concentrations and glutathione peroxidase activities in whole blood of New Zealand residents. *Br J Nutr* 1977; **37**(3): 457-60.
447. Allan CB, Lacourciere GM, Stadtman TC. Responsiveness of selenoproteins to dietary selenium. *Annu Rev Nutr* 1999; **19**: 1-16.
448. Ashton K, Hooper L, Harvey LJ, Hurst R, Casgrain A, Fairweather-Tait SJ. Methods of assessment of selenium status in humans: a systematic review. *Am J Clin Nutr* 2009; **89**(6): 2025S-39S.
449. Li J, Pritchard DK, Wang X, et al. cDNA microarray analysis reveals fundamental differences in the expression profiles of primary human monocytes, monocyte-derived macrophages, and alveolar macrophages. *J Leukoc Biol* 2007; **81**(1): 328-35.
450. Gould NS, Min E, Gauthier S, Chu HW, Martin R, Day BJ. Aging adversely affects the cigarette smoke-induced glutathione adaptive response in the lung. *Am J Respir Crit Care Med* 2010; **182**(9): 1114-22.
451. Kelly FJ. Oxidative stress: its role in air pollution and adverse health effects. *Occup Environ Med* 2003; **60**(8): 612-6.
452. Jones DP, Mody VC, Jr., Carlson JL, Lynn MJ, Sternberg P, Jr. Redox analysis of human plasma allows separation of pro-oxidant events of aging from decline in antioxidant defenses. *Free Radic Biol Med* 2002; **33**(9): 1290-300.
453. Ramirez-Venegas A, Sansores RH, Perez-Padilla R, et al. Survival of patients with chronic obstructive pulmonary disease due to biomass smoke and tobacco. *Am J Respir Crit Care Med* 2006; **173**(4): 393-7.
454. Regalado J, Perez-Padilla R, Sansores R, et al. The effect of biomass burning on respiratory symptoms and lung function in rural Mexican women. *Am J Respir Crit Care Med* 2006; **174**(8): 901-5.
455. Tashkin DP, Clark VA, Coulson AH, et al. Comparison of lung function in young nonsmokers and smokers before and after initiation of the smoking habit. A prospective study. *Am Rev Respir Dis* 1983; **128**(1): 12-6.
456. Reed WW, Diehl LF. Leukopenia, neutropenia, and reduced hemoglobin levels in healthy American blacks. *Arch Intern Med* 1991; **151**(3): 501-5.
457. Kocyigit A, Erel O, Gur S. Effects of tobacco smoking on plasma selenium, zinc, copper and iron concentrations and related antioxidative enzyme activities. *Clin Biochem* 2001; **34**(8): 629-33.
458. Ghayour-Mobarhan M, Taylor A, New SA, Lamb DJ, Ferns GA. Determinants of serum copper, zinc and selenium in healthy subjects. *Annals of clinical biochemistry* 2005; **42**(Pt 5): 364-75.
459. Neurohr C, Lenz AG, Ding I, Leuchte H, Kolbe T, Behr J. Glutamate-cysteine ligase modulatory subunit in BAL alveolar macrophages of healthy smokers. *Eur Respir J* 2003; **22**(1): 82-7.

460. Garbin U, Fratta Pasini A, Stranieri C, et al. Cigarette smoking blocks the protective expression of Nrf2/ARE pathway in peripheral mononuclear cells of young heavy smokers favouring inflammation. *PLoS One* 2009; **4**(12): e8225.
461. Nichenametla SN, Ellison I, Calcagnotto A, Lazarus P, Muscat JE, Richie JP, Jr. Functional significance of the GAG trinucleotide-repeat polymorphism in the gene for the catalytic subunit of gamma-glutamylcysteine ligase. *Free Radic Biol Med* 2008; **45**(5): 645-50.
462. Jung KA, Kwak MK. The Nrf2 system as a potential target for the development of indirect antioxidants. *Molecules* 2010; **15**(10): 7266-91.
463. Brigelius-Flohe R. Tissue-specific functions of individual glutathione peroxidases. *Free Radic Biol Med* 1999; **27**(9-10): 951-65.
464. Kulkarni NS, Prudon B, Panditi SL, Abebe Y, Grigg J. Carbon loading of alveolar macrophages in adults and children exposed to biomass smoke particles. *Sci Total Environ* 2005; **345**(1-3): 23-30.
465. Piacentini S, Polimanti R, Porreca F, Martinez-Labarga C, De Stefano GF, Fuciarelli M. GSTT1 and GSTM1 gene polymorphisms in European and African populations. *Molecular biology reports* 2011; **38**(2): 1225-30.
466. Reddy P, Naidoo RN, Robins TG, et al. GSTM1 and GSTP1 gene variants and the effect of air pollutants on lung function measures in South African children. *Am J Ind Med* 2012.
467. Schwartz J. Air pollution and daily mortality: a review and meta analysis. *Environ Res* 1994; **64**(1): 36-52.
468. Aunan K, Pan XC. Exposure-response functions for health effects of ambient air pollution applicable for China -- a meta-analysis. *Sci Total Environ* 2004; **329**(1-3): 3-16.
469. Schwartz J, Zanobetti A. Using meta-smoothing to estimate dose-response trends across multiple studies, with application to air pollution and daily death. *Epidemiology* 2000; **11**(6): 666-72.
470. Pope CA, 3rd. Respiratory hospital admissions associated with PM10 pollution in Utah, Salt Lake, and Cache Valleys. *Arch Environ Health* 1991; **46**(2): 90-7.
471. Zmirou D, Schwartz J, Saez M, et al. Time-series analysis of air pollution and cause-specific mortality. *Epidemiology* 1998; **9**(5): 495-503.
472. Filleul L, Le Tertre A, Baldi I, Tessier JF. Difference in the relation between daily mortality and air pollution among elderly and all-ages populations in southwestern France. *Environ Res* 2004; **94**(3): 249-53.
473. Lacasana M, Esplugues A, Ballester F. Exposure to ambient air pollution and prenatal and early childhood health effects. *Eur J Epidemiol* 2005; **20**(2): 183-99.
474. Dockery DW, Speizer FE, Stram DO, Ware JH, Spengler JD, Ferris BG, Jr. Effects of inhalable particles on respiratory health of children. *Am Rev Respir Dis* 1989; **139**(3): 587-94.
475. Dockery DW. Epidemiologic evidence of cardiovascular effects of particulate air pollution. *Environ Health Perspect* 2001; **109 Suppl 4**: 483-6.
476. Ezzati M, Kammen DM. The health impacts of exposure to indoor air pollution from solid fuels in developing countries: knowledge, gaps, and data needs. *Environ Health Perspect* 2002; **110**(11): 1057-68.

477. Pandey MR, Boleij JS, Smith KR, Wafula EM. Indoor air pollution in developing countries and acute respiratory infection in children. *Lancet* 1989; **1**(8635): 427-9.
478. WHO. The global burden of disease: 2004 update. Geneva: WHO Press; 2008.
479. Wardlaw T, Salama P, Johansson EW, Mason E. Pneumonia: the leading killer of children. *Lancet* 2006; **368**(9541): 1048-50.
480. Kurosaka K, Takahashi M, Watanabe N, Kobayashi Y. Silent cleanup of very early apoptotic cells by macrophages. *J Immunol* 2003; **171**(9): 4672-9.
481. Xu F, Droemann D, Rupp J, et al. Modulation of the inflammatory response to Streptococcus pneumoniae in a model of acute lung tissue infection. *Am J Respir Cell Mol Biol* 2008; **39**(5): 522-9.
482. Assari T. Chronic Granulomatous Disease; fundamental stages in our understanding of CGD. *Medical immunology* 2006; **5**: 4.
483. Jimenez LA, Drost EM, Gilmour PS, et al. PM(10)-exposed macrophages stimulate a proinflammatory response in lung epithelial cells via TNF-alpha. *Am J Physiol Lung Cell Mol Physiol* 2002; **282**(2): L237-48.
484. Kawasaki S, Takizawa H, Takami K, et al. Benzene-extracted components are important for the major activity of diesel exhaust particles: effect on interleukin-8 gene expression in human bronchial epithelial cells. *Am J Respir Cell Mol Biol* 2001; **24**(4): 419-26.
485. Knapp S, Leemans JC, Florquin S, et al. Alveolar macrophages have a protective antiinflammatory role during murine pneumococcal pneumonia. *Am J Respir Crit Care Med* 2003; **167**(2): 171-9.
486. Serezani CH, Chung J, Ballinger MN, Moore BB, Aronoff DM, Peters-Golden M. Prostaglandin E2 suppresses bacterial killing in alveolar macrophages by inhibiting NADPH oxidase. *Am J Respir Cell Mol Biol* 2007; **37**(5): 562-70.
487. Becher R, Bucht A, Ovrevik J, et al. Involvement of NADPH oxidase and iNOS in rodent pulmonary cytokine responses to urban air and mineral particles. *Inhal Toxicol* 2007; **19**(8): 645-55.
488. Hatch GE, Boykin E, Graham JA, et al. Inhalable particles and pulmonary host defense: in vivo and in vitro effects of ambient air and combustion particles. *Environ Res* 1985; **36**(1): 67-80.
489. Phipps JC, Aronoff DM, Curtis JL, Goel D, O'Brien E, Mancuso P. Cigarette smoke exposure impairs pulmonary bacterial clearance and alveolar macrophage complement-mediated phagocytosis of Streptococcus pneumoniae. *Infect Immun* 2010; **78**(3): 1214-20.
490. Chen H, Cowan MJ, Hasday JD, Vogel SN, Medvedev AE. Tobacco smoking inhibits expression of proinflammatory cytokines and activation of IL-1R-associated kinase, p38, and NF-kappaB in alveolar macrophages stimulated with TLR2 and TLR4 agonists. *J Immunol* 2007; **179**(9): 6097-106.
491. McKusick-Nathans Institute of Genetic Medicine JHUB, MD),. Online Mendelian Inheritance in Man, OMIM®.
492. Iyer SS, Accardi CJ, Ziegler TR, et al. Cysteine redox potential determines pro-inflammatory IL-1beta levels. *PLoS One* 2009; **4**(3): e5017.
493. Kuhn AM, Tzieply N, Schmidt MV, et al. Antioxidant signaling via Nrf2 counteracts lipopolysaccharide-mediated inflammatory responses in foam cell macrophages. *Free Radic Biol Med* 2011; **50**(10): 1382-91.

494. Mukaida N. Pathophysiological roles of interleukin-8/CXCL8 in pulmonary diseases. *Am J Physiol Lung Cell Mol Physiol* 2003; **284**(4): L566-77.
495. Simone RE, Russo M, Catalano A, et al. Lycopene inhibits NF-κB-mediated IL-8 expression and changes redox and PPARgamma signalling in cigarette smoke-stimulated macrophages. *PLoS One* 2011; **6**(5): e19652.
496. Haddad JJ, Saade NE, Safieh-Garabedian B. Redox regulation of TNF-alpha biosynthesis: augmentation by irreversible inhibition of gamma-glutamylcysteine synthetase and the involvement of an IkappaB-alpha/NF-kappaB-independent pathway in alveolar epithelial cells. *Cell Signal* 2002; **14**(3): 211-8.
497. Haddad JJ, Fahlman CS. Redox- and oxidant-mediated regulation of interleukin-10: an anti-inflammatory, antioxidant cytokine? *Biochem Biophys Res Commun* 2002; **297**(2): 163-76.
498. Palacio JR, Markert UR, Martinez P. Anti-inflammatory properties of N-acetylcysteine on lipopolysaccharide-activated macrophages. *Inflamm Res* 2011; **60**(7): 695-704.
499. Pagliei S, Ghezzi P, Bizzarri C, et al. Thioredoxin specifically cross-desensitizes monocytes to MCP-1. *European cytokine network* 2002; **13**(2): 261-7.
500. Desai A, Huang X, Warren JS. Intracellular glutathione redox status modulates MCP-1 expression in pulmonary granulomatous vasculitis. *Laboratory investigation; a journal of technical methods and pathology* 1999; **79**(7): 837-47.
501. Hashimoto S, Gon Y, Matsumoto K, Takeshita I, MacHino T, Horie T. Intracellular glutathione regulates tumour necrosis factor-alpha-induced p38 MAP kinase activation and RANTES production by human bronchial epithelial cells. *Clin Exp Allergy* 2001; **31**(1): 144-51.
502. Mosser DM, Edwards JP. Exploring the full spectrum of macrophage activation. *Nat Rev Immunol* 2008; **8**(12): 958-69.
503. Pi J, Bai Y, Reece JM, et al. Molecular mechanism of human Nrf2 activation and degradation: role of sequential phosphorylation by protein kinase CK2. *Free Radic Biol Med* 2007; **42**(12): 1797-806.
504. Annenkov AY, Baranova FS. Lipopolysaccharide-dependent and lipopolysaccharide-independent pathways of monocyte desensitisation to lipopolysaccharides. *J Leukoc Biol* 1991; **50**(3): 215-22.
505. Didierlaurent A, Goulding J, Patel S, et al. Sustained desensitization to bacterial Toll-like receptor ligands after resolution of respiratory influenza infection. *J Exp Med* 2008; **205**(2): 323-9.
506. Swiston JR, Davidson W, Attridge S, Li GT, Brauer M, van Eeden SF. Wood smoke exposure induces a pulmonary and systemic inflammatory response in firefighters. *Eur Respir J* 2008; **32**(1): 129-38.
507. Tal TL, Simmons SO, Silbajoris R, et al. Differential transcriptional regulation of IL-8 expression by human airway epithelial cells exposed to diesel exhaust particles. *Toxicol Appl Pharmacol* 2010; **243**(1): 46-54.
508. Quay JL, Reed W, Samet J, Devlin RB. Air pollution particles induce IL-6 gene expression in human airway epithelial cells via NF-kappaB activation. *Am J Respir Cell Mol Biol* 1998; **19**(1): 98-106.

509. Kocbach Bolling A, Pagels J, Yttri KE, et al. Health effects of residential wood smoke particles: the importance of combustion conditions and physicochemical particle properties. *Part Fibre Toxicol* 2009; **6**: 29.
510. Werts C, le Bourhis L, Liu J, et al. Nod1 and Nod2 induce CCL5/RANTES through the NF-kappaB pathway. *Eur J Immunol* 2007; **37**(9): 2499-508.
511. Okuma T, Terasaki Y, Sakashita N, et al. MCP-1/CCR2 signalling pathway regulates hyperoxia-induced acute lung injury via nitric oxide production. *International journal of experimental pathology* 2006; **87**(6): 475-83.
512. Brieland JK, Jones ML, Clarke SJ, Baker JB, Warren JS, Fantone JC. Effect of acute inflammatory lung injury on the expression of monocyte chemoattractant protein-1 (MCP-1) in rat pulmonary alveolar macrophages. *Am J Respir Cell Mol Biol* 1992; **7**(2): 134-9.
513. van Zoelen MA, Verstege MI, Draing C, et al. Endogenous MCP-1 promotes lung inflammation induced by LPS and LTA. *Molecular immunology* 2011; **48**(12-13): 1468-76.
514. Gatti S, Faggioni R, Echtenacher B, Ghezzi P. Role of tumour necrosis factor and reactive oxygen intermediates in lipopolysaccharide-induced pulmonary oedema and lethality. *Clin Exp Immunol* 1993; **91**(3): 456-61.
515. Mukherjee B, Dutta A, Roychoudhury S, Ray MR. Chronic inhalation of biomass smoke is associated with DNA damage in airway cells: involvement of particulate pollutants and benzene. *J Appl Toxicol* 2011.
516. Maier KL, Alessandrini F, Beck-Speier I, et al. Health effects of ambient particulate matter--biological mechanisms and inflammatory responses to in vitro and in vivo particle exposures. *Inhal Toxicol* 2008; **20**(3): 319-37.
517. Tamagawa E, Bai N, Morimoto K, et al. Particulate matter exposure induces persistent lung inflammation and endothelial dysfunction. *Am J Physiol Lung Cell Mol Physiol* 2008; **295**(1): L79-85.
518. Kulkarni N, Pierse N, Rushton L, Grigg J. Carbon in airway macrophages and lung function in children. *N Engl J Med* 2006; **355**(1): 21-30.
519. Rybicka JM, Balce DR, Khan MF, Krohn RM, Yates RM. NADPH oxidase activity controls phagosomal proteolysis in macrophages through modulation of the lumenal redox environment of phagosomes. *Proc Natl Acad Sci U S A* 2010; **107**(23): 10496-501.
520. Kampfrath T, Maiseyeu A, Ying Z, et al. Chronic fine particulate matter exposure induces systemic vascular dysfunction via NADPH oxidase and TLR4 pathways. *Circ Res* 2011; **108**(6): 716-26.
521. Amer J, Fibach E. Chronic oxidative stress reduces the respiratory burst response of neutrophils from beta-thalassaemia patients. *British journal of haematology* 2005; **129**(3): 435-41.
522. More JM, Voelker DR, Silveira LJ, Edwards MG, Chan ED, Bowler RP. Smoking reduces surfactant protein D and phospholipids in patients with and without chronic obstructive pulmonary disease. *BMC pulmonary medicine* 2010; **10**: 53.
523. Datla SR, Dusting GJ, Mori TA, Taylor CJ, Croft KD, Jiang F. Induction of heme oxygenase-1 in vivo suppresses NADPH oxidase derived oxidative stress. *Hypertension* 2007; **50**(4): 636-42.

524. Bates SR, Xu J, Dodia C, Fisher AB. Macrophages primed by overnight culture demonstrate a marked stimulation of surfactant protein A degradation. *Am J Physiol* 1997; **273**(4 Pt 1): L831-9.
525. Black MJ, Brandt RB. Spectrofluorometric analysis of hydrogen peroxide. *Anal Biochem* 1974; **58**(1): 246-54.
526. Nyberg K, Johansson U, Johansson A, Camner P. Phagolysosomal pH in alveolar macrophages. *Environ Health Perspect* 1992; **97**: 149-52.
527. Kobzik L, Godleski JJ, Brain JD. Selective down-regulation of alveolar macrophage oxidative response to opsonin-independent phagocytosis. *J Immunol* 1990; **144**(11): 4312-9.
528. Ouadrhiri Y, Pilette C, Monteiro RC, Vaerman JP, Sibille Y. Effect of IgA on respiratory burst and cytokine release by human alveolar macrophages: role of ERK1/2 mitogen-activated protein kinases and NF-kappaB. *Am J Respir Cell Mol Biol* 2002; **26**(3): 315-32.
529. Wu TT, Chen TL, Chen RM. Lipopolysaccharide triggers macrophage activation of inflammatory cytokine expression, chemotaxis, phagocytosis, and oxidative ability via a toll-like receptor 4-dependent pathway: validated by RNA interference. *Toxicol Lett* 2009; **191**(2-3): 195-202.
530. Michel O, Nagy AM, Schroeven M, et al. Dose-response relationship to inhaled endotoxin in normal subjects. *Am J Respir Crit Care Med* 1997; **156**(4 Pt 1): 1157-64.
531. Stone WL, Qui M, Smith M. Lipopolysaccharide enhances the cytotoxicity of 2-chloroethyl ethyl sulfide. *BMC cell biology* 2003; **4**: 1.
532. Don Porto Carero A, Hoet PH, Nemery B, Schoeters G. Increased HLA-DR expression after exposure of human monocytic cells to air particulates. *Clin Exp Allergy* 2002; **32**(2): 296-300.
533. Meyer M, Huaux F, Gavilanes X, et al. Azithromycin reduces exaggerated cytokine production by M1 alveolar macrophages in cystic fibrosis. *Am J Respir Cell Mol Biol* 2009; **41**(5): 590-602.
534. Krausgruber T, Blazek K, Smallie T, et al. IRF5 promotes inflammatory macrophage polarization and TH1-TH17 responses. *Nat Immunol* 2011; **12**(3): 231-8.
535. Pauly JL, Allison EM, Hurley EL, Nwogu CE, Wallace PK, Paszkiewicz GM. Fluorescent human lung macrophages analyzed by spectral confocal laser scanning microscopy and multispectral cytometry. *Microsc Res Tech* 2005; **67**(2): 79-89.
536. Hodge S, Matthews G, Mukaro V, et al. Cigarette smoke-induced changes to alveolar macrophage phenotype and function are improved by treatment with procysteine. *Am J Respir Cell Mol Biol* 2011; **44**(5): 673-81.
537. Williams MA, Rangasamy T, Bauer SM, et al. Disruption of the transcription factor Nrf2 promotes pro-oxidative dendritic cells that stimulate Th2-like immunoresponsiveness upon activation by ambient particulate matter. *J Immunol* 2008; **181**(7): 4545-59.
538. Rangasamy T, Cho CY, Thimmulappa RK, et al. Genetic ablation of Nrf2 enhances susceptibility to cigarette smoke-induced emphysema in mice. *J Clin Invest* 2004; **114**(9): 1248-59.
539. Starrett W, Blake DJ. Sulforaphane inhibits de novo synthesis of IL-8 and MCP-1 in human epithelial cells generated by cigarette smoke extract. *Journal of immunotoxicology* 2011; **8**(2): 150-8.

540. Aoki Y, Hashimoto AH, Amanuma K, et al. Enhanced spontaneous and benzo(a)pyrene-induced mutations in the lung of Nrf2-deficient gpt delta mice. *Cancer Res* 2007; **67**(12): 5643-8.
541. Yageta Y, Ishii Y, Morishima Y, et al. Role of Nrf2 in host defense against influenza virus in cigarette smoke-exposed mice. *J Virol* 2011; **85**(10): 4679-90.
542. Reddy NM, Suryanarayana V, Kalvakolanu DV, et al. Innate immunity against bacterial infection following hyperoxia exposure is impaired in NRF2-deficient mice. *J Immunol* 2009; **183**(7): 4601-8.
543. Marzec JM, Christie JD, Reddy SP, et al. Functional polymorphisms in the transcription factor NRF2 in humans increase the risk of acute lung injury. *FASEB J* 2007; **21**(9): 2237-46.
544. Suzuki M, Betsuyaku T, Ito Y, et al. Down-regulated NF-E2-related factor 2 in pulmonary macrophages of aged smokers and patients with chronic obstructive pulmonary disease. *Am J Respir Cell Mol Biol* 2008; **39**(6): 673-82.
545. Hubner RH, Schwartz JD, De Bishnu P, et al. Coordinate control of expression of Nrf2-modulated genes in the human small airway epithelium is highly responsive to cigarette smoking. *Mol Med* 2009; **15**(7-8): 203-19.
546. Boutten A, Goven D, Boczkowski J, Bonay M. Oxidative stress targets in pulmonary emphysema: focus on the Nrf2 pathway. *Expert opinion on therapeutic targets* 2010; **14**(3): 329-46.
547. Ishii T, Itoh K, Takahashi S, et al. Transcription factor Nrf2 coordinately regulates a group of oxidative stress-inducible genes in macrophages. *J Biol Chem* 2000; **275**(21): 16023-9.
548. Krombach F, Munzing S, Allmeling AM, Gerlach JT, Behr J, Dorger M. Cell size of alveolar macrophages: an interspecies comparison. *Environ Health Perspect* 1997; **105 Suppl 5**: 1261-3.
549. Yasaka T, Mantich NM, Boxer LA, Baehner RL. Functions of human monocyte and lymphocyte subsets obtained by countercurrent centrifugal elutriation: differing functional capacities of human monocyte subsets. *J Immunol* 1981; **127**(4): 1515-8.